Aus dem Adolf-Butenandt-Institut
Lehrstuhl für Stoffwechselbiochemie im Biomedizinisches Zentrum
der Ludwig-Maximilians-Universität München
Vorstand: Prof. Dr. rer. nat. Dr. h.c. Christian Haass

CHARACTERISATION OF THE CLEAVAGE MECHANISM OF SPPL2 PROTEASES

Dissertation
Zum Erwerb des Doktorgrades der Naturwissenschaften
An der Medizinischen Fakultät der Ludwig-Maximilians-Universität zu München

vorgelegt von
CHARLOTTE SPITZ
aus Duisburg

2021

Mit Genehmigung der Medizinischen Fakultät der Universität München

Betreuerin:	Prof. Dr. rer. nat. Regina Fluhrer
Zweitgutachter:	Prof. Dr. rer. nat. Alexander Faußner
Dekan:	Prof. Dr. med. Thomas Gudermann
Tag der mündlichen Prüfung:	19.10.2021

Parts of this thesis have been published in:

Spitz, C., Schlosser, C., Guschtschin-Schmidt, N., Stelzer, W., Menig, S., Götz, A., Haug-Kröper, M., Scharnagl, C., Langosch, D. & Muhle-Goll, C. 2020. Non-Canonical shedding of TNFα by SPPL2a is determined by the conformational flexibility of its transmembrane helix. *iScience*, 101775

TABLE OF CONTENT

LIST OF FIGURES

LIST OF TABLES

ABBREVIATIONS

2-BP	2-bromopalmitate
ABHD	αβ hydrolase domain
ADAM	A disintegrin and metalloprotease
AI	ADAM inhibition
AICD	APP-ICD
ALS	Amyotrophic lateral sclerosis
APH1	Anterior pharynx defective 1
APP	Amyloid precursor protein
APT	Acylprotein thioesterase
BACE1	β-site APP cleaving enzyme 1
BMDC	Bone marrow-derived dendritic cell
Bri	British dementia protein
C9orf72	Chromosome 9 open reading frame 72
CD	Cluster of differentiation
CLR	C-type lectin receptors
CTF	C-terminal fragment
DC	Dendritic cell
ECD	Ectodomain
EGFR	Epidermal growth factor receptor
ER	Endoplasmatic reticulum
ERK	Extracellular-signal-regulated kinase
FasL	Fas ligand
FBD/ FDD	Familiar British/ Danish dementia
FL	Full-length
FTLD	Frontotemporal lobar degeneration
FRMD8	FERM domain-containing protein 8
FVenv	Foamy virus envelope protein
GPCR	G-protein-coupled receptor
HIV	Human immunodeficiency virus
HLA	Human lymphocyte antigen

ICD	Intracellular domain
IFNγ	Interferon γ
IL	Interleukin
IMP	Intramembrane-cleaving protease
iRhom	Inactive rhomboid protease
JMD	Juxtamembrane domain
LDL	Low density lipoprotein
MALDI-TOF	Matrix assisted laser desorption ionization – time of flight
MAPK	Mitogen-activated protein kinase
MHC	Major histocompatibility complex
MIF	Macrophage migration inhibitory factor
MPD	Membrane-proximal domain
MMP	Matrix metalloprotease
NFκB	Nuclear factor 'κ-light-chain-enhancer' of activated B-cells
NK cell	Natural killer cell
NTF	N-terminal fragment
NRG1	Neuregulin 1
PARL	Presenilins-associated rhomboid-like protein
PAT	Protein acyltransferase
PEN	Presenilin enhancer
PDK1	Phosphoinositide-dependent kinase 1
PI3K	Phosphoinositid-3-kinase
PKC	Phosphokinase C
PM	Plasma membrane
PMA	Phorbol 12-myristate 13-acetate
POPC	1-palmitoyl-2-oleoyl-sn-glycero-3-phosphocholine
PPT	Palmitoyl protein thioesterases
PS	Presenilin
PTM	Posttranslational modification
RANK/RANKL	Receptor activator of NFκB (ligand)
Rce1	Ras converting enzyme 1 (glutamyl-intramembrane protease)
RHBDL	Rhomboid-like protein

RIP	Regulated intramembrane proteolysis
RT	Room temperature
S1P	Site-1 protease
S2P	Site-2 protease
sAPP	Soluble APP peptide
sBri2	Soluble Bri2 peptide
SNP	Single nucleotide polymorphism
SREBP	Sterol regulatory element binding protein
sTNFα	Soluble TNFα
sTNFα(L2)	Soluble TNFα generated by SPPL2
SNARE	Soluble N-ethylmaleimide-sensitive factor attachment protein receptors
SPP	Signal peptide peptidase
SPPL	Signal peptide peptidase like protein
TA	Tail-anchored
TACE	TNFα-converting enzyme (ADAM17)
TEV	Tobacco Etch Virus
TFR1	Transferrin receptor 1
TICD	TNFα ICD
TIMP	Tissue specific inhibitors of metalloproteinases
TLR	Toll-like receptor
TM	Transmembrane
TMD	Transmembrane domain
TMEM106b	Transmembrane protein 106b
TNFα	Tumour necrosis factor α
TNFR	TNFα receptor
TRAIL	TNF–related apoptosis-inducing ligand
WB	Western Blot
Wt	Wild type
$(ZLL)_2$	2,2'-(2-Oxo-1,3-propanediyl)bis[N-[(phenylmethoxy) carbonyl]-L-leucyl-L-leucin-amide

SUMMARY

In order to function properly, a cell needs to control the distribution, abundance, and activity of all its proteins. Not only is it important to increase protein expression upon an external stimulus but also removal and downregulation play a key role in cellular homeostasis. The disruption of peptide bonds in order to break down a protein is called hydrolysis and is facilitated by enzymes termed proteases. As this reaction is usually conducted in an aqueous environment, it was surprising to discover a group of proteases that were able to perform this enzymatic reaction within the plane of the membrane. After their discovery, these intramembrane-cleaving proteases (IMPs) have attracted focus, as their processing mechanism seemed to be involved in many regulatory pathways.

The IMPs are grouped according to their active site amino acid. Based on this, presenilins, signal peptide peptidase (SPP), and SPP-like proteases (SPPL) are classified as aspartyl-IMPs that share the same active site motif GxGD. In humans, the SPP/SPPL family comprises five members: SPP, SPPL2a, b, c, and SPPL3. In particular, SPPL2a has demonstrated to be of physiological relevance, as it plays an important role in the immune response of the human body. In contrast to the family of SPPL proteases, presenilins 1 and 2, which form the catalytically active subunit of γ-secretase, have already been well studied. Mutations in presenilins have gained attention as they contribute to the pathomechanism of Alzheimer's disease. Thus, presenilin mutations induce particularly aggressive forms of the disease as they change the processing of their substrates. The characteristic cleavage mechanism, the regulated intramembrane proteolysis (RIP), is common for many IMPs. RIP is a well-controlled process that can be separated into three steps: shedding of the ectodomain (ECD), recognition of the shortened substrate and subsequent processing. So far, little is known about common features of SPPL2 substrates that enable recognition and processing of the substrates in the context of RIP. Therefore, this study aims to provide insights into the individual steps of RIP to establish common requirements for recognition and processing by SPPL2a and SPPL2b.

The first part of the study focuses on the removal of the large substrate ECDs, which is referred to as shedding. Processing of a protein by IMPs often requires a preceding shortening of the substrate by a sheddase such as ADAM. However, more and

more evidence has emerged that ECD shedding is not necessarily a mandatory prerequisite for all substrates to be recognized and processed by IMPs. This study reveals that SPPL2a is able to process tumour necrosis factor alpha (TNFα) without prior shedding and that this non-canonical shedding can be modulated by mutations in different domains of the protein. These mutations most likely affect the secondary structure of the protein, making it better or less assessable for cleavage by SPPL2a or SPPL2b.

So far, no consensus sequence or recognition motif has been identified, which would allow predictions of SPPL2 substrates. Therefore, in the second part of the study, the recognition and initial cleavage of substrates in the context of RIP was investigated by taking advantage of the British dementia protein (Bri) 3, an established non-substrate of SPPL2. While Bri2 is a substrate, its close homologue Bri3 is not processed by SPPL2. Based on this, it was investigated whether sequence specificity or certain domains of substrates are responsible for recognition by SPPL2. By substituting domains of TNFα with the corresponding domains of Bri3, it was shown, that the intracellular domain (ICD) but even more the juxtamembrane domain (JMD) enable recognition and initial cleavage. Within these domains, charged residues are most likely to facilitate this mechanism.

In the third part of the study, the mechanism of further substrate processing by the SPPL2 proteases was investigated in more detail. Sequential cleavage of the substrate's transmembrane domain (TMD) is characteristic for intramembrane cleavage by presenilins and SPPL2b and, as shown in this study, also SPPL2a, even though less prominent. In contrast to presenilins that cleave many of their substrates sequentially, consecutive cleavage by SPPL2a/b seemed to be rather unique to TNFα. While a post-translational modification of TNFα ICD with palmitic acid enabled consecutive cleavage, mutations in the TMD were able to accelerate or reduce this cleavage. Cleavage by SPPL2a and SPPL2b occurred at the same positions within TNFα and in contrast to presenilins were never changed upon mutations.

In conclusion, this study provides a detailed investigation of the cleavage mechanism of SPPL2a and SPPL2b and focuses on commonalities and differences of both proteases. Within this context, not only a new type of substrate processing by SPPL2a is described but also the understanding of substrate selection of IMPs is deepened.

ZUSAMMENFASSUNG

Um ihre Funktionen aufrecht erhalten zu können, muss eine Zelle die Verteilung, Menge und Aktivität ihrer Proteine kontrollieren. Für die Aufrechterhaltung der Homöostase ist es nicht nur wichtig, die Expression der Proteine anzupassen, wenn sich die Bedingungen ändern, sondern auch die bereits vorhandenen Proteine, wenn nötig wieder abzubauen. Der Abbau erfolgt durch die Spaltung der Peptidbindungen in Anwesenheit von Wasser durch spezialisierte Enzyme, den sogenannten Proteasen. Diese Hydrolyse findet meist in wässrigen Lösungen statt, daher überraschte die Entdeckung einer Gruppe von Proteasen, die diese Reaktion in der hydrophoben Umgebung einer Zellmembran durchführen können. Als Grundlage vieler regulatorischer Prozesse ist die Erforschung der Intramembranproteasen (IMPs) heute wichtiger denn je.

Die Kategorisierung der IMPs erfolgt auf Grund der katalytischen Aminosäure im aktiven Zentrum des Enzyms. Presenilin, Signal Peptid Peptidasen (SPP) und SPP- ähnliche (SPPL) Proteasen werden auf Grund des gemeinsamen GxGD Motivs als Aspartyl-IMPs klassifiziert. Im Menschen besteht die Familie der SPP/SPPL Proteasen aus fünf Mitgliedern: SPP, SPPL2a, b, c und SPPL3. Physiologische Bedeutung hat dabei besonders SPPL2a, da es eine wichtige Rolle bei der Immunantwort des menschlichen Körpers spielt. Bereits gut erforscht sind, im Gegensatz zu der Familie der SPPL Proteasen, die Presenilin 1 und 2, die die katalytisch aktive Untereinheit der γ-Sekretase bilden. Kommt es zu Mutationen in Presenilinen, tragen diese zum Pathomechanismus der Alzheimer Krankheit bei und führen dann zu besonders aggressiven Formen dieser Erkrankung. Diese Mutationen verändern dabei die Prozessivität der Enzyme, die normalerweise nach dem Prinzip der regulierten Intramembranproteolyse (RIP) agieren. Bei diesem charakteristischen Mechanismus lassen sich drei Schritte für die meisten IMPs erkennen. Zunächst erfolgt die Abspaltung der Ektodomäne (ECD) des Substrates, danach die Erkennung des nun gekürzten Proteins und als letzter Schritt erfolgt die eigentliche Prozessierung in der Membran durch die IMPs.

Der erste Teil der Arbeit widmet sich dem Prozess der Abspaltung der ECD, dem sogenannten Shedding. In der Regel wird ein Substrat durch eineunabhängige Protease gesheddet. Dieser Vorgang, zum Beispiel durch die Metalloproteasen der ADAM Familie ausgeführt, schien zunächst notwendig für die weitere Prozessierung des Substrates

durch SPPL2. Diese Arbeit zeigt jedoch, dass SPPL2a den Tumor Nekrose Faktor alpha (TNFα) ohne vorangeganges Shedding direkt schneiden kann. Dieses nicht-kanonische Shedding wird durch Mutationen in unterschiedlichen Domänen TNFα entweder verstärkt oder abgeschwächt, da sie vermutlich die Sekundärstruktur in einer Art und Weise beeinflussten, die die Schnittstellen mehr oder weniger zugänglich für SPPL2a machen.

Nach dem heutigen Erkenntnisstand konnte bis jetzt kein spezifisches Spaltungs- oder Erkennungsmotiv identifiziert werden, dass eine Vorhersage von SPPL2-Substraten ermöglicht. Um diese Lücke zu schließen, wurde im zweiten Teil der Studie mit Hilfe des bereits etablierten Nicht-Substrates, Britisches Demenz Protein 3 (Bri3), untersucht, wie ein Protein von SPPL2 als Substrat erkannt wird. Während Bri2 ein Substrat für SPPL2 ist, wird das homologe Bri3 dagegen weder erkannt noch geschnitten. Daher wurde der Frage nachgegangen, ob sequenzspezifische Eigenschaften oder ganze Domänen für die Erkennung eines Proteins durch SPPL2 verantwortlich sind. Dazu wurden einzelne Domänen/ Sequenzen aus TNFα durch entsprechende Bereiche aus Bri3 ersetzt. Das Ergebnis dieses Verfahrens zeigt, dass die intrazelluläre Domäne (ICD) und mehr noch die Juxtamembrandomäne (JMD) die Erkennung des Substrates beeinflussen. Innerhalb dieser Domänen sind vermutlich geladene Aminosäuren für eine korrekte und effiziente Spaltung des Substrates verantwortlich.

Im Fokus des dritten Abschnitts dieser Arbeit steht der Prozessierungsmechanismus der SPPL2 Proteasen. Charakteristisch für SPPL2b und Presenilline ist die sequentielle Spaltung der Transmembrandomäne (TMD) des Substrats. Diese sequenzielle Spaltung konnte, wenn auch weniger ausgeprägt, ebenfalls für SPPL2a beobachtet werden. Im Gegensatz zu Presenilinen, die all ihre Substrate sequenziell schneiden, scheint die konsekutive Spaltung durch SPPL2 substratspezifisch zu sein und wurde bisher nur für TNFα beobachtet. Während die posttranslationale Modifizierung des TNFα ICDs mit Palmitinsäure eine Voraussetzung für die konsekutive Spaltung von TNFα zu sein scheint, konnten Mutationen in der TMD diese beschleunigen oder reduzieren. Die Spaltung von TNFα durch SPPL2a oder SPPL2b erfolgt an den gleichen Positionen innerhalb des Proteins und wurde im Gegensatz zu Presenilinen durch Mutationen nie verändert.

Die Ergebnisse dieser Untersuchung geben einen detaillierteren Einblick in den Schnittmechanismus von SPPL2a und SPPL2b und heben Gemeinsamkeiten und Unterschiede hervor. In diesem Zusammenhang wurde nicht nur eine neue Art der Substratprozessierung durch SPPL2a beschrieben, sondern auch das Verständnis der Substratauswahl von IMPs vertieft.

1. INTRODUCTION

To orchestrate perfect collaboration of body cells, communication is key. The transmission of signals between cells is mediated via direct cell-cell contacts when cells are close to each other. Yet in case of larger distances, information is transmitted via soluble signals. Hence, signalling proteins need to be localised to the cell surface for direct contact or the release of soluble signalling peptides from the surface protein. Not only the correct localisation but also the correct quantity off proteins is necessary for adequate signal transmission to recipient cells. Upon binding of the soluble or membrane-bound peptide to a receptor, the signal is conveyed into the recipient cell, activating or down- regulating signalling pathways to maintain the perfect homeostasis of the recipient cell. If the homeostasis collapses and communication fails, diseases develop, and if permanent, the condition becomes chronic. In many cases, this situation is difficult to restore without compromising the body's integrity. To ensure correct signalling, expression and degradation are tightly regulated, balancing the abundance of cell surface proteins. Throughout all kingdoms of life, and in every cell removal and degradation of membrane proteins is an essential process. The cleavage of peptide bonds within the membrane, termed intramembrane proteolysis, in order to remove residual membrane proteins, was long thought to be highly unlikely. However, a specialised group of enzymes has developed to hydrolyse peptide bonds in a hydrophobic environment.

1.1. PROTEASES AND PROTEOLYSIS

Proteolysis describes an irreversible procedure where peptide bonds are dissolved in the presence of water. This cleavage is facilitated by proteases that account around 60% of all enzymes. According to the international protease network, 2% of the genome encode for almost 500 proteases in a human body (http://www.protease.net.au). They regulate fate, localisation, and activity of many proteins, by modulating protein–protein interactions, generation of peptides, as well as transmission and amplification of

molecular signals. All physiological processes from cell growth to differentiation, in- and outside signalling to apoptosis involve proteases. Thus, proteases are indispensable in all living organisms and misregulation accounts for multiple diseases (Bond, 2019). As a result in 2016, an estimated 5-10% of all pharmaceutical targets pursued for drug development were proteases (Drag and Salvesen, 2010). Thus, the role of proteases and their mechanism in substrate selection and processing needs thorough investigation to ensure efficient drug development and successful treatment of the diseases.

Generally, proteases bind and cleave proteins in aqueous solutions such as the cytoplasm or the extracellular space. Even though hydrolysis of a peptide bond is an energetically favourable reaction, the resolution of a stable biological polymer is extremely slow (Langosch et al., 2015). Peptide bonds withstand high temperatures and acid concentrations within their environment. However, they are broken up easily in the presence of a specific protease. Proteolytic cleavage of surface proteins is an irreversible but important posttranslational modification (PTM), which usually results in the release of a soluble peptide and a membrane-retained fragment. This procedure is referred to as ectodomain (ECD) shedding and enables either release of a signalling competent peptide or activates the membrane-residing protein (Lichtenthaler et al., 2018). The intracellular fragment resulting from this cleavage can have signalling capacities as well or is degraded by independent proteases.

Classification of proteases is dependent on the chemical group that is responsible for catalytic activity in the active centre. If this amino acid is exchanged, the proteases lose their catalytic activity (Urban, 2013). According to this classification, six groups of proteases can be distinguished: cysteine, serine, threonine, glutamyl-, aspartyl- and metalloproteases. Cysteine proteases such as the caspases are involved in almost every aspect of life from plants to humans and thus are targeted in a wide range of human disorders (Gurumallesh et al., 2019). Their active site contains a cysteine and histidine that need reducing agents to develop proper functioning. Serine proteases make up one third of all known proteases (Di Cera, 2009, Kraut, 1977). Trypsin is a serine protease that is used frequently on cell cultures to release attached cells from the petri dish. It cleaves specifically after a lysine or arginine residue. Threonine proteases are largely responsible for intracellular protein turnover as one of the most prominent members is the proteasome. The proteasome that utilises the N-terminal threonine as the active site

removes proteins, which are tagged for degradation with a series of ubiquitin molecules (Budenholzer et al., 2017). Glutamyl- and aspartylproteases are characterised by two glutamic/ aspartic acids at the catalytic site and are therefore acidic proteases working most efficiently at a low pH (Gurumallesh et al., 2019). Pepsin in the gastric fluid, as well as the β-site APP cleaving enzyme 1 (BACE1), which cleaves the amyloid precursor protein (APP), are both aspartylproteases.

Metalloproteases require a divalent metal ion to exhibit proteolytic activity. About 30 families are so far identified one of which is a disintegrin and metalloprotease (ADAM) family. Besides ADAMs, matrix metalloproteases (MMPs) regulate branching morphogenesis, angiogenesis, wound healing, and extracellular matrix degradation (Edwards et al., 2008).

1.1.1. MEMBRANE-BOUND PROTEASES – THE ADAM FAMILY

The ADAM family contains 21 members of which 13 display catalytic activity (Edwards et al., 2008). Some of them are expressed in somatic tissues while most others have a more restricted tissue range (Cho, 2012). As this family is so large, it is not surprising, that they are involved in almost every biological process from sperm-egg interaction, cell fate determination, cell migration, muscle development to the activation of several immunological pathways. Their engagement in diseases such as autoimmune diseases, infection, inflammation, cardiovascular diseases, cancer and neurodegeneration is crucial. Protective roles in the pathogenesis of Alzheimer's disease, but also amplification of malignant tumour growth have been reported (Duffy et al., 2009). Thus, their broad expression and participation in many signalling pathways make it almost impossible to develop suitable inhibitors or modulators for experimental or clinical use.

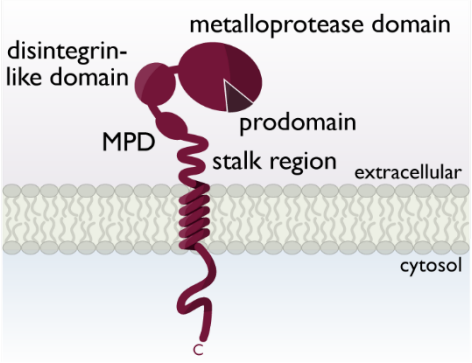

Figure 1.1 Structural elements of ADAM17. ADAM is a type I transmembrane (TM) protein with a C-shaped ECD. The ECD contains the active site of the protease domain and furthermore a disintegrin-like domain, a membrane-proximal domain (MPD) and a stalk region.

ADAMs are type 1 transmembrane (TM) proteins with a signal sequence at their N-terminus, which directs them to the secretory pathway (Zunke and Rose-John, 2017). The pro-domain acts as an intramolecular chaperone to ensure correct protein folding via cysteine-rich sequences and is cleaved off during the transit through the Golgi network. The C-shaped ECD of a functional ADAM consists of three domains: the metalloproteinase domain, the disintegrin-like domain and the cysteine-rich domain. A membrane-proximal domain (MPD) is characteristic only for ADAM10 and ADAM17 (Figure 1.1). The cytoplasmic domain of ADAM17 interacts with proteins involved in intracellular signalling and trafficking, such as iRhom and FRMD8 (Figure 1.2). iRhoms are inactive rhomboid proteases (see below Section 1.1.2.2) that bind to the cytoplasmic tail of immature ADAM17 to guide it to the cell surface, where they are sorted to lipid-rafts. The FERM domain-containing protein (FRMD8) stabilises the complex at the cell surface. Both iRhom and FRMD8 not only prevent the lysosomal degradation of this complex but also contribute to the activation and substrate-specificity by phosphorylation of iRhom (Kunzel et al., 2018).

Regulation of the protease activity differs between members of the ADAM family. Some are constitutively active such as ADAM10, whereas some need additional activation. Physiological activity of ADAM17 is regulated via phosphorylation. Phorbol esters such as PMA activate phosphokinase C (PKC) that phosphorylates ADAM17 (Figure 1.2). Inhibition of ADAMs is endogenously facilitated by tissue-specific inhibitors of metalloproteinases (TIMPs) that bind non-covalently to the cytoplasmic tail. In mammals, four different TIMPs

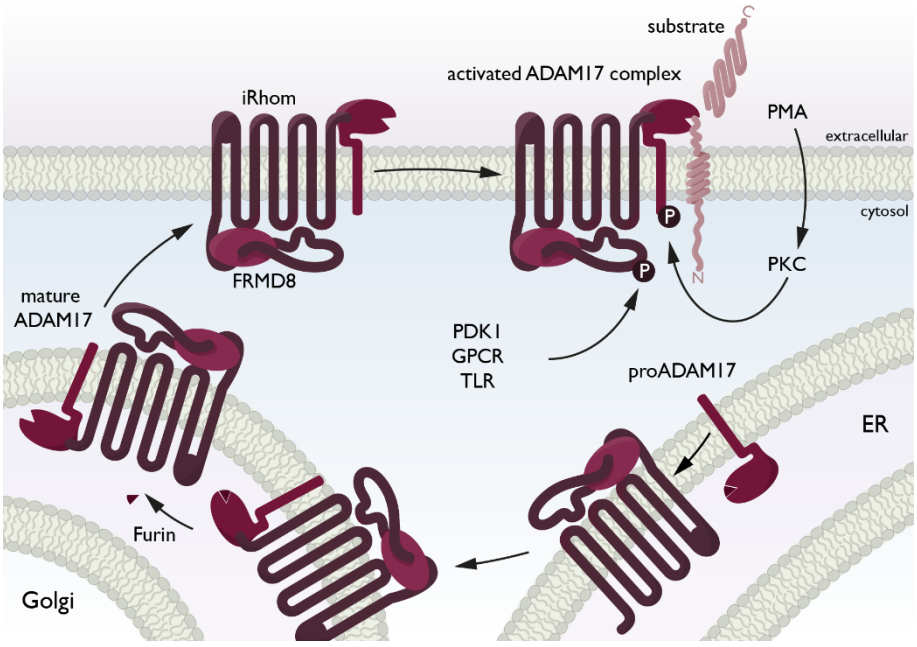

Figure 1.2 Maturation and transport of ADAM17. In the ER iRhom, FRMD8 and proADAM17 form a complex. iRhom ensures stability and correct trafficking of the complex from the Golgi network to the cell surface. Within the Golgi, the Furin-mediated cleavage of a signal peptide allows the maturation of ADAM17. On the cell surface, iRhom and ADAM17 are activated via phosphorylation by phorbol-12-myristat-13-acetat (PMA), Toll-like receptors (TLR), G-protein-coupled receptors (GPCR) or the PDK1 kinase. The activated complex is able to cleave surface proteins.

inhibit ADAM functions, whereas the preferences of binding and inhibitor capacity vary between family members and tissues (Nagase et al., 2006).

ADAMs are an essential upstream regulator for many important signalling pathways in vertebrates. By cleaving their substrates, they partake in the activation of growth factors, chemokines, and other important soluble mediators that influence signalling by binding to the corresponding receptor on a recipient cell. To date, more than 90 different substrates have been described for ADAM17 (Dusterhoft et al., 2019), which makes it the most prominent member of the family. Even though many ADAMs seem to have a specific set of substrates, they can act promiscuously, which means if one ADAM is inhibited another member of the family can resume the cleavage. In humans, ADAM17 (also TNFα converting enzyme, TACE) is essential for releasing soluble TNFα (sTNFα) from the membrane-resident TNFα (TNFα FL). sTNFα controls immune and inflammatory responses via activation of its corresponding receptor (Tseng et al., 2018) (see below Section 1.3.1). Further prominent substrates of ADAM17 but also ADAM10 include ligands of the epidermal growth factor receptor (EGFR) as well as the Notch receptor and APP (Pruessmeyer and Ludwig, 2009). Shedding of these substrates releases a signalling competent peptide into the extracellular space/ lumen and primes many proteins for their subsequent processing by intramembrane-cleaving proteases (IMPs).

1.1.2. INTRAMEMBRANE-CLEAVAING PROTEASES

Soluble and membrane-associated proteases such as ADAMs cleave their substrates in the aqueous solution in- or outside of the cell making water easily assessable for the proteolysis. However, the cleavage becomes much more challenging in the context of a hydrophobic membrane. Nevertheless, such as conventional proteases, IMPs are grouped by their catalytic residues. At present four families that promote intramembrane proteolysis are known: metallo-, serine, glytamyl- and aspartyl-IMPs (Beard et al., 2019, Kuhnle et al., 2019). A cysteine IMP has not been described so far.

The different groups of IMPs are located throughout the cell (Figure 1.3). Many are found in the secretory pathway as a place of vigorous protein modification. But also on

the cell surface and the lysosomal/ endosomal compartment, IMPs partake important roles in signalling and protein degradation.

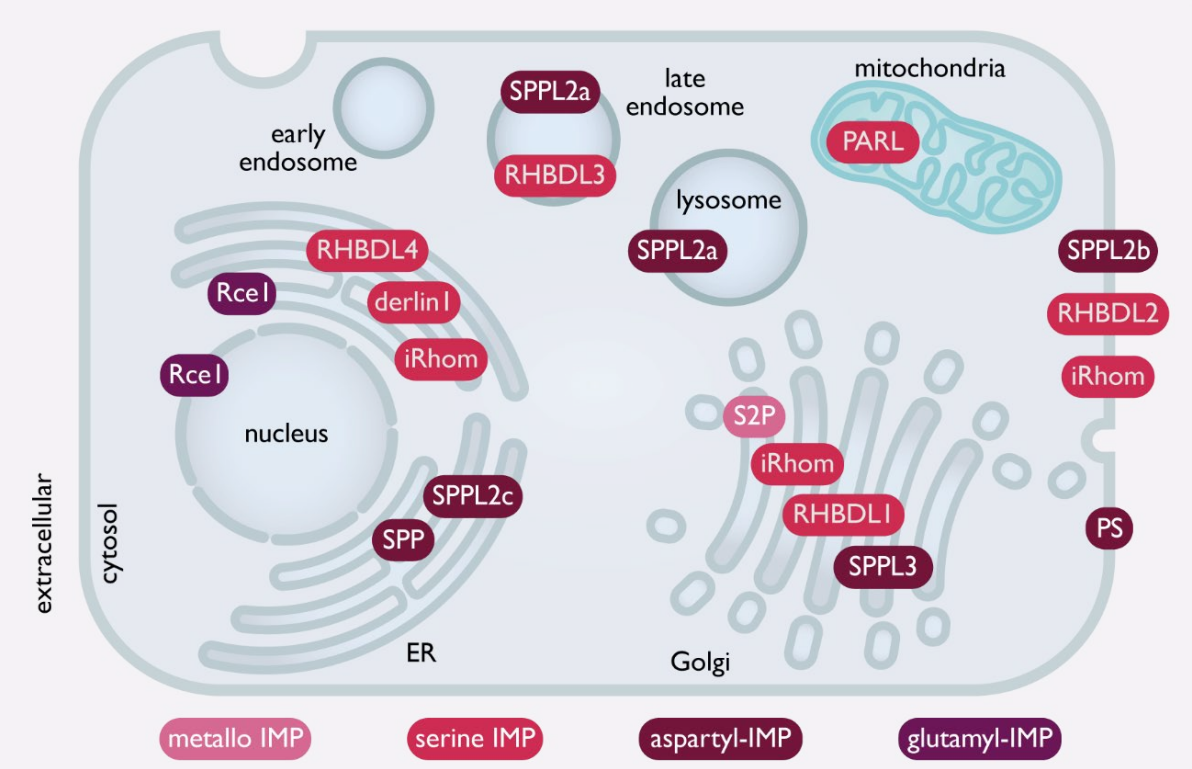

Figure 1.3 Localisation of intramembrane proteases (IMPs) in the cell. Several IMPs are expressed in the ER and Golgi network, as these are central compartments in protein maturation and modification. In compartments such as mitochondria, lysosomes and endosomes more specific IMPs are expressed. It is up to speculate whether SPPL2a and RHBDL3 have a broader substrate spectrum, as their function might be general degradation in the lysosomal compartments. Whereas most of the IMPs are stationary, iRhom appears throughout the entire secretory pathway. It does not display catalytic activity but rather guides other proteins (such as ADAM17) to the correct subcellular location.

1.1.2.1. METALLOINTRAMEMBRANE PROTEASES

The first IMP to be identified was site-2 protease (S2P). It induces a negative feedback loop in the sterol regulatory element-binding protein (SREBP) pathway (Chen and Zhang, 2010). Changes in the cellular demand for cholesterol are signalled via alterations of the lipid composition in the endoplasmic reticulum (ER) membrane. In response to that, SREBPs are shuttled to the Golgi apparatus. Here, the serine protease site-1 protease (S1P) cleaves SREBP within the luminal loop spanning the two TM helices. This cleavage also considered a shedding event, leaves behind two single membrane-spanning fragments of which the N-terminal one is cleaved by S2P at a Leu-Cys bond within the membrane (Duncan et al., 1998). The fragment that is released to the cytosol travels to the nucleus where it activates genes involved in the *de novo* synthesis and uptake of lipids

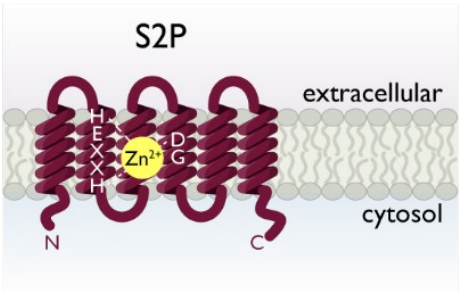

Figure 1.4 Model of the metallointramembrane protease, S2P. S2P displays six TMDs, so both N- and C-terminus are facing the cytosol. The active centre is formed by a HExxH motif in TMD 2 together with a DG motif in TMD 4. The histidine and aspartic acid hold a zinc ion in place.

(Rawson, 2013). In the absence of exogenous lipid, cells lacking S2P cannot survive. Besides SREBPs, S2P also cleaves several stress response transcription factors (Sun et al., 2016).

The crystal structure of an archaeal S2P indicates six TM segments (Figure 1.4). Just as soluble metalloproteases, S2P requires a zinc ion for its proteolytic activity, which is coordinated by a HExxH motif in transmembrane domain (TMD) 2. A GxxxN/G/S motif in TMD 4 is speculated to be involved in substrate binding (Feng et al., 2007).

1.1.2.2. SERINE INTRAMEMBRANE PROTEASES

The serine IMPs are represented by the rhomboid proteases, which were originally identified in *Drosophila*. This group of proteases is highly conserved throughout species and plays an important role in epidermal growth factor receptor (EGFR) signalling. The release of growth factor ligands into the extracellular space is crucial to initiate EGFR signalling (Kandel and Neal, 2020).

The five mammalian rhomboids (RHBDL1-4, PARL) are expressed in different locations throughout the cell indicating a specific function and set of substrates within each localisation (Figure 1.3). PARL is the only IMP that localises to the mitochondrial membrane where it cleaves important substrates related to the mitochondrial homeostasis. Decreased abundancy of PARL is associated with reduced mitochondrial mass and activity and hence, PARL polymorphisms identified in humans are linked to mitochondrial dysfunctions in diabetes type 2 (Hatunic et al., 2009). Furthermore, dysregulation of mitophagy by altered cleavage of the substrate PINK1 by PARL has been implicated in Parkinson's disease (Shi et al., 2011). However, the exact role of PARL in mitochondrial and cellular death has yet to be unravelled.

Rhomboid proteases recognise their substrates based on a combination of structural features and recognition motifs (Lysyk et al., 2020). They require a certain degree of flexibility within the TM helix to cleave their substrates. Unique to this group of

IMPs is that they do not require any preceding processing step such as substrate shedding. Nevertheless, the exact cleavage mechanism is currently under debate. One of the two models suggests structural rearrangements within the protease to facilitate binding and cleavage at the same position within the enzyme. The other model suggests less structural changes and an initial binding step at an exosite with subsequent transport to the active site for cleavage (Lysyk et al., 2020). However, as some of the rhomboid proteases remain orphan, the identification of new substrates is required to give better insights into the cleavage mechanism.

The family of rhomboid proteases comprises additional members that do not display catalytic activities. These rhomboid pseudoproteases include amongst others derlin1 and inactive rhomboids iRhom1 and iRhom2 (Figure 1.5). Even though they share the catalytic dyad GxSG with the catalytically active members of the family, they have acquired a proline in the x-position, which is believed to abolish enzymatic activity (Zettl et al., 2011). Interestingly, while catalytically active IMPs can be inactivated by mutation of the amino acids in their active centre, it is not known whether a pseudoprotease can be turned into an active protease by removal of the proline. Nevertheless, even without catalytic activity, they fulfil crucial tasks within the cell, as they are able to bind proteins in the secretory pathway and control their fate by regulating the trafficking or inducing degradation. As essential co-factors, they were found to be regulators of EGFR and TNFα signalling (Lemberg and Adrain, 2016).

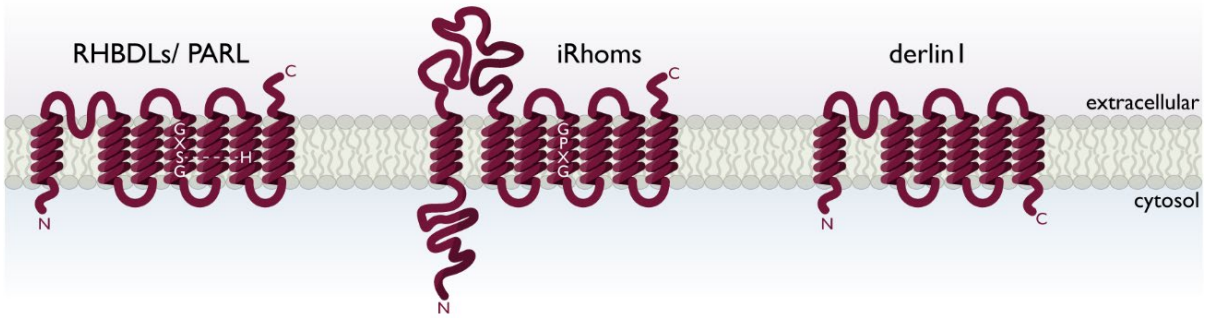

Figure 1.5 Structural overview of serine intramembrane proteases (IMPs). The rhomboids display a topology with six to seven TMDs. Structural elements have been reported that dip into the membrane without really spanning it completely. Not all rhomboids are catalytically active. iRhoms and derlin1 do not display cleavage activity. Nevertheless, they have important functions as adaptor molecules to enable correct trafficking or cleavage by other proteases.

Rhomboid proteases display relatively low sequence similarity and differ within structural elements such as the number of TM segments. However, crystal structures of

the bacterial rhomboid protease GlpG revealed a conserved catalytic His-Ser dyad between the TMD 4 and TMD 6 required for substrate cleavage (Figure 1.5). Initially, rhomboids were thought to cleave exclusively type I TM proteins; however, several exceptions from that rule have been described recently (Bergbold and Lemberg, 2013). This strengthens the hypothesis that rhomboids are in fact recognising sequence specificities paired with certain conformational requirements.

1.1.2.3. GLUTAMYL-INTRAMEMBRANE PROTEASES

In 2013, the crystal structure of Ras converting enzyme (Rce1) revealed that the enzyme previously classified as metallo-IMP comprises a glutamate embedded in a Glu-His-His-Asn motif in its catalytic centre. Therefore, it was re-classified as glutamyl-IMP thus establishing a new group of IMPs (Manolaridis et al., 2013). Rce1 is expressed in the ER and inner nuclear membrane of cells in multiple tissues (Kuhnle et al., 2019) and the structure of an archaeal homologue revealed eight TM segments, even though other topologies have been suggested (Figure 1.6) (Hampton et al., 2018). Although Rce1 shares structural features with the other IMPs, it differs fundamentally in its mechanism. Unlike the other IMPs, Rce1 does not cleave the substrate within its TMD but rather cleaves the Caax motif (C: cysteine; a: aliphatic amino acid; x: random amino acid) at the C-terminal end of the substrate (Manolaridis et al., 2013). GTPases, nuclear laminins, protein kinases and phosphatases comprise a Caax motif and are involved in diverse biological functions such as development, ageing, and parasitic growth. Their implication in cancer has pushed the understanding of the modifications by Rce1 into the focus of current research (Hampton et al., 2018).

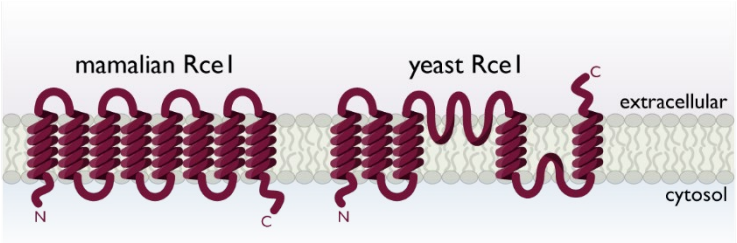

Figure 1.6 Structural overview of mammalian and yeast glutamylintramembrane protease Rce1. An eight TMD containing topology is proposed for this group of IMPs in mammals. However, in yeast and bacteria the topology is not yet clear. Several TMDs and membrane dipping elements are suggested.

1.1.2.4. ASPARTYL-INTRAMEMBRANE PROTEASES

The fourth group of IMPs, the aspartyl-IMPs, contains signal peptide peptidase (SPP) and four related SPP-like proteases (SPPLs), as well as two presenilins. Remarkably, despite low sequence homology between presenilins and SPP(L)s, they all share a signature YD and GxGD catalytic motif and a C-terminal PAL motif, which are unique to this protease family. Mutations of either of the aspartates result in catalytically inactive forms of the proteases (Krawitz et al., 2005). Even though the aspartyl-IMPs share the conserved signature motifs and some topological features, detailed analysis revealed differences in substrate selection, processing and turnover rate.

1.1.2.4.1. PRESENILINS AND γ-SECRETASE

Presenilins manifested their importance in the 1990s when mutations in their genes were linked to early-onset, familiar forms of Alzheimer's disease (Holcomb et al., 1998). They act as the proteolytic subunit of a multiprotein complex, the γ-secretase, and undergo endoproteolysis for activation. The γ–secretase complex embraces a catalytic centre with one of the homologous presenilins (PS1 or PS2) and co-factors nicastrin, presenilin enhancer (PEN) 1 or 2, and anterior pharynx defective 1 (APH1) (Figure 1.7). All parts of the complex are required to generate a functional γ-secretase complex (Kaether et al., 2006).

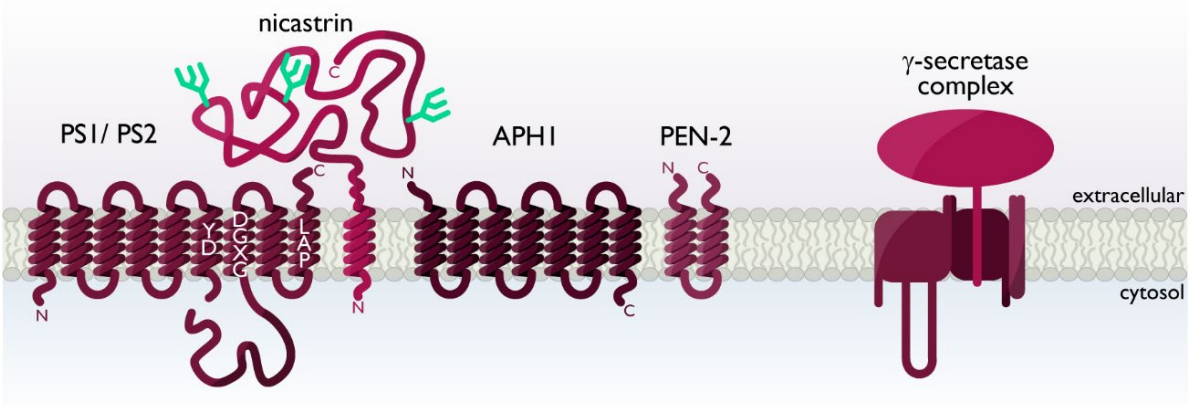

Figure 1.7 γ-secretase is a complex consisting of four proteins. The catalytically active subunit of this complex comprises presenilins (PS). They are aspartyl-IMPs containing the characteristic GxGD and YD motif. The N-terminus is facing the cytosol and the large loop between TM 6 and 7 is auto-catalytically cleaved. Besides PS, nicastrin, presenilin enhancer (PEN) 1 and 2, and pharynx defective 1 (APH1) are part of this complex. Nicastrin has a large ECD with several glycosylation sites. It is debated whether it functions as gatekeeper or is responsible for substrate selection and binding. The function of all the co-factors is not yet fully resolved.

PS1 and PS2 harbour the active site aspartyl-residues and the PAL motif, which contributes to the active site conformation of the γ-secretase complex (Wang et al., 2006). Both presenilins are able to mediate substrate cleavage, suggesting a functional redundancy (Wolfe and Haass, 2001). Nicastrin is discussed as a substrate receptor or gatekeeper and PEN1/2 as stabilizing factor keeping the auto-proteolytically generated presenilin fragments in close contact. No function besides stabilisation of the complex has so far been assigned to APH1 (Pardossi-Piquard et al., 2009).

The cleavage process of one of the most prominent γ-secretase substrates, APP, differs throughout the human body. In the periphery, it undergoes non-amyloidogenic processing by an α-secretase (ADAM10/17), which results in a membrane-bound C-terminal fragment (CTF) that is 83 amino acids (C83) in length (Figure 1.8). C83 is subsequently recognised and cleaved by γ-secretase, generating an APP intracellular domain (AICD) and extracellularly released peptides (p3). The p3 peptides do not form aggregates; therefore, they are considered non-neurotoxic (Kojro and Fahrenholz, 2005).

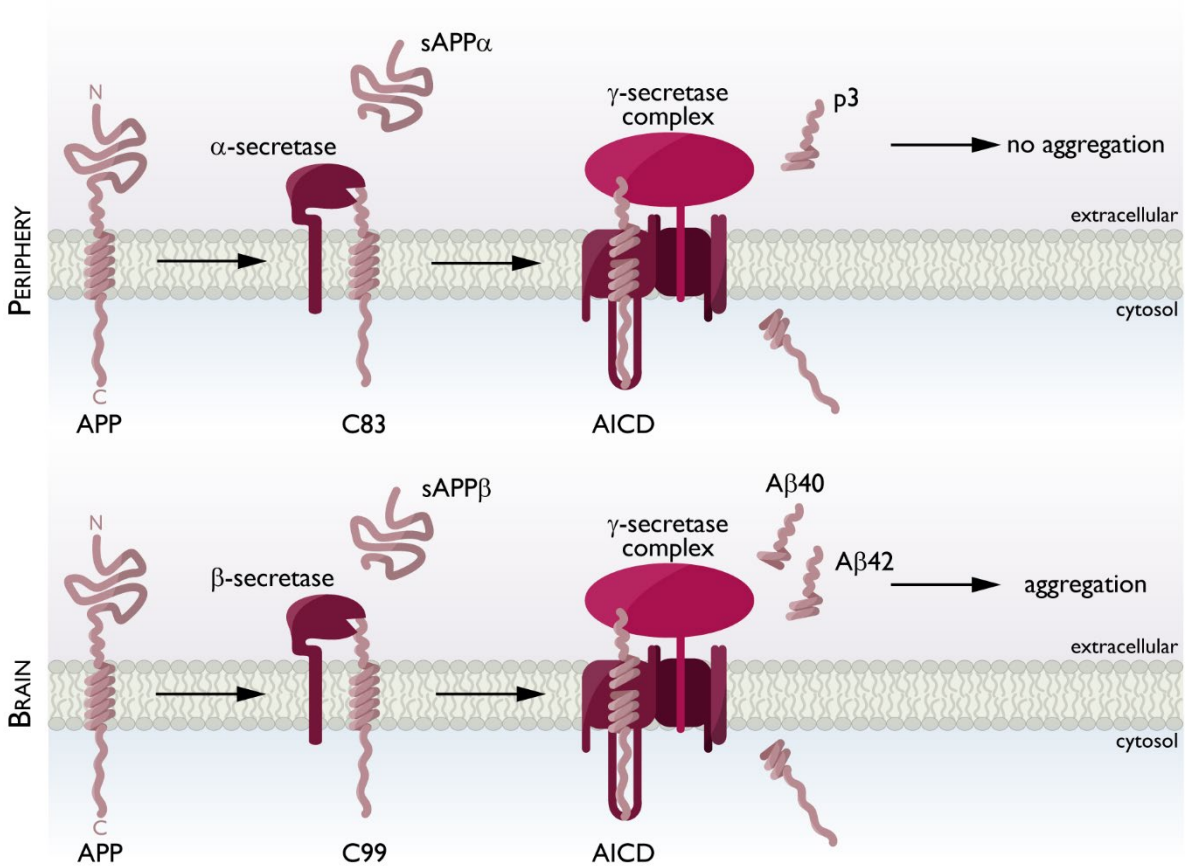

Figure 1.8 Processing of the amyloid precursor protein (APP). APP can be processed by two different sheddases, BACE1 or α-secretase, generating two different membrane-bound fragments, C99 or C83. Both of them are recognised and processed by γ-secretase. However, the cleavage of C99 generates Aβ fragments that are released and prone to aggregation. These aggregates are neurotoxic and suspected to be a major cause of Alzheimer's disease. The cleavage of C83 by γ-secretase generates a fragment, p3 that is not prone to aggregation.

However, on the cell surface of neurons in the brain, APP is mostly cleaved by the membrane-bound aspartyl-protease BACE1, generating a peptide of 99 amino acids (C99). The membrane-resident C99 is consecutively cleaved by γ-secretase, which releases an AICD that can potentially translocate to the nucleus to induce gene expression (Matsuda and Senda, 2019). The fragments that are released into the extracellular space, the so-called Aβ peptides vary in length and are prone to aggregation (Orlando et al., 2020). Currently, more than 350 mutations in PS1/2 are identified as the cause of aberrant Aβ production (http://www.alzforum.org/mutations). The mutations affect precision and cleavage efficiency of γ-secretase. Along with current knowledge, the Aβ aggregates are the major cause of Alzheimer's disease; however, it is debated whether the phosphorylation of tau protein, AICD signalling and abnormal axonal transport add up onto the disease progression or if they contribute to the onset of the disease in a similar manner as Aβ (Hardy, 2003).

1.1.2.4.2. SPP(L) FAMILY

SPP/SPPLs are highly conserved members of the aspartyl-IMP family and have been described in eukaryotes, fungi and protozoa (Voss et al., 2013). A data bank search identified five members of the SPP/SPPL family in humans, SPP, SPPL2a,b,c and SPPL3 (Fluhrer et al., 2009). The SPP members are differentially distributed within the secretory pathway (Figure 1.3), a fact that may reflect their preference for substrates located within the respective compartments. Until now, many degradative functions have been described for SPPLs. However, latest research shows the participation of the proteases in signalling pathways in- and outside of the cell (Mentrup et al., 2020, Papadopoulou et al., 2019, Voss et al., 2013).

In contrast to presenilins, catalytic SPP/SPPL activity does not require endoproteolytic activation or additional components. Nevertheless, they share the topology of nine TM segments, with the most striking difference in the opposite orientation of the catalytic domains within the plane of the membrane (Figure 1.9). While the N-termini of presenilins face the cytosol, SPP/SPPL N-termini face the extracellular space. Because presenilins are known to catalyse intramembrane cleavage of several type I TM proteins,

it is speculated that the opposite orientation of SPP/SPPLs is the reason for cleaving exclusively type II oriented TM proteins (Friedmann et al., 2004).

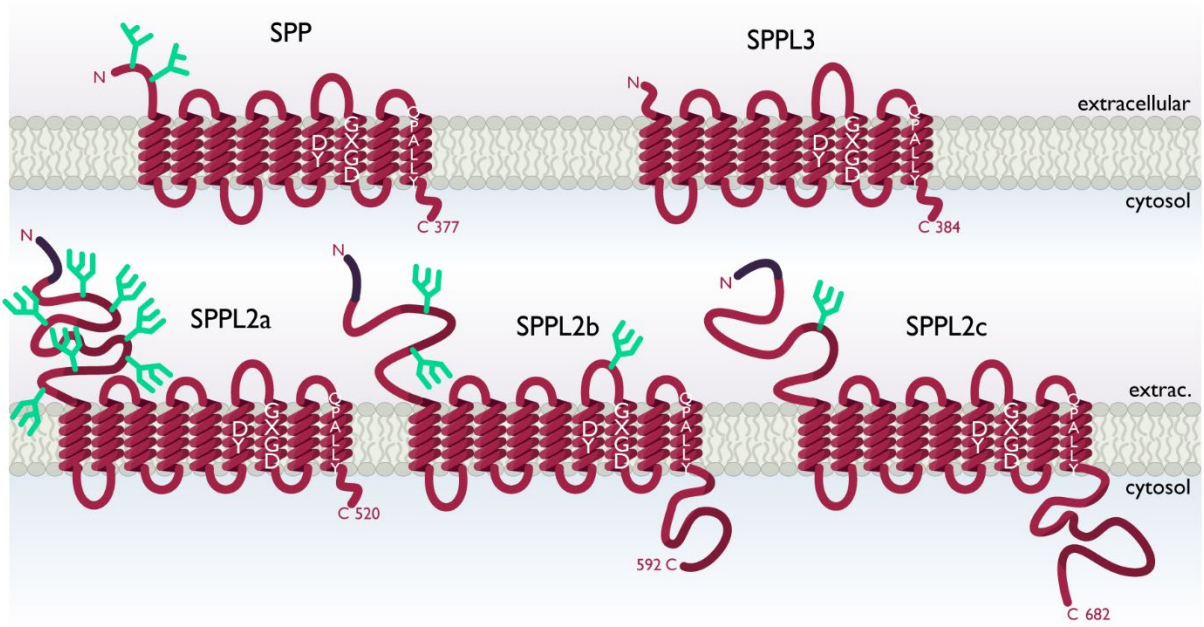

Figure 1.9 Topology of all mammalian members of the SPP/ SPPL family. All members share the nine TMD topology and the characteristic motifs, GxGD, YD and QPALLY. The family members differ especially in the length of the N- and C-termini and glycosylation status. In contrast to presenilins, the N-termini are facing the extracellular space. SPPL2a, b and c contain a signal sequence at the N-terminus.

Although SPP/SPPL proteases lack obvious sequence homologies, they all share the characteristic active site G(L/I/F)GD motif within TMD 7 and the (Y/F)D motif located in TMD 6 (Figure 1.9) (Martin et al., 2009). Besides the active site motifs, SPP/SPPL family members share a conserved QPALLY motif in TMD 9, which is likely to interact with the catalytic centre of GxGD-type proteases (Fluhrer et al., 2008). A direct contribution of this motif to the formation of the catalytic centre is supported by the finding that a transition state analogue inhibitor fails to bind to SPP and PS upon mutagenesis of the PAL sequence (Wang et al., 2006). It is currently unknown how the QPALLY motif affects SPPL activity; however, close proximity of all three conserved domains in the native enzyme forming the catalytic centre is assumed for aspartyl-IMPs (Torres-Arancivia et al., 2010). The lack of specific antibodies, inhibitors or *in vitro* assays for SPP/SPPL proteases makes these proteases difficult to study. A commonly used active site inhibitor for SPPL2 is $(Z\text{-}LL)_2$-ketone (2,2'-(2-Oxo-1,3-propanediyl)bis[N-[(phenylmethoxy) carbonyl]-L-leucyl-L-leucine-amide). It is specific towards SPPL2a/b and SPP whereas SPPL3 activity is not inhibited

(Weihofen et al., 2002, Voss et al., 2014). To complicate the research on SPPLs further, it seems that some of the family members have such fundamental functions that growth and development of cells or mice are strongly affected upon depletion of the protease (Papadopoulou, unpublished data).

1.1.2.4.2.1. SPP

SPP was the first member of the family to be discovered (Lemberg and Martoglio, 2004). Even though SPP does not need any co-factors for proteolytic function, it has been shown that it mostly functions as a homodimer (Voss et al., 2013) and recruits other proteins such as derlin1 (see above Section 1.1.2.2) or the EC3 ubiquitin ligase TCR8 (Chen et al., 2014b). These proteins allow recognition and cleavage of additional proteins that otherwise are not part of the SPP substrate collection (Chen et al., 2014b).

A specific signalling sequence, the signal peptide, is guiding proteins destined for the ER to their correct location where this sequence is cleaved off upon arrival. Thereafter, the remaining signal peptides that comprise a type II orientation can undergo intramembrane proteolysis by SPP, which is maintained in the ER by a retention motif (KKxx) at its C-terminus. Requirements for intramembrane cleavage by SPP are helix-destabilising residues within the substrate's TMD. Positively charged residues in juxtamembrane domain (JMD) have an inhibitory effect on the cleavage efficiency (Lemberg and Martoglio, 2002). The cleavage of signal peptides by SPP results in their liberation from the ER membrane (Mentrup et al., 2017). SPP processes a broad variety of these signal peptides such as prolactin, major histocompatibility complex (MHC) class I molecules human lymphocyte antigen (HLA)-E and calreticulin (Lemberg and Martoglio, 2002). Release of the epitope-containing signal peptides from the ER membrane toward the cytosol plays a central role in the activation of a cellular immune response. This cleavage is essential for the generation of HLA-E epitopes that upon surface presentation protect cells against natural killer (NK) cell-mediated elimination (Bland et al., 2003). In addition to eukaryotic substrates, SPP plays a central role in the processing of viral peptides such as human immunodeficiency virus (HIV) gp130 and hepatitis virus C core protein (Mentrup et al., 2017). As SPP has such a central role in cell homeostasis, an implication in breast, lung and colon cancers is suggested. SPP is strongly upregulated in certain tumours and the

expression correlates with progression and malignancy of tumours (Hsu et al., 2019). However, it has not been investigated whether this is cause or causality of the cancer.

1.1.2.4.2.2. SPPL2A/B

The members of SPPL2 subfamily all share a large, glycosylated N-terminus (Figure 1.9). Regarding their sequence, SPPL2a and SPPL2b are 50% identical and 70% homologous (Golde et al., 2009). Even though closely related, SPPL2a and SPPL2b show substantial differences considering their localisation. SPPL2a is expressed in all tissues with the lowest abundancy in brain while SPPL2b is more restricted in its expression and mostly found in the brain and with lower abundancy in the lymphatic system (Mentrup et al., 2020). On a subcellular level, SPPL2b is located at the cell surface, while SPPL2a resides in lysosomes/ late endosomes due to a C-terminal tyrosine-based sorting signal (Behnke et al., 2011). Even though differences in subcellular localisation restrict the number of potential substrates within the organism, it has been shown that the set of substrates overlaps partially *in vitro* (Martin et al., 2009). TNFα, British dementia protein 2 (Bri2), CD74, Clec7a, Clec8a, type III neuregulin 1 and foamy virus envelope protein (FVenv) are cleaved by both proteases. FasL and TMEM106b are exclusively cleaved by SPPL2a and the transferrin receptor 1 (TFR1) only by SPPL2b (Voss et al., 2013, Brady et al., 2014, Fleck et al., 2016, Mentrup et al., 2019). For most of the substrates, the fate and function of the cleavage products is a central unresolved question. First evidence suggests that the cleavage mechanism differs depending on the substrate. Whether this is a characteristic controlled by the protease or the substrate is not known.

The physiological relevance of SPPL2a becomes apparent in patients with a single nucleotide polymorphism (SNP) in the SPPL2a gene. In psoriasis patients, an SPPL2a SNP increases epidermal SPPL2a expression (Liu et al., 2008). It is speculated that this increase leads to an enhanced local release of TNFα ICD that induces IL-12 expression (Arican et al., 2005, Friedmann et al., 2006). Besides other interleukins, levels of TNFα and IL-12 correlate with disease severity.

Contrary to an increased expression, SPPL2a-deficiency in humans has been linked to augmented susceptibility to mycobacterial infections (Kong et al., 2018). This mechanism is mostly conveyed via misregulated CD74 cleavage as CD74 NTF accumulates in B cells and dendritic cells (DCs) upon loss of SPPL2a (Schneppenheim et al., 2014).

Interestingly, the accumulation mostly induces depletion of DCs, which results in a subsequent reduction of chemokine release. The lack of chemokines leads to an impaired activation of immune cells that are needed to orchestrate the depletion of mycobacteria. Therefore, patients suffer from infections of low-virulent mycobacteria. The loss of SPPL2a function also decreased TNFα expression in CD4 T cells; however, overall levels of sTNFα were normal.

Furthermore, SPPL2a has been described as a potential risk factor in Alzheimer's disease (Bis et al., 2018, Novikova et al., 2019). The correlations and causal effects of SPPL2a expression in Alzheimer's disease have not yet been identified. A possible connection of SPPL2a as a potential risk factor for Alzheimer's disease and immune deficiencies lies within its location on chromosome 15q21.2. Patients with a disruption of this gene locus display amongst the accumulation of CD74 (Schneppenheim et al., 2014) idiopathic neurological condition with severe disabilities (Moreno-De-Luca et al., 2011).

A physiological function of SPPL2b has yet to be identified.

1.1.2.4.2.3. SPPL2C

Just until as recent as 2019, SPPL2c was marked a pseudoprotease. However, proteomic screens identified several soluble N-ethylmaleimide-sensitive factor attachment (SNARE) proteins as substrates for SPPL2c. The vesicle fusion proteins syntaxin 5, 8 and 18 are cleaved by SPPL2c, therefore cellular transport is impaired in the presence of active SPPL2c (Papadopoulou et al., 2019). The monoglycosylated SPPL2c resides in the ER of elongated spermatids and exists in a long and C-terminally truncated version. When isolated it exceeds its calculated size suggesting that it is also part of a larger complex (Mentrup et al., 2020). So far, the composition of this complex remains unknown.

Increased expression of SPPL2c in cells leads to the accumulation of proteins in the ER and disassembly of the Golgi apparatus (Papadopoulou et al., 2019). Due to this strong impact on cellular homeostasis, the expression of SPPL2c is limited to differentiating male germ cells that are destined to undergo major intracellular rearrangements during spermatogenesis. In the absence of SPPL2c, mature spermatozoa differ in morphology and motility. However, this controls fertility only to a minor extent and only when combined with SPPL2c-deficient females, litters drastically decrease (Niemeyer et al.,

2019, Papadopoulou et al., 2019). This surprising effect hints towards an additional effect of SPPL2c in female mice, even though no expression was found in the reproductive system so far.

Despite SPPL2c and SPP sharing the same intracellular localisation, they only overlap partially in substrate selection, indicating unique biological functions for each protease. The recognition of substrates appears to be highly protease-specific even though SPP, SPPL2a, b and c seem to prefer substrates with short ECDs.

1.1.2.4.2.4. SPPL3

SPPL3 is the smallest member of the SPPL family, as its N-terminus is short and not glycosylated. Presence of murine SPPL3 has been demonstrated in NK and T cells in brain, lung, spleen and embryonic fibroblasts (Voss et al., 2013). A constitutive deficiency in cultured cell lines and mice strongly increases lethality, impeding the research on this protease but demonstrating its importance within the organism. Nevertheless, the important role of SPPL3 expression in NK cells is emphasised by the observation that SPPL3-deficient mice lack mature, therefore functioning NK cells (Hamblet et al., 2016). Whether this maturation defect is directly correlating with cleavage of a specific SPPL3 substrate or whether it is a secondary effect is not yet clear.

On a subcellular level, SPPL3 resides in the Golgi apparatus where numerous glycosyltransferases and glycosidases add glycans to proteins on their way through the secretory pathway. SPPL3 cleaves off the catalytic domain of such glycosyltransferases and glycosidases, therefore, decreasing the glycosylation of many proteins in the Golgi apparatus. Thus, increased SPPL3 expression leads to hypoglycosylation, while reduction results in hyperglycosylation, which makes SPPL3 expression an important switch that allows adaptation to environmental factors (Voss et al., 2014).

Unlike the other SPPL family members, SPPL3 displays no favour towards proteins with short ECDs. This property distinguishes the protease from the other aspartyl-IMPs and resembles the class of rhomboid proteases. In addition, SPPL3 selects substrates not purely based on structural elements but rather prefers methionine and tyrosine in the P1 cleavage position (Kuhn et al., 2015). However, it remains to be elucidated whether this is a true consensus sequence or based on the structural impact of these amino acids.

1.2. REGULATED INTRAMEMBRANE PROTEOLYSIS

The process of regulated intramembrane proteolysis (RIP) has been a subject of intensive research during the last decades. Generally, RIP can be divided into three steps (Figure 1.10). The first step is the cleavage of the ECD by an accompanying sheddase. This shedding is required to allow the second step of RIP, the recognition and binding of substrates by an IMP. During the third step, the substrate is cleaved within the TMD in the plane of the membrane. This intramembrane cleavage has been described for many substrates and is required either for the generation of an intracellular signalling peptide or the removal of membrane-retained fragments (Fluhrer et al., 2008). In the following section, all three steps of RIP are described in more detail focusing on the SPP/ SPPL family.

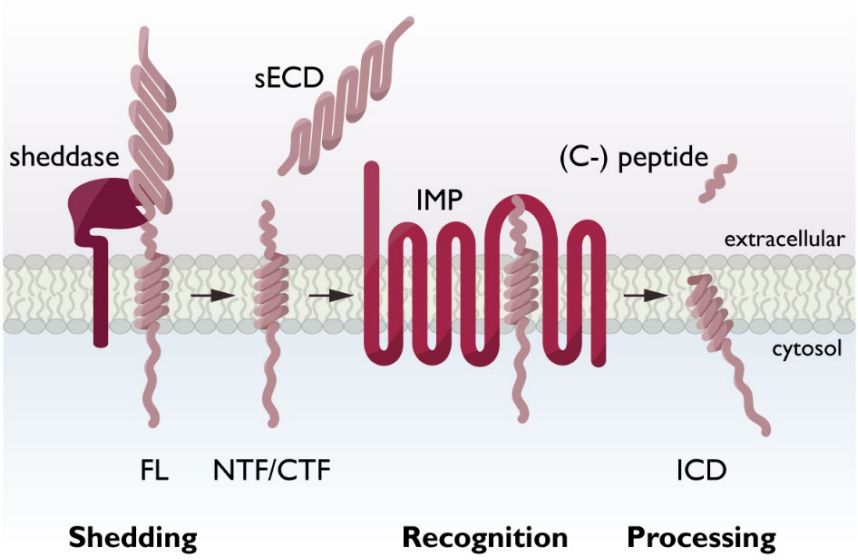

Figure 1.10 The three basic steps of regulated intramembrane proteolysis (RIP) of a type II TM protein. After an initial shedding of the full-length (FL) protein, which releases a soluble ectodomain (sECD), the membrane-bound N/C-terminal fragment (NTF/ CTF) is recognized by an IMP. The IMP cleaves the NTF/ CTF, which releases a small (C-) peptide to the extracellular space and an intracellular domain (ICD) to the cytosol.

1.2.1. RIP STEP 1 - SHEDDING

According to Lichtenthaler et al. shedding is defined as the removal of a large part of the ECD releasing it into the extracellular space or lumen of an organelle (Lichtenthaler et al., 2018). Shedding is an irreversible modification of the protein and can alter the structure and function of the substrate, thus, it controls the abundance and activation status of many membrane proteins. Cleavage occurs 10-35 amino acids distant from the membrane, in the JMD of the substrate (Figure 1.11). These usually membrane-bound

sheddases are referred to as canonical or full-time sheddases. Some of these sheddases act redundantly on many substrates such as BACE1, others have only a limited substrate selection (Lichtenthaler et al., 2018). Besides membrane-bound sheddases, more and more soluble proteases such as the MMPs have been reported to facilitate canonical shedding as well. This type of shedding does not only describe the release of an ECD but rather the cleavage of a loop spanning two TM helices (Figure 1.11).

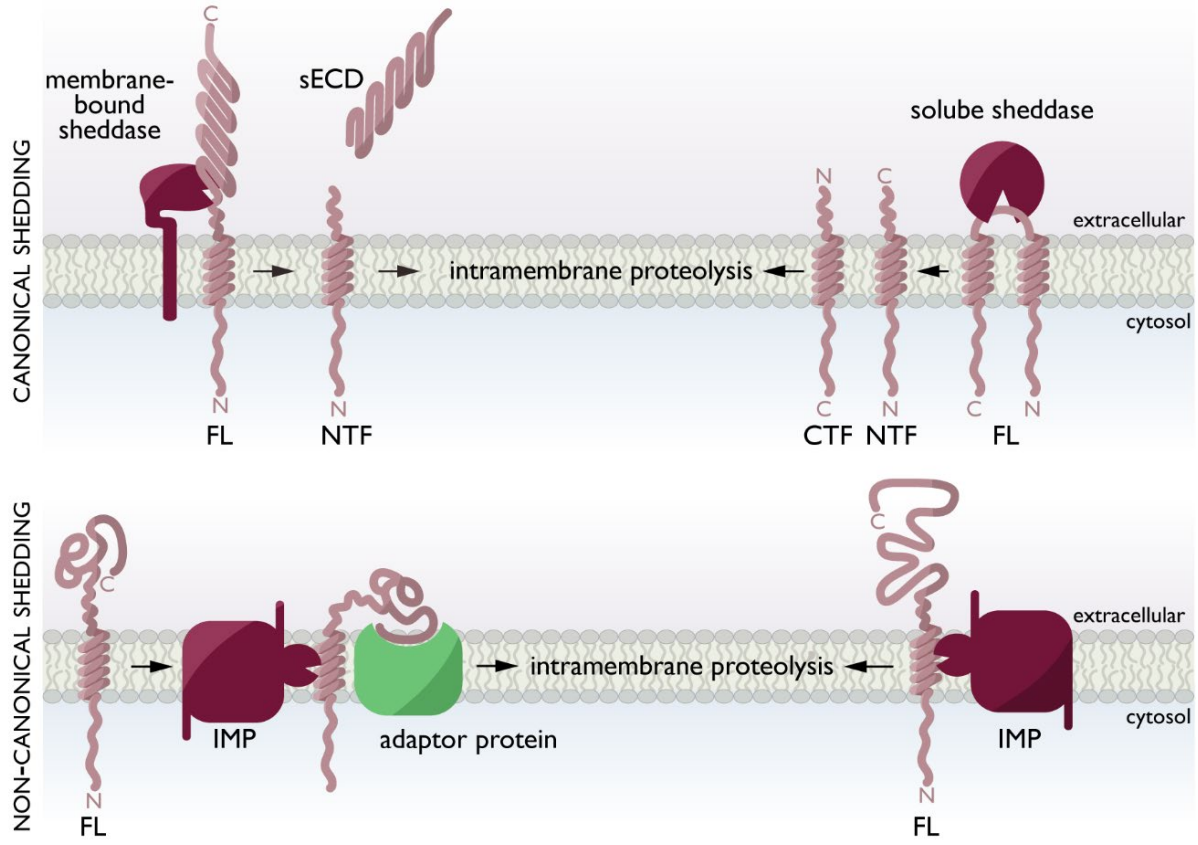

Figure 1.11 Different types of shedding. In the conventional way of shedding, a single span TM protein is cleaved close to the membrane, which releases the majority of the ECD. Furthermore, a protein, which spans the membrane twice, can be cleaved in the loop connecting both TMDs. This generates two single span TM proteins, which can both be subjected to further intramembrane proteolysis. This is termed conventional shedding. However, recently intramembrane proteases (IMPs) have been described to be able to cleave TM proteins either directly or with the help of adaptor proteins. This is termed non-canonical shedding.

Even though, RIP might imply that an initial shedding is required to allow subsequent substrate binding to and cleavage by IMPs, there are some exceptions to the rule. Rhomboid proteases and SPPL3 are able to cleave full-length (FL) proteins directly without any preceding shedding event (Figure 1.11). These intramembrane sheddases are referred to as non-canonical sheddases. The newest addition to this group is SPP. With the help of the catalytically inactive rhomboid derlin1, SPP is able to process Xbp1u FL directly. It is suggested that binding of the ECD to derlin1 alters the structure of the

substrate making the TMD accessible for SPP intramembrane cleavage (Figure 1.11) (Chen et al., 2014a).

Other modifications of the three-step process are represented by Bri2 that is generated in a pro-form. This pro-form is cleaved by Furin in the Golgi compartment, preventing premature cleavage before the substrate has reached its final destination (Kim et al., 1999). Pro-protein convertases like Furin are soluble serine proteases. They are not considered sheddases as they do not cleave in close proximity to the membrane neither do they remove the majority of the ECD. However, it is difficult to assign clear functional definitions as to whether a protease becomes a sheddase and always needs to be discussed individually (Lichtenthaler et al., 2018).

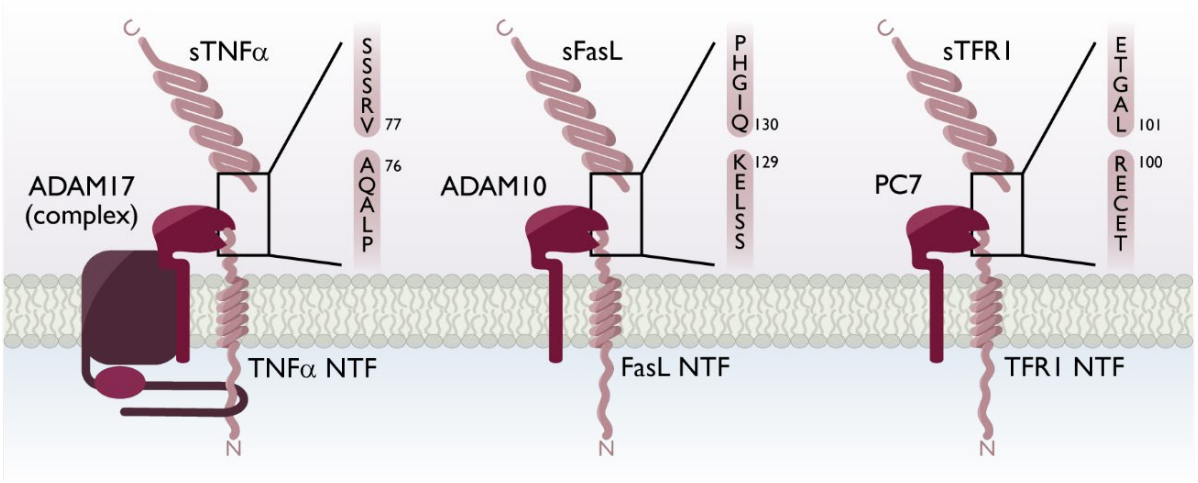

Figure 1.12 Known shedding sites in SPPL2 substrates. Even though soluble fragments are detectable for almost all substrates, the identification of the exact shedding site is more complicated. TNFα is shedded mainly by ADAM17 at A76/V77. FasL is shedded by ADAM10 at position K129/Q130 and transferrin 1 (TFR1) is shedded at R100/L101. In hepatocytes, TFR1 is shedded by PC7. Whether PC7 is the main sheddase also in other organs has not been investigated so far. Cleavage by a sheddase generates a soluble peptide and a membrane-retained stub, the N/C-terminal fragment (NTF/ CTF).

Many membrane-bound sheddases are assumed to work as monomers or dimers. This is not surprising as many substrates also form dimers or trimers on the cell surface. However, growing evidence suggests that some sheddases assemble into larger complexes. In case of ADAM17, iRhom and FRMD8 are required for trafficking and supposedly responsible for substrate interaction and selection (Section 1.1.1). ADAM10 can interact with γ-secretase during the cleavage of APP (Chen et al., 2015). Hence, it might be possible that many sheddases use adaptor proteins; however, not all of them are stable and just form quickly upon substrate binding or during trafficking. Even though many proteins are shedded and produce activated soluble components of a signalling

pathway, the exact cleavage sites have only been identified for very few, among them only three SPPL2 substrates (Figure 1.12).

1.2.2. RIP STEP 2 - SUBSTRATE RECOGNITION

Whereas several proteases (and also sheddases) display sequence-specific cleavage preferences, it seems more complicated for many IMPs. It appears as if the primary sequence within the TMD or adjacent domains is not the main criteria for substrate recognition and turnover (Martin et al., 2009). Since ECD shedding is a mandatory prerequisite for numerous IMP substrates, a short ECD was established as one of the substrate criteria. Within the γ-secretase complex, nicastrin is considered a gatekeeper aggravating the binding of proteins with large ECDs (De Strooper, 2005). Whether a certain domain of SPPL2 proteases conducts gatekeeper functions is the topic of ongoing research. However, it is unlikely that a short ECD is the only requirement for IMPs accepting proteins for cleavage as the non-substrate Bri3 is still not processed by SPPL2 proteases even if the ECD is removed (Martin et al., 2008).

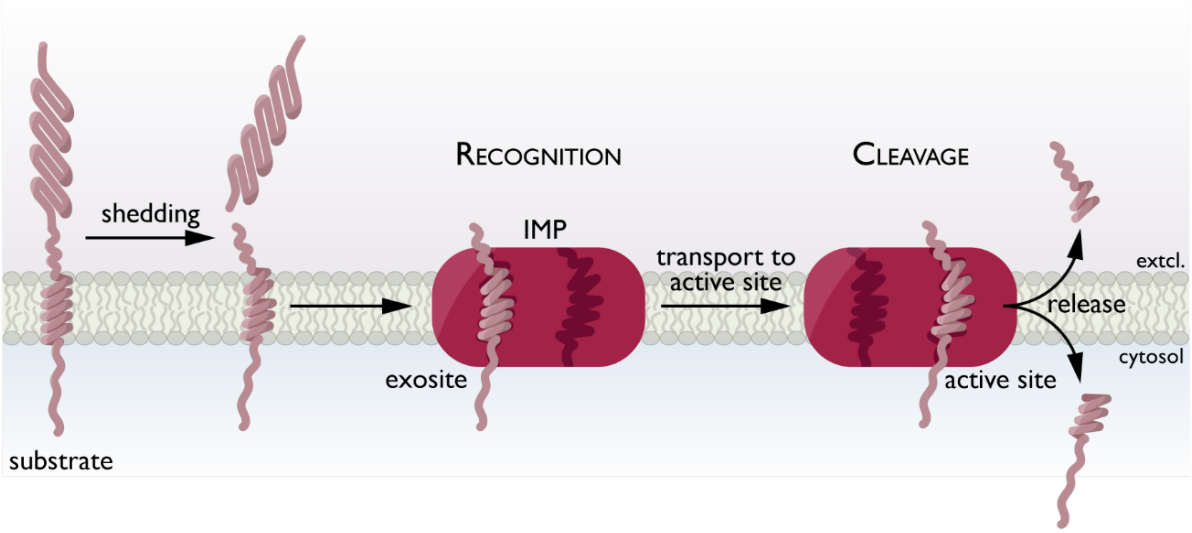

Figure 1.13 Exosite model. Substrate binding and substrate processing happen in different places within the intramembrane protease (IMP). As full-length proteins are not processed by many IMPs, it is speculated whether shedding induces structural rearrangements in the protein. Thus, the substrate can be recognised either within the IMP or by cofactors (nicastrin in γ-secretase) and is subsequently transported to the active site where the cleavage occurs. As this is highly speculative, it remains to be determined where these domains are within each IMP.

Growing interest is focusing on a new model of substrate recognition for IMPs where recognition depends on structural properties of protease and enzyme. This model proposes that substrate binding and cleavage happen in different locations within the enzyme. Hence, the cleavage site of the substrate might not necessarily be the same as the recognition site. Within the protease, so-called exosites facilitate binding/ selection of substrates before the substrates are relocated within the enzyme to the active site where they are cleaved (Figure 1.13) (Chávez-Gutiérrez and De Strooper, 2016, Hitzenberger and Zacharias, 2019).

1.2.3. RIP STEP 3 - SUBSTRATE CLEAVAGE

Once the substrate has undergone shedding and subsequent recognition by the protease, it is cleaved in the TMD within the lipid bilayer. Most proteases cleave their substrates in one specific position. This results in the immediate release of two fragments. However, for γ-secretase and SPPL2b, a sequential cleavage that occurs roughly every third amino acid has been described (Fluhrer et al., 2008, Fluhrer et al., 2006, Fukumori et al., 2010, Matsumura et al., 2014, Olsson et al., 2014). Mutations in γ-secretase shift the start of the product line of APP cleavage, which results in an altered product line and, thus, in larger, amyloidogenic peptides (Figure 1.14).

A similar effect has been observed for Notch, proposing that consecutive cleavage is a general mechanism of γ-secretase (LaVoie and Selkoe, 2003). The consecutive cleavage mechanism of SPPL2b has been shown for TNFα where after recognition, initial cleavage releases a C-peptide while the remaining ICD is cleaved sequentially (Figure 1.14) (Fluhrer et al., 2006). Mutations in the GxGD motif slow down the consecutive cleavage of SPPL2b, resulting in longer TNFα N-terminal cleavage products (Fluhrer et al., 2008). So far, it has not been investigated whether consecutive cleavage is a general feature of all (aspartyl-) IMPs.

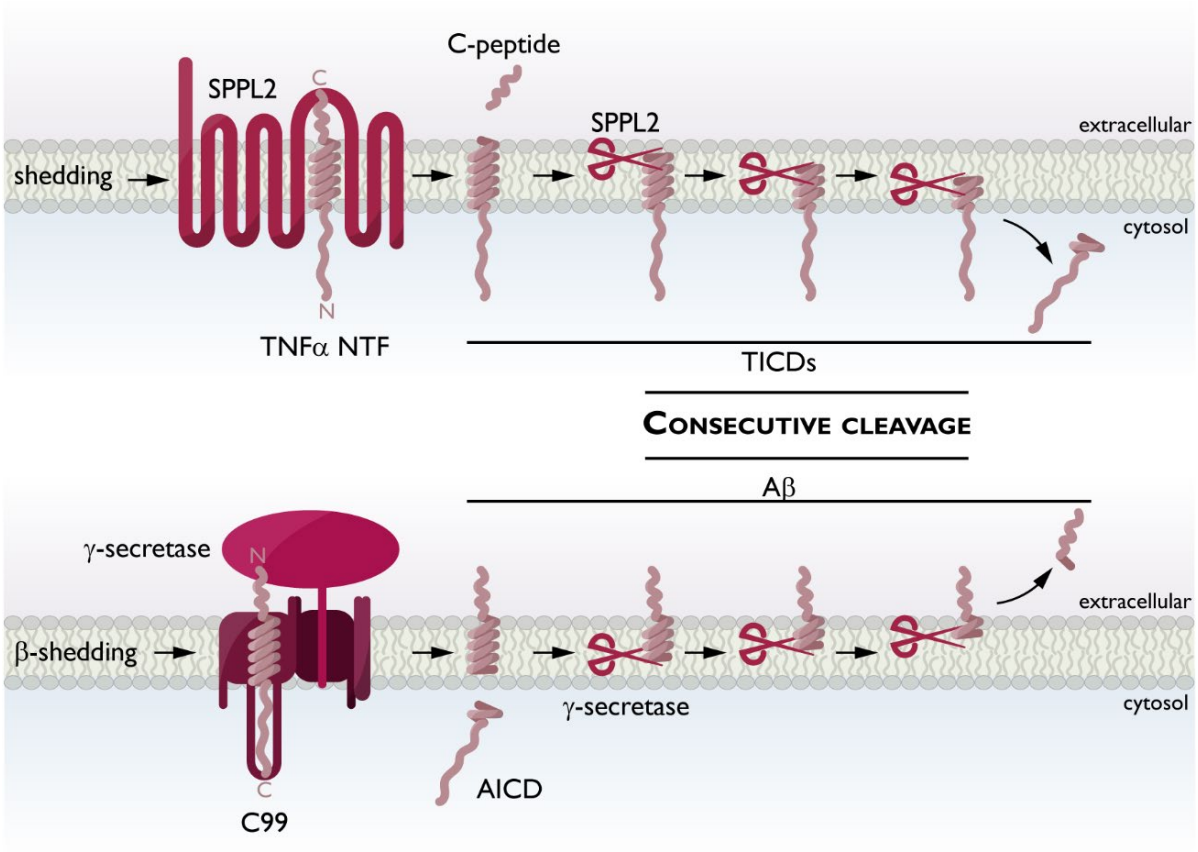

Figure 1.14 Consecutive cleavage mechanism of SPPL2b and γ-secretase. SPPL2b recognises TNFα NTF. After an initial cleavage, which releases the C-peptide, the remaining TNFα intracellular domain (TICD) is cleaved roughly every third amino acid, releasing TICDs of different lengths into the cytosol. As membrane-orientation of γ-secretase is flipped, it cleaves type I proteins such as APP. After shedding by β–secretase, a C-terminal fragment remains in the membrane that is termed according to its length (C99). The consecutive cleavage of C99 releases an APP ICD (AICD) into the cytosol and N-terminal fragments into the extracellular space (Aβ). The consecutive cleavage in APP has multiple starting positions resulting in different product lines. Therefore, released Aβ fragments can vary in length.

1.3. SPPL2 SUBSTRATES

So far, only a few substrates for SPPL2 have been identified but the spectrum is continuously growing. In the following section, current knowledge about all SPPL2 substrates will be summarised. As many of them are involved in complex immune reactions and are investigated in the context of many diseases, the summary is far from being complete.

1.3.1. TNFα – THE MASTER REGULATOR OF INFLAMMATION

Over 60 years ago, TNFα was identified as a factor that induces haemorrhagic necrosis of tumours in mice upon LPS stimulation (Carswell et al., 1975, O'Malley et al., 1962). Since its discovery, over 40 proteins with similar properties have been grouped into the TNF/TNFR superfamily that is continuously growing. Besides TNFα, the TNF/TNFR superfamily includes prominent members such as lymphotoxin, Fas/FasL, TRAIL, CD40/CD40L and RANK/RANKL. Nowadays, TNFα is not considered a tumour necrosis factor but rather a pleiotropic cytokine that is produced by neutrophils and cells of monocytic lineage such as macrophages, astrocytes, microglia, Langerhans cells and Kupffer cells (Flynn et al., 1995, Pfeffer et al., 1993).

TNFα is, amongst others, the first and most abundant cytokine released after infection or trauma, stimulating the expression of other inflammatory mediators and recruiting immune cells to the place of injury (Kalliolias and Ivashkiv, 2016). It perpetuates inflammation and apoptosis; thus, is considered an upstream regulator of the immune response and its expression needs precise regulation. TNFα expression is induced by activation of Toll-like receptors and release of interferon gamma (IFNγ) (Parameswaran, 2010). Once upregulated and expressed on the cell surface, TNFα is shedded by ADAM17 to release its ECD that can bind to one of the two TNFα receptors (TNFR1, TNFR2). The removal of the membrane-retained N-terminal stub is facilitated through cleavage by SPPL2a or SPPL2b (Fluhrer et al., 2006). The cytosolic domain that is released by SPPL2 cleavage can travel to the nucleus and activate expression of interleukin (IL-) 12 (Friedmann et al., 2006).

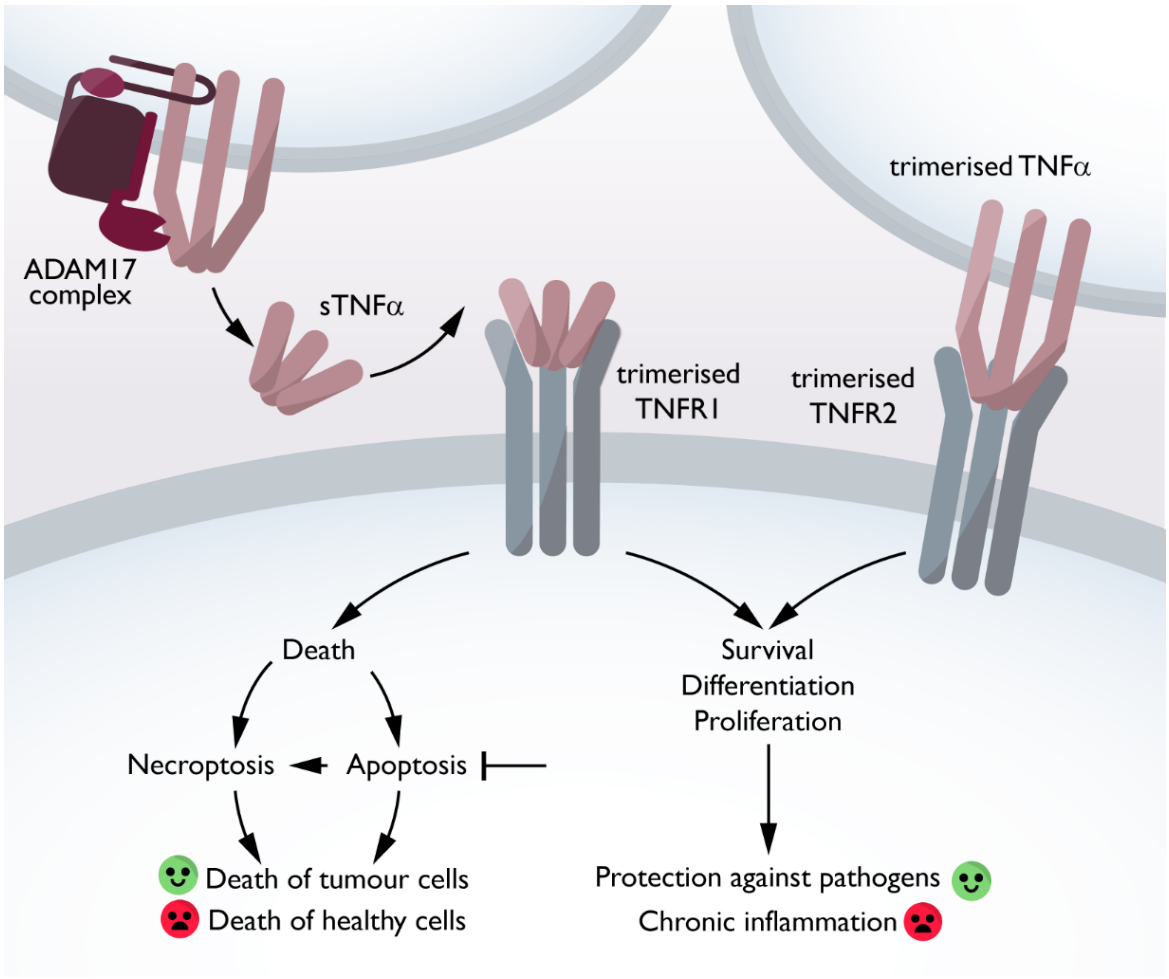

Figure 1.15 TNFα conducts various cellular responses. TNFα is shedded on the cell surface by ADAM17. The trimerised soluble ECD binds to the TNFα receptor 1 (TNFR1). Upon stimulation, the receptor can induce either a death or a survival response. Membrane-bound TNFα is able to bind directly to TNFR2. This induces a survival response. However, neither response is healthy if not regulated correctly.

In addition to apoptotic functions, TNFα also induces an extensive array of protective and renewing properties. The at first glance contradicting functions of TNFα are mediated via signalling through the two distinct receptors. While cell death is mostly induced via pathways activated by TNFR1, survival is mediated via TNFR2 (Figure 1.15) (Tartaglia et al., 1991). TNFR1 is ubiquitously expressed and its activation induces a large number of inflammatory responses that are usually attributed to TNFα signalling (Tseng et al., 2018). Upon ligand binding, TNFR1 initiates apoptosis and necroptosis that lead to tissue degeneration. However, induction of TNFR1 signalling can also facilitate cell proliferation, migration and differentiation (Parameswaran, 2010). The regulation of these conflicting processes depends on the formation of different molecular complexes that diverge in their kinetic and special distribution within the receiving cell (Workman and Habelhah, 2013). TNFR2, mostly found on immune cells, induces proliferation of lymphoid

cells (Tartaglia et al., 1991). It lacks the intracellular death domains and therefore mediates homeostatic effects such as survival, proliferation and tissue regeneration via the MAPK and ERK pathway (Kalliolias and Ivashkiv, 2016). Even though these are two very different functions, both receptors can contribute to the fuelling of inflammation by inducing cell death in abnormal cells and stimulating proliferation in immune cells (Figure 1.15). Furthermore, they are able to induce negative feedback loops to downregulate the inflammatory response.

Interestingly, even though a central player of the immune response, TNFα deficiency in mice is not lethal. Amongst other defects, these animals display a high susceptibility to infectious diseases but are resistant to sepsis (Marino et al., 1997). Interestingly, no TNFα variations on protein level have so far been described. In contrast, variations in the promoter region of the TNFA gene have been reported extensively (El-Tahan et al., 2016, Yi et al., 2018). These SNPs affect the susceptibility for certain auto-immune disorders, infectious diseases and sleep disorders (Hohjoh and Tokunaga, 2001). The SNPs modify transcription factor binding, which leads to altered expression of TNFα protein. Due to its central role in the question of death vs. survival, the inhibition of TNFα activity has been a focus of drug development. Anti-TNFα antibodies are extremely successful in the treatment of chronic inflammatory diseases. Etanercept – a recombinant human soluble fusion protein of TNFR2 coupled to Fc domain of IgG – improves the clinical course of rheumatoid arthritis (RA) and psoriasis (Strand et al., 2012). Infliximab (anti-TNFα human-murine chimeric IgG1 monoclonal antibody) and Adalimumab (human anti-human TNF antibody produced by phage display) are used in patients with inflammatory bowel diseases (Ordás et al., 2012). These antibodies that inhibit the interaction with TNFR by antagonizing the receptor or neutralize sTNFα are the gold standard for treatment of TNFα-related diseases and among the most sold drugs worldwide (Parameswaran, 2010).

1.3.2. FASL (CD95L) – THE APOPTOTIC CYTOKINE

The Fas ligand (FasL, or CD95L) is another cytokine of the TNF superfamily (TNFSF6) that binds primarily to its receptor Fas but is also able to bind to TNFR (Linkermann et al., 2003). Fas/FasL interaction is involved in the induction of apoptosis mediated by cytotoxic

T cells and NK cells but also in T cell development and peripheral tolerance. These cells eliminate harmful cells such as cancer or virus-infected cells and obliterate autoreactive lymphocytes, or activated lymphocytes during an infection (Levoin et al., 2020).

As TNFα and FasL belong to the same family of cytokines, they share many structural and functional features. On the cell surface, FasL can directly bind to the receptor on a recipient cell inducing signalling events in the receptor-expressing cell. If shedded by ADAM10, the sFasL fails to induce cell death upon binding to the receptor. Thus, ADAM10 negatively regulates FasL-induced cell death and the processing of the FL protein ends its cytotoxic function (Guardiola-Serrano et al., 2010, Schulte et al., 2007). The remaining NTF is removed from the membrane by SPPL2a (Kirkin et al., 2007). Activation of Fas-mediated cell death occurs similarly to TNFα-mediated apoptosis via caspases. Besides cell death initiation, FasL also induces cell survival pathways or non-death functions such as cytokine production or differentiation (Rossin et al., 2019). In certain cancers, e.g. NK cell lymphomas, ovarian or breast cancer and autoimmune disease sFasL peptides accumulate in the bloodstream (Fouque et al., 2014).

1.3.3. BRI2 (ITM2B) – THE DEMENTIA PROTEIN

The family of the British dementia proteins consists of three members, Bri1, Bri2 and Bri3. Bri2 has gained attention when it was found to be mutated in patients with familiar British/ Danish dementia (FBD/ FDD) (Kim et al., 1999). Given their role in dementia, it is not surprising that Bri2 but also Bri3 reside in the brain. Bri1 expression is however restricted to chondrocytes suggesting no engagement in dementia development (Del Campo and Teunissen, 2014).

The three proteins are highly homologous in sequence and structure. The large ECD contains the BRICHOS domain, which is involved in targeting the secretory pathway and chaperoning the formation of β-sheets (Del Campo and Teunissen, 2014, Tsachaki et al., 2008). In Bri2, a GxxxG motif, as well as a cysteine (C89) close to the extracellular plane of the membrane, are involved in dimer formation (Figure 1.16).

Even though very similar, the Bri proteins diverge significantly regarding their processing. While all members of the family are cleaved by the Pro-protein convertases

Furin, which releases a rather small pro-peptide (~25 amino acids), Bri1 and Bri3 are subsequently not shedded and therefore not subjected to RIP. Even truncated versions of Bri3 that bypass shedding are not a substrate of SPPL2 (Martin et al., 2009). In contrast, Bri2 is a RIP substrate of SPPL2b and shedded by ADAM10 after Furin-mediated cleavage (Figure 1.16) (Martin et al., 2008). Even though the cleavages happen sequentially, *in vitro* experiments showed that the cleavage of ADAM10 and SPPL2 can occur without prior removal of the pro-peptide (Del Campo and Teunissen, 2014). Exact cleavage sites of ADAM10 in Bri2 have yet to be determined. The membrane-remaining fragment of Bri2 is subject to cleavage by SPPL2a or SPPL2b, which release a C-peptide and an ICD with unknown fate. A consecutive cleavage of the Bri2 TMD such as for TNFα has not been observed so far.

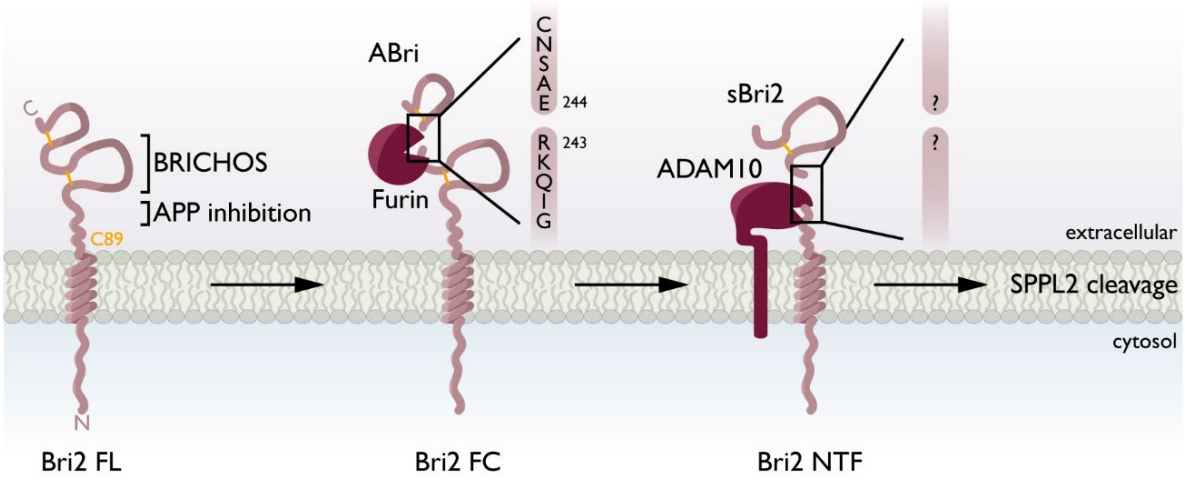

Figure 1.16 Structural overview of Bri2 and its cleavage in the extracellular space by Furin and ADAM10. Bri2 comprises a large ECD with a BRICHOS domain, a domain, which binds to APP and inhibits its turnover by γ-secretase, and several cysteins involved in folding. The full-length (FL) protein is first cleaved by Furin between R243 and E244 (Bri2 FC). It is not known whether the released fragment has any physiological role. However, in FBD/FDD patients a mutation causes this fragment to become longer thereby forming toxic aggregates. The majority of the Bri2 ECD is released by the cleavage of ADAM10. The exact cleavage site of ADAM10 has yet to be identified.

In patients with FBD/ FDD, the BRI2 gene exhibits a point mutation affecting the stop codon and thus adding 10/ 11 amino acids to the Furin-released fragment. This longer ABri peptide tends to form amyloidogenic aggregates in the brain causing severe forms of dementia with patients exhibiting progressive dementia, cerebellar ataxia and spasticity (Del Campo and Teunissen, 2014). Additionally, patients develop extensive cerebral amyloid angiopathy, neurofibrillar tangles and an increased microglial response that goes in hand with the activation of the complement system. Early eye problems

(cataracts) manifest at an average age of onset of 48 years and most patients die within 10 years after disease onset (Mead et al., 2000). Developing suitable mouse models to investigate the physiological processes has turned out to be difficult. Even though Bri2 or an amyloidogenic Bri2 precursor protein are expressed in mice, they do not exhibit the clinical and pathological characteristics of the disease (Pickford et al., 2006). Cognitive deficits are either not present or cannot be measured due to abnormal movements and severe kyphosis (Del Campo and Teunissen, 2014).

Besides the involvement of Bri2 in dementia, the physiological function of the protein has yet to be determined. An idea about its function was derived from observations of increased Bri2 in brain injuries suggesting an implication in plasticity of neuronal processes (Choi et al., 2004). Bri2 might also act as a tumour-suppressor gene (Tsachaki et al., 2008) and has potentially protective functions in Alzheimer's disease. By masking the docking site of α- and β-secretases or interacting with C99 but not C83, Bri2 is discussed to reduce Aβ deposition (Matsuda and Senda, 2019). Even though the interaction is mediated by a short specific juxtamembrane region, which is unique to Bri2 (Figure 1.16), Bri3 has been attributed with similar APP-binding capacity that is however mechanistically different from Bri2 (Matsuda et al., 2009). Moreover, reports hint towards an involvement in TNF-induced cell death and neuronal differentiation (Gong et al., 2008, Wu et al., 2003). A physiological function for Bri1 has been established in chondrocyte differentiation; however, nothing is known about its cleavage mechanism so far (Boeuf et al., 2009).

1.3.4. CD74 (INVARIANT CHAIN) – THE REGULATOR OF IMMUNITY

CD74 was identified as a chaperone for the MHC class II while trafficking from the ER to endosomal compartments (Dijkstra and Yamaguchi, 2019). MHC class II presents peptides on the surface of antigen-presenting cells that are then recognised by the T cell receptor on T helper or regulatory T cells. Peptides are buried in a groove pocket that is specific for the presented peptide and ensures efficient and long-lasting (up to weeks) presentation (Yin et al., 2012). Since the groove displays a high affinity to misfolded proteins, CD74 blocks the MHC II peptide groove from premature peptide binding. In late

endosomes, CD74 is degraded by several proteases one of which is SPPL2a (Figure 1.17) (Huttl et al., 2015). Misregulation of the CD74 degradation leads to maturation defects in B cells and DCs and increased susceptibility to infections. These results have been mostly established in SPPL2a-deficient mouse lines. However, a few patients deficient for SPPL2a have been described that mimic the effects observed in mice (Kong et al., 2018, Schneppenheim et al., 2014).

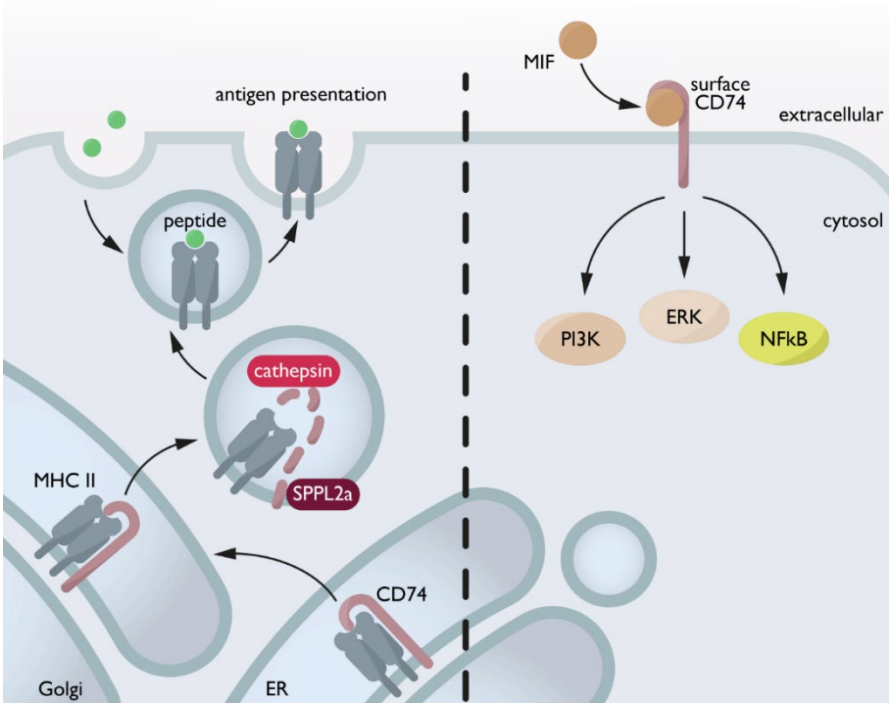

Figure 1.17 CD74 chaperones MHC II on the way through the secretory pathway and has receptor functions on the cell surface. To protect the high-affinity groove of the MHC II receptor from improper binding of peptides, CD74 binds to it. CD74 is then degraded by cathepsins and SPPL2a in endosomes. Afterwards, foreign peptides are loaded into the groove and thus, presented to immune cells on the surface of the antigen-presenting cell. CD74 is also expressed on the cell surface where it can bind ligands such as the macrophage inhibitory factor (MIF). This induces several intracellular pathways.

Recent studies show that CD74 is able to chaperone other proteins besides MHC class II and even displays non-chaperone functions on the cell surface. CD74 can serve as receptor on the surface of non-immune and epithelial cells inducing ERK, PI3K-Akt and NFκB pathways (Figure 1.17) (Schroder, 2016). One of the most prominent ligands is the secreted macrophage migration inhibitory factor (MIF). MIF is ubiquitously expressed and its secretion is rapidly upregulated during the early stages of inflammation. Thus, high levels of CD74 can be found in injury, inflammation and cancer defining it as another key player in the context of inflammation. Interestingly, failure of anti-TNFα therapy in inflammatory bowel disease are connected to CD74 polymorphisms (Farr et al., 2020). Whether processing of CD74 on the cell surface follows the same mechanism as in endosomes is under investigation.

1.3.5. TMEM106B – A DEMENTIA RISK FACTOR

TMEM106b was identified as a risk factor for frontotemporal lobar degeneration (FTLD) and amyotrophic lateral sclerosis (ALS) (Nicholson and Rademakers, 2016). In a large cohort of FTLD patients, several SNPs were determined to boost the pathology besides progranulin and C9orf72 (chromosome 9 open reading frame 72) mutations (Feng et al., 2020).

The TMEM106 family consists of three members: A, B and C. TMEM106b is expressed in endosomes/ lysosomes of neurons, glial and endothelial cells. Even though it is known that TMEM106b undergoes RIP on the surface of the lysosomes, a specific sheddase has not yet been identified (Brady et al., 2014). The remaining NTF is processed by SPPL2a that generates an ICD, which is rapidly degraded. With so little known about the cleavage process, it is not surprising that the significance of physiological or mis-regulated RIP of TMEM106b is uncertain. First observations from *in vitro* experiments show that TMEM106b is involved in controlling lysosome size, acidification and function (Nicholson and Rademakers, 2016). The overexpression of TMEM106b leads to larger, less functional lysosomes, which are reduced in total numbers. Further observations, e.g., that TMEM106b is important for myelination are only descriptive and do not explain the exact mechanism of how TMEM106b exerts its molecular function (Feng et al., 2020).

1.3.6. TRANSFERRIN RECEPTOR 1 (CD71) – THE REGULATOR OF IRON UPTAKE

The transferrin receptor 1 (TFR1) is a homodimeric protein that is ubiquitously expressed in most cell membranes (Naito et al., 2020) even though expression levels are generally low except for differentiating cells and immature erythrocytes (Testi et al., 2019). Upregulation upon certain stimuli controls the expression levels of TFR1 and subsequent iron uptake. TFR1 regulates the uptake of plasma iron-carriers e.g., transferrin or ferretin that upon interaction are internalised and iron is released into the cell by endocytosis. The receptor is recycled to the surface (Figure 1.18) (Naito et al., 2020).

Deficiency in the receptor leads to severe heart diseases as it is detrimental in maintaining mitochondrial function especially in the heart and skeletal muscles (Xu et al.,

2015). Due to its primary role in iron uptake, storage and release, exceptionally tight regulation is needed to sustain an optimal balance. Several intracellular protein interactions fine-tune the binding affinity and trafficking of the receptor (Testi et al., 2019). In the liver, TFR1 is shedded by the metalloprotease PC7 (Figure 1.12) and the soluble peptide is used as a diagnostic marker for anaemia caused by iron deficiency (Guillemot et al., 2013). Whether it exerts any physiological functions is not yet clear. The membrane-retained TFR1 stub is subsequently processed by SPPL2b. Even though it has been shown that SPPL2a is able to cleave TFR1, it does not account for the majority of the degradational process (Zahn et al., 2013).

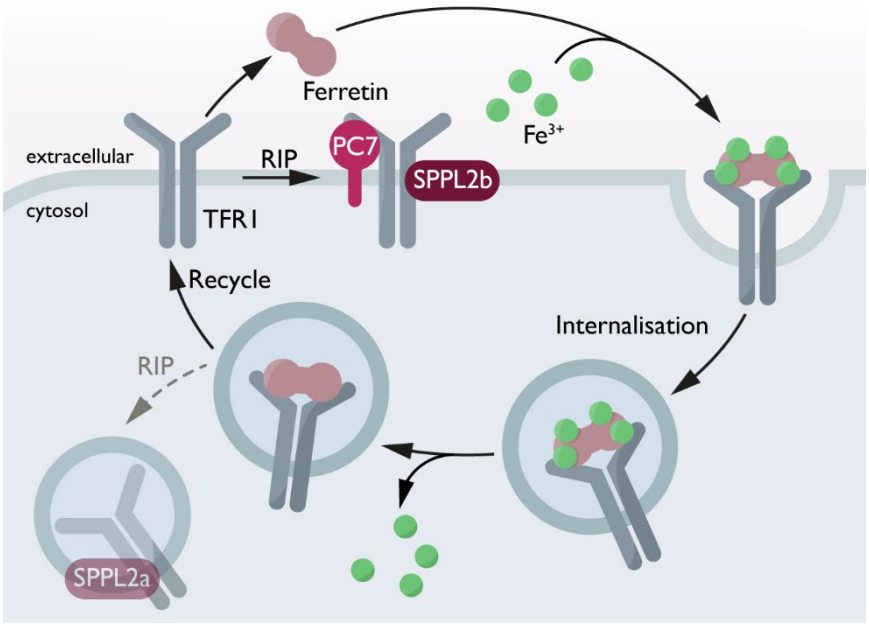

Figure 1.18 The transferrin receptor 1 (TFR1) enables iron uptake. Ferretin-bound iron binds to the TFR1. After internalisation of the complex, the iron is released into the cell. TFR1 and ferretin are recycled to the cell surface. This process can be governed by RIP, therefore reducing the amount of cell surface TFR1 and subsequent iron uptake. Only a small portion of TFR1 is degraded in the lysosomal system (grey, dashed arrow), the majority is subjected to RIP by PC7 and SPPL2b.

1.3.7. CLEC7A (DECTIN-1)/ CLEC8A (LOX-1) – THE NEW SUBSTRATES

Clec7a and Clec8a are C-type lectin receptors (CLRs) that recognize sugars (e.g., zymosan) in the cell wall of bacteria, plants and fungi. The over 1 000 CLRs are grouped into 17 families based on their function and/ or structure and most of them play a crucial role in immunity and homeostasis (Tone et al., 2019).

Clec8a is mostly expressed in low amounts on endothelial cells but is rapidly upregulated upon stimulation by inflammatory cytokines and oxidised low-density lipoprotein (LDL). Once bound, the ligand is internalised, activating intracellular signalling as well as the production of cytokines, upregulation of adhesion molecules, apoptosis and

NFκB signalling (Tone et al., 2019). Shedding of Clec8a is mediated by ADAM10 releasing a soluble fragment that is detectable in serum. The levels correlate with cardiovascular diseases and stroke; thus, they are used as diagnostic markers. The NTF is further processed by SPPL2a or SPPL2b (Mentrup et al., 2019). Whether the FL protein or the NTF mediate intracellular signalling is not yet clear.

Clec7a is expressed on myeloid cells but also in B cells and some subsets of T cells (Tone et al., 2019). In humans, two isoforms are expressed of which one is lacking the stalk region. Besides the activation via β-glucans, endogenous ligands exist such as galactosylated immunoglobulins and galectins (Gross et al., 2006). Activation of the receptor induces phagocytosis, autophagy, DC maturation, inflammasome activation, a respiratory burst and the production of cytokines and chemokines (Sun and Zhao, 2007). Therefore, polymorphisms of Clec7a are associated with reduced host defence and increased risk of fungal diseases (Kalia et al., 2018). The processing of Clec7a by SPPL2a is a fairly new observation (Schlosser, unpublished data) and not yet well understood.

1.3.8. NEUREGULIN1 AND FVENV - UNCONVENTIONAL SUBSTRATES

So far, most of the substrates identified for SPPL2 are type II TM proteins, with two exceptions. NRG1 and FVenv protein are type III TM proteins, which span the membrane twice. When shedded, two single TM proteins remain one of which is in type II orientation (Figure 1.11). This fragment is then cleaved by SPPL2 (NRG1) or SPPL3 (FVenv).

NRG1 is indispensable for neuronal and cardiac development as it is most abundant in brain and heart tissue (Hu et al., 2016). Misregulation of NRG1 cleavage is associated with Alzheimer's disease and schizophrenia (Hu et al., 2016, Willem, 2016). The neuregulin gene is one of the largest genes in the human genome. Its expression and regulation are highly complex involving different transcriptional isoforms and several splice variants. All isoforms contain an EGF-like domain that can be secreted or directly bind to its receptor. The activation of the receptor induces MAPK and PI3K-AKT pathways (Baliga et al., 1999). Unless the soluble form is directly synthesised as a functional isoform, NRG1 needs ADAM10/17 and BACE1 shedding twice to release the EGF-like domain to the extracellular space, leaving behind a single span type I and a type II TM fragment (Figure

1.19). The type I TM fragment contains a short luminal domain and therefore is directly processed further by γ-secretase. The type II TM protein exhibits a larger ECD and is shedded again by an unknown protease, which generates an NTF' that is processed by SPPL2a or SPPL2b (Fleck et al., 2016). The cleavage occurs in the C-terminal region of the TMD, but the function of ICD and C-peptide are unknown. As they lack conserved domains this cleavage might only fulfil a degradational purpose.

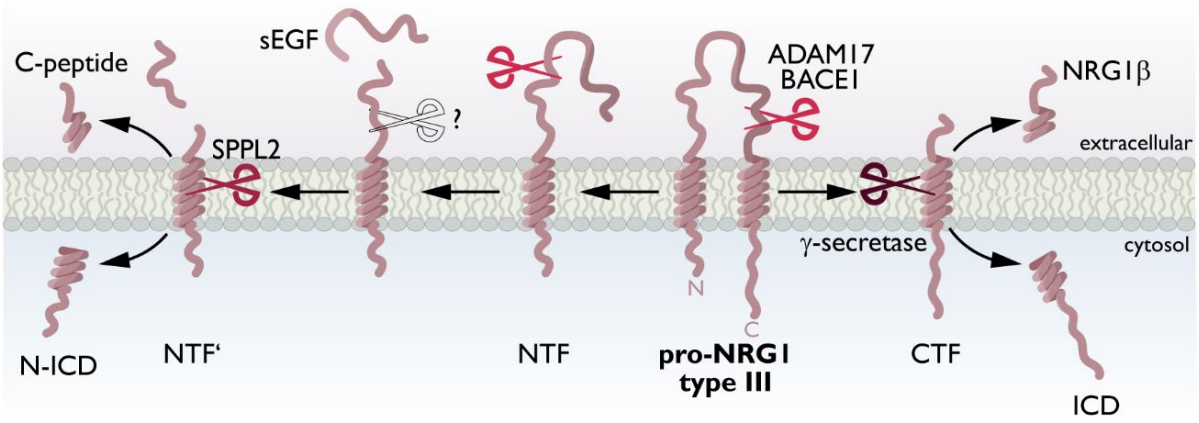

Figure 1.19 Processing of neuregulin 1 (NRG1) is a multi-step process. NRG1 spans the membrane twice. It is cut twice in the luminal domain by ADAM17 or BACE1. This cleavage releases the soluble EGF domain (sEGF). The C-terminal membrane resident fragment (CTF) is cleaved by γ-secretase. The NTF is shortened by an unknown protease, which generates the NTF'. This fragment is cleaved by SPPL2a or SPPL2b releasing a C-peptide to the extracellular space and an N-ICD to the cytosol.

The foamy virus (FV) belongs to a subfamily of retroviruses that infect non-human primates. The persistent but mostly non-pathogenic infection is transmitted by primates biting or licking each other but is generally restricted to epithelial cells in the mouth and pharynx (Buseyne et al., 2018). So far, only a small cohort of African hunters have been investigated in the context of a clinical study displaying signs of anaemia and differences in blood count after infection (Buseyne et al., 2018). So far, no mechanism is identified linking the FV to the clinical symptoms.

The FVenv protein is a type III TM protein with both C- and N-terminus facing the cytosol. Its interaction with the viral capsid makes it most likely that it is involved in the release from the host cell. Furin or a Furin-like proprotein convertase sheds the protein in the extracellular loop twice enabling subsequent SPPL3 cleavage. Even though FVenv is canonically shedded, SPPL3 is able to process the protein without prior shedding. Besides SPPL3, SPPL2a and b are also able to process FVenv, but only after the preceding shedding by Furin (Voss et al., 2012).

The table below summarises the current knowledge of SPPL2 substrates in the context of RIP. Most of the substrates are characterised incompletely, information about cleavage sites of sheddases and SPPL2 are still missing. Some substrates like FasL and CD74 have been studied in more detail because of their central role in disease development.

The question, whether SPPL2a and SPPL2b are generally able to cleave the same substrates is also not entirely answered, even though *in vitro* experiments indicate at least partially overlapping substrate acceptance by both proteases. However, taking into account that enzyme and possible substrate may differ in subcellular localisation *in vivo* studies are necessary to proof physiological relevance. Thus, the definition of what is a potential or a physiological substrate is pending.

Table 1.1 Summary of human SPPL2 substrates. PM: plasma membrane. (References on page 15548)

	TNFα	FasL	Bri2	CD74	TMEM106b	Clec7a	Clec8a	TFR1	NRG III	FVenv
Protein type	Type II	Type II	Type II	Type II	Type II	Type II	Type II	Type II	Type III	Type III
Subcellular localisation	PM [1]	PM [11] Lysosome [12]	PM[17] Endosome[18] Golgi[19]	Secretory pathway [21] PM [22]	Lysosome Endosome [28]	PM	PM [30]	PM [34]	PM[40]	- Viral
Crystal structure	yes [2]	yes [13]	no	yes [23]	no	no	yes [31]	yes [35]	yes [41]	no
Sheddases	ADAM17 [3]	ADAM10/17 MMP7 [11]	ADAM10 [20]	Cathepsins [24]	?	?	ADAM10 [30]	PC7 [36]	ADAM10/ ADAM17 BACE1 [40]	Furin [44]
Shedding site	A76 [4]	S126 E128 K129 [14]	?	?	?	?	N72-N92 N-terminally of N92 [30]	Arg100 [36]	NTF: F293,Y286, F285, A283 EGF release: H234, L217 [40]	R126 [44]
Substrate for SPPL2	a + b	a	a + b	a + b	a	a + b	a + b	(a) + b	a + b	a + b
SPPL2 cleavage site	L51 (b) C49 (b) L39 (b) R28 (b) [5]	?	?	?	?	?	L52 (a) T51 (b) [30]	G84 I83 [37]	C92 [42]	?
Consecutive cleavage	yes [6]	?	no	?	?	?	?	?	?	yes [45]
ICD signalling	yes [7]	yes [15]	?	yes [25]	?	?	?	?	yes [43]	yes [45]
PTM	Glycosylation S80 [8] 2x Myrisoylation [9] Palmitoylation C30 [10]	3x Glycosylation* Palmitoylation C82 [16]	Glycosylation N170 [17]	5x Glycosylation [26] Palmitoylation C28 [27]	5x Glycosylation [28] Myrisolation G2[29]	Glycosylation N91	2x Glycosylation [32] 2x Palmitoylation [33]	4x Glycosylation [38] 2x Palmitoylation [39]	3x Glycosylation*	no
Identified as SPPL2 substrate by	(Fluhrer et al., 2006, Friedmann et al., 2006)	(Kirkin et al., 2007)	(Martin et al., 2008)	(Schneppenheim et al., 2014)	(Brady et al., 2014)	(Schlosser unpublished data)	(Mentrup et al., 2019)	(Zahn et al., 2013)	(Fleck et al., 2016)	(Voss et al., 2012)

1.4. SUBSTRATE MODIFICATION

PTMs are believed to induce or enhance function, increase stability or provide guidance of proteins to certain subcellular locations. The modifications occur throughout the entire secretory pathway and can involve multiple steps and several types of modifications. Proteins can be modified by proteolytic removal of peptides (Section 1.1 and 1.2.1) or by addition of lipids or glycans. While removal of peptides and addition of glycans are irreversible and depend on the homeostatic status of the cell, the addition of certain lipids is a highly dynamic process. The questions of how, when and where a protein is modified is unique to each protein.

All SPPL2 substrates are glycosylated (Table 1.1); however, the function of this modification is rarely investigated. Differently glycosylated proteins can alter surface stability, signalling capacity and localisation therefore affecting the cell homeostasis. In TMEM106b, the correct localisation to endosomes/ lysosomes is maintained by glycosylation in five positions in the luminal domain and its loss leads to retention in the ER (Nicholson and Rademakers, 2016). A similar function has been reported for the glycosylation of Bri2, which is needed for the correct localisation on the cell surface; however, it seems not to be crucial for protein processing (Tsachaki et al., 2011). In contrast, elimination of FasL glycosylation does not seem to affect the protein at all (Levoin et al., 2020). Therefore, it remains to be investigated how and to what extent glycosylation affects the SPPL2 substrates in more detail.

Attachment of lipids is another common PTM that can alter protein localisation, stability and even function. Depending on the fatty acid that is attached to the protein, the process is called myristoylation (C14), farnesylation (C15) or palmitoylation (C16). When a palmitate is transferred to the functional group of a cysteine residue via a thioester linkage this process is referred to as S-palmitoylation. S-palmitoylation is the only reversible protein lipidation. Thus, this process occurs within seconds and lasts up to several hours (Ko and Dixon, 2018). Protein acyltransferases (PATs) catalyse S-palmitoylation and are multi-pass TM proteins with a conserved zinc-finger Asp-His-His-Cys (zDHHC) motif that is important for catalytic activity (Figure 1.20) (Zmuda and Chamberlain, 2020). Most of the PAT family members are found in the Golgi apparatus; however, some of them localise to the ER and the cell surface. Half of all zDHHC PATs are

expressed in the brain, explaining the large number of palmitoylated synaptic proteins (40%) (Globa and Bamji, 2017). Substrate selection of zDHHC PATs remains elusive as no consensus sequence for palmitoylation is known so far (Ko and Dixon, 2018). Often, more than one PAT is able to palmitoylate a substrate; however, not every cysteine within a protein becomes palmitoylated.

Whereas the PAT family consists of 23 members, only a few depalmitoylating enzymes have been described so far. Removal of the palmitate is facilitated by acylprotein thioesterases (APTs), a group of serine hydrolases and palmitoyl protein thioesterases (PPT) that have emerged as depalmitoylating enzymes (Figure 1.20) (Koster and Yoshii, 2019, Won et al., 2018). In addition, a group of αβ hydrolase domain (ABHD) containing proteins have been described to enable depalmitoylation of cancer-related and SNARE-like proteins (Lin and Conibear, 2015).

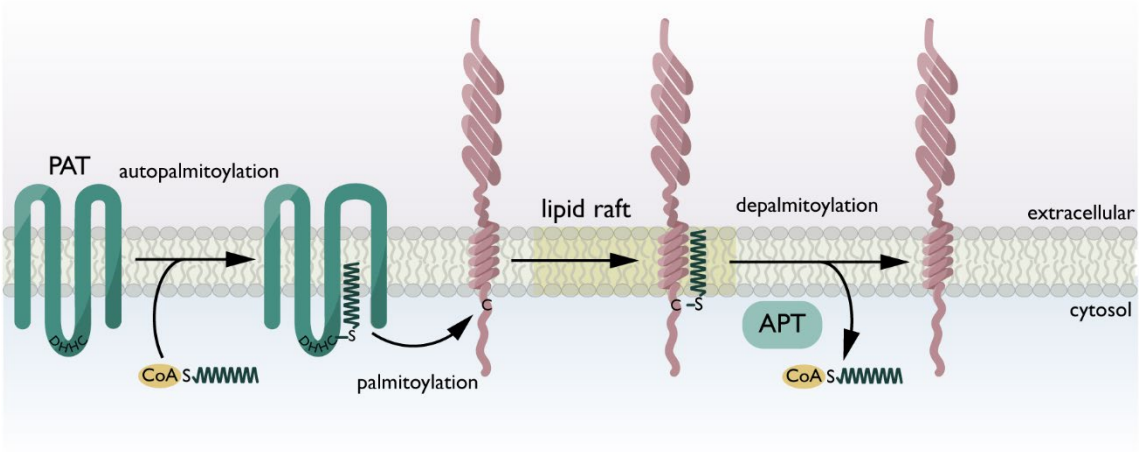

Figure 1.20 Protein acyltransferases (PAT) palmitoylate proteins, whereas acylprotein thioesterases (APT) depalmitoylate proteins. PATs are autopalmitoylated at the DHHC motif before they transfer the palmitate to the thiol group of the target protein. The palmitoylation guides the protein to lipid rafts. Palmitoylation is removed by APTs.

To investigate the effects of lipidation two categories of palmitoylation inhibitors exist, lipid-based and non-lipid compounds. Even though lipid-based inhibitors such as 2-bromopalmitate (2-BP), tunicamycin and cerulenin analogues have been used to inhibit palmitoylation *in vitro*, their mechanism of action is poorly understood and lacks substrate specificity. It has been suggested that 2-BP inhibits palmitate incorporation unspecifically as it is converted into 2-BP-CoA inside the cell (Davda et al., 2013). Nevertheless, besides inhibiting palmitoylation, all lipid-based inhibitors have shown to interfere with numerous metabolic processes, thus their effect on palmitoylation might

not be direct (Draper and Smith, 2009). In an attempt to bypass the tremendous effects on cell homeostasis when interfering with the lipid state, non-lipid compounds were designed to inhibit specifically palmitoylation of certain proteins. They do not act as palmitoyl-CoA competitors but rather target the protein-binding site. Based on this and the fact that they do not interrupt fatty acid synthesis, these inhibitors are tested as anti-cancer drugs (Ko and Dixon, 2018, Zheng et al., 2013).

Many SPPL2 substrates undergo lipidation (Table 1.1). Palmitoylation has been shown for TNFα (Utsumi et al., 2001), FasL (Guardiola-Serrano et al., 2010), CD74 (Schroder, 2016), and TFR1 (Zahn et al., 2013). The physiological role of this modification is pending for most of the substrates, as effects of palmitoylation are difficult to investigate. Results on FasL and CD74 strengthen the assumption that palmitoylation of SPPL2 substrates is critically involved in surface stability. However, while TFR1 palmitoylation enhances endocytosis (Drecourt et al., 2018), palmitoylation of CD74 increases cell surface stability (Huttl et al., 2015). Furthermore, effects on localisation to lipid rafts and proper function are assumed. The regulation of the palmitoylation/ depalmitoylation cycle is complex and that depends on many factors such as availability of fatty acids, enzyme activity and substrate localisation.

2. AIM OF THE STUDY

Aspartyl-intramembrane cleaving proteases emerged as important regulatory players in health and disease, thus the understanding of their function is of great importance. Their participation in the process of RIP requires several steps to complete substrate processing successfully. However, many details about substrate selection and the detailed processing mechanism remain elusive. The goal of this thesis is to increase understanding of the function and cleavage mechanism of SPPL2a and SPPL2b. So far, most information available on the cleavage mechanism of SPPL2 proteases is only based on analysis of SPPL2b and SPPL2a data is incomplete. Here, both proteases will be compared to judge whether substrate recognition and cleavage are actually as similar as suggested.

To this end, domains in TNFα that allow recognition by SPPL2a or SPPL2b will be identified and specific features of these domains will be analysed. It will be investigated how the proteases distinguish substrates from non-substrates and if the subsequent processing mechanism differs between substrates. Previous reports have shown that a short luminal substrate domain seems to be an important requirement for SPPL2 cleavage; therefore, the JMD but also the effect of the TMD and ICD on recognition and processing will be investigated in detail, to answer whether the proteases detect sequence specificities or structural properties. Furthermore, the study aims to explore the question of whether SPPL2a and SPPL2b apply a common recognition/ processing mechanism to all substrates or whether the cleavage mechanism is substrate specific. The resulting data on the substrate selection and processing mechanism will be used to predict new potential substrates to expand the knowledge on SPPL2a and SPPL2b proteases further.

3. MATERIAL AND METHODS

3.1. MATERIALS

3.1.1. INSTRUMENTS, CONSUMABLES, REAGENTS, SOFTWARE

Table 3.1 Instruments and consumables

Instrument	Company
Accu Jet pro	Brand
Agarose electrophorese	Peq Lab
Cawomat 2000IP X-ray developer	Cawo
Centrifuges	Heraeus Pico, Heraeus Frisco 17, 21, Megafuge 40 R
FACS Melody	BD
Gel Electrophorese/ Western Blotting equipment	Biorad
ImageQuant LAS-4000	FUJIFILM
Incubator	Heraeus, Thermo Fisher
Laminar Flow Hood	Thermo Scientific
NanoPhotometer	Implen
Thermomixer C	Eppendorf
Reaction tubes/ pipette tips	Sarstedt
Research plus pipettes	Eppendorf
RX-N X-ray films	FUJIFILM
4800 MALDI TOF/TOF Analyzer	Applied Biosystems
7500 Fast Real-Time PCR System	Applied Biosystems

Table 3.2 Software

Software	Company
CLC Main Workbench, Version 6.9.1	CLC bio
Prism 8 Version 8.4.1	GraphPad Software,LLC
Data Explorer TM Version 4.4	Applied Biosystems
Illustrator/ Photoshop 2021 25.0.0	Adobe
Multi Gauge V3.0	FUJIFILM
PyMOL Molecular Graphics System, Version 2.0	Schrödinger, LLC

Table 3.3 Chemicals used in this study

Chemical	Company
1 kb Plus DNA ladder	Invitrogen
2-bromopalmitate	Sigma Aldrich
α-cyano-4-hydroxycinnamic acid matrix	Sigma Aldrich
Acetic Acid	Merck
Acetonitrile	Sigma Aldrich
Acrylamide/ Bis 40% 29:1	Biorad
Acrylamid/ Bis 40% 37.5:1	Invitrogen
Agarose	Invitrogen
APS (10 %)	Merck
Brilliant Blue R	Sigma Aldrich
Bromphenolblue	Fluka
BSA	Uptima
$CaCl_2$	Merck
DDM	Calbiochem
DMSO	Roth
dNTP	Roche
DTT	Biomol
EDTA	Merck
EGTA	Serva
EtOH	Merck
GelRed	Biotium
Glucose	Merck
Glycerine	Merck
Glycine	Biomol
Hepes	Biomol
Hydroxylamid	Sigma Aldrich
Tropix® I-Block	Applied Biosystems
Isopropanol	Merck
KCH_3COO	Sigma Aldrich
KH_2PO_4 * H_2O	Merck
$Mg(CH_3COO)_2$	Fluka
NaN_3	Merck
$NaHPO_4$ * $2H_2O$	Merck
NaCl	Roth
$NaHCO_3$	Merck
NaOH	Merck
N-octyleglycopyranoside	Sigma Aldrich
NP-40	USB 19628

Orange G	Sigma Aldrich
Pierce TM ECL Western Blotting Substrate & Plus	Thermo Fisher
Protease inhibitor cocktail	Sigma Aldrich
SDS	Serva
See Blue Plus 2 Standard	Invitrogen
Sucrose	Sigma Aldrich
TEMED	Roth
Trifluoroacetic acid (TFA)	Roth
Tris	Biomol
Tricine	PanReac AppliChem
Triton X100	Merck
Tween20	Merck
Westar Antares	Cyanogen
β-mercaptoethanol	Sigma Aldrich

3.1.2. PLASMIDS AND CONSTRUCTS

Table 3.4 Plasmids

Plasmid	Company
pcDNA3.1 Hygro(+)	Invitrogen
pCMV-Cas9-GFP	Sigma Aldrich

Table 3.5 cDNA constructs established in this study for transient transfection. FL: full-length protein, NTF: N-terminal fragment.

Tag N-terminal	Construct name	Tag C-terminal
Flag	TNFα FL S34L	V5
Flag	TNFα FL S34P	V5
Flag	TNFα FL S37L	V5
Flag	TNFα FL S37P	V5
Flag	TNFα FL G43L	V5
Flag	TNFα FL G43P	V5
Flag	TNFα FL C49L	V5
Flag	TNFα FL C49P	V5
Flag	TNFα FL H52L	V5
Flag	TNFα FL H52P	V5
Flag	TNFα FL AGA42-44L	V5
V5	TNFα NTF S34P	Flag AP
V5	TNFα NTF S37P	Flag AP

V5	TNFα NTF G43P	Flag AP
V5	TNFα NTF C49P	Flag AP
V5	TNFα NTF H52P	Flag AP
Flag	TNFα FL EED61,62,66QQN	V5
Flag	TNFα FL EED61,62,66QQA	V5
Flag	TNFα FL EED61,62,66AAA	V5
Flag	TNFα FL FlagTEV	V5
Flag	3TT FL	V5
Flag	33T FL	V5
Flag	T3T FL	V5
Flag	3T3 FL	V5
Flag	TT3 FL	V5
Flag	T33 FL	V5
Flag	3TT NTF	V5
Flag	33T NTF	V5
Flag	T3T NTF	V5
Flag	3T3 NTF	V5
Flag	TT3 NTF	V5
Flag	T33 NTF	V5
V5	3TT NTF	FlagAP
V5	33T NTF	FlagAP
V5	T3T NTF	FlagAP
V5	3T3 NTF	FlagAP
V5	TT3 NTF	FlagAP
V5	T33 NTF	FlagAP
Flag	3T3 FL S66P	V5
Flag	3T3 FL G73P	V5
Flag	TNFα FL juxBri3_1	V5
Flag	TNFα FL juxBri3_2	V5
Flag	TNFα FL juxBri3_3	V5
Flag	TNFα NTF juxBri3_1	V5
Flag	TNFα NTF juxBri3_2	V5
Flag	TNFα NTF juxBri3_3	V5
V5	TNFα NTF juxBri3_1	FlagAP
V5	TNFα NTF juxBri3_2	FlagAP
V5	TNFα NTF juxBri3_3	FlagAP
Flag	SACA3	V5
Flag	ENTPD6	V5
Flag	GOLM1	V5
Flag	TNFSF15	V5

Flag	NKG2D	V5
Flag	Bri2 FL	V5
Flag	Bri2 G60L	V5
Flag	Bri2 G60P	V5

All constructs were cloned into a pcDNA3.1 Hygro (+) vector via the HindIII and XhoI cleavage sites.

Bri proteins contain an additional pro-peptide, which is removed by Furin-mediated cleavage. As this cleavage does not affect further processing the pro-peptide was removed. Throughout the study, these constructs are still referred to as full-length (FL).

3.1.3. KITS

Table 3.6 Kits

Kit	Company
Novex™ AcTEV™ Protease	Thermo Fisher Schientific
Clean up kit NucleoSpin®	Macherey Nagel
NucleoBond Xtra Midi kit	Macherey Nagel

3.1.4. CELL LINES AND CELL CULTURE

Table 3.7 Cell lines

Cell line name	Genetic alteration	Antibiotic resistance	Source
T-RexTM-293 (TR)	pcDNATM6/TR	Blasticidin	Invitrogen
TR SPPL2a wt HA	pcDNATM6/TR pcDNA4/TO-SPPL2a wt HA	Blasticidin Zeocin	Martina Haug-Kröper (Martin et al., 2008)
TR SPPL2b wt HA	pcDNATM6/TR pcDNA4/TO-SPPL2b wt HA	Blasticidin Zeocin	Martina Haug-Kröper (Martin et al., 2008)
TR SPPL2a ko clone 36.3	pCMV-Cas9-GFP gRNA hSPPL2a	Blasticidin	Current study (Spitz et al., 2020)
TR SPPL2b ko clone 36.19	pCMV-Cas9-GFP gRNA hSPPL2b	Blasticidin	Current study (Spitz et al., 2020)
TR SPPL2a/b ko clone 115	pCMV-Cas9-GFP gRNA hSPPL2a	Blasticidin	Current study (Spitz et al., 2020)

Table 3.8 Reagents

Name	Company
Blasticidin	Life Technologies
DEMEM GlutaMAX TMI	Life Technologies
Doxycycline	Carl Roth
Fetal Bovine Serum (FBS)	Sigma Aldrich
GI254023X	Sigma Aldrich
L-Glutamine (L-Gln)	Life Technologies
Lipofectamine TM 2000	Thermo Fisher
OptiMEM® I + GlutaMAX TM I	Life Technologies
Penicillin/ Streptomycin (P/S)	Life Technologies
Phorbol 12-myristate 13-acetate (PMA)	Enzo lifesciences
Poly-L-lysine	Sigma Aldrich
Trypsin (0.05 %) –EDTA (1 x)	Life Technologies
Zeocin	Life Technologies
2,2'-(2-Oxo-1,3-propanediyl)bis[N-[(phenylmethoxy) carbonyl]-L-leucyl-L-leucin-amide ($(Z\text{-}LL)_2$-ketone)	Merck
BMS-561395	Kindly provided by Haass Lab

Table 3.9 Composition of cell culture media

Name	Composition
Antibiotic free medium + Doxycycline (ABF+Dox)	DMEM GlutaMAX 10 % (v/v) FCS 1 µg/ ml Doxcycline
Basic medium	DMEM GlutaMAX 10 % (v/v) FCS 1 % (v/v) P/S 1 % L-Gln
Blasticidin Medium (B)	Basic medium 5 µg/ ml Blasticidin
Blastcidin/ Zeocin medium (B/Z)	Basic medium 5 µg/ ml Blasticidin 200 µg/ ml Zeocin

3.1.5. ANTIBODIES

Table 3.10 Primary antibodies. WB: western blot, FC: flow cytometry, IP: immunoprecipitation.

Antigen	Host/ Type	Source	Clone	Method	Dilution
FlagM2	Mouse	Merck	M2	WB	1 : 1 000
V5-mono	Mouse, mIgG2A	Life Technologies	R960-25	WB FC	1 : 2 000 1 : 400
Calnexin	Rabbit, pAB	Enzo Life Sciences		WB	1 : 1 000
Anti-TNFα	Rabbit, pAB	Abcam	ab9739	WB	1 : 1 000
V5-mono	Mouse	Haass Lab	29H	IP	1 : 50
V5 poly	Rabbit, pAB	Millipore	AB3792	IP	1 - 1 : 10

Table 3.11 Secondary antibodies. WB: western blot, FC: flow cytometry.

Target organism	Host	Coupling	Source	Method	Dilution
Mouse	Goat	HRP	Promega	WB	1 : 10 000
Rat	Goat	HRP	Millipore	WB	1 : 10 000
Rabbit	Goat	HRP	Promega	WB	1 : 20 000
Mouse	Donkey	Alexa488	Thermo Fisher	FC	1 : 2 000

3.1.6. BUFFERS

Table 3.12 List of buffers used for analysis.

Name	Composition
Acrylamide Solution 29.5 %	48 g Acrylamid 1.5 g Bisacrylamid ad. 100ml H_2O
Anode buffer	1 M Tris-HCL pH 8,9
Basic buffer	40 mM Tris pH 7.8 40 mM KCH3COO 1.6 mM $Mg(CH_3COO)_2$ 100 mM sucrose 0.8 mM DTT 1:500 PI mix
Binding buffer	100mM HEPES 1mM EDTA 1% SDS
Cathode buffer	0.1 M Tris HCl 0.1 M Tricine 0.1 % SDS

$CaCl_2$ buffer	50 mM $CaCl_2$ 10 mM Tris pH 8,0
$CaCl_2$ Glycerin buffer (fresh)	7.5 ml $CaCl_2$ buffer 2.5 ml Glycerin sterile
FACS buffer	1 x PBS 0.5 % BSA 0.01 % NaN_3
gDNA Lysis Buffer	10 mM Tris-HCl pH 7.5 10 mM 0.5M EDTA 10 mM NaCl 0.5 % sarcosyl (N-lauryl sarcosine) 10 mg/ ml Proteinase K (before use) ad. 1 L H_2O
gDNA precipitation buffer	0.15 M NaCl ad. 10 ml 98 % EtOH
Hypotonic buffer	10 mM Tris pH 7.6 1 mM EDTA 1 mM EGTA, pH 7.6 PI mix 1:500
I-Block	2 % (w/v) Tropix I-Block™ 0.1 % (v/v) Tween 20 in PBS
LB agar plates	LB medium 15 g/ L agar autoclaved at 120°C at 1.2 bar 20 min 100 mg/ ml ampicillin
LB medium	1 % (w/v) bactotrypton 0.5 % (w/v) yeast extract 1 % (w/v) NaCl
Lower Tris	1.5 M Tris 0.4 % (w/v) SDS, pH 8.8
Mass Spec washing buffer (20 x)	2.8 M NaCl 2 % N-octyleglycopyranoside 200 mM Tris-HCl pH 8 100 mM EDTA
PBS pH 7.4	140 mM NaCl 10 mM Na2HPO4 1.75 mM KH2PO4
Quenching buffer	100mM HEPES pH 7.5 1mM EDTA 2.5% SDS 2.5% NEM

Running buffer	25 mM Tris 200 mM Glycine 0.1 % (w/v) SDS
Sample buffer (5 x)	50 % (v/v) glycerol 7.5 % (w/v) SDS 7.5 % (w/v) DTT bromophenol blue (traces) dissolved in 4 x upper Tris buffer
SDS Gel buffer	3 M Tris-HCl 0,3 % SDS
Solution 1	50 mM Glucose 25 mM Tris pH 8 10 mM EDTA pH 8
Solution 2 (fresh)	0.2 M NaOH 1 % SDS ad. 6 ml H_2O
Solution 3	3 M Acetic potassium 11.5 % acetic acid
SPP Stock buffer	50 mM Tris pH 7.8 50 mM KCH_3COO 2 mM $Mg(CH_3COO)_2$ 125 mM sucrose 1 mM DTT
STEN-lysis buffer	400 ml STEN buffer 1 % Triton X-100 1 % NP-40 0.2 % BSA
STEN buffer	50 mM Tris pH 7.5 150 mM NaCl 2 mM EDTA 0.2 % NP-40
TBE buffer (10 x)	50 mM Tris pH 7.5 150 mM NaCl 2 mM EDTA 1 % NP-40 PI mix 1:500
TBS-T pH 7.6	50 mM Tris 150 mM NaCl 0.05 % (v/v) Tween 20
TE buffer	10 mM Tris HCl pH 8 1 mM EDTA

Transfer buffer	25 mM Tris 200 mM glycine
Upper Tris (4 x) pH 6.8	0.5 M Tris 0.8 % (w/v) SDS

3.1.7. ACRYLAMID GELS

Table 3.13 Acrylamide gel composition for 12 % SDS gel

	Separating gel (12 %)	Stacking Gel
H_2O	1.8 ml	1,625 ml
Acrylamide/ Bis 37, 5:1	1.2 ml	0.25 ml
Lower Tris	1 ml	-
Upper Tris	-	0.625 ml
TEMED	7.5 µl	7.5 µl
APS (10 %)	7.5 µl	7.5 µl

Table 3.14 Acrylamide gel composition for a Schägger gel

	Separating gel	Spacing gel	Stacking gel
Acrylamide solution	2 ml	0.75 ml	0.25 ml
Tris-tricine gelbuffer	1.75 ml	1.25 ml	0.75 ml
H_2O	-	1.75 ml	2.1 ml
32 % (v/v) glycerol	1.5 ml	-	-
TEMED	32.5 µl	35 µl	25 µl
APS (10 %)	3.25 µl	4 µl	5 µl

Table 3.15 Acrylamide gel composition for DNA analysis

	Running Gel (8 %)
H_2O	8.4 ml
Acrylamide/ Bis 29:1	2.4 ml
10 x TBE	1.2 ml
TEMED	10 µl
APS (10 %)	200 µl

3.1.8. MOUSE SAMPLES

Samples of bone marrow-derived dendritic cells (BMDCs) of wildtype (wt) and SPPL2a-deficient mice were kindly provided by Dr. Bernd Schröder in Dresden

(Schneppenheim et al., 2014). BMDCs were isolated and treated with LPS and the ADAM inhibitor marimastat for 6 h or 24 h. Cells and media were collected by the collaborators.

3.2. METHODS

3.2.1. MOLECULAR CLONING

3.2.1.1. STANDARD PCR, QUICKCHANGE, GBLOCK

cDNA constructs were designed using the CLC software. Either mutations were inserted via PCR or cDNA was purchased at IDT (https://eu.idtdna.com/pages). Tags were added on both N- and C-terminus as shown in

Table 3.5 (Flag: DYKDDDDK(AP) or V5: GKPIPNPLLGLDST). To change tags or to fuse larger cDNA fragments an optimised PCR protocol was used (Table 3.16). This protocol was also used to amplify the cDNA received from IDT. The composition of the PCR mix is listed in Table 3.17.

Table 3.17 Optimised PCR Program

Cycle	Temp.	Time
1	95°C	2 min
2	95°C	1 min
3	42°C	1 min
4	72°C	2 min
5		Go to 2, Repeat 20 x
6	94°C	1 min
7	42°C	1 min
8	72°C	2 min
9		Go to 6, Repeat 30 x
10	72°C	7 min
11	4°C	Hold

Table 3.16 PCR mix for standard PCR

cDNA (10 - 50 ng)	1 µl
Primer fwd (25nM)	1 µl
Primer rv (25nM)	1 µl
dNTP	2 µl
5x Go Taq polymerase buffer (Promega)	10 µl
Go Taq polymerase (Promega)	1 µl
H_2O	ad. 50 µl

To introduce point mutations the Quick-Change PCR was used (Table 3.18). Primers were designed using the online webtool of Agilent Technologies (http://www.genomics.

agilent.com/primerDesignProgram.jsp) and purchased at Sigma Aldrich. The composition of the Quick-Change PCR mix is listed in Table 3.19.

Table 3.19 Program for Quick Change PCR

Cycle	Temp.	Time
1	95°C	1 min
2	95°C	30 s
3	55°C	30 s
4	68°C	2 min/ 1 kb
5		Go to 2, Repeat 16 x
6	68°C	20 min
7	4°C	Hold

Table 3.18 PCR mix for Quick Change PCR

Template cDNA (10 ng)	1 µl
Primer fwd (125 ng)	1 µl
Primer rv (125 ng)	1 µl
dNTP	2 µl
10x buffer (Agilent technologies)	5 µl
Pfu Turbo polymerase (Agilent technologies)	1 µl
H_2O	ad. 50 µl

PCR products were analysed on 1.5% TBE buffered agarose gels containing 0.2µg/µl GelRed. For analysis samples were mixed 1:10 with DNA sample buffer. A 1 kb Plus DNA ladder was used to estimate the size of the PCR products. Correctly sized bands were cut under UV light and extracted from the agarose using the NucleoSpin Gel and PCR clean-up kit.

3.2.1.2. RESTRICTION

The PCR products or gBlocks were subcloned into the HindIII and XhoI sites of a pcDNA3.1 Hygro(+) vector. Restriction was performed for 2 h at 37°C. Restriction endonucleases were obtained from Thermo Fisher or New England Biolabs and used according to the manufacturer's instructions. Restriction products were cleared from enzymes using the NucleoSpin Gel and PCR clean-up kit.

Table 3.20 Restriction mix per sample

PCR product	20 µl
Restriction enyme 1 (HindIII)	1 µl
Restriction enzyme 2 (Xho I)	1 µl
Buffer (buffer red)	3 µl
H_2O	ad. 30 µl

3.2.1.3. LIGATION

The digested PCR products were ligated into the pcDNA3.1 Hygro(+) vector for 4 h at RT or overnight at 4°C. The composition of the ligation mix is shown in Table 3.21.

Table 3.21 Ligation mix

Cleaved vector	2 µl
Insert	15 µl
T4 ligase buffer 10x	2 µl
T4 ligase	1 µl

3.2.1.4. TRANSFORMATION INTO COMPETENT CELLS

For transformation, competent *E.coli* DH5α cells were generated. To this end, *E.coli* were cultured overnight in 3 ml of LB media. This pre-culture was transferred into 800 ml fresh LB media and incubated at 37°C until an OD_{600} of 0.5 was reached. The suspension was centrifuged at 1 500 g for 10 min and pellets were resuspended in $CaCl_2$ buffer. The bacteria were incubated for 30 min on ice and centrifuged again at 1 500 g for 10 min at 4°C. The pellet was resuspended in $CaCl_2$-Glycerin buffer and stored at -80°C until use.

PCR-generated cDNA constructs were transformed into the competent cells via heat shock. 50 µl of competent cells were thawed 10 min on ice and then 10 µl of the cDNA-containing plasmid was added. The samples were incubated for 10 min on ice, 2 min at 42°C and 2 min on ice again. 1 mL of sterile LB media was added before the samples were incubated for an hour at 37°C and subsequently plated on LB agar plates containing ampicillin. The plates were incubated at 37°C overnight to select for ampicillin resistant clones.

3.2.1.5. PLASMID PREPARATION

Ampicillin resistant clones were selected and transferred into 4 ml LB media with ampicillin and incubated overnight at 37°C. The bacteria were centrifuged at 1 500 g for 10 min and the pellet was resuspended in 100 µl Solution 1. 200 µl Solution 2 and 150 µl Solution 3 were added. In between, the samples were softly shaken. Then, samples were centrifuged at 17 000 g for 10 min at 4°C. The supernatant was collected in a new reaction tube and 1 ml 98 % EtOH was added. Samples were again centrifuged as before. After

centrifugation, the supernatant was removed and the pellets were washed with 500 µl 70 % EtOH. After another centrifugation step, the pellets were dried and resuspended in 20µl H_2O with 10 % RNase. Insertion of cDNA was verified by restriction endonuclease digestion and agarose gel electrophorese. Photometric analysis of DNA concentration was performed using a UV-Vis Nano-Photometer (Table 3.1).

3.2.1.6. SEQUENCING

All constructs were sequence-verified prior to experimental use. DNA was sequenced by GATC Biotech (Konstanz, DE). For the Sanger sequencing, either standard GATC or self-designed primers were used. Sequence analysis was performed using the CLC Main Workbench (Table 3.2).

3.2.2. CELL CULTURE

Cell culture procedures were performed under laminar flow hoods. Cells were cultivated in the according media (Table 3.9) in water-jacket incubators with a humidified atmosphere containing 5 % (v/v) CO_2. Cells were passaged every 3 - 4 days by Trypsin-EDTA digest. Therefore, cells were washed with PBS to remove all traces of serum. Trypsin-EDTA was added for 5 min, detached cells were collected in a reaction tube and centrifuged at 1 200 g for 5 min. The pellet was resuspended in 4 - 5 ml of the according culture media and plated into a new petri dish.

When plated for experiments, cells were seeded onto Poly-L-lysine coated plates. Plates were coated for at least 45 min with 100 µg/ ml Poly-L-lysine, followed by one wash with PBS and one wash with H_2O. Cell culture media used during experiments did not contain any antibiotics.

3.2.2.1. TRANSFECTION

HEK293 cells stably expressing ectopic SPPL2a or SPPL2b have been described earlier (Martin et al., 2008). To induce expression of the respective SPPL2 protease, cells were incubated with 1 µg/ ml doxycycline added to an otherwise antibiotic free medium,

at least 24 h before transient transfection of SPPL2 substrates. Transient transfection of cells was carried out using Lipofectamine 2000 and OpitMEM according to the manufacturer's instructions. Cells were transfected with 2µg of the according cDNA at a density of 60 - 80 %.

3.2.2.2. INHIBITOR/ ACTIVATOR TREATMENT

To inhibit SPPL2 activity cells were treated with a final concentration of 30-50 µM $(Z\text{-}LL)_2$-ketone. Treatment with 5 µM of GI + 1 µM of BMS-561395 or 50 µM TAPI was applied to inhibit ADAM10/17 enzymatic activity. Inhibitors were added directly after transient transfection of the cells. Treatment lasted up to 24 h after transfection. DMSO was added to the untreated control cells in equal volumes as the respective inhibitor. To activate ADAM17 activity, cells were treated 4 h before collection with 1 µM PMA.

3.2.2.3. GENERATION OF SPPL2A/B KNOCKOUT HEK293 USING CRISPR/ CAS9

Depletion of SPPL2a and/ or SPPL2b was performed according to the protocol of Ran et al. in T-RexTM 293 HEK (TR) cells (Ran et al., 2013). Commercially available guide RNAs (Sigma Aldrich) were used for targeting the SPPL2a or SPPL2b gene. For SPPL2a, a human GFP-tagged guide RNA binding to exon 1 was used. Studies of SPPL2a-deficient patients showed that disruption of exon 1 depletes protein expression completely (Schneppenheim et al., 2014). SPPL2b GFP-tagged guide RNA was chosen to bind to exon 4 to target all different splice variants. SPPL2a/b double knockout was achieved by transfecting validated TR SPPL2b knockout clones with SPPL2a guide RNA.

24 h after transfection, GFP expression was controlled using a LSM 710 Zeiss Observer Z.1 confocal microscope. 48 h after transfection cells were submitted to FACS based single cell sorting and sorted for the GFP signal. The sorting was carried out at the sorting facility of the Institute for Cardiovascular Prevention (IPEK, Munich, DE) with a BD FACSAria™III. The cells were sorted into flat bottom 96-well plates. After two weeks, colonies were progressively transferred into larger plates. Clones were subsequently washed with PBS, centrifuged at 1 200 g and frozen at -80°C until further use.

3.2.2.4. VALIDATION OF KNOCKOUT BY PCR AND WESTERN BLOTTING

Knockout of SPPL2a was validated on protein level using Western Blot (WB) analysis. Only clones with undetectable levels of SPPL2a were subjected to genomic DNA (gDNA) analysis. Knockout of SPPL2b could not be validated via WB due to inefficient antibody detection, so all clones were analysed using PCR.

gDNA was extracted by adding 500 µl of gDNA Lysis buffer to the cells and subsequent incubation at -80°C for 1 h. Then, 1.5 ml gDNA precipitation buffer was added and samples were incubated for 30 min at RT. Samples were centrifuged at 17 000 g for 15 min at 4°C and washed with 1 ml 70 % ethanol. After an additional centrifugation step, the pellet was dried and resuspended in 100 µl of TE buffer. 1 µl of DNA was subjected to PCR amplification. As a control, gDNA from non-modified TR cells was used.

In order to ensure specific amplification, nested PCR was performed with two sets of primers for each gRNA. The first primer pair amplified a region of 700 - 1 000 bp, while the second primer pair amplified a region of 200-400 bp within the first region (Table 3.22). PCR samples from the second PCR were run on an 1.5 % agarose gel in TBE. After confirming a single band on the agarose gel, samples were denatured and reannealed either with themselves or in combination with the wt DNA isolated from control HEK293 cells. Composition of the PCR mix and PCR program are listed in Table 3.23 and Table 3.24 respectively.

Table 3.22 Primers used for nested PCR

1st SPPL2a	Primer fw: AGTGAGCAACTATCGAGAAG
	Primer rv: AGCCGGAAAGCGACA
2nd SPPL2a	Primer fw: GCGAGGAGTAGGGGAAG
	Primer rv: GGGTTTCCGCATCTTACG
1st SPPL2b	Primer fw: AGAGTGCCATCCCTGTC
	Primer rv: GAGGCAGGCGTCAGA
2nd SPPL2b	Primer fw: GCGAATGGGCACAGAG
	Primer rv: CCTGATCCCACCAACTGA

Table 3.24 Denaturing and reannealing sample composition

Self-reannealing	Reannealing with WT
2 µl 2nd PCR product	1.5 µl 2nd PCR product + 1.5 µl TR wt PCR
2 µl T7 buffer	2 µl T7 buffer
16 µl H2O	15 µl H2O

Table 3.23 Denature/ reannealing PCR program

Temperature	Time
95°C	2 min
-2°C/ s to 85°C	-
-0.1°C/ s to 25°C	-
16°C	hold

After reannealing, 4 µl DNA loading buffer were added to 15 µl of sample and loaded on a DNA acrylamide gel (Table 3.15). The gels were run for 4-5 h in 1 x TBE at 30 V and subsequently stained with 0.2 µg/ml GelRed for 30 min in TBE. 1 kb Plus DNA ladder was used to assess the length of the DNA fragment under UV light.

Clones with homozygous dsDNA showed only one band, whereas mismatched DNA ran as multiple bands. Clones that differed in their band pattern from the wt control but were homozygous were selected for sequencing (Section 3.2.1.6). For each single knockout and for the SPPL2a/ b double knockout one clone with an early stop codon was selected for further use. Potential off target effects were excluded using NCBI Nucleotide BLAST.

3.2.3. BIOCHEMICAL METHODS

3.2.3.1. PROTEIN EXTRACTION FROM CELLS (MEMBRANES/ LYSATE)

Depending on the location of the proteins, two different methods of extraction were used. The first method extracted and enriched for proteins in the cellular membranes. For this, cells were washed with PBS and harvested on ice before mixing and lysis for 10 min in ice-cold hypoton buffer supplemented with protease inhibitor mix (1:500) followed by a homogenising using a 23 G needle. Membranes were isolated by two centrifugation steps, first for 5 min at 16 000 g to remove cell debris and second for 45 min at 17 000 g to pellet the membranes. The pellet was resuspended in basic buffer and samples were incubated at 37°C for indicated times to allow proteolysis. Subsequently proteins were precipitated with chloroform/ methanol (2:1) and, most commonly, resuspended in 20 µl 2 x sample buffer.

The second method was used to isolate proteins and peptides from total cell lysates. Cells were shortly mixed and lysed for 20 min in ice-cold STEN lysis buffer. Cell debris was removed by centrifugation for 20 min at 16 000 g. Anti-Flag®M2 affinity gel (Sigma Aldrich) was used to precipitate all soluble protein fragments. After overnight incubation on a shaker, beads were washed 3 x with STEN buffer. 10 µl 5 x sample buffer was added and all probes were incubated 10 min at 95°C before subjection to gel electrophoresis.

For detection of palmitoylated proteins cell membrane were isolated as described above until the second centrifugation step. Then the pellet was resuspended in quenching buffer and incubated for 2 min at 40°C to block free thiol groups. Afterwards samples were precipitated with $CHCl_3$/ MeOH as described above. After centrifugation, the pellet was resuspended in 400 µl binding buffer and split into two. One half was treated with 0.5 M NH_2OH to remove the palmitic acid from the protein and the other half was treated with 0.5 M Tris-HCl. 15 µl Thiopropyl-Sepharose®6B was added and samples were incubated overnight at 4°C. After 5 min centrifugation at 1 200 g at 4°C the supernatant was transferred into a new tube and residual protein was immunoprecipitated with anti-Flag®M2 agarose affinity gel. Immunoprecipitated samples were washed 3 x with 1 x STEN. 10 µl 5 x sample buffer was added and probes were incubated 10 min at 95°C before gel electrophoresis.

3.2.3.2. ISOLATION OF PEPTIDES FROM MEDIA

Proteins that were secreted into the conditioned cell culture media were immunoprecipitated using the V5 polyclonal antibody with protein A sepharose beads, the V5 monoclonal antibody (Table 3.10) with protein G sepharose beads or anti-Flag®M2 agarose affinity gel. After overnight incubation, samples were washed 3 x with STEN buffer, 10 µl 5 x sample buffer was added and probes were incubated for 10 min at 95°C.

For samples that released high amounts of peptide into the media, 5 x SB buffer was directly added 1:5 to the conditioned media. The samples were denatured at 95°C for 10 min before gel electrophoresis.

3.2.3.3. ELECTROPHORESIS/ IMMUNOBLOTTING

For separation of proteins smaller than 16 kDa a modified Tris-tricine gel was used (Table 3.14) (Fluhrer et al., 2006). Larger proteins were separated on 12 % Tris-glycine gel (Table 3.13). The gels were run at 70 V until the samples were concentrated at the border of stacking and separating gel and then run at 120 V. The See Blue Plus Protein ladder was used for estimating the molecular weight of the proteins.

Samples were blotted on isopropanol activated polyvinylidene fluoride (PVDF) membranes or – for cleavage products tagged with a V5-tag and smaller than 6 kDa - on nitrocellulose membranes by wet transfer for 1 h at 400 mAmp/ chamber. Blocking of unspecific antibody binding was performed by using Tropix® I BlockTM solution for 1 h at RT. The membranes were incubated with primary antibodies (Table 3.10) overnight at 4°C and washed 3 x with TBS-T before incubation for 1 h at RT with secondary HRP coupled antibodies (Table 3.11). After additional three washing steps, proteins were incubated with Pierce™ ECL Western Blotting Substrate or Westar Antares for increased sensitivity. The chemiluminescence was detected on X-ray films (Table 3.1). To digitalize the films, they were scanned with an Epson Perfection V700 Photo scanner. The brightness was adjusted using Photoshop. For quantification of the protein signal, the chemiluminescence was detected with a CCD camera-based imaging system (Table 3.1) and analysed using the Multi Gauge software (Table 3.2).

3.2.3.4. FLOW CYTOMETRY

To detect proteins on the cell surface, samples were subjected to flow cytometry. Cells were washed with PBS and harvested on ice. The cell count was adjusted to 1-5 x 10^6 cell/ ml in FACS buffer. 100 µl of cell suspension were transferred into a new reaction tube and centrifuged at 400 g for 5 min. The cell pellet was resuspended in PBS supplemented with 3 % FCS and V5 monoclonal antibody (Table 3.10). Controls of untransfected cells and transfected cells without primary antibody staining were included in the analysis. The samples were incubated for 30 min at RT or on ice. Afterwards samples were washed 3 x with PBS and stained with anti-mouse Alexa 488 (Table 3.11). Samples were again incubated for 30 min on ice or RT in the dark and afterwards washed 3 x with PBS before flow cytometry. Viable cells were gated for side scatter (SSC-A) vs. front scatter (FSC-A). These cells were then gated for single cells by side scatter-width (SSC-W) vs. side scatter-

height (SSC-H) and front scatter-width (FSC-W) vs. front scatter-height (FSC-H). GFP positive cells were gated from this population.

3.2.3.5. MASS SPECTROMETRY WITH MALDI-TOF

To identify the exact length of peptides that resulted from protease cleavage, samples were analysed with matrix-assisted laser desorption/ionisation – time of flight (MALDI-TOF) mass spectrometry. Secreted peptides from media were precipitated as described above (Section 3.2.3.2). Membrane proteins were isolated as described in section 3.2.3.1 and solubilized in SPP stock buffer supplemented with 2 % of DDM and incubated 30 min on ice before centrifugation at 16 000 g at 4°C. Solubilized peptides were immunoprecipitated using anti-Flag®M2 agarose affinity gel. All samples were washed 3 x with mass spec washing buffer and de-salted by two washes with dH_2O.

For the analysis of peptides generated from Flag TNFα FlagTEV V5, the fragments were immunoprecipitated with anti-Flag®M2 agarose affinity gel overnight and subsequently eluted from the beads with 100 mM glycine pH 2.5. Cleavage at the TEV site was facilitated with a commercially available kit according to the manufacture's instructions (Table 3.6). Resulting peptides were precipitated with the anti-Flag®M2 agarose affinity gel for 1 h at RT followed by 3 washes with mass spec washing buffer and 2 washes with dH_2O.

Samples were subjected to analysis by mass spectrometry using a α-cyano-4-hydroxycinnamic acid matrix mixed 1:1 with acetonitrile and 0,6 % TFA. Three times 0,4 µl of sample were spotted on a 384-spot plate (Applied Biosystems) and left to dry at RT. Mass spectra were recorded in the linear mode and analysed with the Data Explorer Software (Table 3.2). Intensities were normalised to the internal maximum.

3.2.4. STATISTICAL ANALYSIS

Quantifications and differences in surface expression were statistically analysed with GraphPad (Table 3.2). If not stated differently, at least three biological replicates were performed for the statistical analysis. To enable comparison of increased vs. decreased

samples, measured values were transformed to log2 and the wt samples was set to 0. For the comparison of two groups, an unpaired, two-tailed student's t-test was applied if groups comprised equal sample numbers and a Welch's test in case of unequal group size. For comparison of more than two groups, a two-way ANOVA test was used. Significance is indicated in the respective figure legend.

4. RESULTS

4.1. GENERATION OF SPPL2A/B-DEFICIENT CELL LINES

In order to investigate the proteolytic mechanism of human SPPL2a and SPPL2b, the proteases were ectopically expressed in T-Rex™-293 (HEK293) cells (Fluhrer et al., 2008). As control, single and double SPPL2a/b-deficient cell lines were generated using the CRISPR/ Cas9 genome-editing technique. With commercially available guide RNAs (gRNA), the SPPL2a and SPPL2b genes were targeted, which resulted in several homozygous clones. Due to the deletion of several nucleotides, frameshift mutations occurred. However, not all of them induced a premature stop codon. An SPPL2a clone with a deletion of 4 bp generating a stop codon at position 20 was chosen for further analysis (Figure 4.1). In this clone no SPPL2a protein was detectable (Figure 4.2B). To target all splice variants of SPPL2b a gRNA was chosen that induced a frameshift by deleting 11 bp generating a stop codon at position 135 (Figure 4.1). Protein levels of SPPL2b could not be tested, as no antibodies detecting endogenous SPPL2b in HEK293 cells are available.

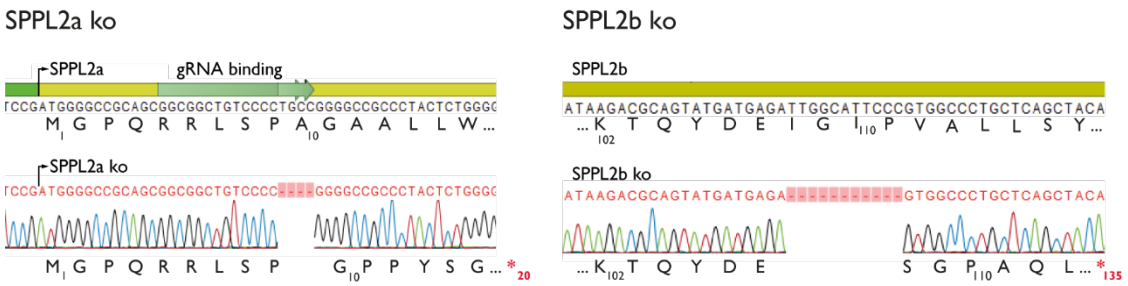

Figure 4.1 Genomic sequences of SPPL2a and SPPL2b-deficient cell lines. SPPL2 guide RNA (gRNA) generated frameshift mutations leading to a premature stop codon. The SPPL2a protein was translated up to amino acid 20, and SPPL2b protein up to amino acid 135 (Spitz et al., 2020).

In addition to single knockout clones, a cell line deficient for SPPL2a and SPPL2b was generated. To this end, the previously established SPPL2b-deficient clone was transfected with SPPL2a gRNA. This resulted in the deletion of 17 bp and a premature stop codon at position 40 of the SPPL2a protein (Figure 4.2A). The double deficient clone was tested for SPPL2a protein and no SPPL2a was detectable (Figure 4.2B).

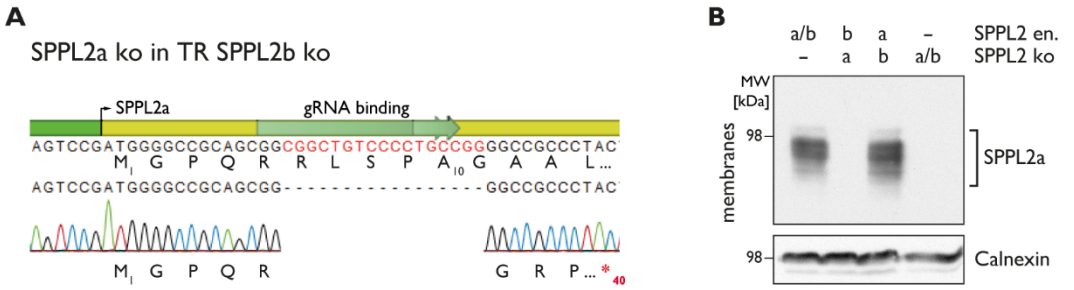

Figure 4.2 Characterisation of the SPPL2a/b-deficient cell line. (A) To generate an SPPL2a/b-deficient cell line, SPPL2a guide RNA was applied to SPPL2b-deficient cells. SPPL2a guide RNA generated a frameshift resulting in a premature stop codon at amino acid 40. **(B)** Expression of SPPL2a in CRISPR/Cas9 treated cell lines. Endogenous (en.) SPPL2a levels were not affected in SPPL2b knockout cells, while no SPPL2a was detectable in the single SPPL2a and the double SPPL2a/b-deficient cell lines (Spitz et al., 2020).

4.2. SHEDDING

4.2.1. SPPL2A ACTS AS A NON-CANONICAL SHEDDASE

Among the above-mentioned substrates, TNFα has the most prominent functions throughout the human body and is well characterised. When TNFα is transported to the cell surface, it is usually shedded by ADAM10 or ADAM17 to release the majority of its ECD (McGeehan et al., 1994). T-Rex™-293 (HEK293) cells with endogenous expression of ADAM17, SPPL2a and/ or SPPL2b were transiently transfected with C-terminally V5-tagged TNFα. The ECD released upon shedding is detected at about 22kDa (sTNFα) (Figure 1.3). However, a second, slightly larger fragment was isolated along with the ADAM-cleaved ECD (sTNFα) in cells with endogenous SPPL2a expression (sTNFα(L2)). As ADAM10/17 levels were not changed it seems that TNFα is shedded by another protease. Based on the fact that the larger fragment was not detectable in SPPL2a-deficient cells irrespectively of SPPL2b expression, it seems that SPPL2a is able to cleave TNFα full-length (FL) directly without a preceding shedding by ADAM17. According to the definition of shedding (Section 1.2.1), this process was termed non-canonical shedding.

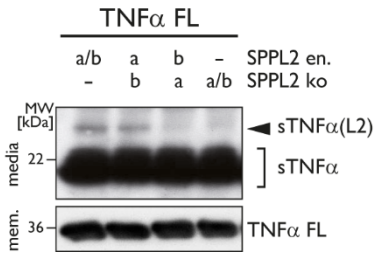

Figure 4.3 Non-canonical TNFα shedding by endogenous SPPL2a. Soluble TNFα ECDs were isolated from conditioned media of HEK293 cell lines expressing endogenous (en.) levels of SPPL2a, SPPL2b, both or none (ko). The V5-mono antibody was used for visualisation. Detection of TNFα full-length (FL) in the membranes served as transfection control. sTNFα(L2): TNFα ECD secreted by SPPL2-mediated shedding; sTNFα: TNFα ECD secreted by ADAM-mediated shedding (Spitz et al., 2020).

To further support the hypothesis of TNFα non-canonical shedding by SPPL2a and to exclude that sTNFα(L2) production by SPPL2b was not just missed due to low endogenous SPPL2b expression, SPPL2a or SPPL2b were ectopically expressed in HEK293 cells that additionally express endogenous SPPL2a or SPPL2b. While ectopic SPPL2a expression significantly increased sTNFα(L2) secretion compared to control cells, ectopic expression of SPPL2b did not (Figure 4.4). This supports that SPPL2a is capable of non-canonical shedding, while SPPL2b hardly accepts TNFα FL as substrate.

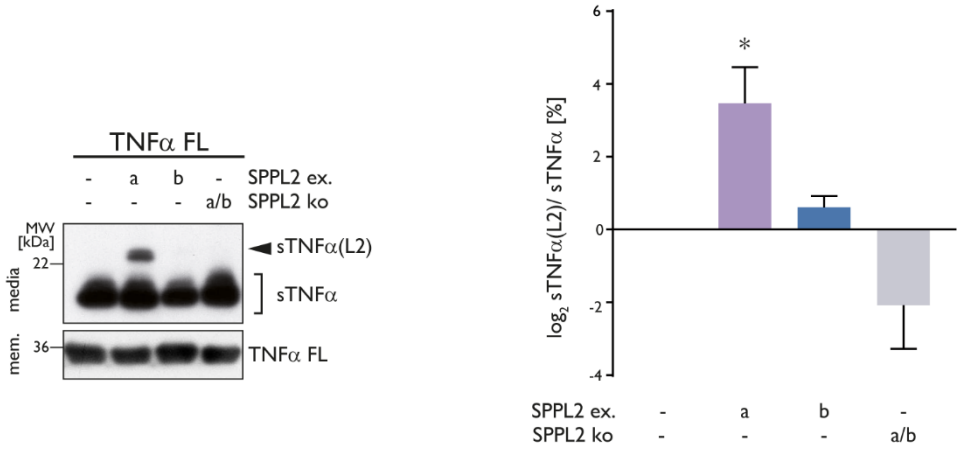

Figure 4.4 sTNFα(L2) secretion is increased upon ectopic SPPL2a expression (ex.). Soluble TNFα(L2) was directly analysed from conditioned media, quantified relative to sTNFα from Western Blots (WB) by densitometric analysis and normalized to untreated controls, n=3. Data are represented as mean +/- SD. Statistical significance was calculated applying an unpaired, two-sided Student's t-test. *: $p<0.05$. The WB shows one representative experiment. TNFα FL was used as transfection control (Spitz et al., 2020).

Whereas ectopic expression of SPPL2a enhanced non-canonical shedding of TNFα, treatment with $(Z\text{-}LL)_2$-ketone, an SPP/ SPPL specific inhibitor, significantly reduced generation of sTNFα(L2). Canonical shedding by ADAM was unaffected by this treatment (Figure 4.5). Even though ADAM17 is considered the major sheddase for TNFα, other ADAMs are able to partake in the release of the ECD (Zheng et al., 2004). Therefore, cells were treated with ADAM10 and ADAM17-specific inhibitors (AI), which resulted in a significant reduction of sTNFα, while sTNFα(L2) remained unchanged compared to the

respective non-treated cells (Figure 4.5). Treatment with the ADAM activator, phorbol 12-myristate 13-acetate (PMA) stimulates ADAM17 activity and thus, increased canonical shedding and sTNFα secretion, but not sTNFα(L2) release (Figure 4.5). This demonstrated that sTNFα(L2) secretion is independent of sTNFα secretion, suggesting that ADAM10/17 and SPPL2a are not competing for cleavage of TNFα.

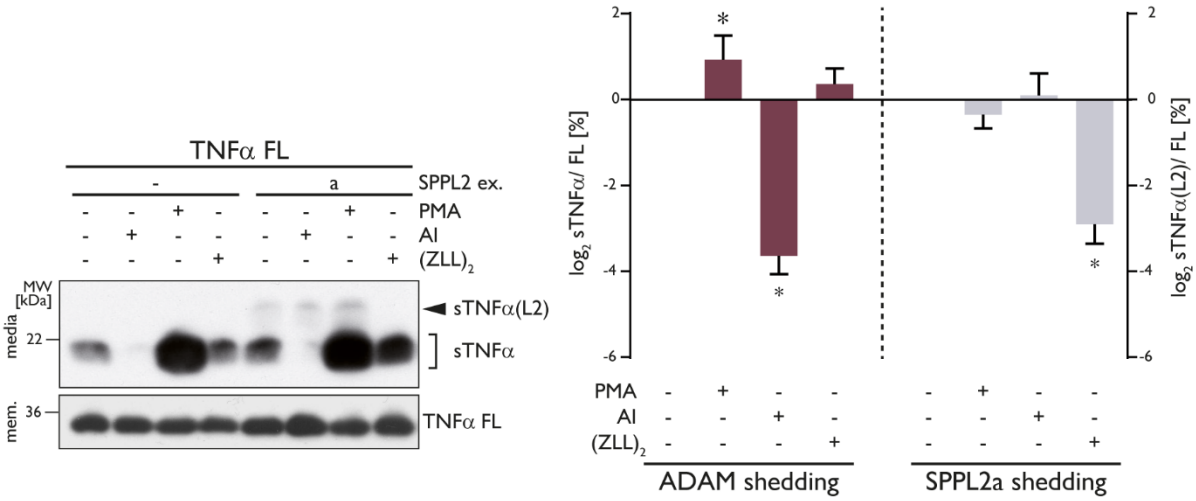

Figure 4.5 Canonical and non-canonical shedding of TNFα are two independent processes. TNFα ECDs from conditioned media of the indicated HEK293 cell lines were isolated and detected with the V5-mono antibody. Cells were treated with either 50µM Z-LL_2-ketone (+ $(ZLL)_2$) to inhibit SPPL2 catalytic activity, with 5µM GI 254023X and 1µM BMS-561395 (+ AI) to inhibit ADAM proteases or 1µM phorbol 12-myristate 13-acetate (PMA) to activate ADAM17 cleavage. Controls were treated with DMSO (-). The expression of TNFα FL was used as transfection control. Quantification of sTNFα(L2) was calculated relative to intracellular TNFα FL by densitometric analysis from WB and normalized to untreated controls; n=3. Data are represented as mean +/- SD. Statistical significance was calculated applying a two-way ANOVA, *: p<0.05. (Experiments depicted in this figure were conducted by Christine Schlosser.) (Spitz et al., 2020)

4.2.2. IDENTIFICATION OF SPPL2A CLEAVAGE SITES IN TNFα

A previous study has identified SPPL2b cleavage sites in TNFα in the context of RIP (Fluhrer et al., 2006). To investigate whether SPPL2a cleavage sites differ from that of SPPL2b, SPPL2a-mediated cleavage of truncated TNFα was analysed by MALDI-TOF mass spectrometry. To detect C-peptides that are released by SPPL2 proteases in context of RIP, a short TNFα protein that carried a C-terminal Flag-tag stabilized by alanine and proline (TNFα NTF-FlagAP) was used. Analysis of TNFα C-peptides released by SPPL2b cleavage confirmed the previously described major cleavage sites at L50 and H52 (Figure 4.6). Moreover, two smaller C-peptides were identified resulting from cleavages at V55 and R60. Surprisingly, these cleavages occurred in the JMD, outside of the membrane. Due to the use of radiosequencing, these cleavage sites had not been detected in the previous

study. Essentially, SPPL2a secreted the same peptides, although the shorter C-peptide species were less abundant (Figure 4.6). Untransfected cells were included to control for background signals. Table 4.1 lists the exact masses of the measured and calculated peptides.

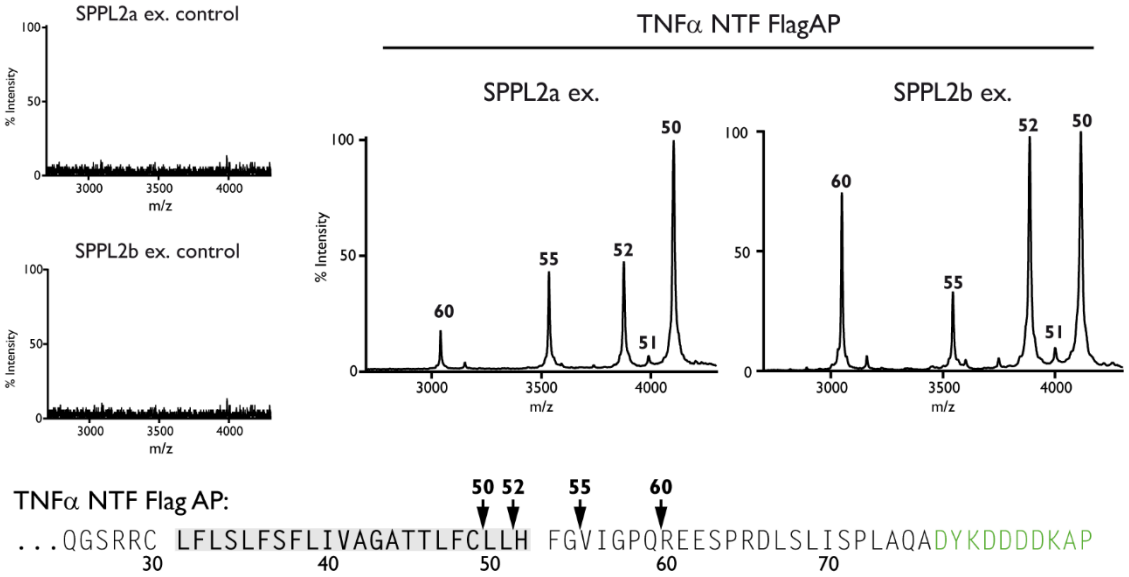

Figure 4.6 C-terminal cleavage sites in TNFα NTF. Mass spectrometric analysis of TNFα C-peptides generated by SPPL2a or SPPL2b, respectively. Numbers indicate the position of the most N-terminal amino acid of the respective cleavage product. Media of untransfected controls were included to decipher unspecific peaks. Cleavage sites are indicated in the TNFα sequence with arrows. The TMD is indicated in grey and the FlagAP-tag in green (Spitz et al., 2020).

Table 4.1 Masses of TNFα C-peptides measured by MALDI-TOF compared to calculated masses. Measured values are normalised to the calculated mass of the peptide resulting from cleavage at position 50.

C-Peptide (cleavage position)	Calculated mass (in Da)	Measured mass (in Da)	
		SPPL2a	SPPL2b
60	3045	3044	3041
55	3540	3539	3537
52	3881	3881	3879
51	3987	3993	3982
50	4107	4107	4107

To solidify whether SPPL2a cleavage sites in the context of non-canonical shedding and RIP differed, an internal Flag-tag followed by a TEV cleavage site was inserted into TNFα FL (Figure 4.7A). The TEV cleavage site enabled removal of the large TNFα ECD just before subjecting the samples to mass spectrometry and thus allowed detection of the SPPL2a cleavage sites in TNFα FL. In addition, the FlagTEV site was inserted four amino

acids C-terminal of the ADAM cleavage site to ensure also detection of peptides generated by canonical shedding.

It was confirmed that TNFα FlagTEV was similarly processed as TNFα wt (Figure 4.7B). Both proteins were shedded by ADAM10/17 and SPPL2a resulting in the release of sTNFα and sTNFα(L2) respectively. Due to the insertion of the Flag-tag and the TEV site, TNFα FlagTEV, as well as its soluble peptides, are slightly larger. The NTF, which results from canonical shedding, was detectable and further processed into TNFα ICDs (TICD) in both TNFα proteins. Intracellular sTNFα/ sTNFα(L2) has continuously been observed in other experiments (data not shown). Here it was visualised only in the TNFα FlagTEV transfected cells due to the internal Flag-tag. Using flow cytometry, it was confirmed that TNFα FlagTEV was expressed on the cell surface in equal amounts as TNFα wt (Figure 4.7C).

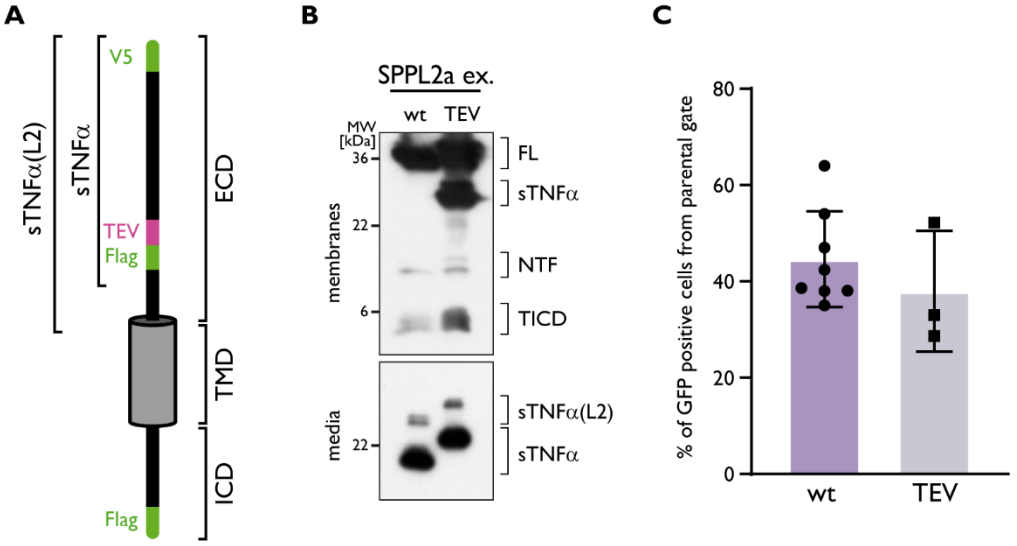

Figure 4.7 Processing of TNFα FlagTEV. (A) Schematic representation of TNFα FlagTEV. **(B)** Processing of TNFα wt and TNFα FlagTEV is essentially similar. Membranes of HEK 293 cells co-expressing (ex.) SPPL2a and the indicated TNFα variant were analysed on WB using the monoclonal FlagM2 antibody to detect intracellular TNFα N-terminal fragment (NTF) and TNFα intracellular domain (TICD). The respective conditioned media were visualised with the monoclonal V5 antibody to detect secreted TNFα ECD variants. **(C)** Surface expression of TNFα wt and TNFα FlagTEV is similar. Cells transiently transfected with the respective TNFα variants were surface stained with V5 mono antibody and then analysed by flow cytometry. GFP positive cells were gated from a single cell population. wt n=8, TEV n=3. Data are represented as mean +/- SD (Spitz et al., 2020).

To analyse the cleavage sites of SPPL2a in TNFα FlagTEV, cleavage products were isolated from conditioned media by immunoprecipitation utilizing the Flag-tag. The isolated protein fragments were enzymatically digested with TEV-protease and peptide fragments containing a Flag-tag were again immunoprecipitated and subjected to MALDI-TOF mass spectrometry. The results revealed two groups of peptides, one reflecting cleavages at previously established SPPL2 sites. The other group comprised smaller

peptides one matching the known ADAM10/17 cleavage sites at position V77 (Figure 4.8) (Mohan et al., 2002). Other minor cleavage sites were detected at L73, L79 and D66. To ensure the larger peptides were indeed generated by SPPL2a cleavage, cells were treated with the SPP/SPPL inhibitor $(Z\text{-}LL)_2$-ketone prior to analysis. This treatment abolished the secretion of all peptides ranging from 4 - 6 kDa, while the secretion of the smaller peptides resulting from ADAM10/17 cleavage remained unchanged (Figure 4.8). This indicates that non-canonical shedding by SPPL2a occurred at the same positions as cleavage in the context of RIP and thus demonstrates that shortened TNFα variants display a valid technique of investigating the C-terminal cleavage sites generated by SPPL2 proteases. Interestingly however, the most dominant cleavage site of SPPL2a-mediated non-canonical shedding mapped to cleavage at V55, while the dominant cleavage sites of RIP-related processing were detected at L50 and H52 (Figure 4.6). Moreover, this result indicates that SPPL2 proteases are able to cleave TNFα at the luminal-membrane border. However, even though unlikely, it cannot be fully excluded that an unrelated exopeptidase present in the conditioned media partakes in the cleavage of TNFα or the released peptides. Table 4.2 lists the exact masses of the measured and calculated peptides.

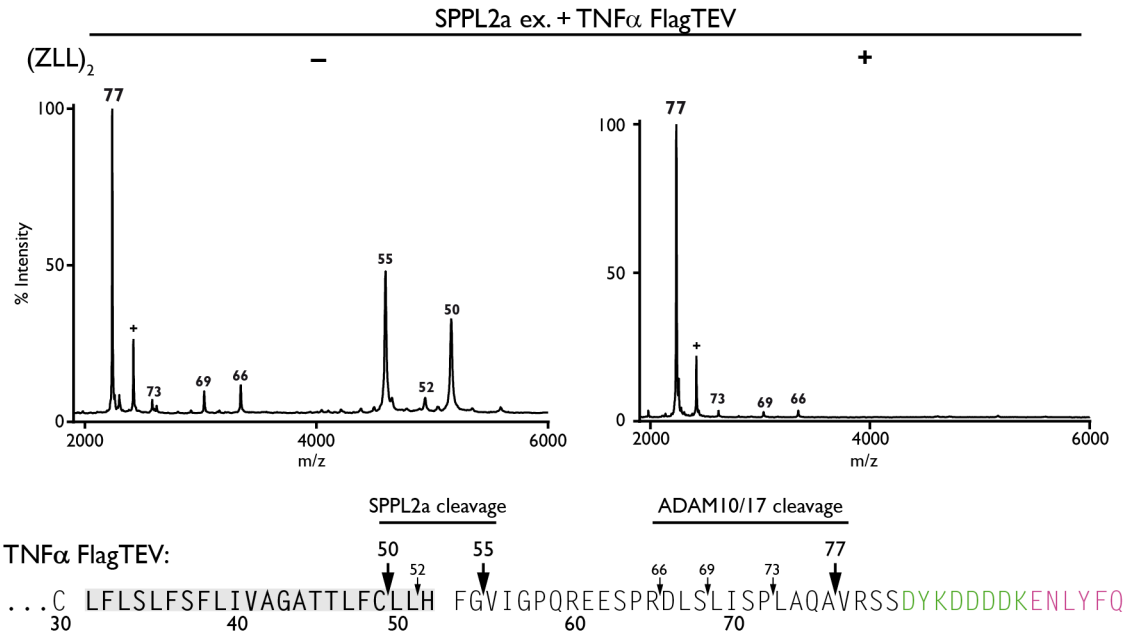

Figure 4.8 C-terminal cleavage sites in TNFα FlagTEV. HEK293 cells co-expressing (ex.) SPPL2a and TNFα FlagTEV were treated with 50µM $(Z\text{-}LL)_2$ or DMSO and secreted ECDs were isolated. Numbers indicate the position of the most N-terminal amino acid of the respective cleavage product. Peaks from 66-77 reflect cleavage of TNFα by ADAM proteases. Peaks from 50-55 reflect cleavage of TNFα by SPPL2a. x marks peak of unknown identity. Cleavage sites are indicated in the TNFα sequence with arrows. The TMD is indicated in grey, the Flag-tag in green and the TEV site in pink (Spitz et al., 2020).

Table 4.2 Masses of C-terminally cleaved TNFα FlagTEV products measured by MALDI-TOF compared to calculated masses. Measured values are normalised to the calculated mass of the peptide resulting from cleavage at position 50.

C-Peptide (cleavage position)	Calculated mass (in Da)	Measured mass (in Da)
77	2237	2233
73	2620	2616
69	3031	3027
66	3346	3343
55	4595	4594
52	4937	4936
50	5163	5163

4.2.3. SHEDDING OF MOUSE TNFα

So far, non-canonical shedding of TNFα was observed only *in vitro*. However, sTNFα is a strong upstream regulator of many cellular signalling pathways (Tseng et al., 2018). To establish a physiological relevance of non-canonical shedding, mouse BMDCs were isolated and analysed for sTNFα and sTNFα(L2) secretion.

While in previous experiments, sTNFα was detected via a C-terminal V5-tag, endogenous mouse TNFα antibodies recognizing both sTNFα and sTNFα(L2) had to be established. Several commercially available antibodies against mouse sTNFα were tested with the Abcam antibody ab9739 recognising both soluble TNFα peptides *in vitro* the best. However, comparing *in vitro* shedding from ectopically expressed mouse and human TNFα, already revealed a different shedding process of mouse TNFα (Figure 4.9A). Detection of soluble peptides with ab9739 resulted in the identification of several mouse TNFα peptides (#1-3, Figure 4.9). In addition to this, the detection of C-terminally V5-tagged mouse TNFα with the V5 mono antibody was inefficient compared to human TNFα. It can only be speculated that mouse TNFα ECD might fold differently impeding accessibility of the tag for the antibody. Moreover, treatment with the SPPL-inhibitor did not diminish the release of any of the soluble peptides (+(Z-LL)$_2$ Figure 4.9A) and they were also detectable in SPPL2a/b-deficient cells. However, fragments were absent when ADAM activity was inhibited (+AI, Figure 4.9A). Thus, mouse TNFα generally seems to be

processed differently. Even though several soluble ECDs are released, they all seemed to originate from canonical shedding by ADAM proteases.

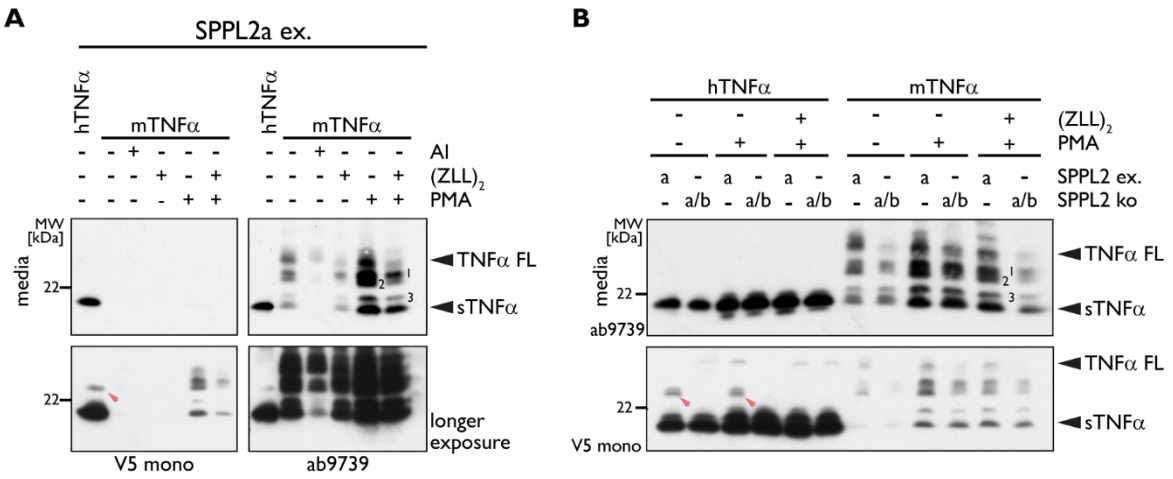

Figure 4.9 Shedding of mouse TNFα is different from human TNFα. (A) ECDs of human (hTNFα) and mouse TNFα (mTNFα) were isolated from HEK293 cells co-expressing (ex.) human SPPL2a. Cells were treated with either 5µM GI 254023X and 1µM BMS-561395 (AI), 50µM $(ZLL)_2$, 1µM PMA, or DMSO as control. Samples were analysed with the V5-mono antibody and with an antibody directed against mouse TNFα ECD (ab9739). sTNFα(L2) is indicated with red arrows. **(B)** The ECDs of TNFα were isolated from conditioned media of cells co-expressing SPPL2a or cells deficient for SPPL2a/b (ko). Cells were treated with either 50µM $(ZLL)_2$ or 1µM PMA and detected as in (A).

These results were confirmed by experiments in BMDCs derived from wt and SPPL2a-deficient mice. Breeding of the mice, as well as isolation of the cells and treatment with or without LPS and ADAM inhibitors, was conducted by collaborators at Dr. Bernd Schröder's Lab. Conditioned media was analysed for the secretion of soluble TNFα peptides. After 24h of LPS stimulation, which induces the secretion of sTNFα, several soluble fragments were detectable (Figure 4.10). However, the secretion of all fragments was reduced when the cells were treated with ADAM inhibitors (Figure 4.10; + AI) and no fragment was notably absent in SPPL2a-deficient mice. These results indicate that SPPL2a does not shed mouse TNFα and that processing of mouse TNFα is generally different compared to human TNFα.

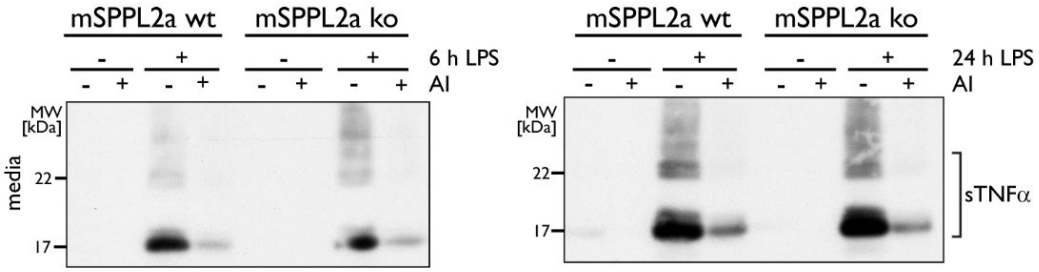

Figure 4.10 TNFα shedding in mice is only facilitated by ADAM proteases. BMDCs of wt (mSPPL2a wt) or SPPL2a-deficient (mSPPL2a ko) mice were isolated and treated for the indicated period with LPS and 20µM marimastat (AI) or DMSO as control. TNFα ECDs were detected with an antibody against mouse TNFα ECD (ab9739).

4.2.4. NON-CANONICAL TNFα SHEDDING CAN BE MODULATED BY TM MUTATIONS

Earlier experiments suggested that cleavage capacity of aspartyl-IMPs is affected by the conformational flexibility of the substrate TMD (Fluhrer et al., 2012, Götz et al., 2019, Langosch et al., 2015, Langosch and Steiner, 2017). The domains of the protein that are embedded in the lipid membrane are usually compacted as α–helix. Amino acids that can affect helix properties in TMDs are asparagine, cysteine, glycine, histidine, proline and serine (Li and Deber, 1994). Amino acids with polar side chains are able to form stabilizing hydrogen bonds with upstream residues (Gray and Matthews, 1984, Scharnagl et al., 2014), while glycine facilitates local helix bending and changes the TMD dynamics (Hӧgel et al., 2018). The positive charge of histidine influences back-bone stability, thus disturbing the helix (Armstrong and Baldwin, 1993). Analysis of the TNFα TMD revealed five of these structurally important residues: S34, S37, G43, C49 and H52. Each residue was substituted by alanine, leucine or proline to specifically alter the TMD dynamics. Alanine but even more leucine have stabilising effects by enabling a rigid helical structure (Quint et al., 2010). In contrast, proline is a strong helix-destabilizer enhancing flexibility of the substrate's TMD (Cordes et al., 2002). All TNFα mutants were co-expressed at similar amounts with SPPL2a in HEK293 cells (Figure 4.11A). Substitutions of S34, S37, G43 and C49 by proline significantly enhanced non-canonical TNFα shedding, while an H52P mutation had no effect. On the contrary, leucine substitutions in all positions decreased non-canonical TNFα shedding, with C49L and H52L having the strongest effect (Figure 4.11C). Alanine substitutions in all positions had only a minor impact on non-canonical shedding. Interestingly, substitution with a proline at G43 had the most pronounced effect of all proline variants on non-canonical shedding, but substitution with leucine in this position barely reduced non-canonical shedding. However, additional substitutions of the flanking alanines with leucines (AGA42,43,44LLL) resulted in an almost complete loss of SPPL2a-mediated non-canonical shedding (Figure 4.11B/C).

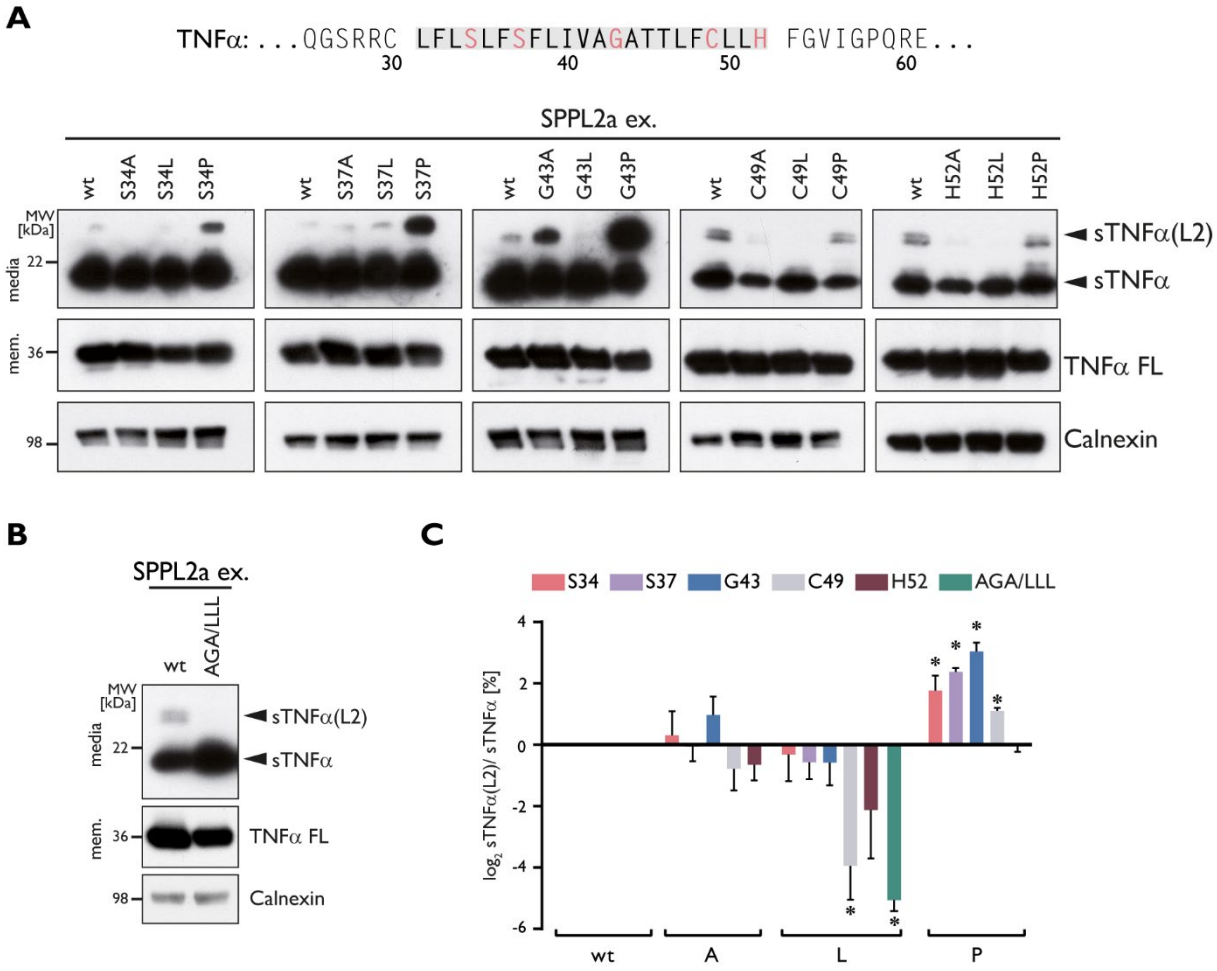

Figure 4.11 Modulating non-canonical TNFα shedding by mutations in the TMD. In the TMD of TNFα, leucine substitutions reduce and proline mutations increase non-canonical shedding significantly. **(A)** Secreted TNFα from media of cells co-expressing (ex.) SPPL2a and the respective TNFα mutant was analysed using the V5-mono antibody. Detection of TNFα FL from membranes served as transfection and calnexin as loading control. **(B)** Representative WB of the AGA/LLL mutant. **(C)** Quantification of (A) and (B). sTNFα(L2) was quantified relative to sTNFα from respective WB by densiometric analysis and normalized to TNFα wt, n=3. Data are represented as mean +/- SD. Statistical significance was calculated applying an unpaired two-sided Student's t-test. *: p<0.05 (Spitz et al., 2020).

Although SPPL2b did not act as a non-canonical sheddase on TNFα wt (Figure 4.4), proline substitutions at positions S34, S37 and again most pronounced at position G43 allowed non-canonical shedding also by SPPL2b (Figure 4.12).

These data demonstrate that the dynamics of the TNFα TMD affect its non-canonical shedding. While increased dynamics and less contact with neighbouring residues induced by proline enhanced non-canonical shedding, tight packing of TMD residues caused by leucines had the opposite effect. Interestingly, leucine substitutions had the strongest impact in the C-terminal part of the TMD, whereas the increase of non-canonical shedding by proline substitutions was most pronounced in the N-terminal half.

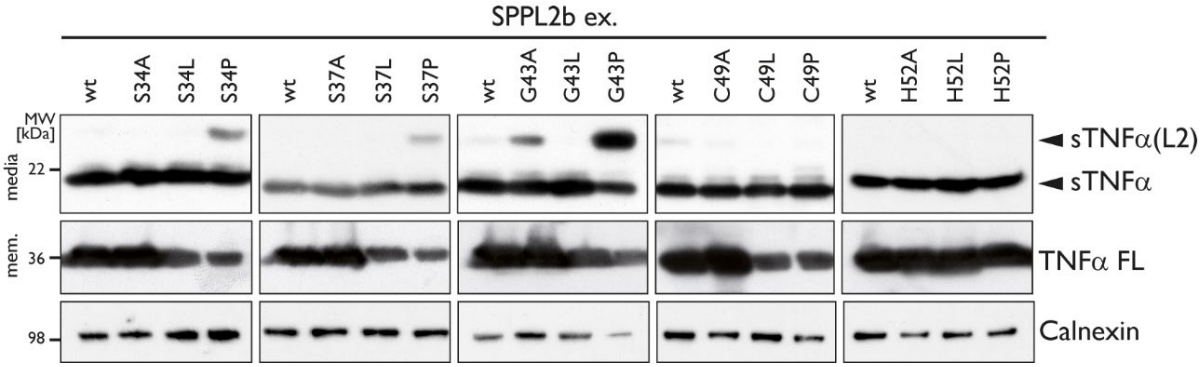

Figure 4.12 Non-canonical shedding of TNFα mutants by SPPL2b. Mutations in the TMD of TNFα induce shedding by SPPL2b. In the media of cells co-expressing (ex.) SPPL2b and the respective TNFα variant secreted TNFα was detected with the V5-mono antibody. Detection of TNFα FL in the membranes served as transfection and calnexin as loading control (Spitz et al., 2020).

To elucidate whether increased non-canonical shedding induced by proline substitutions also altered the SPPL2a cleavage sites, TNFα variants were analysed by mass-spectrometry. Proline substitutions that significantly increased non-canonical shedding (S34P, S37P, G43P and C49P) did not change SPPL2a cleavage sites (Figure 4.13). Interestingly, H52P substitution, which had no effect on non-canonical shedding, resulted in an almost complete loss of the major cleavages close to the substitution site. In contrast, exchange at position C49, which also locates close to an SPPL2a cleavage site, did not result in loss of any specific cleavage product. Proline substitutions at S34 and S37 relatively increased cleavage at H52 and G43P cleavage at R60. The triple leucine substitution enabled an additional cleavage site at I56, but overall position L50 remained the major cleavage site.

These data may indicate that cleavage by SPPL2a is to a certain degree dependent on primary sequence requirements as the cleavage at H52 is disrupted by a proline substitution. However, the secondary structure and charges of amino acids close to the cleavage site seem to be more important since amino acids that introduced disruptions or tightened the TMD helix as well as the change of the charges significantly changed cleavage efficiency. By altering the TMD structure substitutions were able to exert effects on cleavage even if not placed at a cleavage site directly. Table 4.3 lists the exact masses of the measured and calculated peptides.

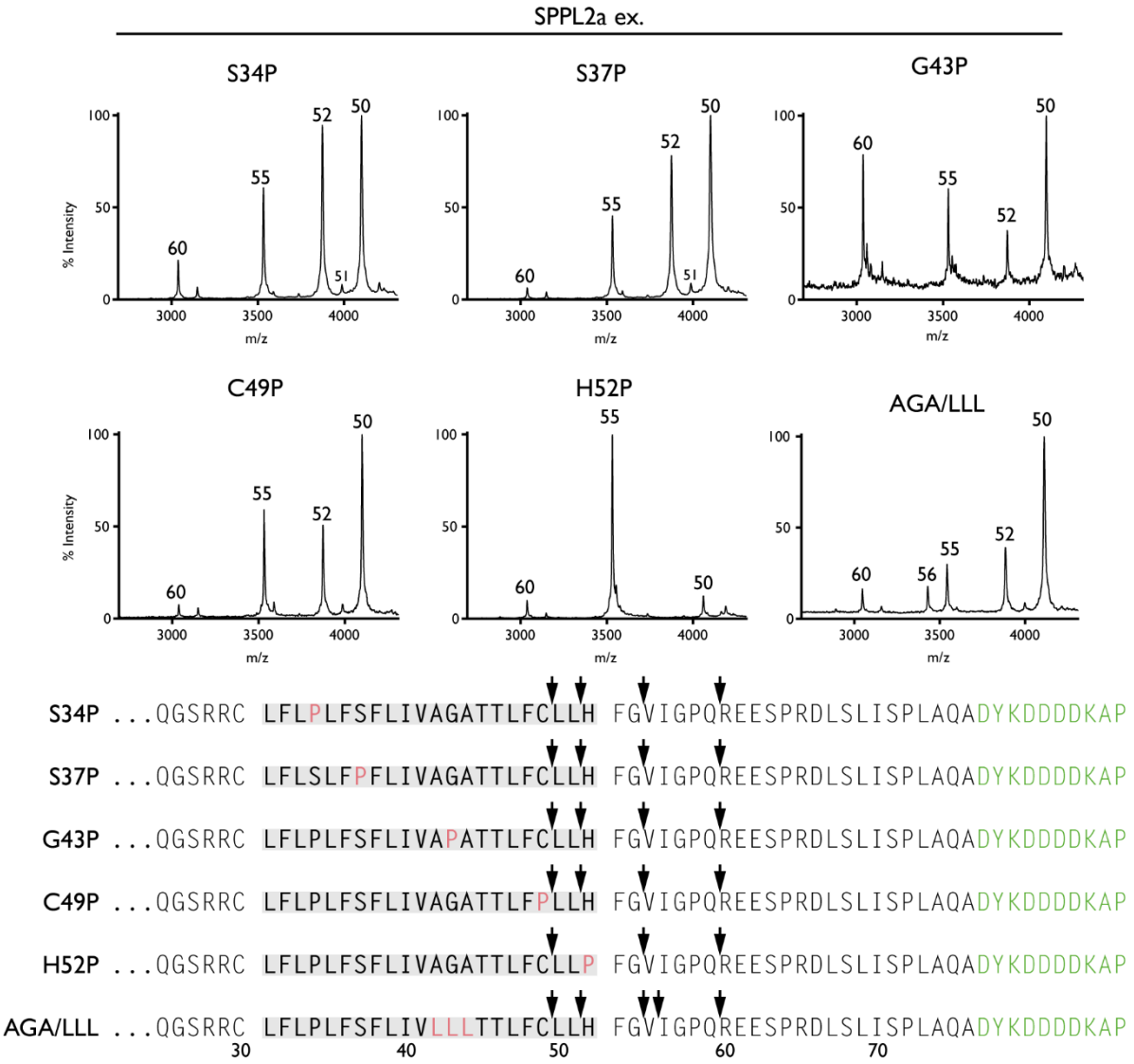

Figure 4.13 C-terminal cleavage sites in TNFα TMD mutants largely remain unchanged. Secreted ECD from HEK293 cells co-expressing (ex.) SPPL2a and the indicated TNFα variants were isolated with the FlagM2 antibody. Numbers indicate the position of the most N-terminal amino acid of the respective cleavage product. Cleavage sites are indicated with arrows. Substituted amino acids are indicated in pink, the TMD in grey and the FlagAP-tag in green (Spitz et al., 2020).

Table 4.3 Masses of TNFα variant C-peptides measured by MALDI-TOF compared to calculated masses. Measured values are normalised to the calculated mass of the peptide resulting from cleavage at position 50.

TNFα variant	C-Peptide (cleavage position)	Calculated mass (in Da)	Measured mass (in Da)
S34P	60	3045	3044
	55	3540	3539
	52	3881	3881
	51	3994	3994
	50	4107	4107
S37P	60	3045	3044
	55	3540	3539
	52	3881	3880

	51	3994	3993
	50	4107	4107
G43P	60	3045	3045
	55	3540	3539
	52	3881	3881
	50	4107	4107
C49P	60	3045	3045
	55	3540	3540
	52	3881	3880
	50	4107	4107
H52P	60	3045	3045
	55	3540	3540
	50	4067	4067
AGA/LLL	60	3045	3041
	56	3441	3435
	55	3540	3537
	52	3881	3880
	50	4107	4107

4.2.4.1. SUBSTRATES WITH NATURALLY OCCURRING PROLINE IN THE TMD

Since proline substitutions drastically increased non-canonical TNFα shedding to levels comparable with canonical shedding, it is tempting to speculate whether further substrates exist that are efficiently shed by SPPL2a. The previous experiments showed that a proline especially in the N-terminal half of the TNFα TMD improved non-canonical shedding. Thus, TNFα characteristics such as the length of the TMD of around 22 amino acids, a cysteine close to the TMD/ ICD border plus at least one proline in the N-terminal half of the TMD provided the basis for a tailored prediction algorithm identifying potential substrates. The analysis, performed by Stephan Beilmann, resulted in 26 type II TM proteins matching these criteria. Due to their localisation and function, five potential substrates, SACA3, ENTPD6, GOLM1, TNFSF15 and NKG2D were chosen for a more in-depth investigation (Table 4.4). The cDNAs were fused to an N-terminal Flag-tag and a C-terminal V5-tag to allow collective detection.

Table 4.4 Overview of type II TM proteins with at least one naturally occurring proline in the TMD. Unknown and therefore suggested functions are quoted from www.uniprot.org. PM: plasma membrane

Name	TMD sequence	Mass in kDa incl. tags	Localisation	Function
SACA3	WCPAGIMLLALVCLLSCLLPS	25.8	PM of sperm	○ Sperm-egg plasma membrane adhesion and fusion during fertilization ○ Receptor for the egg oligosaccharide residue N-acetylglucosamine (Mandal et al., 2003)
ENTPD6	VAKVAYPLGLCVGVFIYVAYI	55.6	PM and Golgi	○ Unknown (Support of glycosylation reactions, catalyses the hydrolysis of extracellular nucleotides)
GOLM1	SPPLVLAALVACIIVLGFNYWIA	47.7	Golgi	○ Unknown (Cellular response protein to viral infection)
TNFSF15	ALTCCLVLLPFLAGLTTYLLV	30.5	PM / secreted	○ Activation of NF-kB. ○ Inhibition of vascular endothelial growth and angiogenesis *(in vitro)*. ○ Activation of caspases and apoptosis (Valatas et al., 2019)
NKG2D	PFFFCCFIAVAMGIRFIIMVA	27.6	PM	○ Immunosurveillance by scavenging various cellular stress-inducible ligands ○ Activation of NK cells, leading to cytotoxic activity (Lanier, 2015)

Secretion of soluble peptides from the potential substrates was investigated in HEK293 cells and HEK293 cells ectopically expressing either SPPL2a or SPPL2b. SACA3, ENTPD6 and GOLM1 secreted only a single fragment, which was also detected in SPPL2a/b-deficient cells. Since no change in the secretion pattern was detected when comparing cells ectopically expressing SPPL2 proteases with cells deficient for them, it suggests that non-canonical shedding did not occur in these proteins (Figure 4.14). Since ENTPD6 and GOLM1 ECDs are glycosylated and therefore are quite large, the shift of

canonical vs. non-canonical shedding might have been missed. However, de-glycosylation assays did not reveal multiple fragments (data not shown), concluding that a proline residue in the N-terminal half of the substrate's TMD is not the only determinant for non-canonical shedding by SPPL2a. TNFSF15 ECDs could not be detected at all. Several detection methods did not yield any results, which suggests a very rapid degradation of the sECD or generally a low expression/ transfection efficiency in HEK293 cells.

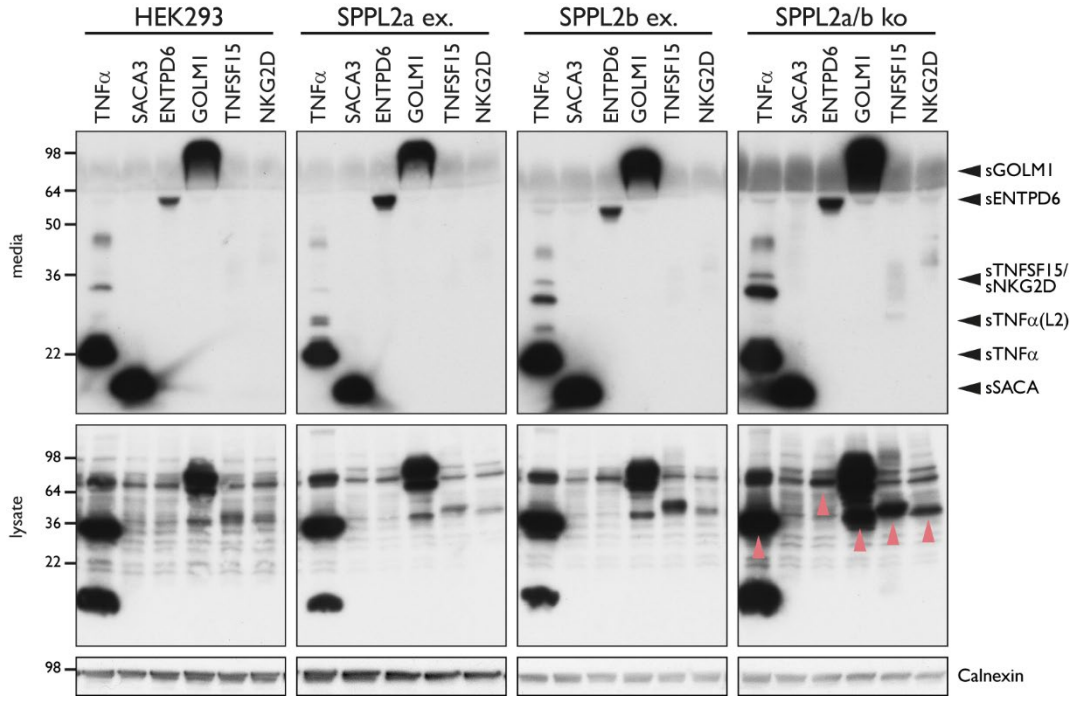

Figure 4.14 An N-terminal proline in the substrate's TMD is not the only determinant for non-canonical shedding by SPPL2a. HEK293 cells, cells ectopically expressing (ex.) either SPPL2a or SPPL2b or HEK293 cells deficient for SPPL2a/b (ko) were transiently transfected with the indicated proteins. Soluble ECDs of the proteins were detected with the monoclonal V5 antibody. Isolation of the FL protein (red arrows) from cell lysates serves as transfection and calnexin as loading control. SACA FL was not unambiguously identified and thus is not marked.

4.2.5. MODULATION OF SHEDDING BY INSERTION OF NON-SUBSTRATE DOMAINS

From accompanying studies on biophysical properties of the TNFα TMD, it is known that single amino acids influence the dynamics of the TMD even over a certain distance from the cleavage sites (Section 4.2.4) (Spitz et al., 2020). The data described above demonstrated that proline itself is not sufficient to induce non-canonical shedding in type II TM proteins generally. To unravel other important determinants for non-canonical shedding subdomains of TNFα were substituted with the corresponding subdomains of the non-substrate Bri3.

In the context of Leonie Wittmann's bachelor thesis, the TMDs of TNFα, Bri2 and Bri3 were validated to reassure correct exchange of the protein's subdomains (Wittmann, 2017). Molecular dynamics simulations in 1-palmitoyl-2-oleoyl-sn-glycero-3-phosphocholine (POPC) bilayers and multiple prediction algorithms confirmed the annotated TMDs for TNFα and Bri2. For Bri3 the analysis indicated that the TMD is not correctly annotated but rather assigns five amino acids further C-terminal (Figure 4.15). TNFα/Bri3 chimeras were designed according to these results. However, previously the processing and recognition of Bri2 by SPPL2b was investigated via the same method using Bri2/Bri3 chimeras solely based on the annotated TMDs (Martin et al., 2009). However, comparing processing of published Bri2/Bri3 chimeras with TMD-adjusted Bri2/Bri3 chimeras showed only very little changes (data not shown).

Figure 4.15 Sequence of Bri3. The annotated TMD according to www.uniprot.org is underlined, the newly predicted TMD according to Wittmann, 2017 is highlighted in grey.

Bri proteins contain an additional pro-peptide, which is removed by Furin-mediated cleavage. As this cleavage does not affect further processing (Section 1.3.3) the pro-peptide was removed. Throughout the study, those proteins are referred to as full-length (FL).

Since Bri3 is not canonically shedded by ADAM10/17 and also not cleaved by SPPL2a, the TICD and/ or TMD were fused to the Bri3 ECD, to evaluate whether this allows non-canonical shedding by SPPL2a (Figure 4.16). To test whether Bri3 exhibits inhibitory functions on non-canonical shedding, the Bri3 ICD and/ or TMD were fused to the TNFα ECD. All cDNAs were fused to an N-terminal Flag- and a C-terminal V5-tag to allow simultaneous detection.

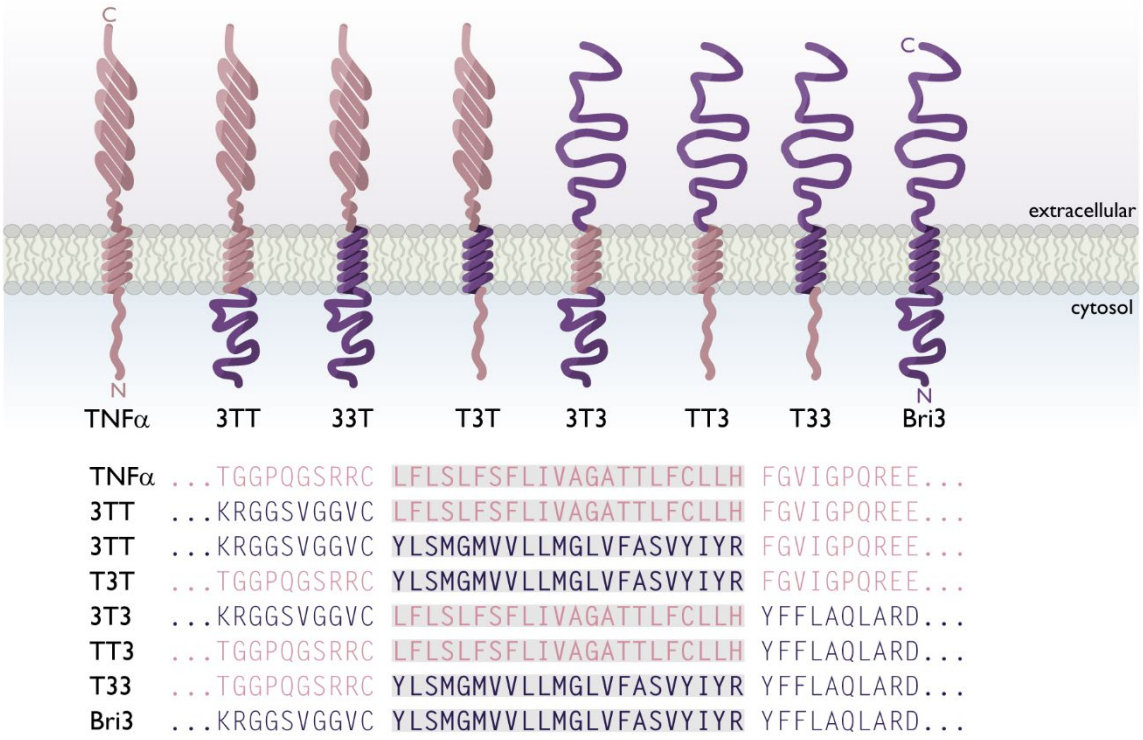

Figure 4.16 Schematic representation of the TNFα/Bri3 chimeras. TMD, ECD and ICD of TNFα and Bri3 were exchanged. The amino acid sequence displays the exact transition between the individual domains. TNFα is depicted in pink, Bri3 in purple. The TMDs are indicated in grey.

To allow comparison of processing, surface expression of all chimeras was tested via flow cytometry (Figure 4.17). Except 3T3, all chimeras were expressed in similar amounts on the cell surface compared to TNFα. 3T3 was expressed less and its detection on WB varied strongly between experiments indicating enhanced degradation.

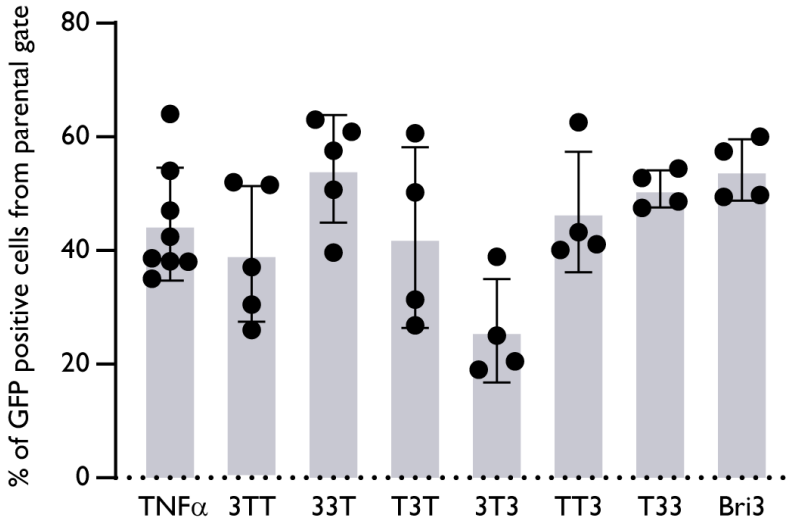

Figure 4.17 All TNFα/Bri3 chimeras are expressed on the cell surface. HEK293 cells were transiently transfected with the indicated chimera and surface stained with the V5-mono antibody prior to analysis by flow cytometry. GFP positive cells were gated from a single cell population. n=4-8. Data are represented as mean +/- SD.

As established in this study, cleavage of the TNFα ECD results in the release of two fragments, sTNFα (Figure 4.18; #4) and sTNFα(L2) (Figure 4.18; #1). Chimeras comprising

the Bri3 ECD are not shedded by ADAM10/17. Interestingly, non-canonical shedding by SPPL2a was also not detected in these chimeras. Conversely, chimeras with a TNFα ECD and a Bri3 TMD were shedded by SPPL2a, ADAM10/17 and even additional intermediate fragments were observed (Figure 4.18; #2, #3). Of note, substitution of only the TICD with Bri3 (3TT) resulted in reduced non-canonical shedding compared to the control and also canonical shedding seemed to be reduced slightly (see also Figure 4.19) whereas substitution of TICD and TNFα TMD (33T) increased non-canonical shedding by SPPL2a and even allowed SPPL2b non-canonical shedding.

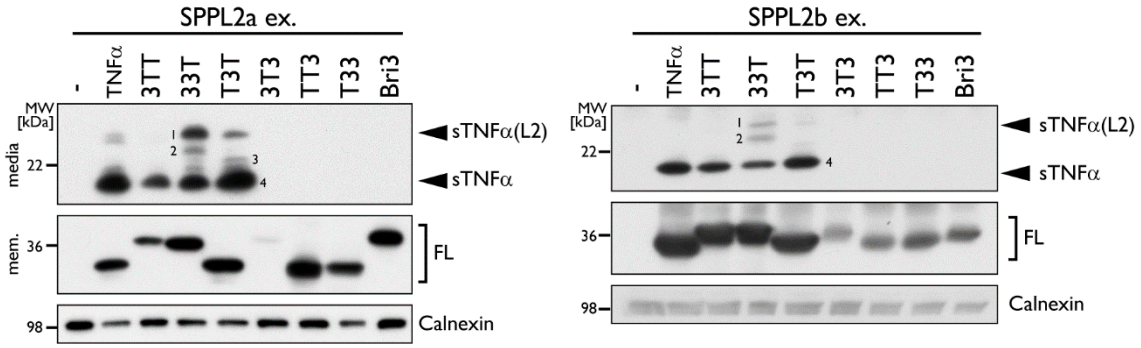

Figure 4.18 Non-canonical shedding does not occur in chimeras comprising Bri3 ECD. HEK293 cell lines co-expressing (ex.) SPPL2a or SPPL2b were transiently transfected with the indicated TNFα/Bri3 chimera. Soluble ECDs were isolated using the monoclonal V5 antibody. Detection of the FL proteins isolated from membranes was used as transfection and calnexin as loading control.

To ensure secreted fragments were generated by ADAM10/17 and SPPL2a cleavage, chimeras were expressed in SPPL2a/b-deficient cells and treated with ADAM inhibitors. As expected, canonical shedding of TNFα wt was inhibited by application of ADAM inhibitors (+AI) and non-canonical shedding was abolished in SPPL2a/b-deficient cells (Figure 4.19). 3TT and T3T chimeras behaved similarly; however, Bri3 ICD and TMD seem to exhibit impeding effects on non-canonical shedding when present individually. Surprisingly, the substitution of both domains at the same time did not enhance the reducing effect of Bri3 but in contrast, increased non-canonical shedding. In addition, 33T chimera displayed intermediate fragments (Figure 4.19; #2, #3). Fragment #2 was diminished in ADAM inhibitor-treated cells and fragment #3 absent in SPPL2a/b-deficient cells. This indicates that the Bri3 TMD can be cleaved by SPPL2a generally and non-canonical shedding sites exist. Furthermore, the presence of Bri3 TMD generates additional canonical cleavage sites for ADAM10/17. However, secretion of sTNFα(L2) was not completely abolished in SPPL2a/b-deficient cells but strongly reduced. Furthermore,

additionally secreted intermediate fragments in T3T were also not diminished by the inhibition of ADAM activity or SPPL2a/b deficiency (Figure 4.19; #3). This may suggest that an unrelated protease is contributing to the cleavage and the generation of sTNFα(L2) in chimeric proteins with a Bri3 TMD (Figure 4.19; #1).

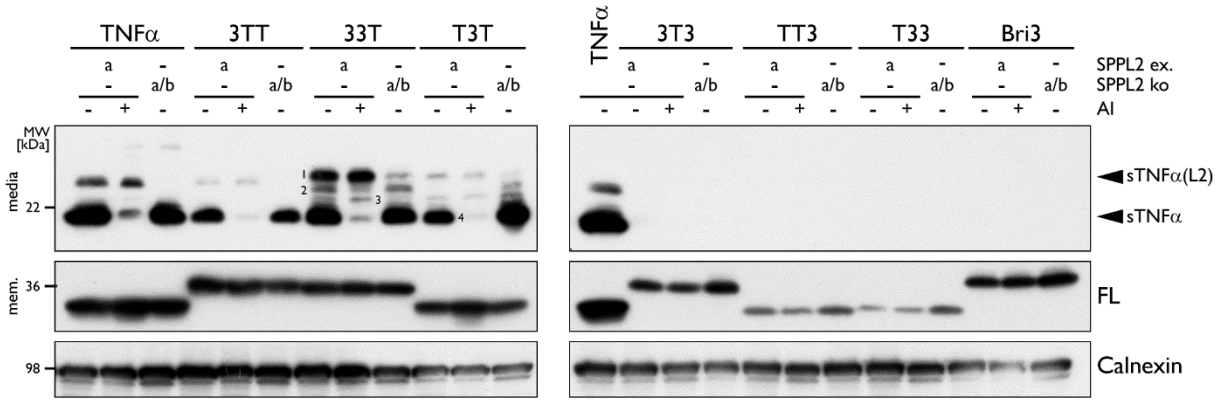

Figure 4.19 Bri3 ICD and TMD display inhibitory effects on non-canonical shedding individually but not synergistically. Cells ectopically expressing SPPL2a (ex.) and SPPL2a/b-deficient cells (ko) were transfected with the respective TNFα/Bri3 chimera. Where indicated, cells were treated with 5µM GI 254023X and 1µM BMS-561395 (+AI) or DMSO as control (-). Soluble ECDs were isolated using the monoclonal V5 antibody. Detection of the FL protein isolated from membranes was used as transfection and calnexin as loading control.

4.2.5.1. INSERTION OF A PROLINE INTO TMD OF CHIMERIC PROTEINS

To unravel the reason for the strong inhibitory effect of the Bri3 ECD on non-canonical shedding even in the presence of a substrate's TMD, a proline was introduced in the TMD of 3T3. As shown above, S37P and G43P substitutions strongly increased non-canonical TNFα shedding. Therefore, S66 and G72 of 3T3 were substituted by proline and shedding was investigated.

Chimeric proteins substituted with prolines did not show any release of soluble peptides by neither ADAM10/17 nor SPPL2a/b (Figure 4.20). Substitution of the central glycine with proline (G73P) even led to premature degradation of the protein as no FL protein was detected. Even if non-canonical shedding in this mutant was theoretically enabled, the lack of successful surface transport hindered analysis and final conclusions. Nevertheless, technical problems like reduced transfection or blotting efficiency and decreased viability of SPPL2a/b-deficient cells might need to be considered additionally (Figure 4.20, right).

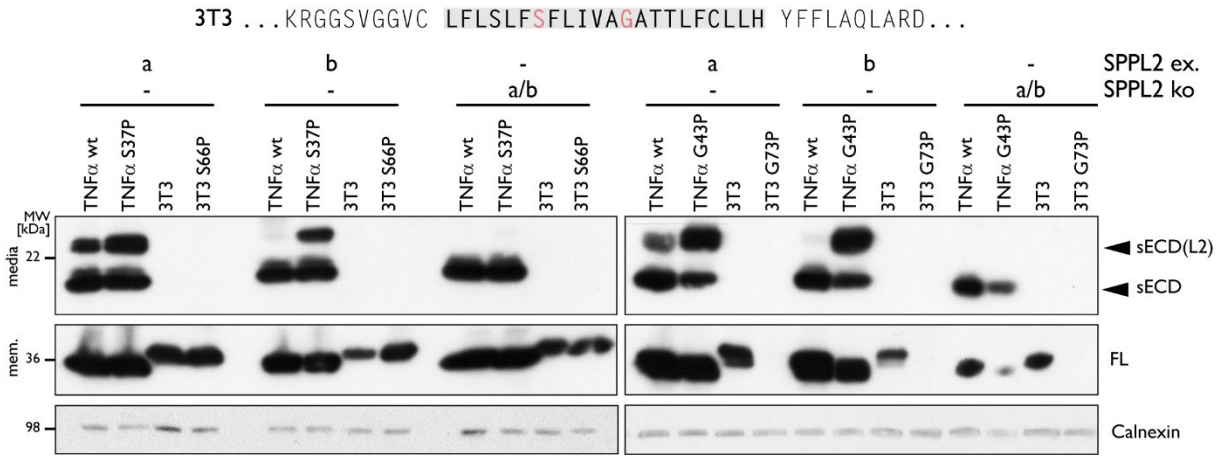

Figure 4.20 Proline in the TMD of 3T3 does not enable non-canonical shedding. SPPL2a or SPPL2b overexpressing and SPPL2a/b-deficient cells were transfected with the respective TNFα/Bri3 chimera. Soluble ECDs were isolated using the monoclonal V5 antibody. Detection of the FL protein isolated from membranes was used as transfection and calnexin as loading control. The TMD of 3T3 is highlighted in grey and the position of the substituted amino acids in pink.

4.2.6. SHEDDING CAN BE MODULATED BY JMD MUTATIONS

4.2.6.1. DISTINCT JMD SEGMENTS INFLUENCE SHEDDING DIFFERENTLY

Since the presence of the Bri3 ECD abolished both canonical and non-canonical shedding, changes in the luminal JMD were introduced to evaluate their impact on processing. The ADAM10/17 cleavage site in TNFα is located 24 amino acids C-terminal of the luminal border of the TMD at position A76. The JMD was split into three sections, each substituted with the corresponding section of the Bri3 JMD to investigate whether these parts have an inhibitory effect on shedding.

Whereas the substitution of the entire TNFα ECD with Bri3 diminished both types of shedding (Figure 4.18), exchanges of smaller JMD sections still enabled the release of the TNFα ECD (Figure 4.21). Substitution of the second or third TNFα JMD section with Bri3 abolished canonical shedding (almost) completely (Figure 4.21A; juxBri3_2, juxBri3_3) while substitution of the first section selectively diminished non-canonical shedding (Figure 4.21A; juxBri3_1). Interestingly, non-canonical shedding was not affected by substitution of the second and only slightly reduced by substitution of the third section. This not only suggests that it is possible to inhibit canonical TNFα shedding and only enable non-canonical shedding by SPPL2a but also corroborates that both cleavage mechanisms are not co-dependent. Additionally, the Bri3 JMD seems to comprise a certain inhibitory capacity for SPPL2a and ADAM10/17 cleavage as substitutions at the respective

cleavage site inhibited corresponding peptide release. However, it was interesting to see that the second section of the Bri3 JMD displayed inhibitory effects on ADAM10/17-mediated shedding even though several amino acids distant from the actual cleavage site. This suggests that this section comprises certain characteristics important for TNFα processing by ADAM10/17.

Again, several intermediate fragments were detected (Figure 4.21; #2-4). These intermediate peptides that were released upon substitution of the first JMD section were partially insensitive to ADAM inhibition and did not decrease in SPPL2a/b-deficient cells (Figure 4.21B). Thus, cleavage by an unrelated protease might not only interfere with shedding of chimeric proteins when the TMD is substituted (Figure 4.19) but also sections close to the TNFα TMD.

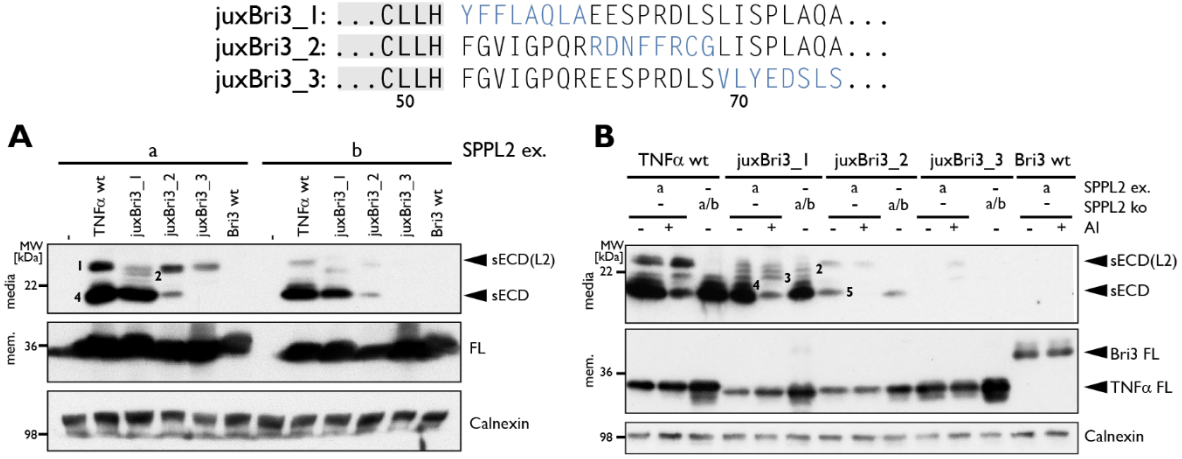

Figure 4.21 Bri3 substitutions in the TNFα JMD affect shedding. (A) Cells ectopically expressing SPPL2a or SPPL2b (ex.) were transiently transfected with the respective TNFα mutants. Soluble ECDs were isolated using the monoclonal V5 antibody. Detection of the FL proteins isolated from membranes was used as transfection and calnexin as loading control. **(B)** Indicated cell lines were treated with 5µM GI 254023X and 1µM BMS-561395 (+ AI) to inhibit ADAM proteases. Soluble ECDs and controls were isolated as in (A). The TNFα TMDs of the juxBri3 mutants are highlighted in grey and substituted amino acids in blue.

4.2.6.2. REMOVAL OF NEGATIVELY CHARGED RESIDUES FROM TNFα JMD AFFECTS SHEDDING

To pinpoint the inhibitory effect of the Bri3 JMD on shedding the primary sequence of both TNFα and Bri3 was analysed in more detail. A study on the cleavage mechanism of SPP showed that positively charged residues in the JMD have an inhibitory effect on substrate processing (Lemberg and Martoglio, 2002). When comparing the JMD of TNFα with that of Bri3 the distribution of the charged residues stands out. In the TNFα JMD the charged residues cluster in the middle (R60, E61, E62, R65, D66), whereas the charges in

the Bri3 JMD are more spread (R90, D91, R95, E101). As both JMDs contain two positively charged residues in similar positions, the effect of the negatively charged residues was analysed. Thus, residues E61, E62 and D66 of the TNFα JMD were mutated into asparagine or glutamine (E61Q, E62Q, D66N; QQN) to eliminate the charge but keep structural changes to a minimum. However, substitution of D66N generated a glycosylation site that was indeed glycosylated (Figure 4.22). Therefore, D66 was substituted by alanine (E61Q, E62Q, D66A; QQA). Additionally, a mutant with all three positions substituted by alanine was generated (E61A, E62A, D66A; AAA).

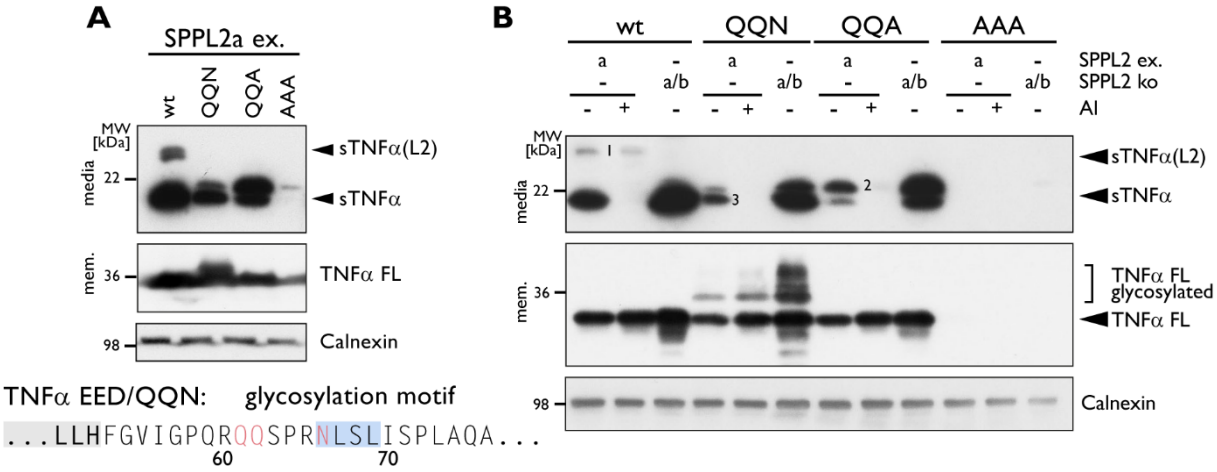

Figure 4.22 Removal of negative charges from the JMD abolishes non-canonical shedding. (A) Cells ectopically expressing SPPL2a (ex.) were transiently transfected with the respective TNFα variants. Soluble ECDs were isolated using the monoclonal V5 antibody. Detection of the FL proteins isolated from membranes was used as transfection and calnexin as loading control. The generation of a glycosylation motif by substitution of D66N in the TNFα JMD is indicated in blue. **(B)** The removal of charges from the JMD shifts the usage of the ADAM cleavage site (#3) more N-terminally (#2) and abolishes sTNFα(L2) release (#1). Cells ectopically expressing SPPL2a and SPPL2a/b-deficient cells (ko) were transiently transfected with the indicated TNFα variant. Indicated cell lines were treated with 5µM GI 254023X and 1µM BMS-561395 (+ AI) to inhibit ADAM proteases or DMSO as a control. Soluble ECDs and controls were isolated as in (A).

The removal of charges from the JMD with minimal changes in the structural integrity resulted in reduced canonical shedding at the major cleavage site (Figure 4.22B; #3). In addition, a second soluble fragment was detected but depleted when treated with an ADAM inhibitor (Figure 4.22B; #2). Thus, removal of the negative charges shifted the primary cleavage site of canonical cleavage by ADAM10/17 a few amino acids further N-terminal. It was established previously that ADAM10/17 mainly cleaves at position A76. Nevertheless, other cleavages sites such as position P73, L69 and D66 were observed (Figure 4.8) and are likely to be used in the TNFα QQN and QQA mutants. Since the cleavage shift was not as prominent in the QQN mutant, it might be speculated that the artificial glycosylation of the TNFα ECD affected accessibility of the cleavage site, resulting

in reduced shedding by ADAM10/17. However, as the shift of canonical shedding also occurred in the QQA mutant, which was not artificially glycosylated, the effect on shedding may be attributed to the removal of the negative charges. Interestingly, replacement of all three charged residues by alanines resulted in reduced surface expression, thus no analysis of this mutant was possible. These results conclude that ADAM10/17-mediated cleavage is not only abolished when negatively charged residues are inserted close to the cleavage site (Figure 4.21; juxBri3_3) but is also reduced when negatively charged residues distant from the cleavage site are reduced (Figure 4.21; juxBri3_2) or removed (Figure 4.22; QQN/QQA).

Interestingly, non-canonical shedding was completely abolished in the charge mutants. Even though SPPL2a-mediated cleavage seemed not to be affected by the reduction of charges (Figure 4.21; juxBri3_2), their removal abolished non-canonical shedding. These results support the conclusion that negatively charged residues in the TNFα JMD seem to play a crucial role not only for canonical but also non-canonical shedding. Furthermore, the effect is conducted over the distance of several α-helical turns, as the modifications of the second section of the TNFα JMD are distant from the actual SPPL2a and ADAM10/17 cleavage sites in contrast to substitutions of the first and second section of the TNFα JMD.

4.2.7. SHEDDING CAN BE MODULATED BY PALMITOYLATION OF THE TICD

The previous results indicate that substitution of TICD with Bri3 ICD reduced non-canonical shedding (Figure 4.18). One characteristic of the TICD is a palmitoylated cysteine at position 30 that affects the processing of TNFα by SPPL2b (Poggi et al., 2013, Utsumi et al., 2001). Therefore, the effect of lipid modification on non-canonical shedding was investigated in more detail. To confirm lipid modification of the cysteine, TNFα wt and two cysteine mutants (C30S, C30A) were treated with hydroxylamine to remove a possible palmitoylation. Depletion of the palmitoylation resulted in free thiol groups at the cysteine, which enabled isolation of the protein using thiopropyl beads. The detection of

a fragment bound to the beads confirms palmitoylation of TNFα wt (Figure 4.23). As both mutants were not palmitoylated, peptides were not isolated.

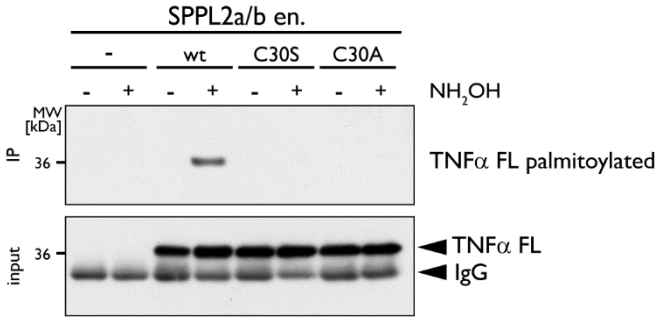

Figure 4.23 TNFα is palmitoylated at C30. TNFα wt and the indicated variants were isolated from cells endo- genously (en.) expressing SPPL2a/b. Free thiol groups were quenched before palmitate was removed via hydroxylamine treatment (+NH_2OH). Release of palmitate resulted in accessible thiol groups that were used to immunoprecipitate the proteins using thiopropyl beads. Isolation of the FL protein using the FlagM2 antibody served as control.

After validating that TNFα undergoes palmitoylation in the cellular system used for the analysis, shedding of the non-palmitoylated C30S and C30A mutants was compared to that of palmitoylated TNFα wt. The results showed that non-canonical shedding by SPPL2a increased in non-palmitoylated mutants compared to the wt (Figure 4.24). Since the increased effect was not as pronounced as in the proline TMD mutants (Section 4.2.4) it is not surprising that non-canonical shedding by SPPL2b was not enabled.

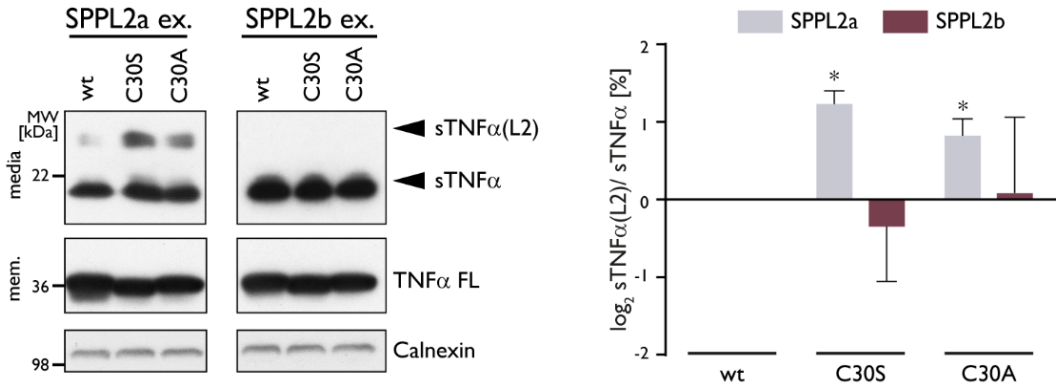

Figure 4.24 Non-canonical shedding increases when palmitoylation is abolished. Soluble TNFα species were isolated from conditioned media of the indicated cell lines and quantified relative to sTNFα from respective WB by densitometric analysis and normalized to the wt, n=3. Data are represented as mean +/- SD. Statistical significance was calculated applying an unpaired, two-sided Student's t-test. *: $p<0.05$. The WB shows one representative experiment. TNFα FL was used as transfection and calnexin as loading control.

4.2.8. NON-CANONICAL SHEDDING OF OTHER SPPL2 SUBSTRATES

The results on non-canonical TNFα shedding raised the question whether this shedding is a general feature of SPPL2a and if other substrates are processed similarly. In order to confirm a general shedding capacity of SPPL2a, the known substrates Bri2, FasL, TMEM106b and CD74 were analysed for the release of sECDs into the conditioned media.

All proteins except TMEM106b were successfully expressed on the cell surface. Despite successful expression, no sFasL was detected (Figure 4.25A). Multiple secreted fragments were generated from Bri2 and CD74. In CD74 however, the secreted fragments probably represent differently matured peptides, as the CD74 ECD is glycosylated multiple times (Table 1.1).

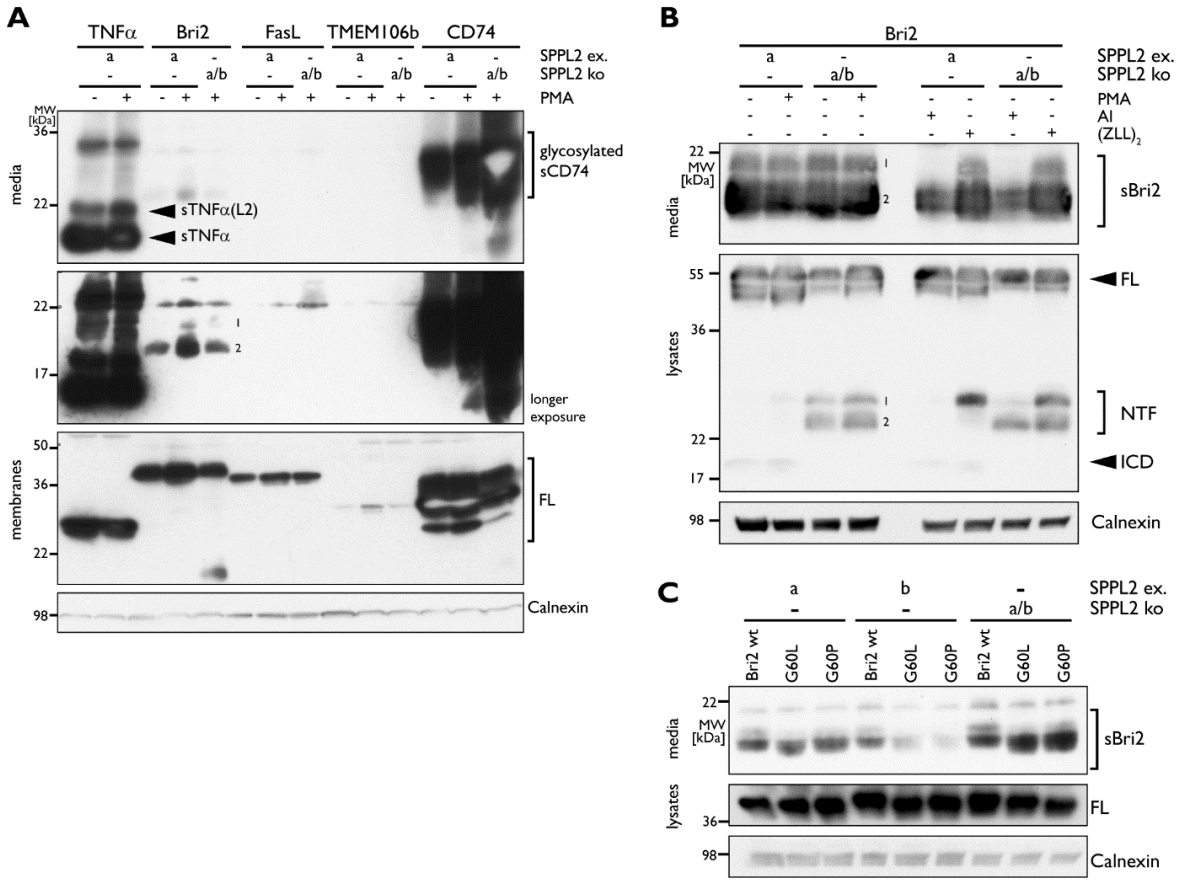

Figure 4.25 SPPL2a-mediated non-canonical shedding is probably an exclusive characteristic of TNFα. ECDs from conditioned media of HEK293 cell lines co-expressing the indicated substrates and SPPL2a, SPPL2b or none of the proteases (ko) were isolated and detected with the V5-mono antibody. **(A)** Cells were treated with 1µM PMA to activated ADAM cleavage. **(B)** Cells were treated with either 1µM PMA to activated ADAM cleavage, 50µM Z-LL$_2$-ketone (+ (ZLL)$_2$) to inhibit SPPL2 catalytic activity or with 5µM GI 254023X and 1µM BMS-561395 (+ AI) to inhibit ADAM proteases. Controls were treated with DMSO (-). **(C)** sBri2 secreted from the indicated mutant was isolated as in (A). The expression of the FL protein was used as transfection and calnexin as loading control.

Even though Bri2 secreted several soluble fragments as well, no fragment was decreased in SPPL2a/b-deficient cells or by the application of the SPPL2 inhibitor (+(ZLL)$_2$) (Figure 4.25B). Not all of the secreted ECDs were inhibited by the treatment with an ADAM10/17 inhibitor, thus, Bri2 might be shedded in several positions by more than just the ADAM-proteases. Even insertion of a proline in the centre of the TMD did not induce non-canonical shedding; it rather even decreased canonical shedding in SPPL2b-expressing cells (Figure 4.25C). This implies that Bri2 does not undergo SPPL2a mediated

non-canonical shedding and substitutions of the central TMD glycine by either leucine or proline even negatively affect canonical shedding. The secreted sBri2 peptides might as well result from the release of differently matured Bri2 ECD, as Bri2 just as CD74 is glycosylated at several sites (Table 1.1). To conclude, it appears that SPPL2a mediated non-canonical shedding exclusively occurs in TNFα and the other so far known SPPL2 substrates are not directly cleaved by SPPL2a.

4.3. SUBSTRATE RECOGNITION AND INITIAL CLEAVAGE

So far it was assumed that most SPPL2 substrates are shedded by a accompanying (metallo-) protease, then recognised by SPPL2 and subsequently processed. However, the previous data showed that TNFα is shedded as FL protein by SPPL2a, which indicates that the protease is able to recognise not only the NTF but already the FL protein. Indeed, previous studies have shown that SPPL2 proteases are able to bind FL proteins, but yet binding does not necessarily result in the cleavage of the protein (Bri3) (Martin et al., 2008, Fluhrer et al., 2006). Thus, it seems that binding is rather unspecific and further protein features determine which proteins are cleaved by SPPL2. Therefore, assuming that SPPL2 proteases are capable of binding most type II TM proteins, other substrate criteria determine which proteins are finally cleaved.

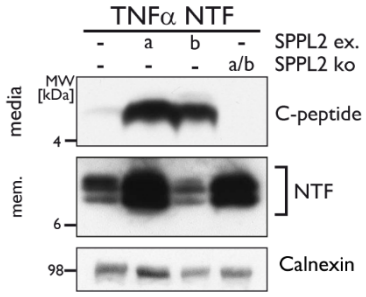

Figure 4.26 Secretion of C-peptide by SPPL2. C-peptides were isolated from conditioned media of HEK293 cell lines expressing exogenous (ex.) levels of SPPL2a, SPPL2b or none of the proteases (ko) and ectopically expressing TNFα NTF using the polyclonal V5 antibody. For visualization on WB, the monoclonal V5 antibody was employed. Calnexin served as loading control (Spitz et al., 2020).

In the context of RIP, the shedded substrate NTFs are cleaved by SPPL2 releasing a small C-peptide into the conditioned media. This first cleavage is referred to as initial cleavage. To investigate initial cleavage of TNFα by SPPL2a and SPPL2b, a TNFα variant

lacking the ECD (TNFα NTF) was established. TNFα NTF was C-terminally V5-tagged to enable detection of the C-peptide. Co-expression of TNFα NTF and SPPL2b resulted in secretion of TNFα C-peptides (Figure 4.26), which confirmed previously published results (Fluhrer et al., 2006). SPPL2a triggered the secretion of comparable amounts of TNFα C-peptide, suggesting that the initial endoproteolytic processing step by both protease, which follows canonical shedding, occurs with similar efficiency. As a result of SPPL2a/b-depletion, TNFα NTF accumulated within the cell and no C-peptide was released. TNFα NTF also accumulated in cells co-expressing SPPL2a, which was probably due to a higher transfection efficiency and higher cell desity as indicated by the detection of calnexin.

4.3.1. INITIAL CLEAVAGE IN TNFα/ BRI3 CHIMERAS

To identify determinants that enable initial cleavage in the context of RIP TNFα/Bri3 chimeras lacking the ECD were established. Confirming earlier results, co-expression of SPPL2a or SPPL2b with Bri3 NTF did not result in release of a C-peptide (Figure 4.27) (Martin et al., 2008).

Release of a C-peptide by SPPL2a or SPPL2b was detected in all chimeras comprising a TNFα JMD. However, initial cleavage and therefore release of a C-peptide in 3TT and 33T NTF was reduced, indicating that Bri3 ICD has an inhibitory effect on the initial cleavage by SPPL2. Bri3 TMD seemed not to affect initial cleavage, as C-peptide release from T3T was as efficient as in TNFα wt. In line with this, the TNFα TMD did not enable cleavage by SPPL2 in the context of Bri3 (Figure 4.27; 3T3). Since 3TT and TT3 were still cleaved by SPPL2, Bri3 ICD and JMD seemed to both comprise a certain inhibitory effect which when combined abolished initial cleavage of TNFα by SPPL2. Interestingly, while the addition of the whole Bri3 ECD inhibited shedding and subsequent processing (Figure 4.18), Bri3 JMD in short chimeras was not able to abolish release of the C-peptide completely but reduced the cleavage slightly. Surprisingly, even if the TMD seemed not to influence initial cleavage by SPPL2 in 33T, it was able to reduce/ abolish cleavage by SPPL2 when combined with the Bri3 JMD (T33). These results demonstrate that Bri3 JMD and ICD

are able to reduce TNFα cleavage by SPPL2 and that the TMD does not play a role in the initial cleavage.

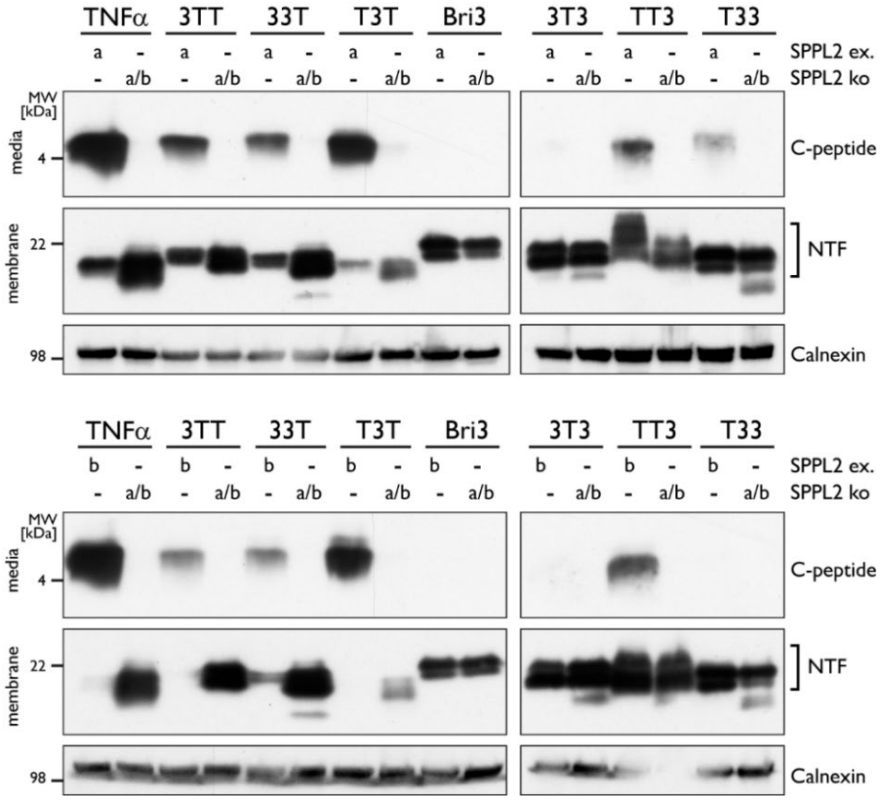

Figure 4.27 Initial cleavage by SPPL2 is reduced in chimeras comprising Bri3 ICD and/ or Bri3 JMD. C-peptides were isolated from conditioned media of HEK293 cell lines expressing exogenous (ex.) levels of SPPL2a, SPPL2b or none of the proteases (ko) using the poly-clonal V5 antibody. For visualization on WB, the monoclonal V5 antibody was employed. Calnexin was used as loading control.

Further analysis of the SPPL2a cleavage sites in TNFα/Bri3 chimeras revealed changes of cleavage sites induced by the respective Bri3 segments. While Bri3 ICD did affect the general cleavage capacity of SPPL2 (Figure 4.27), it did not alter cleavage sites (Figure 4.28; 3TT). Bri3 TMD influenced initial cleavage capacity rather less in WB analysis; however, it did induce additional cleavage sites in the TNFα JMD (33T, T3T). Furthermore, detection of secreted peptides in SPPL2a/b-deficient cells was used to ensure specificity of SPPL2a-mediaited cleavage. Interestingly, cleavages in 33T and T3T were not or only partially reduced in SPPL2a/b-deficient cells indicating that an unrelated protease is indeed cleaving TNFα/Bri3 chimeras. Even though mass spectrometry results supported the hypothesis that the Bri3 TMD can actually be cleaved by SPPL2 (Figure 4.28; 33T, T3T, T33) it also showed that a so far unidentified protease is partaking in the cleavage at the same positions as SPPL2 proteases.

Even though Bri3 JMD was not sufficient to inhibit cleavage by SPPL2a completely it abolished (TT3) or reduced (3T3) cleavage at specific sites in the TNFα TMD. Additionally, the combination of TNFα TMD and Bri3 JMD (TT3, 3T3) increased the amount of cleavage

sites in the Bri3 JMD. However, when combined with the Bri3 TMD (T33) cleavage sites in the Bri3 JMD were reduced, while presence of TNFα ICD induced cleavage by SPPL2 in the Bri3 TMD. Surprisingly, while 3T3 cleavage was not observed in WB analysis, cleavage sites in mass spectrometry were detectable. The soluble fragment might have been missed in WB analysis as peptide properties such as hydrophobicity enabled better detectability in mass spectrometry then on WB. Table 4.5 lists the exact masses of the measured and calculated chimeric peptides.

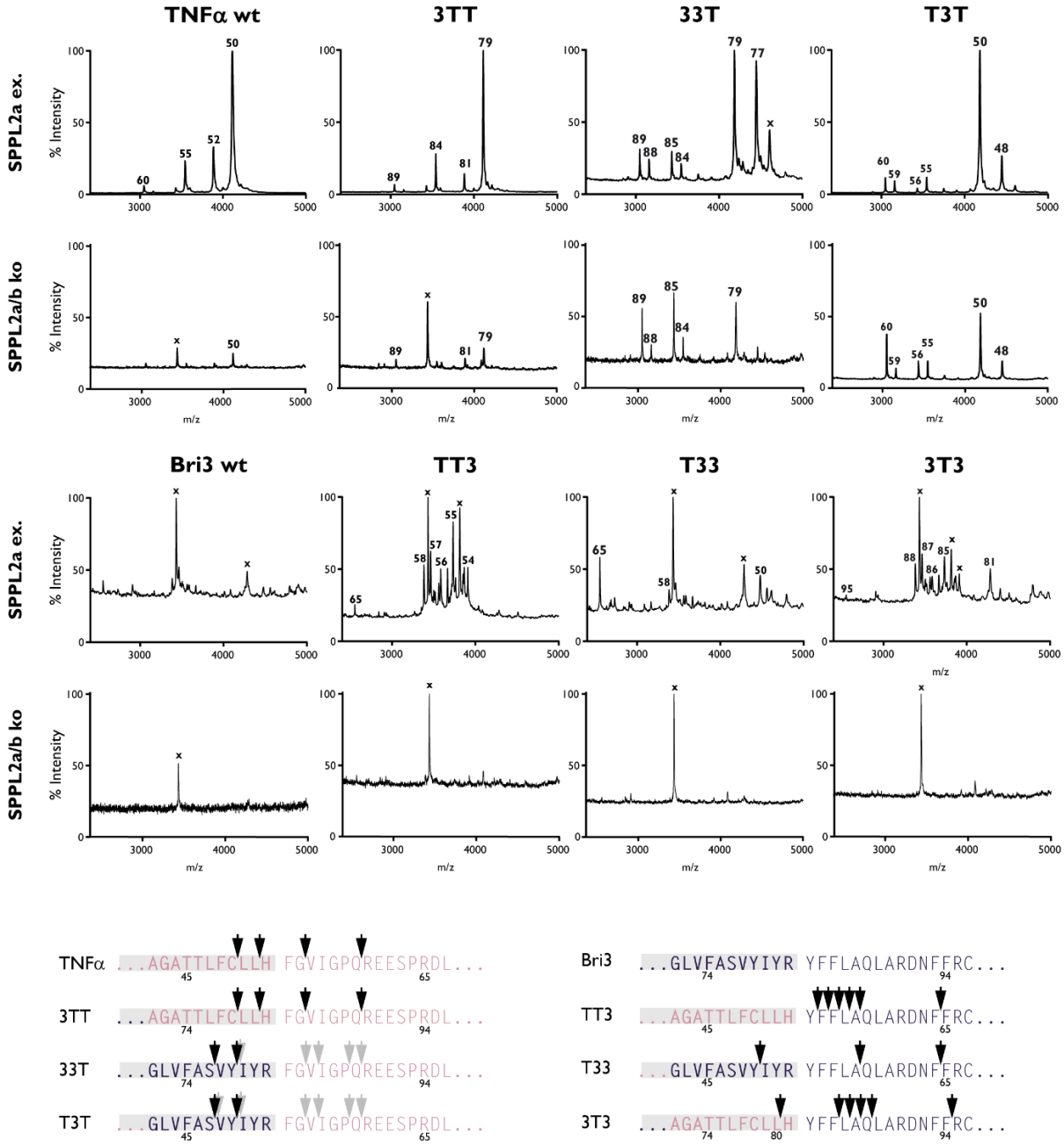

Figure 4.28 Identification of C-terminal cleavage sites in TNFα/Bri3 chimeras by mass spectrometry. Secreted ECDs from HEK293 cells co-expressing SPPL2a (ex.) or deficient for SPPL2a/b (ko) and indicated chimeras were isolated using the FlagM2 antibody and were analysed via mass spectrometry. Black arrows indicate the position of SPPL2a cleavage. Grey arrows indicate cleavage by an unknown protease. The TMD is highlighted in grey, TNFα in pink and Bri3 in blue. x marks peaks of unknown identity.

Table 4.5 Masses of TNFα/Bri3 chimeric cleavage products measured by MALDI-TOF compared to calculated masses. Measured values of samples with a TNFα TMD are normalised to the calculated mass of the peptide resulting from cleavage at position H52/ H81. Measured values of samples with a Bri3 TMD are normalised to the calculated mass of the peptide resulting from cleavage at position I50/ I79.

TNFα/Bri3 chimera	C-Peptide (cleavage position)	Calculated mass (in Da)	Measured mass (in Da)
3TT	89	3044	3041
	84	3539	3537
	81	3880	3879
	79	4106	4106
33T	89	3044	3043
	88	3172	3168
	85	3440	3434
	84	3539	3539
	79	4176	4176
	77	4469	4471
T3T	60	3044	3043
	59	3172	3165
	56	3440	3444
	55	3539	3539
	50	4176	4176
	48	4438	4440
3T3	95	2551	2553
	88	3396	3389
	87	3467	3469
	86	3580	3585
	85	3728	3732
	81	4288	4288
TT3	65	2551	2552
	58	3396	3393
	57	3467	3473
	56	3580	3584
	55	3728	3732
	54	3875	3875
T33	65	2551	2554
	58	3396	3385
	50	4470	4470

4.3.2. INITIAL CLEAVAGE IN JMD CHIMERAS

The results shown above demonstrated that the Bri3 JMD decreases the initial cleavage but increases cleavage sites especially in the section close to the TNFα TMD. Thus, sectional JMD substitutions (Section 4.2.6.1) lacking the majority of the TNFα ECD were investigated for their influence on the initial cleavage by SPPL2.

The analysis of the short Bri3 JMD chimeras suggests that especially the second section of the JMD is crucial for initial cleavage by SPPL2 (Figure 4.29). Release of the C-peptide was abolished when the second and reduced when the first section of the TNFα JMD was substituted with the respective Bri3 sequence. Even though increased initial cleavage and subsequent C-peptide release would suggest a reduction of NTF and reduced C-peptide release implies an accumulation of the NTF, this did not correlate in WB analysis. This phenomenon has also been observed for other RIP substrates such as APP (Sastre et al., 2001). It might be caused by an accelerated processing of the short compared to the FL protein. Nevertheless, these results imply that the second and - to a lesser extent - also the first part of the TNFα JMD is crucial for initial cleavage by SPPL2 in the context of RIP.

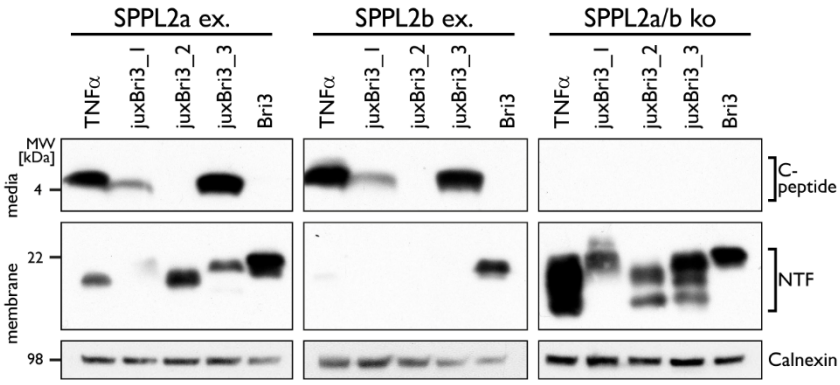

Figure 4.29 The first and second part of the TNFα JMD are important for initial cleavage. (A-B) C-peptides of the indicated TNFα JMD chimeras were isolated from conditioned media of HEK293 cell lines using the polyclonal V5 antibody. Cells expressed either exogenous (ex.) levels of SPPL2a, SPPL2b or none of the proteases (ko). For visualization on WB, the monoclonal V5 antibody was employed. Calnexin was used as loading control.

To investigate whether SPPL2a-mediated cleavage sites in JMD chimeras differed compared to TNFα wt and whether a certain section of the Bri3 JMD induced the before mentioned cleavage by an unknown protease, JMD mutants were investigated by mass spectrometry. Cleavage sites in TNFα with the third section of the JMD substituted with Bri3 were not changed (Figure 4.30; juxBri3_3). The substitution of the second section of the TNFα JMD with the corresponding Bri3 section resulted in the loss of the most C-terminal cleavage site at position 60 and shifted the most N-terminal cleavage site at

position 50 one amino acid further N-terminal. In addition, two major peaks that did not correlate with any possible secreted peptide were detected in SPPL2a-expressing cells and absent in SPPL2a/b-deficient cells, which indicates that - even though unidentified - these peptides are probably specific for an SPPL2a-mediated cleavage. The peptides might originate from smaller peptides (#55, #52) that became modified. Both unidentified peaks are ≈ 80 Da larger than the corresponding peptide. However, it seems puzzling that the peptides become modified only in this chimera and not in TNFα wt or juxBri3_1. Furthermore, small, unidentified peaks were detected in juxBri3_3; however, these peptides were ≈ 55 Da larger.

Besides the major SPPL2 cleavage positions 50 and 55, juxBri3_1 displayed additional cleavage sites in the area of substitution that were not abolished in SPPL2a/b-deficient cells. This indicates that besides SPPL2a an unrelated protease is cleaving the chimeric protein. Moreover, it seems that the unknown protease cleaves the TNFα chimera at the same positions as SPPL2a, as cleavages at positions 55 and 50 were only reduced and not abolished in SPPL2a/b-deficient cells. Table 4.6 lists the exact masses of the measured and calculated peptides.

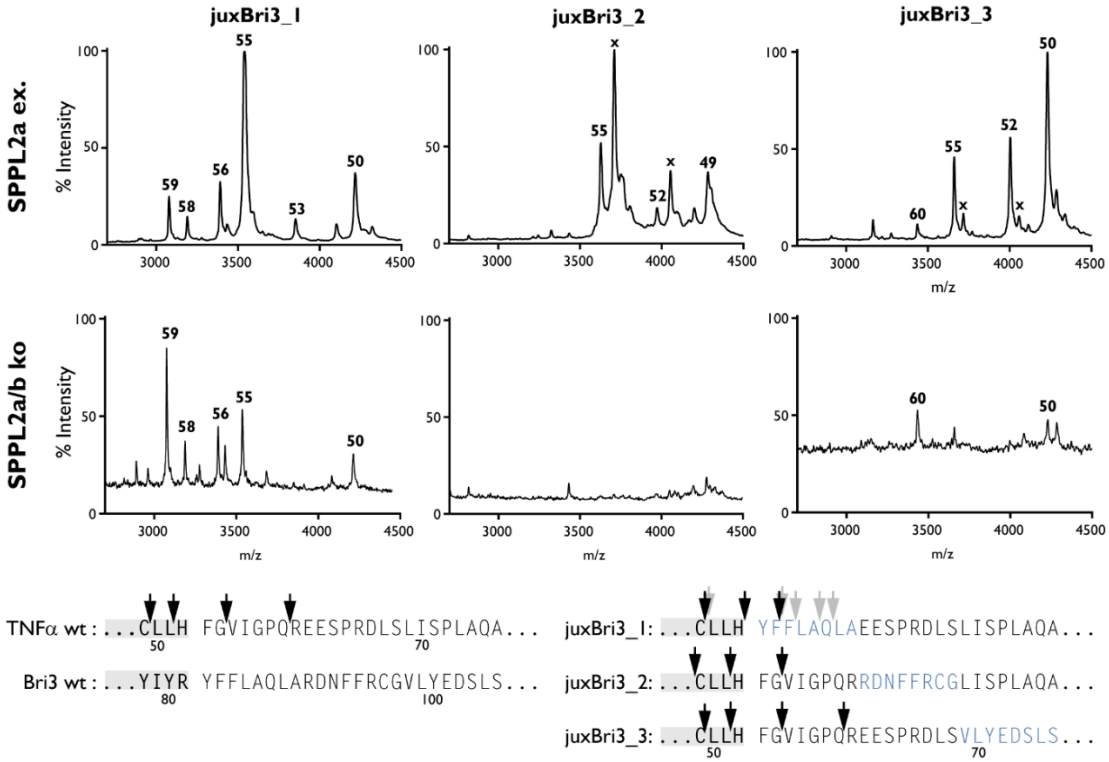

Figure 4.30 Identification of cleavage sites in JMD chimeras by mass spectrometry. Secreted ECDs from HEK293 cells co-expressing SPPL2a (ex.) or deficient for SPPL2a/b (ko) and the indicated TNFα variants were isolated using the FlagM2 antibody. Numbers indicate the position of the most N-terminal amino acid of the respective cleavage product. x marks peaks of unknown identity. Cleavage positions in the sequence are indicated with arrows. The TMD is highlighted in grey and Bri3 substitutions in blue.

Table 4.6 Masses of TNFα JMD variant C-peptides measured by MALDI-TOF compared to calculated masses. Measured values are normalised to the calculated mass of the peptide resulting from cleavage at position 55.

Mutant	C-Peptide (cleavage position)	Calculated mass (in Da)	Measured mass (in Da)
juxBri3_1	59	3073	3070
	58	3201	3193
	56	3385	3378
	55	3532	3532
	53	3843	3844
	50	4206	4209
juxBri3_2	55	3622	3622
	52	3963	3967
	49	4292	4286
juxBri3_3	60	3158	3156
	55	3652	3652
	52	3994	4995
	50	4220	4223

4.4. CONSECUTIVE SUBSTRATE PROCESSING

4.4.1. CONSECUTIVE CLEAVAGE OF TNFα BY SPPL2A

After initial cleavage, the TNFα counterpart that remains in the membrane after C-peptide release is further processed by SPPL2. The conversion of TNFα NTF into TICDs is best visualised when the FL protein is co-expressed with exogenous levels of SPPL2 (Fluhrer et al., 2008, Fluhrer et al., 2006). Consecutive cleavage of TNFα in HEK293 cells endogenously expressing SPPL2a/b is barely detectable (Figure 4.31) and co-expression of TNFα NTF and SPPL2 accelerate turnover to the point where TICDs cannot be observed on WB anymore. Therefore, to monitor TICD production, N-terminally Flag-tagged TNFα FL was co-expressed with either SPPL2a or SPPL2b, which resulted in the reduction of TNFα NTF and the release of several TICDs (Figure 4.31). Turnover of TNFα NTF provides further evidence for the efficiency of initial cleavage, whereas the amount of TICDs and

their turnover hints towards the efficiency of the consecutive cleavage. Co-expression of TNFα wt with SPPL2a or SPPL2b confirms previous findings on SPPL2b (Fluhrer et al., 2006, Fluhrer et al., 2008) and supports evidence that SPPL2a is able to consecutively cleavage TNFα as well. Both initial cleavage and consecutive cleavage were eradicated when SPPL2a/b were absent, which resulted in accumulation of the NTF.

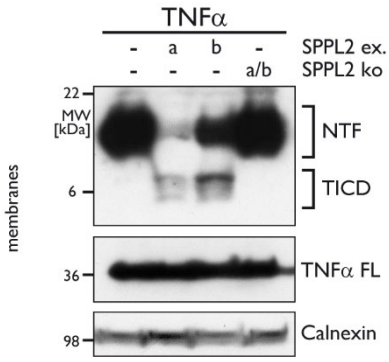

Figure 4.31 Consecutive TICD generation by SPPL2a and SPPL2b. Membranes of the indicated HEK293 cell lines ectopically expressing TNFα FL were isolated. Intracellular TNFα species were visualised by the monoclonal FlagM2 antibody. Isolation of TNFα FL was used as transfection and calnexin as loading control (Spitz et al., 2020).

To address whether SPPL2a utilizes processive cleavages within the TMD similar to SPPL2b, an *in vitro* conversion assay was performed (Fluhrer et al., 2008). Membrane preparations from cells co-expressing either SPPL2a or SPPL2b and TNFα were incubated at 37°C for different time intervals. The efficiency of the consecutive cleavage is defined by the number and amount of detected fragments and their size. Hence, the detection of less or smaller fragments hints towards an increase and accumulation or larger fragments hints towards a decrease in consecutive cleavage efficiency. Similar to SPPL2b, SPPL2a evinced processive activity, converting longer TICD species into shorter ones (Figure 4.32). However, SPPL2b was more efficient in the turnover since the decrease of TNFα NTF was much faster and TICD conversion more efficient. Generally, less and smaller TICDs were detected when TNFα was co-expressed with SPPL2b while co-expression of TNFα with SPPL2a resulted in accumulation of larger TICDs. While SPPL2b converted the largest TICD (Figure 4.32; #1) within two hours into three smaller TICDs (Figure 4.32; #2-4), SPPL2a only showed two cleavages (Figure 4.32; #2, #3) within five hours.

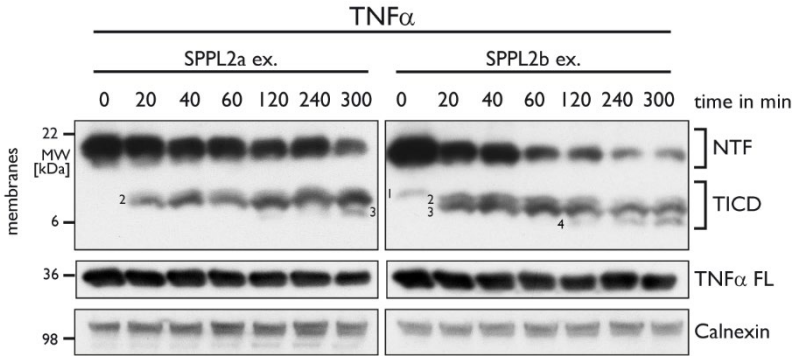

Figure 4.32 Processive turnover of TNFα by SPPL2 proteases. Membranes of HEK293 cell lines co-expressing either SPPL2a or SPPL2b and TNFα FL were incubated for the indicated time periods. ICD conversion was monitored using WB and the Flag M2 antibody for detection. TNFα FL served as transfection and calnexin served as a loading control. (Experiments displayed in this figure were conducted by Martina Haug-Kröper.) (Spitz et al., 2020)

Due to the differences of both SPPL2 proteases in the kinetic of consecutive cleavage, MADLI-TOF mass spectrometry was used to determine whether the N-terminal cleavage sites generated during sequential cleavage also differ. Analysis of TICDs produced by SPPL2b cleavage confirmed previously reported cleavage sites in the TMD after amino acids S34 and L39 (Fluhrer et al., 2006) and the release of additional smaller peptides resulting from the cleavages after position P18, G26 and R28 (Figure 4.33). The most prominent cleavage at position R28 displayed a modification of the cleavage site in SPPL2b-expressing cells. To this end, it can only be speculated whether it originates from a C-terminal modification of the arginine or whether the peptide is modified at a more N-terminal residue. The ≈40 Da mass difference between the peaks could correlate to an acetylation of either Lys19 or Lys20. However, the second peak could also result from the formation of sodium adducts (Zhu and Papayannopoulos, 2003). The reason why this modification primarily occurred in SPPL2b-expressing cells could not be identified.

In addition to the earlier study (Fluhrer et al., 2006), a new consecutive cleavage site at S37 was identified. Even though SPPL2a appeared less efficient in the consecutive cleavage on WB analysis, more cleavage sites and smaller TICDs compared to SPPL2b were identified by mass spectrometry. While the most dominant cleavage of SPPL2a in the TMD was at S34, SPPL2b main cleavage occurred at L39. Additionally, to the SPPL2b cleavage sites, SPPL2a cleaved the TNFα TMD at L35 and L31 and at position K20 in the TICD. The exact masses measured in mass spectrometry are compared to the calculated masses in Table 4.7.

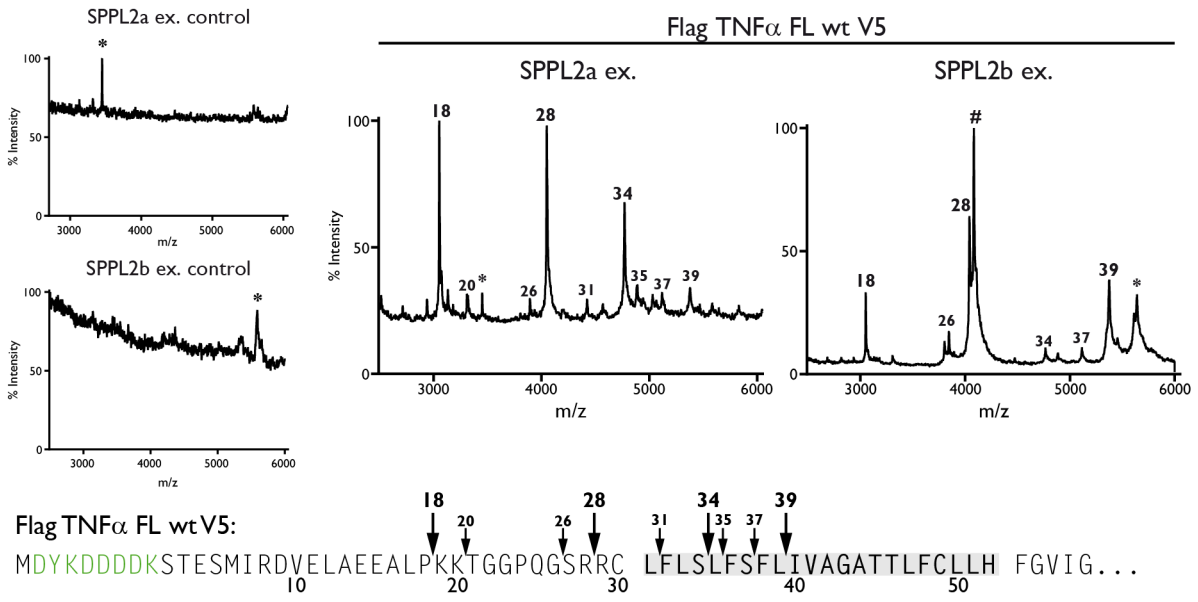

Figure 4.33 N-terminal cleavage sites in TNFα. Mass spectrometric analysis of the TICD generated from SPPL2a or SPPL2b, respectively. Numbers indicate the position of the most C-terminal amino acid of the respective cleavage product. Lysates of untransfected controls were included to decipher unspecific peaks (*). A modification of a cleavage product is indicated with a #. Arrows indicate the cleavage sites in the TNFα sequence. The TMD is indicated in grey and the Flag-tag in green (Spitz et al., 2020).

Table 4.7 Masses of TICDs measured by MALDI-TOF compared to calculated masses. Measured values are normalised to the calculated value of cleavage at position 39.

TICD (cleavage position)	Predicted mass (in Da)	Measured mass (in Da)	
		SPPL2a	SPPL2b
18	3058	3059	3058
20	3314	3315	
26	3811	3810	3312
28	4055	4056	4050
#			4090
31	4427	4429	
34	4774	4776	4775
35	4888	4892	
37	5122	5126	5124
39	5383	5383	5383

4.4.2. PROCESSIVITY CAN BE MODULATED BY TMD MUTATIONS

The consecutive cleavage of IMPs is also termed processivity. Since the exchange of structurally important amino acids within the TMD had shown to affect non-canonical

shedding of TNFα (Section 4.2.4), the effect of these mutations on processivity was investigated. The most prominent effects were again observed when amino acids were substituted by leucine and proline, while as expected alanine substitutions mainly displayed similar effects as leucine substitutions but less prominent. Leucine and alanine in positions S34, S37 and H52 increased the amount of TICD, pointing to a reduced processivity. In contrast, proline induced the opposite effect in all positions tested, except at C49 and H52 (Figure 4.34). NTF and TICD in these mutants were barely detectable, providing evidence for a faster turnover. SPPL2a/b-deficient cells served as a control demonstrating that decrease of NTF and therefore the generation of TICD was specific for SPPL2a activity.

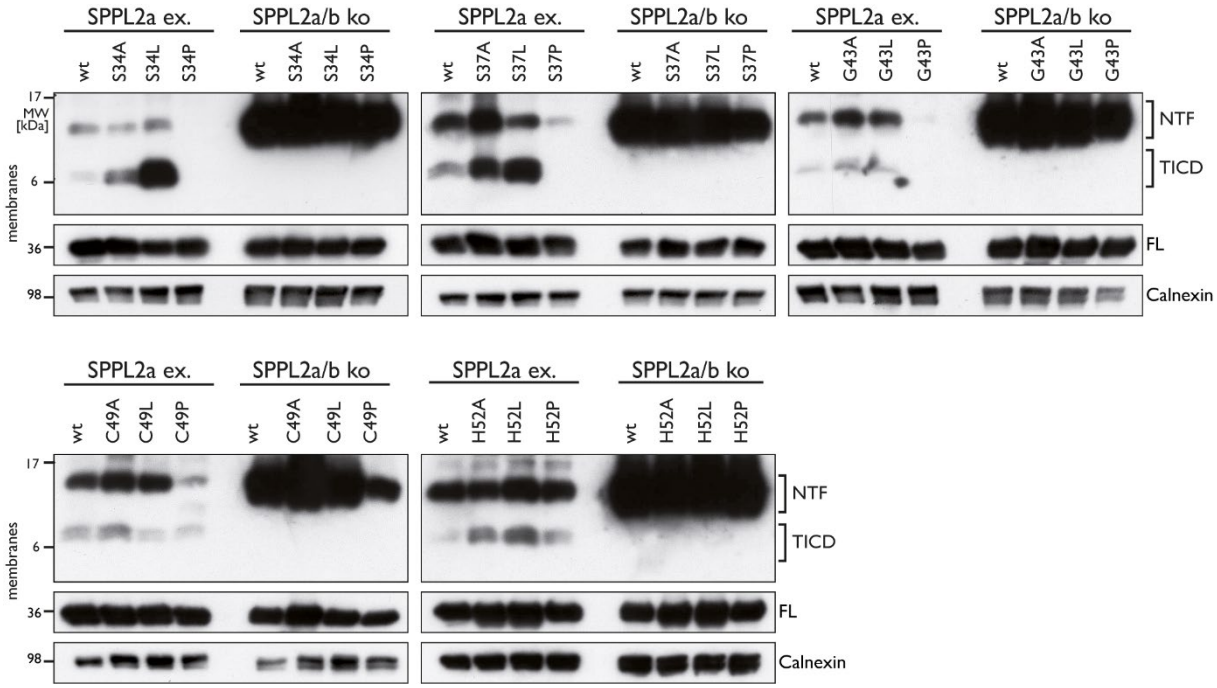

Figure 4.34 Mutations in TMD affect the processivity of SPPL2a. Membranes of HEK293 cell lines either co-expressing SPPL2a (ex.) or neither of the SPPL2a/ SPPL2b proteases (ko) with the indicated TNFα variant were isolated. TNFα cleavage products were monitored using WB analysis and FlagM2 antibody for detection. Detection of the FL protein served as transfection and calnexin as a loading control.

To better monitor consecutive cleavage of the TNFα variants over time, an *in vitro* conversion assays was performed as described above (Section 4.4.1) (Fluhrer et al., 2008). The accumulation of TICD compared to the respective wt control supported the evidence that single leucine mutants in position S34, S37, H52 but also G43 and the triple leucine substitution (AGA/LLL) slowed down consecutive cleavage by SPPL2a (Figure 4.35). It seemed as if the initial cleavage was generally slowed down in S37L, C49L, H52L and

AGA/LLL, as the NTF was not processed as quickly as in the corresponding wt. To no surprise also over a longer period of time no fragments were detectable in proline substituted TNFα variants, further supporting an improved processivity by increased TMD dynamics. Similar effects were observed for SPPL2b (data not shown).

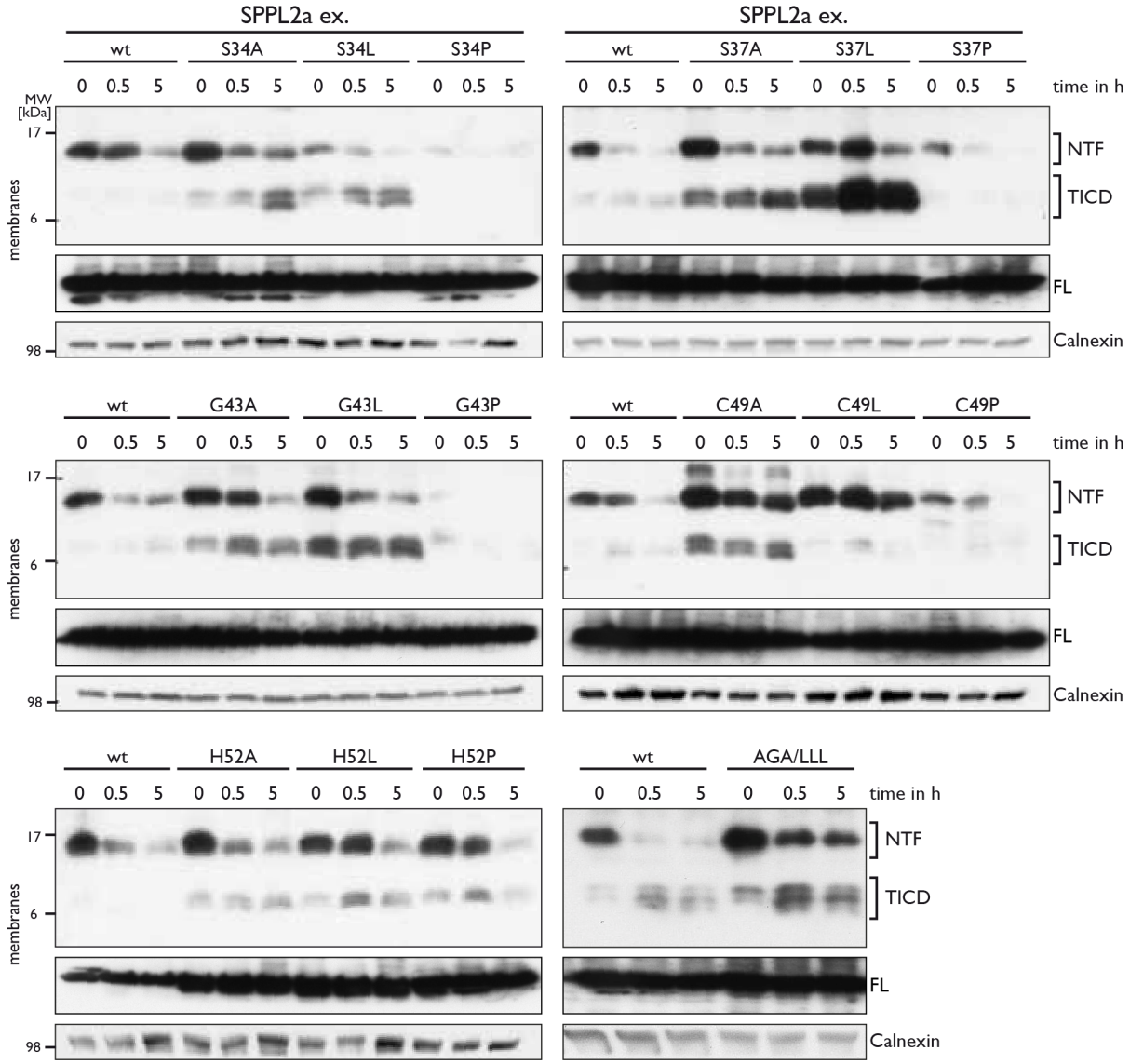

Figure 4.35 Substitutions in the TMD affect processivity of SPPL2a. Membranes of HEK293 cell lines co-expressing SPPL2a (ex.) and the indicated TNFα variant were incubated for the indicated time periods. TICD conversion was monitored using WB and the Flag M2 antibody for detection. The FL protein served as transfection and calnexin as a loading control.

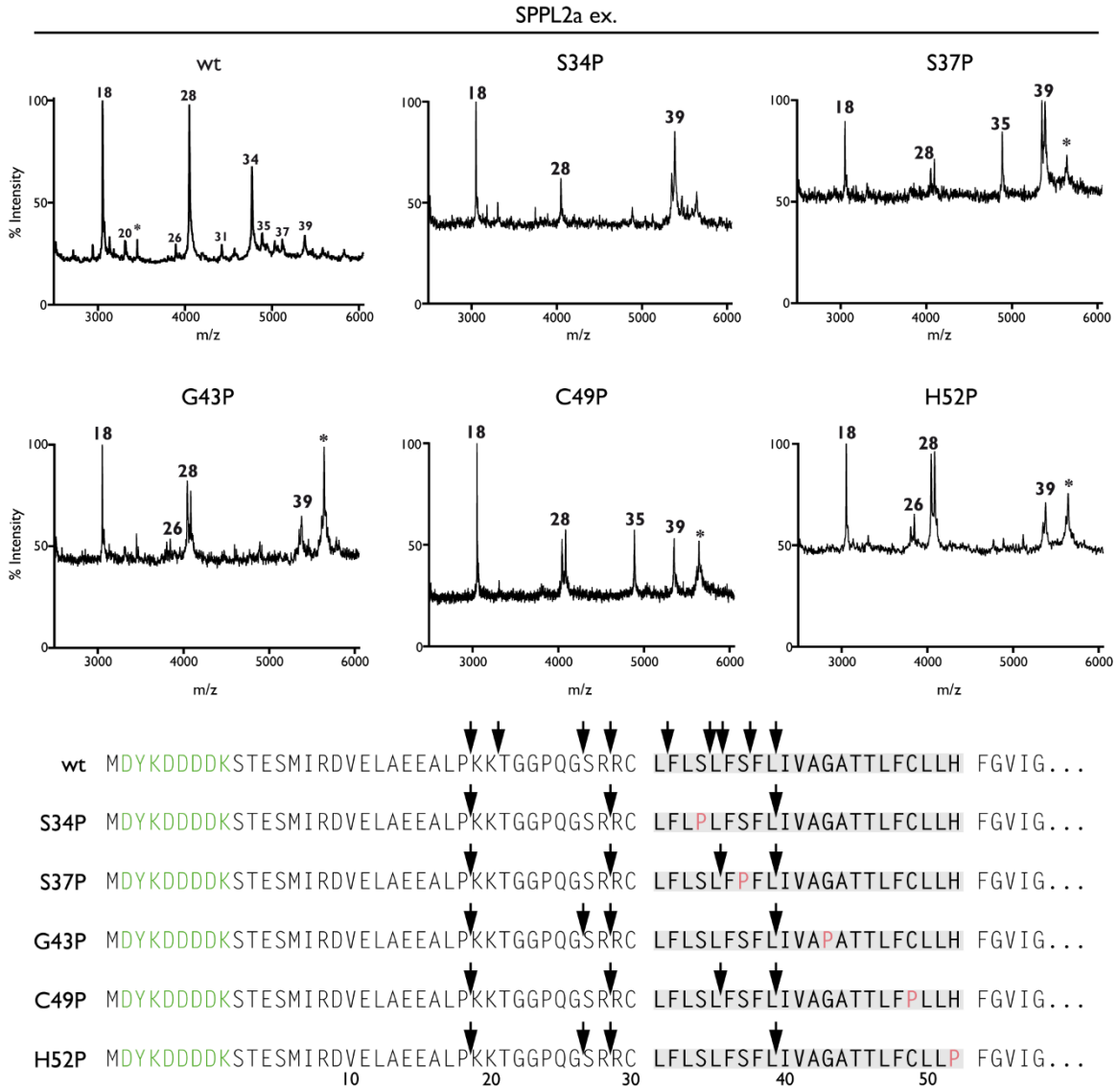

Figure 4.36 Use of N-terminal cleavage sites in the TNFα TMD proline variants is changed. TICDs were isolated from membranes of cells ectopically expressing SPPL2a (ex.) and the indicated TNFα variant and isolated using the FlagM2 antibody. Numbers indicate the position of the most C-terminal amino acid of the respective cleavage product. The TMD is highlighted in grey, the Flag-tag in green and the substituted amino acid in pink.

To elucidate whether the altered processivity induced by proline substitutions also affected the SPPL2a cleavage sites, TNFα variants were analysed by mass spectrometry. Positions of the cleavage sites in TNFα variants did not change; however, the overall number of cleavage sites was strongly reduced upon proline substitution (Figure 4.36). Whereas in TNFα wt S34 was the major cleavage site within the TMD, all mutants displayed a most prominent cleavage at L39. Except for TNFα variants S37P and C49P that were also cleaved at L35 within the membrane, cleavage sites in all other variants within the TMD were diminished. R28 remained the most prominent N-terminal cleavage site. Therefore, the increased processivity of the proline substitutions was probably caused by increased

cleavage kinetics or the reduction of cleavage sites compared to the wt. Proline in the TNFα TMD might have triggered a structural rearrangement, which resulted in an earlier release of the TICD from the membrane and thus these mutants display a reduced consecutive cleavage and subsequent release of TICDs in WB analysis. Exact masses of calculated and measured ICD peptide masses are displayed in Table 4.8.

Table 4.8 Masses of N-terminally cleaved TNFα variants measured by MALDI-TOF compared to calculated masses. Measured values are normalised to the calculated value of cleavage position 39.

TNFα variant	TICD (cleavage position)	Calculated mass (in Da)	Measured mass (in Da)
S34P	18	3058	3059
	28	4055	4056
	39	5393	5393
S37P	18	3058	3058
	28	4055	4055
	35	4888	4893
	39	5393	5393
G43P	18	3058	3057
	26	3811	3808
	28	4055	4050
	39	5382	5382
C49P	18	3058	3051
	28	4055	4047
	35	4888	4888
	39	5382	5382
H52P	18	3058	3051
	26	3811	3806
	28	4055	4048
	39	5382	5382

4.4.3. PROCESSIVITY CAN BE MODULATED BY INSERTION OF NON-SUBSTRATE DOMAINS

Since Bri3 ICD exhibited strong inhibitory effects on the initial cleavage (Figure 4.27) the impact of the ICD but also TMD and ECD on the processivity of SPPL2 proteases were also tested. Therefore, TNFα/Bri3 FL chimeras were co-expressed with either SPPL2a or

SPPL2b. As already established, the Bri3 ECD abolished shedding by ADAM10/17 or SPPL2a (Figure 4.18), thus no consecutive cleavage could be monitored in chimeras with a Bri3 ECD (Figure 4.37A). In line with the results described above, Bri3 ICD also slowed down consecutive cleavage, as ICDs of 3TT and 33T accumulated compared to TNFα wt ICD. While Bri3 TMD in the context of TNFα did not affect initial cleavage, it seemed to increase consecutive cleavage drastically. However, as already observed in the context of initial cleavage, opposing effects of Bri3 ICD and TMD were not additive, as the consecutive cleavage of 33T was not restored to TNFα wt processing. To ensure that all cleavages resulted from SPPL2 processing TNFα/Bri3 FL chimeras were expressed in SPPL2a/b-deficient cells. Elimination of ICD production and accumulation of chimera NTFs in these cells demonstrates that consecutive cleavage of the mutants is mediated by SPPL2 proteases and is indeed accelerated by the substitution of the TNFα TMD with Bri3 (Figure 4.37B). This shows that even if the TMD has rather a low impact on shedding and initial cleavage it becomes important for consecutive cleavage. However, while Bri3 exhibited an inhibitory effect on initial cleavage by SPPL2 it increased consecutive cleavage.

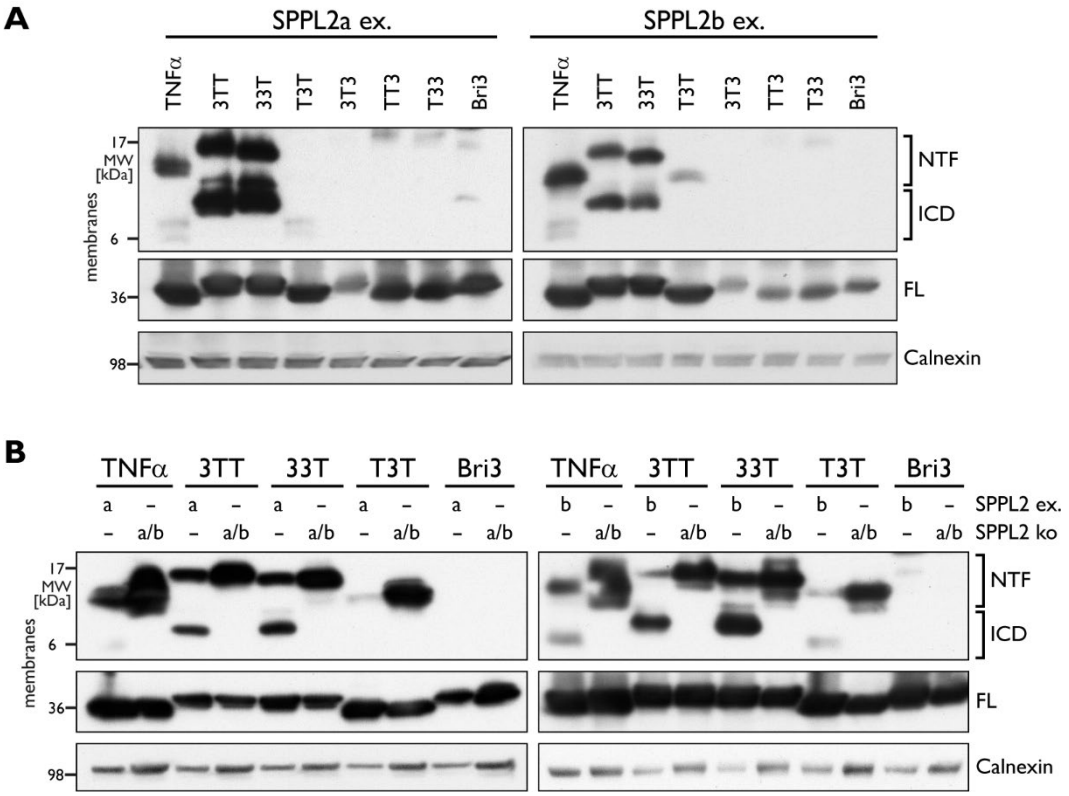

Figure 4.37 SPPL2 processing of TNFα/Bri3 chimeras is reduced by the Bri3 ICD. HEK293 cell lines co-expressing either SPPL2a or SPPL2b were transfected with the indicated TNFα/Bri3 chimera. ICD conversion was monitored using WB and the FlagM2 antibody for detection. The expression of the FL chimera served as transfection and calnexin served as a loading control.

5. DISCUSSION

Intramembrane proteases are involved in a wide variety of processes that range from transcriptional control over cellular signalling to prevention of parasitic and bacterial invasion. They act in the context of RIP. RIP of TM proteins can either activate or terminate a signalling process or remove membrane-resident protein fragments (Figure 5.1). The regulation of this cleavage mechanism can occur on many levels, e.g., the activity of the enzyme can be controlled by expression, co-factors or localisation. If the enzyme is constitutively active, the regulation of cleavage can be modulated by substrate determinants such as consensus cleavage site or substrate enzyme affinity. This ensures that the enzyme cleaves specific proteins and not, for instance, all membrane proteins. However, even though for some IMPs no specific cleavage sequence has been identified, their substrate selection and processing mechanism seem to be highly specific. The question of what characteristics determine a substrate of a specific protease is still pending. Thus, in the context of this thesis, features of the SPPL2 substrate TNFα were exploited in order to increase the understanding of substrate selection and cleavage mechanism of SPPL2 proteases. The following sections will discuss these findings and identify commonalities and differences between the SPPL2 substrates and substrate recognition by other (aspartyl-) IMPs.

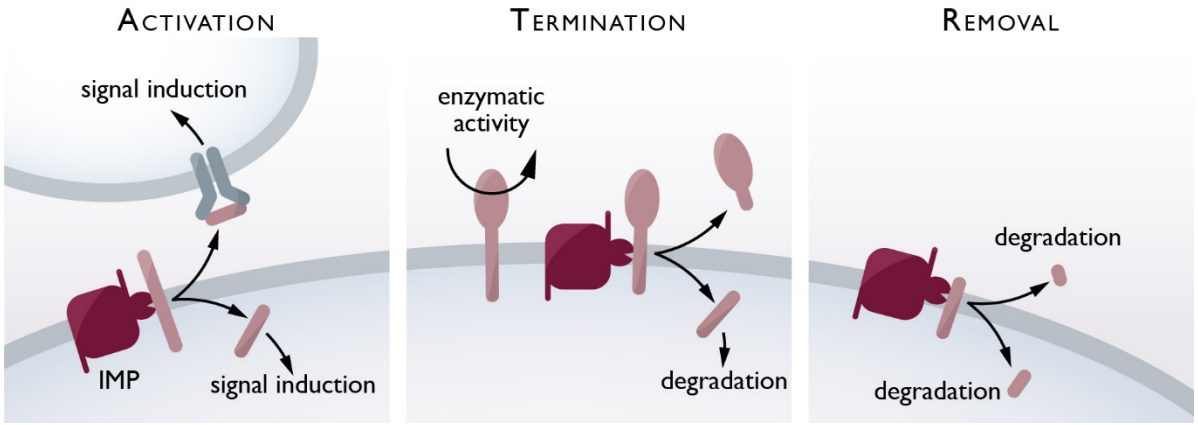

Figure 5.1 Functions of intramembrane proteases (IMPs). By cleaving a TM protein, the intramembrane protease (IMP) releases an intracellular and extracellular peptide. The IMP can terminate a signal by cleaving a TM protein that is active in its membrane-bound state. The probably best-known function is the removal of the TM segment of the protein by sequential cleavage.

5.1. IDENTIFICATION OF NON-CANONICAL SHEDDING BY SPPL2 PROTEASES

Shedding of proteins is one of the key mechanisms within a cell that contributes to the termination or activation of a protein's function. Signalling between cells is often facilitated via soluble peptides that originate from the release of a TM protein's ECD. For TNFα, ADAM17 is the major sheddase that releases sTNFα to signal to recipient cells to induce their survival or death (Coeshott et al., 1999, Kalliolias and Ivashkiv, 2016). The remaining membrane-bound NTF is subsequently processed by the aspartyl-IMPs SPPL2a and SPPL2b (Fluhrer et al., 2006). This study showed that SPPL2a besides ADAM17 contributes to the release of the TNFα ECD by directly cleaving the FL protein (Figure 4.3). This direct cleavage by SPPL2a generated a slightly larger fragment termed sTNFα(L2). Overexpression of either SPPL2a or SPPL2b indicates that non-canonical shedding of TNFα wt is only efficiently catalysed by SPPL2a and not SPPL2b (Figure 4.4). These results go in line with previous studies showing that SPPL2b does not accept Bri2 FL as substrate but needs a preceding shortening of the Bri2 ECD by ADAM10 (Martin et al., 2009).

SPPL2a-mediated non-canonical shedding was sensitive to an SPPL-specific inhibitor and abolished in SPPL2a/b-deficient cells. Thus and in line with the definition of shedding (Lichtenthaler et al., 2018), SPPL2a qualifies as a part-time sheddase for TNFα. In addition, non-canonical shedding occurred independently of canonical shedding, as the inhibition of ADAM17 did not affect shedding by SPPL2a (Figure 4.5).

Because sTNFα(L2) is slightly larger than regular sTNFα, it is not surprising that the SPPL2a shedding sites mapped to cleavage sites within or close to the TMD while the canonical shedding site of ADAM17 located more N-terminal (Figure 5.2). Direct analysis of SPPL2a non-canonical shedding sites in TNFα is not possible, as large fragments are not reliably distinguished by MALDI-TOF mass spectrometry. Therefore, a TEV cleavage site was introduced into the ECD of TNFα. Comparing the surface expression and SPPL2 processing of TNFαTEV to TNFα wt showed that the insertion of the FlagTEV did not affect processing. Thus, both canonical and non-canonical shedding most likely occurred on the physiological cleavage sites. Cleavage of TNFα FlagTEV by SPPL2a mainly mapped to position V55. Of note, cleavage sites of SPPL2a in the context of RIP have previously not been determined. Therefore, it was interesting to see that even though different in their cleavage mechanism, SPPL2a and SPPL2b were using the same cleavage sites in the

context of RIP (R60, V55, H52 and L50), although with different intensities (Figure 4.6). Comparing the cleavage sites generated from RIP (Figure 4.6) with the ones from non-canonical shedding (Figure 4.8), showed that the major cleavage site in RIP (L50) occurred five amino acids more N-terminally and within the TMD. This may suggest that either binding of TNFα FL and TNFα NTF to SPPL2a occurs differently or that the ADAM-shedded TNFα NTF is positioned differently within the membrane due to the lack of its ECD. In addition, a possible effect of the FlagTEV introduction cannot be fully excluded even though it seems unlikely, as the overall quality of cleavage sites in TNFα FlagTEV was essentially similar as in TNFα NTF. Therefore, these results further solidify previously found cleavage sites in TNFα and show that non-canonical shedding and cleavage in the context of RIP occur at similar positions.

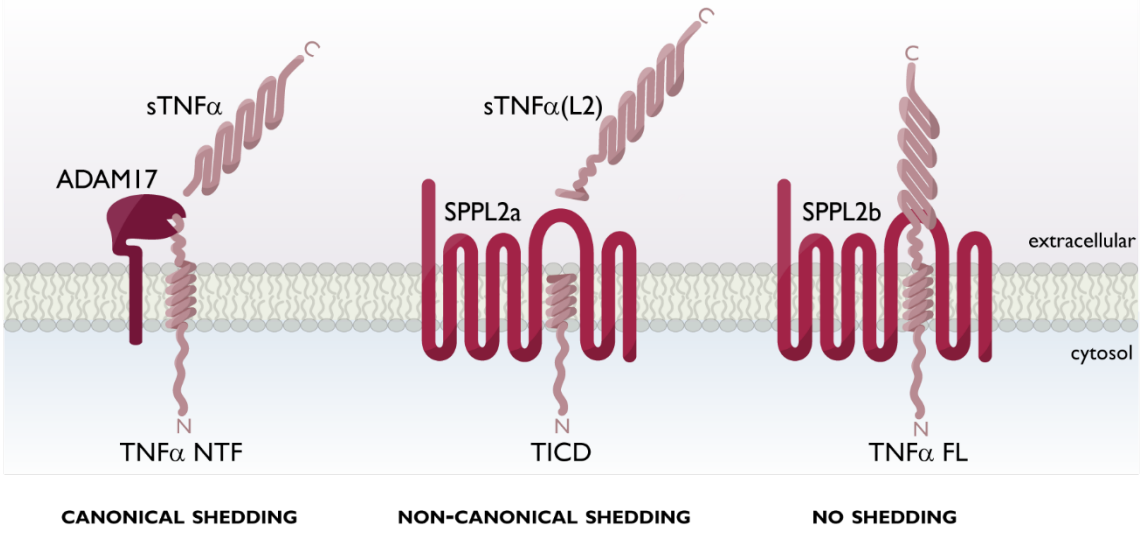

Figure 5.2 TNFα can be shedded by ADAM17 and SPPL2a but not by SPPL2b. The canonical shedding by ADAM17 generates a soluble ECD (sTNFα) and a membrane-bound N-terminal fragment (NTF). The non-canonical shedding by SPPL2a generates a slightly larger ECD (sTNFα(L2)) and directly a TNFα intracellular domain (TICD). SPPL2b is not able to cleave TNFα FL.

Other members of the aspartyl-IMP family have been investigated for their shedding function showing that γ–secretase, SPP and SPPL3 can act as non-canonical sheddases that directly cleave most or at least some of their substrates without any prior shedding.

So far, Nicastrin was suggested as the gatekeeper of γ-secretase ensuring adequate shortening of the substrate's ECD. The APP-homolog APLP1 however, has a large ECD of several hundred amino acids. Nevertheless, in addition to its canonical shedding by ADAM10 and BACE1, γ-secretase was able to process APLP1 directly (Schauenburg et al.,

2018). While the exact mechanism of how APLP1 bypasses the strict short ECD length requirement imposed by nicastrin is unknown, the mechanism of non-canonical shedding by SPP has been investigated more precisely. Generally, SPP is not able to process FL proteins and needs preceding shortening of the ECD by signal peptidases. Nevertheless, with the help of the inactive rhomboid protease derlin1 SPP cleaves Xbp1u without prior shedding (Figure 1.11) (Chen et al., 2014a). Shedding capacity of SPPL3 has been described for several substrates (Voss et al., 2014) and it exceeds that of SPPL2a, as the FVenv protein is processed by SPPL2a, SPPL2b and SPPL3 but only SPPL3 is also capable of shedding this substrate (Voss et al., 2012).

As so far only one substrate for each SPP, SPPL2a and γ-secretase has been described, which is non-canonically shedded by the respective protease, they qualify as non-canonical part-time sheddases while SPPL3 might be considered a non-canonical full-time sheddase.

5.2. PROCESSING OF TNFα BY SPPL2A IS AFFECTED BY DETERMINANTS…

5.2.1. …IN THE TMD

The TNFα TMD was investigated, in order to determine specific characteristics that enable non-canonical shedding and subsequent processing by SPPL2. As expected, exchanging the TNFα TMD with the non-substrate Bri3 TMD did not affect canonical shedding. Nonetheless, the Bri3 TMD in the context of TNFα still enabled non-canonical shedding by SPPL2a (Figure 4.19) and initial cleavage in the context of RIP (Figure 4.27). Vice versa, the substrate TNFα TMD in the context of Bri3 did not result in cleavage of 3T3 by ADAM10/17 or SPPL2a on WB analysis. However, investigation of the cleavage sites by MALDI-TOF mass spectrometry showed that T3T and 3T3 are both processed by SPPL2a. Additionally, T3T was not only processed by SPPL2 proteases but also by an unrelated and unidentified protease. In contrast, 3T3 displayed cleavages only generated by SPPL2. Since chimeric 3T3 was generally lower in surface abundance (Figure 4.17) the detection of

soluble fragments was generally aggravated. Consecutive cleavage was strongly increased when TNFα TMD was substituted with Bri3 (Figure 4.37), which indicates that the individual amino acid composition and therefore the secondary structure of the TMD can affect the processivity of SPPL2. The effects of all TNFα TMD alterations on shedding and subsequent processing are summarized in Table 5.1.

Taken together, results from TNFα/Bri3 TMD chimeras indicate that the TMD itself is neither sufficient to generate a substrate from a non-substrate nor able to inhibit cleavage of a substrate. These results go in line with observations on γ-secretase. A substrate TMD (TNR12) is not cleaved in the context of a non-substrate (Itgβ/DAP12), whereas the non-substrate TMD is cleaved in the context of the substrate (Güner, unpublished data). While results on TNFα/Bri3 TMD exchange and TMD exchange in γ–secretase substrates are consistent, Bri2/Bri3 TMD exchange experiments reveal contradictory results. While the substitution of the Bri2 TMD with Bri3 consistently increased processing, vice versa insertion of the Bri2 TMD in Bri3 still enabled processing (Martin et al., 2008). It rather seemed as if the Bri3 TMD even accelerated cleavage. Additionally, non-canonical shedding could not be identified in these substrates. This strengthens the hypothesis that the cleavage mechanism is defined by substrate rather than protease properties.

Studies in the context of other aspartyl-IMPs such as presenilins and SPPL2b suggested that intramembrane proteolysis is indeed influenced by the conformational flexibility of the substrate TM helix (Fluhrer et al., 2012, Götz et al., 2019, Langosch et al., 2015, Langosch and Steiner, 2017). In line with these observations, proline substitutions especially in the N-terminal half of the TNFα TMD increased non-canonical shedding (Figure 4.11) and overall processivity of SPPL2a (Figure 4.34). Structural analysis of proline-substituted TNFα revealed the destabilisation of the N-terminal TM helix and shift of the hinge bending as cause for the increase in non-canonical shedding (Spitz et al., 2020). The reduced capacity of prolines to form amide hydrogen bonds and its cyclic side chain encounter the N-terminal neighbours, therefore disturbing stabilising interactions (Cordes et al., 2002). Furthermore, proline substitutions in TNFα lead to an increase in the tilt angle of the helix, thus repositioning the protein within a lipid bilayer. In conclusion, proline substitutions affected helix flexibility and positioning, which may explain their long-distance effect on shedding and processing of TNFα. These effects not only increased

SPPL2a-mediated shedding and processivity but also enabled non-canonical shedding and increased processing of TNFα by SPPL2b.

Conversely, leucine, especially a triple leucine motif in the centre of the TMD (AGA/LLL) stabilised the TM helix reducing non-canonical shedding (Figure 4.11) and slowing down processivity of SPPL2a (Figure 4.34, Figure 4.35). The central motif mimics a glycine hinge that upon leucine substitution reduced flexibility and thus cleavage by SPPL2. Such a glycine hinge can also be found in the APP TMD and reduces cleavage by γ-secretase upon substitution with leucine (Götz et al., 2018). Similar to TNFα, the APP glycine hinge is distant from the initial cleavage sites of γ-secretase.

Even though certain TNFα TMD mutations were placed at cleavage positions of SPPL2a (S34, C49, H52), a shift of the cleavage sites, and thus alternative product lines as in APP were not observed. Furthermore, even though N-terminal proline and the C-terminal leucine mutations significantly changed the efficiency of non-canonical shedding, they did not affect the cleavage position (Figure 4.13). However, cleavage sites were abolished when proline was inserted C-terminally next to the cleavage position (Figure 4.13, Figure 4.36), which suggests that SPPL2a might not accept any amino acid at the site of cleavage.

Table 5.1 Effect of TMD mutations in TNFα on shedding and processing. Shedding was measured by the release of the proteins ECD into the conditioned media. Initial cleavage was measured by the release of C-peptide from a short chimera while consecutive cleavage was measured by ICD detection in FL chimeras. TMD: transmembrane domain. =: levels of shedding/ processing were not changed. x: no cleavage was detected. v: reduction of shedding/processing. ^ : increase of shedding/ processing.

Mutation		ADAM17 shedding	SPPL2a shedding	SPPL2a processing	
				Initial cleavage	Consecutive cleavage
S34	A	=	=		v
	L	=	=		v
	P	=	^		^
S37	A	=	=		v
	L	=	=		v
	P	=	^		^
G43	A	=	=		v
	L	=	=		v
	P	=	^		^
C49	A	=	=		v
	L	=	x		v
	P	^	^		^
H52	A	=	=		v

	L	v	x		v
	P	=	=		v
AGA/LLL		v	x		v
TMD	T3T	=	=	= + Protease X	^
	3T3	x	x	x	x

Similar to TNFα, several other aspartyl-IMP substrates exhibit flexible hinge regions in the TMD that upon substitution with leucines (or alanines) significantly reduce the processing (Götz et al., 2019). Cleavage of Xbp1u by SPP and APP by γ-secretase were shown to be reduced upon leucine insertions in the respective TMD (Yucel et al., 2019). Interestingly, removal of an N-terminal but not C-terminal glycine in the TMD of Bri2 reduced cleavage by SPPL2b (Fluhrer et al., 2008). In contrast, reduction of CD74 processing was only observed when all three helix-destabilizing glycine residues were substituted. However, the individual roles of the three glycines were not tested (Hüttl et al., 2016). Nevertheless, a helix-break-helix structure in the substrate's TMD might be one of the key features affecting the processing mechanism of aspartyl-IMP substrates, even though it does not necessarily have to be located in the centre of the TMD (Lemberg and Martoglio, 2002).

A model explaining how increased TMD flexibility possibly affects the cleavage is depicted in Figure 5.3. The substrate is recognised at one or more exosites in the protease, which is followed by translocation to the active site. While the N-terminal part of the helix already occupies its final binding sites, the C-terminal is able to bypass the extra-cellular loop due to the flexible hinge in the TMD (Hitzenberger et al., 2020). The glycosylation of this loop spanning TMD 6 and 7 in SPPL2b might display an additional structural hindrance that cannot be bypassed by TNFα wt. Thus, SPPL2b is not able to non-canonically shed TNFα wt; however, increased TMD flexibility by proline substitutions can enable this mechanism. In contrast, leucine mutations reduce the TM flexibility and therefore the substrate fits less efficiently to the active site, which results in reduced shedding.

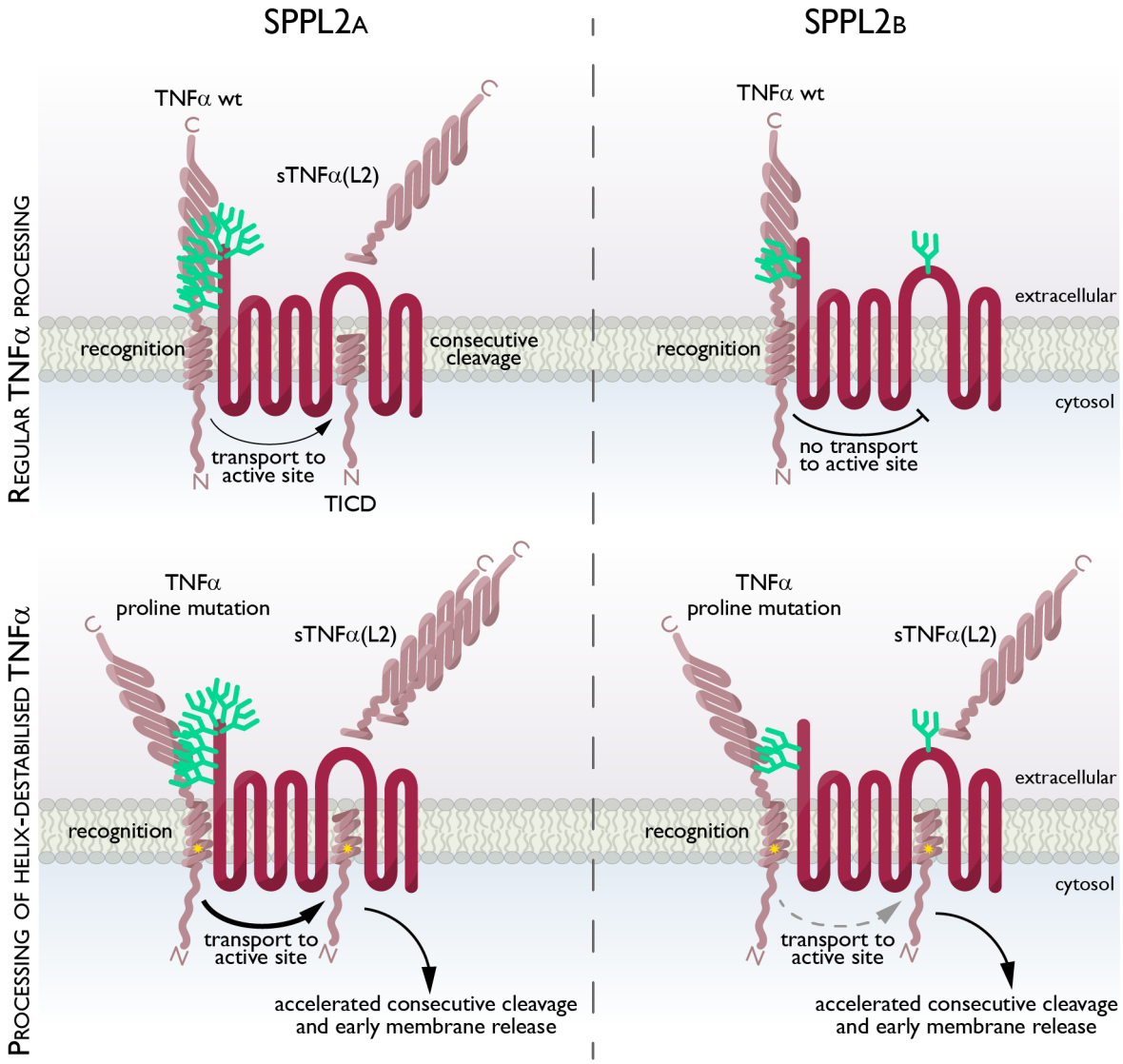

Figure 5.3 Hypothetical mechanism of how proline mutations increase non-canonical shedding by SPPL2a and enable shedding by SPPL2b. TNFα wt even though recognised by both proteases is only shedded by SPPL2a but not SPPL2b. It can be speculated whether the glycosylation of the extracellular loop spanning TMD 6 and 7 inhibits transport to the active site. However, destabilisation of the TM helix by proline substitutions increases the shedding by SPPL2a and even enables shedding by SPPL2b. The proline might induce a structural change in TNFα that enables bypassing the structural hindrance. However, the question whether the accessibility of the TMD is the cleavage-determining factor or the rearrangement of the ECD is necessary as well cannot be answered so far. Furthermore, a specific exosite in SPPL2 proteases that is responsible for recognition has not been described so far.

This model however, only provides information on the shedding mechanism. To explain the changed processivity of the SPPL2 proteases, it is speculated that besides rearranging itself within the protease, the substrate needs local unfolding of the helix at the cleavage sites to allow hydrolysis. Local helix destabilization by proline facilitates access of the helix backbone to the catalytic residues of the protease (Langosch et al., 2015). Due to its strong interactions with neighbouring residues, leucine in contrast may inhibit the necessary unfolding of the helix. Whether the effects of proline and leucine are

actually due to their influence on the flexibility of the helix or direct interaction with the residues of the protease is still debated.

While results on TMD exchange of SPPL2 and γ–secretase substrates were consistent, differences emerge regarding the substitution of single amino acids in the TMD. While leucine substitutions in the APP TMD consistently reduce non-canonical shedding and processivity by γ-secretase, proline substitutions reduce cleavage even stronger (Werner, unpublished data). Hence, it is possible that the degree of helix flexibility would need to match the flexibility of the protease and the extent of steric hindrance presented by the enzyme. Besides bypassing structural hindrances, affecting the TMD flexibility might affect transport within the enzyme to the active site. Therefore, increased flexibility reduces transport, which results in decreased processivity of the substrate. However, structural data of a substrate-enzyme complex have only been resolved for γ-secretase and its substrates (Bai et al., 2015, Cai and Tomita, 2020, Osenkowski et al., 2009). As the required substrate-flexibility will most likely depend on the type of protease, information on SPPL2 substrate interaction cannot be drawn from γ–secretase models and 3D structures of SPPL2 proteases would be of great help to support the SPPL2 cleavage model.

Nevertheless, the flexibility of the TMD seemed to be one key element for non-canonical shedding in TNFα. However, increasing flexibility with a proline substitution of an in principle cleavable TMD in the context of a non-substrate did not enable shedding (Figure 4.20). Substitution of the central glycine with proline in the 3T3 chimera abolished cell surface expression and thus no conclusion about possible effects on shedding or cleavage can be drawn. Inhibition of the proteasome showed that this protein was prematurely degraded, which accounts for the tight control mechanisms of the cell controlling for inappropriate folding of a protein.

Since the introduction of a proline into a TNFα/Bri3 chimera did not help to answer the question if increased TM flexibility generally enables non-canonical shedding by SPPL2a, a screen for potential substrates comprising a natural proline within the TMD was applied. Out of five proline-containing type II TM proteins, none displayed non-canonical shedding by SPPL2a (Figure 4.14). Thus, generating a substrate from a non-substrate by solely enhancing the flexibility of the TMD is not possible, indicating that further substrate properties are necessary for efficient cleavage by SPPL2 proteases. Nevertheless,

computing approaches might help in the future to narrow down the possible substrates; however, *in vitro* experiments are still needed to verify the results, especially to pinpoint actual substrate requirements to increase again the precision of the prediction algorithm.

5.2.2. ...IN THE LUMINAL JMD/ ECD

Substitutions of the TNFα TMD with Bri3 did not impact on shedding in particular; however, exchange of the TNFα ECD with Bri3 (TT3, T33, 3T3) resulted in a complete loss of canonical and non-canonical shedding despite the presence of TNFα ICD and/ or TMD (Figure 4.18). Thus, consecutive cleavage by SPPL2 in these chimeras was also not observed (Figure 4.37). However, initial cleavage of the short TNFα/Bri3 chimeras comprising the Bri3 JMD (TT3, T33) was not completely abolished but rather reduced when TNFα ICD was present (Figure 4.27). Moreover, several cleavage sites were detectable by mass spectrometry, which resulted from SPPL2a-mediated cleavage (Figure 4.28). These results indicate that the Bri3 JMD is not sufficient to inhibit SPPL2-mediated cleavage and that the Bri3 JMD such as the TMD can be cleaved by SPPL2 even though less efficient. The effects of all JMD mutations on shedding and subsequent processing are summarized in Table 5.2.

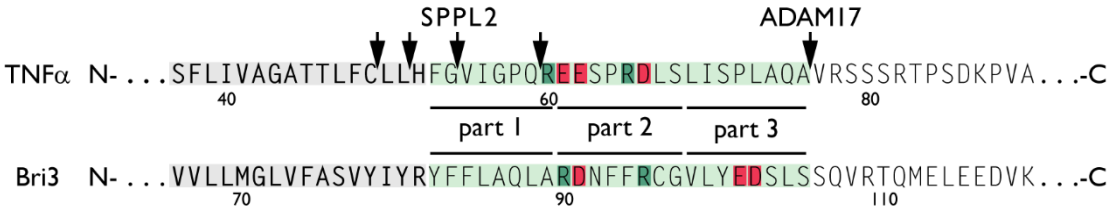

Figure 5.4 Negatively charged residues in the JMD of TNFα and Bri3. Known cleavage sites in TNFα by SPPL2a and ADAM17 are indicated with arrows. The TMD is indicated in grey and the luminal JMD in green. Negatively charged residues in the JMD are highlighted in red and positively charged residues in dark green. JMD sections that were exchanged are underlined.

In order to determine in more detail the features of the Bri3 JMD that display the impeding effects on shedding and initial cleavage, the TNFα JMD was split into three sections that were individually substituted with the corresponding section of the Bri3 JMD (Figure 5.4). Exchange of the first part of the JMD with Bri3 reduced non-canonical shedding (Figure 4.21) and initial cleavage (Figure 4.29). Even though the major SPPL2

cleavage site within the TNFα TMD (L50) was still detectable, additional cleavage sites in the altered JMD section occurred (Figure 4.30). Since these cleavage sites were still present in SPPL2a/b-deficient cells, it is most probable that they were generated by an unrelated and so far unidentified protease. In the context of a cellular assay, other proteases may interfere with cleavage, as indicated by mass spectrometry results. Interestingly, substitution of only the first section of the TNFα TMD with Bri3 did not abolish the cleavages in the Bri3 section in SPPL2a/b-deficient cells, whereas cleavages in chimeras with the whole TNFα JMD substituted with Bri3 were generated by SPPL2 as indicated by their elimination in SPPL2a/b-deficient cells. Whether these results display a valid effect, where Bri3 JMD attracts an unrelated protease for cleavage or whether technical problems such as the contamination of the SPPL2a/b-deficient cells interfered with the analysis needs to be validated in the future.

While the substitution of the second JMD section reduced canonical shedding, it did not affect non-canonical shedding (Figure 4.21). In contrast, initial cleavage by SPPL2a was strongly reduced (Figure 4.29, Figure 4.30). Thus, it seems that this section of the JMD is crucial for initial cleavage in the context of RIP but rather less important for non-canonical shedding. These results indicate that either non-canonical shedding and cleavage in the context of RIP are two independent processes or that the FL protein is positioned and processed differently than the short substrates.

The exchange of the third section of the TNFα JMD, which comprises the ADAM17 cleavage site, abolished canonical shedding while still keeping a reduced amount of non-canonical shedding (Figure 4.21). As initial cleavage was not affected by the substitution, it seems that this part of the TNFα JMD does not affect the cleavage by SPPL2.

These results conclude that the first and second section of the TNFα JMD contains SPPL2 substrate-defining properties. Generally, the luminal JMD of TNFα is an un-structured domain connecting the helical TMD and the β-sheet structured ECD (Eck and Sprang, 1989, Idriss, 2000). Analysis of the primary structure revealed that the TNFα JMD contains three negatively (E61, E62, D66) and two positively charged residues (R60, R65), most of them in the second section of the JMD. The importance of charges on processing by an aspartyl-IMP was previously demonstrated by a study on the SPP cleavage mechanism, where positively charged residues in the JMD had an inhibitory effect on cleavage efficiency of several substrates (Lemberg and Martoglio, 2002). When comparing

TNFα and Bri3 JMD it becomes apparent that the Bri3 JMD contains also two positively (R80, R85) three negatively charged residues (D81, E91, D92). However, whereas the positively charged arginines of Bri3 and TNFα are in similar positions, the negatively charged residues are distributed differently in the Bri3 JMD (Figure 5.4). Substitution of the whole TNFα JMD with Bri3 did not change the balance of the charges but repositioned them. Since initial cleavage was still enabled in these chimeric proteins (Figure 4.27) but canonical shedding abolished, these results suggest that SPPL2 is more accepting of diverse positions of the charges whereas ADAM10/17 does not accept negatively charged residues in the proximity of its cleavage site. This conclusion corresponds with the observations when the third TNFα JMD section was substituted with Bri3. This exchange kept the negatively charged residues of the second TNFα JMD section in place and inserted two additional negatively charged residues close to the ADAM10/17 cleavage site, which eradicated canonical shedding (Figure 4.21).

The substitution of the second section of the TNFα JMD with the corresponding section of Bri3 reduced the negatively charged residues and even added a positively charged residue to the chimeric JMD. This modification abrogated initial cleavage completely (Figure 4.29); therefore, it can be speculated that negative charged residues enable cleavage while positive charges have an inhibitory effect at least for the initial cleavage by SPPL2.

Since these mutations affected the number of negative charges in the substrate JMD, the respective residues were substituted with their structurally similar amino acids (EED/QQN). This resulted in a shift of canonical shedding but also abolished non-canonical shedding completely (Figure 4.22). Thus, it seems that ADAM is dependent on the correct localisation of the negatively charged residues to enable proper cleavage. Furthermore, it indicates that SPPL2 but also ADAM10/17 need a certain balance of charged residues in the middle of the TNFα JMD for processing.

Because substitution of the charged residues with alanines abolished surface expression of the TNFα variant, their importance in maintaining the structure of the TNFα protein is further highlighted. As modifications of the TNFα JMD impact on both shedding and initial cleavage, it is not surprising that also the consecutive cleavage in the chimeric proteins was reduced if even detectable (data not shown).

The presented data show that canonical shedding of TNFα is less sensitive to modifications in the substrates since amino acid substitutions and thus structural changes throughout the protein did not affect canonical shedding unless changes were placed close to the actual cleavage site. The removal of the negative charges in the second part of the JMD and engrafting charges very close to the cleavage site diminished the shedding. How exactly the charges affect the cleavage by ADAM17 remains to be investigated. Possible explanations are electrostatic forces between substrate and enzyme or the induction of favourable structures by the charges that are more easily recognised by the enzyme.

Table 5.2 Effect of mutations in the luminal JMD of TNFα on shedding and processing. Shedding and consecutive cleavage were monitored in FL proteins whereas initial cleavage was measured by the release of C-peptide in proteins lacking the ECD. Therefore, initial cleavage might have been detected even though in the FL protein shedding was abolished. JMD: juxtamembrane domain. TMD: transmembrane domain. ECD: ectodomain. Shift: A change in fragment size was monitored; however, cleavage was still facilitated by the indicated protease as inhibitors or protease knockout were able to diminish the cleavage. =: Levels of shedding/processing were not changed. x: No shedding/processing was detected. v: Reduction of shedding/ processing. ^: Increase of shedding/processing. Protease X: Intermediate fragments were detected and could not be abrogated with ADAM or SPPL inhibitors/ ko, thus cleavage is most likely facilitated by an unknown protease. (_) indicates finding from experiments that were conducted but not shown in the result section.

Mutation		**ADAM17 shedding**	**SPPL2a shedding**	**SPPL2a processing**	
				Initial cleavage	Consecutive cleavage
JMD charge	QQN	v + shift	x		(v)
	QQA	v + shift	x	(=)	(v)
	AAA			(v)	
juxBri3_1		=	v + Protease X	v	(v)
juxBri3_2		v	=	v	(v)
juxBri3_3		v	v	=	(v)
ECD	TT3	x	x	v	x
ECD+TMD	T33	x	x	v	x

5.2.3. ...IN THE ICD

Besides ECD/ JMD and TMD, also the ICD affected processing and unexpectedly even shedding of TNFα. By exchanging the TICD with Bri3 ICD (3TT), non-canonical shedding was abolished and even canonical shedding was slightly reduced (Figure 4.18). Surprisingly, the effect was not enhanced but rather reversed by the additional exchange of the TMD (33T), even though substitution of only the TMD (T3T) had no effect on non-

canonical shedding (Table 5.1). Consecutive processing (Figure 4.37), as well as initial cleavage (Figure 4.27) of 3TT and 33T, were reduced. Since C-terminal cleavage sites in these chimeric proteins were not affected (Figure 4.28), this indicates that the ICD is able to affect cleavage efficiency even in distant domains. Comparing Bri3 ICD and TICD shows an obvious size difference, however previous studies on SPP observed no impact of the size of the cytosolic domain on cleavage (Lemberg and Martoglio, 2002). It would be interesting to know whether charges also in the ICD affect positioning of the substrate within SPPL2 and thus affect the cleavage. In contrast to the negative charges in the JMD (Figure 5.4), TNFα ICD comprises two positive charged residues at the cytosolic membrane border whereas Bri3 positive charges are shifted towards the N-terminus (Figure 5.5). Upon ICD exchange positive charges at this membrane border are eliminated, which might be the reason for the reduction of cleavage by SPPL2. Further research will be needed on whether negative charges in the JMD and positive charges in the ICD coordinate a balance that is necessary for efficient SPPL2 cleavage. The effects of all ICD modifications on shedding and processing are summarised in Table 5.3.

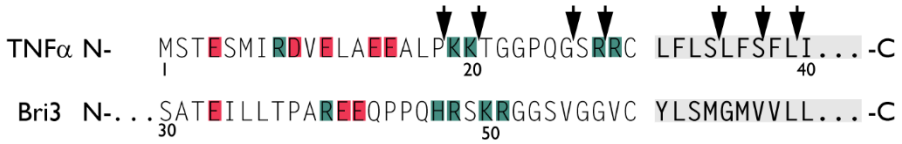

Figure 5.5 Charged residues in the ICD of TNFα and Bri3. The TMD is highlighted in grey and cleavage sites of SPPL2 are indicated with arrows. Negatively charged residues are highlighted in red and positive residues in green.

In addition to the differently located charged residues in TNFα and Bri3 ICD, TNFα undergoes palmitoylation at C30 (Figure 4.23) (Utsumi et al., 2001). To investigate the effect of palmitoylation on SPPL2 cleavage, the cysteine was substituted by serine or alanine. Even though this might induce structural changes, this is the most reliable method to abolish palmitoylation. Inhibitors such as 2-BP inhibit several enzymes involved in lipid metabolism as well as triacylglycerol biosynthesis (Planey and Zacharias, 2010). Therefore, it is important to note that the effects observed upon 2-BP treatment are not necessarily only due to its effects on protein palmitoylation. The research on lipid modifications of TNFα is further complicated by the fact that the PATs and APTs that add and remove palmitoylation are unknown. Thus, specific inhibition of TNFα palmitoylation or depalmitoylation was not possible. Nevertheless, removal of the palmitoylation by

substituting TNFα C30 with serine or alanine enhanced non-canonical shedding (Figure 4.24) which indicates that palmitoylation of TICD might display a structural hindrance for the access of SPPL2 to its substrate. When removed, SPPL2a gains easier access to the cleavage sites and thus shedding and processivity are improved.

Table 5.3 Effect of ICD mutations on shedding and processing. ICD: intracellular domain. TMD: transmembrane domain. =: Levels of shedding were not changed. x: No shedding was detected. v: Reduction of shedding. ^: Increase of shedding. Protease X: Intermediate fragments were detected and could not be abrogated with ADAM or SPPL inhibitors/ ko, thus cleavage might be facilitated by an unknown protease. (_) indicates findings from experiments that were conducted but not shown in the result section.

Mutants		**ADAM17 shedding**	**SPPL2a shedding**	**SPPL2a processing**	
				Initial cleavage	Consecutive cleavage
C30	S	=	^		(^)
	A	=	^		(^)
ICD	3TT	v	x	v	v
ICD+TMD	33T	=	^ + Protease X	v	v

5.3. CLEAVAGE DETERMINANTS OF SPPL2A AND SPPL2B

Based on previous results this study provides further information about the cleavage mechanism of SPPL2 proteases and their substrate characteristics. The side-by-side comparison of SPPL2a and SPPL2b showed that the proteases share a common mechanism by which they process their substrates but yet are distinct from each other regarding the details. (Figure 5.6).

The most prominent indication that SPPL2 substrates are not only determined by a pure size-exclusion mechanism is the fact that the non-substrate Bri3 that is lacking its ECD (Bri3 NTF) is not processed by SPPL2 (Figure 4.28) (Martin et al., 2009). Therefore, properties within the ECD, TMD and ICD of TNFα were determined in this study. Furthermore, it was investigated whether the identified TNFα properties also apply to other SPPL2 substrates.

While ADAM10/17-mediated shedding was only affected by changes close to its cleavage site, non-canonical shedding of TNFα by SPPL2a was affected by changes

throughout the substrate. It requires the proper positioning of the substrate within the enzyme, which may be facilitated by a balance of positive and negative charges in the JMD and ICD. Furthermore, a certain flexibility of the TM helix is necessary (Figure 5.6). As structural elements distant from the actual cleavage sites affect cleavage efficiency, this study supports the hypothesis of SPPL2 proteases comprising an exosite for substrate recognition that is spatially different from the active site. Whether substrate properties only determine binding to the exosite and subsequent transport to the active site or directly influence the cleavage at the active site as well is yet to be determined.

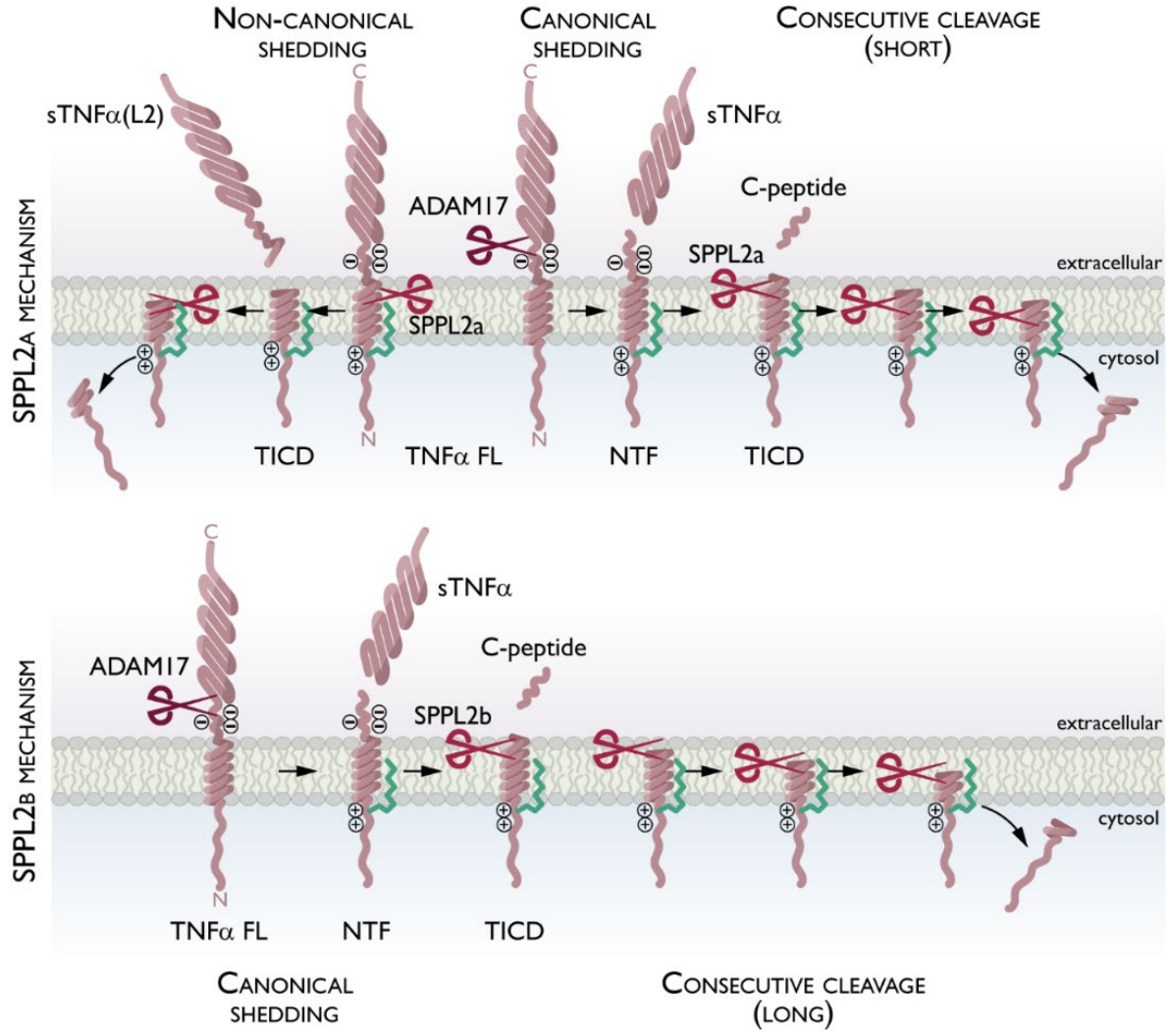

Figure 5.6 Summary of the SPPL2a and SPPL2b cleavage of TNFα. TNFα FL is usually shedded by ADAM17 releasing sTNFα. Canonical shedding by ADAM17 is influenced by negative charges in the JMD (-). Besides canonical shedding by ADAM17, TNFα FL is also shedded by SPPL2a, a process termed non-canonical shedding releasing sTNFα(L2) into the extracellular space. TNFα non-canonical shedding and processing in the context of RIP are influenced by many substrate properties. Both proteases most likely need a balance of negatively charged residues in the JMD and positive ones (+) in the ICD for correct positioning of the substrate in the protease. Furthermore, palmitoylation (green) is able to reduce non-canonical shedding and slow down subsequent consecutive cleavage. Even though both SPPL2 proteases are able to cleave TNFα consecutively, it is less pronounced in SPPL2a resulting in longer TNFα ICDs (TICDs) that are quicker released into the cytosol. Consecutive cleavage of TNFα NTF by SPPL2b occurs in more steps, releasing smaller TICDs.

With these substrate-defining properties, other SPPL2 substrates were investigated to determine whether non-canonical shedding by SPPL2a is a general characteristic of the protease. A comparison of the primary sequence of known SPPL2 substrates with Bri3 did not uncover obvious criteria that distinguish the substrates from a non-substrate (Figure 5.7). Furthermore, characteristics such as the distribution of the charges are not shared amongst all substrates. Therefore, it is not surprising that substrates differed regarding processing in the context of RIP. Already the detection of the ECD was highly variable and substrate-specific (Figure 4.25). Several soluble CD74 fragments of different size were observed. However, they were also present in SPPL2a/b-deficient cells, arguing against a non-canonical shedding mechanism. As published before, these different soluble fragments probably account for differently glycosylated peptides. Whether these represent various maturation states or actually fulfil different functions is not yet investigated.

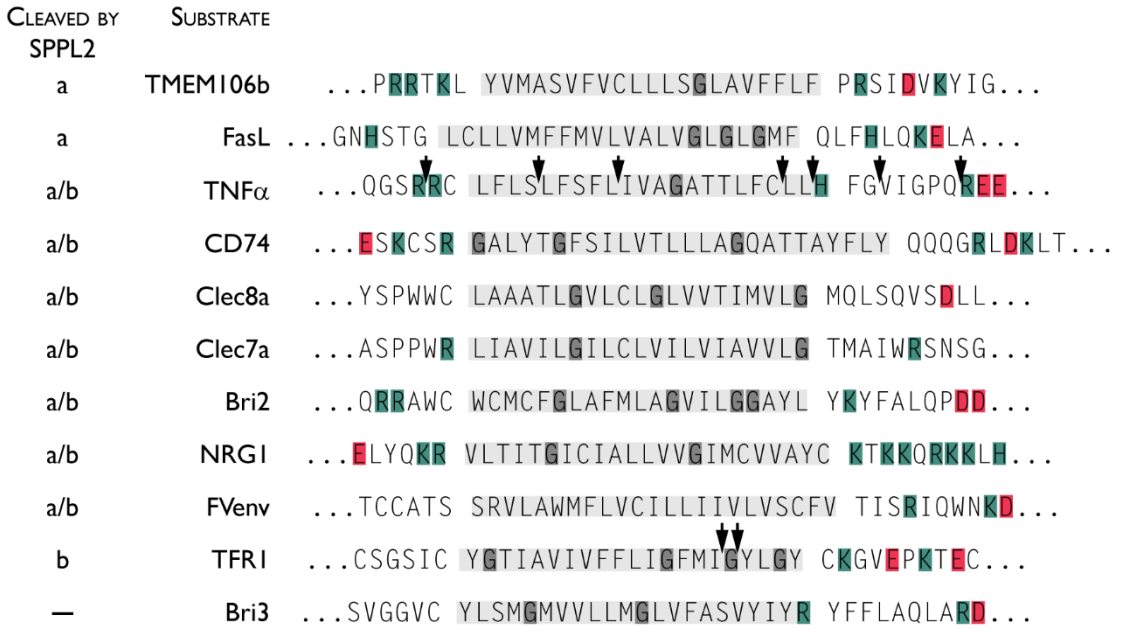

Figure 5.7 Alignment of human SPPL2 substrates with the non-substrate Bri3. Common characteristics that decipher an SPPL2 substrate from the non-substrate Bri3 are not apparent from the primary sequences. Arrows indicate SPPL2 cleavage sites in human substrates that have been determined experimentally. Negatively charged residues are highlighted in red and positively charged residues in green. The TMD is highlighted in light grey and (potentially) destabilising glycines in the TMD in dark grey.

Even though cells secreted several sBri2 fragments, SPPL2a-mediated non-canonical shedding of Bri2 was not observed (Figure 4.26) as the secretion of none of the fragments was impaired in SPPL2a/b-deficient cells. Even substitution of the central glycine with proline did not induce non-canonical shedding. The analysis of Bri2

processing is generally aggravated, as the exact cleavage sites of neither canonical shedding nor subsequent SPPL2 processing are not known. Even though efforts were made to identify the cleavage sites of SPPL2b in Bri2, results were not reliable. Furthermore, the question of whether Bri1 is indeed a substrate or at least shedded could not be answered to full satisfaction in the context of this thesis.

Secreted ECDs of the other substrates (FasL, TMEM106b) could not be detected at all, which complicated the identification of SPPL2a non-canonical shedding. Even stimulation with PMA did not result in the release of soluble peptides. So far, little is known about TMEM106b processing and the identification of a sheddase and detection of a soluble fragment are pending. Interestingly and in contrast to many other SPPL2 substrates, ADAMs, MMPs and cathepsins appear not to act as TMEM106b sheddases (Brady et al., 2014). The release of sFasL however, is additionally to ADAM10/17 induced by MMP7. MMP7 as well as ADAM17 are not constitutively active and need transcriptional activation (Craig et al., 2015). The fact that even with PMA stimulation no sFasL was detected suggests that ADAM17 might not be the major sheddase in the model used. Thus, further experiments with specific activation of MMP7 shedding or a change of the expression system would be needed to gain insight into FasL processing.

These results indicate that SPPL2a-mediated non-canonical shedding is a mechanism unique to TNFα. Nevertheless, it is intriguing to speculate that the SPPL2 substrate-specific cleavage capabilities might change throughout different physiological conditions of the cell. It is imaginable that the cleavage capacity of SPPL2 proteases might change under cellular stress such as starvation or apoptosis. Additionally, the proteases differ in their sub-cellular localisation. SPPL2a is mainly expressed in lysosomes and SPPL2b most likely on the cell surface (Kuhnle et al., 2019) and different conditions, such as the pH, could affect the protease function and selectivity. For instance, the acidic pH in the lysosome might cause a structural rearrangement in the substrate allowing easier access of the cleavage sites for SPPL2a.

Furthermore, cells throughout the body are equipped differently so that in the context of a different cellular system non-canonical shedding might be enabled with the help of cell type-specific adaptor proteins. Based on the discovery that ADAM17 is part of a complex with iRhom and FRMD8, it is possible that the sheddase itself or its co-factors play a role in substrate selection and processing. So far, an interaction of SPPL2 and

ADAM17 could not be validated. Thus, it would be of interest to see whether ADAM17 adaptor proteins specifically interact with TNFα and adaptor proteins of different sheddases with other SPPL2 substrates. In other words, a basic mode of action for SPPL2 proteases might exist, that is then modified by the specific interaction of additional cell/ organ-specific adaptor proteins. This would also allow different processing mechanisms of the same protein throughout the body by the interaction of varying adaptor proteins. In contrast, if co-factors actually contribute to the SPPL2 cleavage mechanism it might be the lack of these in certain subcellular locations that enable shedding whereas the interaction inhibits non-canonical shedding.

Even though it might be intriguing to speculate that co-factors are responsible for substrate selection such as iRhom for ADAM17 (Maretzky et al., 2013), it appears more likely that the differences in function are to find in the protease itself. The SPPL proteases differ significantly in regard to size and glycosylation of their N-termini (Figure 1.9). While the full-time non-canonical sheddase SPPL3 exhibits a rather small N-terminus without glycosylation, part-time non-canonical sheddase SPPL2a carries the largest N-terminus of all SPP/ SPPL-family members and additionally multiple glycosylation sites (Voss et al., 2013). Since SPPL2b comprises an intermediate-sized N-terminus with only three glycosylation sites it seems unlikely that size and modification of the N-terminus enable the shedding function. However, only SPPL2b carries an additional glycosidic chain in the extracellular loop connecting the active site containing TMDs 6 and 7 (Friedmann et al., 2004). This steric hindrance close to the active site may act as gatekeeper in SPPL2b to exclude binding of proteins with a large ECD (Figure 5.3) (Spitz et al., 2020).

While non-canonical shedding seems to have rather strict requirements, initial cleavage seems to occur more promiscuous, as indicated by both SPPL2 proteases preferring substrates with a short ECD. Generally, SPPL2a accepts more changes within the substrate suggesting a lesser specificity towards substrate determinants. While modifications of the area around the C-terminal cleavage site reduced initial cleavage by SPPL2b, SPPL2a cleavage was less affected (Figure 4.29). Furthermore, the distribution of charged residues in luminal and probably also the cytosolic JMD greatly influenced the initial cleavage by both proteases.

The subsequent processing that follows the initial cleavage of TNFα occurs in a sequential manner that is facilitated by SPPL2a and SPPL2b (Figure 4.32). However,

SPPL2b is more efficient in consecutive cleavage. While SPPL2a and SPPL2b cleave TICD in the same major positions, additional SPPL2a cleavage sites were detected (Figure 4.33). It has not been determined whether this resulted from slower proteolytic cleavage or whether a stronger attachment of TNFα NTF to SPPL2a allows more cleavages to occur while SPPL2b releases TICD species more easily.

As for the shedding, consecutive cleavage seems to be substrate-dependent, since the analysis of Bri2 cleavage did not result in several ICD peptides (Figure 4.25). Instead of indicating a consecutive turnover the detection of several NTF fragments rather suggests that many maturation and dimerization states of Bri2 cleavage products exist (Tsachaki et al., 2008).

Whether variations of substrate processing are determined by structural differences in the protease or deviation of localisation and thus diverging environmental factors is so far unknown. The results only account for the processing of TNFα as similar processing mechanism so far could not be observed for other SPPL2 substrates. In contrast to γ-secretase, which seems to process at least some substrates similarly (Okochi et al., 2006), SPPL2 proteases seem to process each substrate slightly different. However, as the consecutive cleavage of APP by γ-secretase is a central mechanism in the development of Alzheimer's disease it remains an open question to what extent consecutive cleavage and non-canonical shedding of TNFα by SPPL2a contribute to the physiological state of the cell.

5.4. PHYSIOLOGICAL RELEVANCE…

5.4.1. …OF NON-CANONICAL SHEDDING IN TNFα

Since SPPL2a accepts TNFα for non-canonical shedding, but SPPL2b does not, this might indicate that sTNFα(L2) generation is not just a general by-product. This hypothesis is supported by the detection of non-canonical shedding in cell lines with endogenous expression of SPPL2a. Hence, to identify a physiological relevance of SPPL2a-mediated

shedding BMDCs of wt and SPPL2a-deficient mice were investigated for the release of sTNFα(L2). Unfortunately, non-canonical shedding of TNFα could not be detected since TNFα processing appeared to be fundamentally different in mice (Figure 4.10). Even though several different soluble fragments were secreted into the conditioned media of cultured mouse BMDCs, release of all fragments was inhibited by a broad-spectrum MMP inhibitor. This indicates that in mice, either ADAM10 and ADAM17 are less specific regarding their cleavage sites or other MMPs contribute to a larger extent to the secretion of mouse sTNFα. Comparing rodent and human TNFα, the primary sequence shows a high level of conservation, especially within the TMD (Figure 5.8). The ECD contains several conserved stretches of ≈10 amino acids, interrupted by less conserved regions. The residues that facilitate binding of human TNFα to the receptor (Van Ostade et al., 1991) are also conserved throughout the species (Figure 5.8, highlighted red). Interestingly, the JMD and the region of ADAM17 cleavage are much less conserved. This might explain also the less conserved mechanism of ECD shedding in rodents compared to humans even though the binding to and activation of the receptor might be similar.

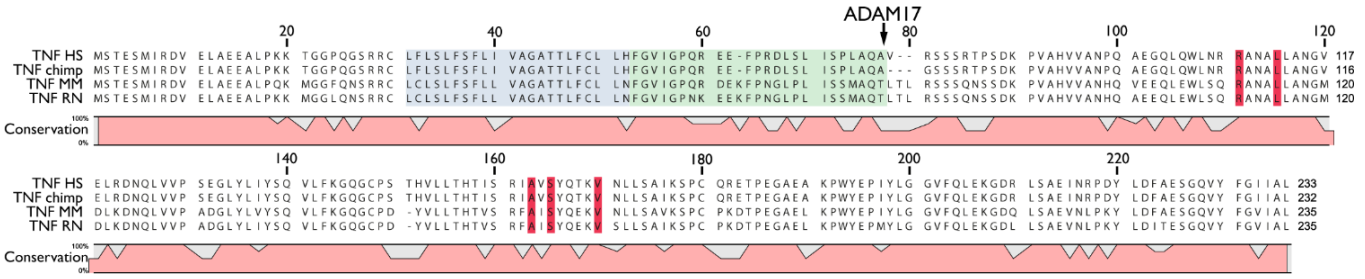

Figure 5.8 Alignment of mammalian TNFα. The protein sequence of human (HS), chimpanzee (chimp), mouse (MM) and rat (RN) display high levels of homology. The TMD is highlighted in grey, the JMD in green and residues mediating binding to the receptor in TNFα HS in red. The arrow indicates the major shedding site in human TNFα by ADAM17.

In order to analyse the specific role of ADAM17 cleavage in mouse vs. human processing, a knockout of the protease would foster the interpretation of the experimental results. However, due to its promiscuity and large set of substrates, investigating the effects of ADAM17 is difficult, as the huge amount of off-target effects would impede a conclusive analysis. Moreover, ADAM17-deficient mice are not viable and also cell lines are affected majorly in their growth behaviour (Peschon et al., 1998). To enable the analysis of ADAM17-mediated shedding nonetheless, it either is knocked out conditionally or cell type-specific. For example, irradiated mice reconstituted with ADAM17-deficient leukocytes only showed an 80-90% reduction of sTNFα (Bell et al.,

2007), which indicates that up to a fifth of the sTNFα production is resumed by other proteases. In mouse models, for instance, MMP7 contributes to a great extent to the secretion of sTNFα (Haro et al., 2000). Studies on the participation of other sheddases in humans show that *in vivo* contributions of ADAM9, 10 and 19 are rather low (Zheng et al., 2004). However, during acute local inflammation sTNFα secretion is enhanced by the serine protease proteinase 3 (Coeshott et al., 1999). Thus, even though ADAM17 is the major sheddase of TNFα, many other proteases are able to partake in this cleavage, depending on the protease expression profile and activation status of the cell. Nevertheless, most of these sheddases cleave human TNFα in a similar position as ADAM17, generating soluble peptides of similar sizes (Table 5.4) and so far, the release and mode of action of a ≈20-25 amino acid longer peptides has not been described. Furthermore, it can be speculated whether the larger mouse sTNFα peptides are differently matured and glycosylated fragments or actually originate from a cleavage within the TNFα TMD. Nevertheless, as the human and mouse TNFα TMD is highly conserved it is surprising to see that the proteins are processed differently. This might be due to the fact that other sheddases contribute to the release of sTNFα, therefore SPPL2a does not encounter TNFα FL. As SPPL2 cleavage sites are conserved between the two species the difference in cleavage might be due to differences in human and mouse SPPL2a. To determine which peptide is released by which protease, mass spectrometry analysis of mouse TNFα in mouse cell lines would be needed. However, it was beyond the scope of this study to scrutinize the cleavage sites of ADAM proteases and SPPL2 in mice.

Table 5.4 Cleavage position of several sheddases in TNFα (Spitz et al., 2020, Zheng et al., 2004).

Protease	Cleavage site in TNFα
ADAM9	...SPLA$_{74}$-QAVRS$_{79}$-SSR...
ADAM10	...SPLAQA$_{76}$-VRSSSR...
ADAM17	...SPLAQA$_{76}$-VRSSSR...
ADAM19	...SPLAQAVR$_{78}$-SSSR...
MMP7	?
Serine protease proteinase 3	?
SPPL2a	...ATTLFC$_{49}$-LL$_{51}$-HFG$_{54}$-VIGPQ$_{59}$-REEFP...

The different proteases releasing sTNFα account for the importance of the soluble peptide in general and commend for a fine-tuned regulatory mechanism. Based on this, the cell/ organ-specific expression of different sheddases may not only allow a local regulation of the amount of secretion but the different peptides of TNFα may also exert different functions. This hypothesis is further supported by data indicating that approximately up to a third of the patients that receive treatment with anti-TNFα drugs do not respond to the treatment (Parameswaran, 2010). The lack of responsiveness and the mechanisms behind it are still unclear.

sTNFα exerts central immunological functions by inducing cell survival or death (Kalliolias and Ivashkiv, 2016, Tartaglia et al., 1991). Misregulated cleavage of TNFα accounts for or exacerbates many autoimmune diseases such as rheumatoid arthritis, chronic bowel diseases (Crohn's disease) and skin diseases like psoriasis (Parameswaran, 2010). Usually, the release of sTNFα via cleavage of ADAM17 leads to interaction with either one of the two TNFα receptors (TNFR1, TNFR2). The crystal structure suggests that sTNFα consists of several β-sheets that associate in homotrimers resembling a pyramidal shape (Figure 5.9A) (Eck and Sprang, 1989, Mukai et al., 2010), which binds to the receptor with the tip facing the membrane. Based on the crystal structure of sTNFα resolved already in 1989, the residues responsible for binding to the receptor have been determined by amino acid exchange. They cluster in two regions at 108/112 and 160/162/167 (Figure 5.9B) (Van Ostade et al., 1991). Interestingly, the more N-terminal cluster facilitates binding mostly to TNFR1, while the more C-terminal one facilitates binding to TNFR2 (Mukai et al., 2009). Since TNFR1 binds sTNFα and TNFR2 binds membrane-bound TNFα (Tartaglia et al., 1993b, Grell et al., 1995), sTNFα is probably able to dip deeper into the binding groove of TNFR1 utilising the more N-terminal residues for interaction and binding of membrane-bound TNFα may display a steric hindrance. However, another explanation for utilisation of different binding motifs might be a different folding of the membrane-bound TNFα ECD compared to sTNFα. Additionally, binding kinetics vary greatly between the receptors as binding of sTNFα to TNFR1 is considered irreversibly while the interaction of TNFα with TNFR2 displays rapid on and off dynamics (Tartaglia et al., 1993a). Even though many crystal structures of TNFα without or in combination with the receptor are available, the model of membrane-bound TNFα with TNFR2 does not fully copy the physiological situation as both receptor and ligand lack their membrane

anchoring domain to allow crystallisation (Mukai et al., 2010). Nevertheless, subtle differences in folding of TNFR2 were detected compared to TNFR1. Even though receptors differ in interaction dynamics and the form of TNFα they bind, so far little is known about the correlation of ligand binding and subsequent intracellular complex formation. Upon binding of sTNFα to TNFR1, formation of either complex I, which induces the NFκB pathway and thus cell survival or complex II, which activates caspase 8 and consequently cell death decide the fate of the receptor cell. As these are two very different functions, the question emerges whether sTNFα variants of different sizes might affect the activation status of the receptor and thus signalling capacity. Modelling of sTNFα(L2) shows that the longer N-termini of the trimerised peptide are facing the extracellular space and not the binding sites of the receptor. However, the additional 20-25 amino acids of sTNFα(L2) might be able to widen the bottom of the pyramidal structure thus affecting binding to the receptor as it is not able to bring interacting residues close to each other. This might weaken the activation of the receptor. If the elongated N-terminus interferes with the correct folding or trimerisation of sTNFα, interacting residues might not become exposed in the direction of the receptor. Again, these changes would weaken the binding of sTNFα(L2) to the receptor or even induce a shift of preference towards one of the TNFRs.

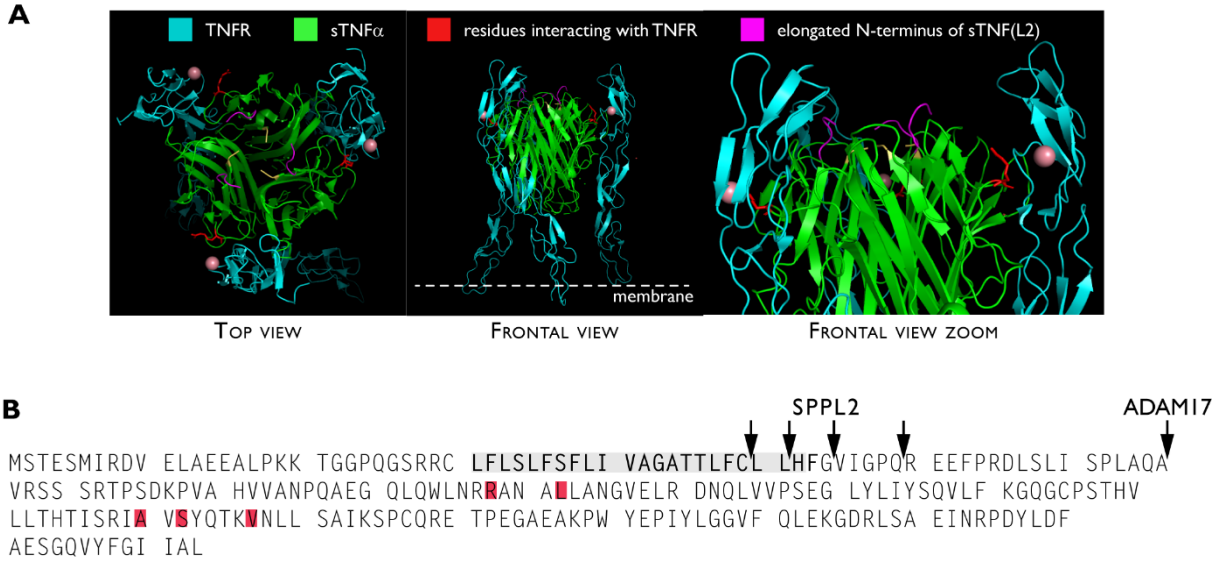

Figure 5.9 sTNFα(L2) structure. (A) 3D structure of sTNFα(L2) binding to the soluble TNFR. sTNFα (green) trimerises in a pyramidal shape. It binds to the receptor (blue) with the tip of the pyramid facing the membrane. In the top view, binding of each sTNFα(L2) monomer to a trimerised TNFR is indicated. The interacting residues are shown in red. The elongated N-terminus of sTNFα(L2) is highlighted in pink (PyMol ID: 3alq, the modelling was kindly conducted by Dr. Sabine Höppner). **(B)** Cleavage sites and receptor interaction sites in the TNFα primary sequence. Shedding sites of SPPL2a and ADAM17 are marked with arrows and the TMD is highlighted in grey.

Addition of several amino acids on the N-terminus of sTNFα could induce aggregation similar to Aβ. The shift of γ-secretase cleavage in APP generates peptides that are just a few amino acids longer but display a strongly increased capacity of aggregation (Cukalevski et al., 2015, Moore et al., 2017). Even though the binding of sTNFα(L2) to its receptor might not be influenced directly, the longer fragments could affect trimerisation by aggregation into larger multimers. If these aggregates accumulated in the extracellular space and form plaques, this would subsequently result in reduced receptor binding, thus altering signalling. Consistently, in Bri2 the duplication of 10/11 amino acids leads to a severe form of dementia due to the aggregation of the altered Bri2 pro-peptide (Tsachaki et al., 2008). Therefore, additional of ≈25 amino acids in sTNFα(L2) could have severe effects on the fragment's characteristics.

Considering the localisation of SPPL2a on the cell surface but also in lysosomes, non-canonical TNFα shedding would release the soluble peptides into the extracellular space but also to the inside of the lysosome. Both, sTNFα and sTNFα(L2) were detected within the cell (Figure 4.7). Thus, it might be speculated that sTNFα(L2) is especially generated by lysosomal SPPL2a to cleave surface-escaped TNFα FL. If this cleavage only served a degradational purpose for misfolded or dysfunctional proteins, SPPL2a would have been expected to cleave other substrates in a similar manner and not only specifically TNFα. Therefore, it is conjectured that intracellular sTNFα/ sTNFα(L2) may have additional functions within the cell. Whether intracellularly generated sTNFα(L2) can be secreted from lysosomes to the extracellular space was not determined within this study.

5.4.2. …OF CONSECUTIVE CLEAVAGE

Mechanistically, the consecutive cleavage may be explained by TNFα passing through the hydrophilic, pore-like active site of SPPL2. While TNFα is moving along the enzymatic domain, SPPL2 remains locked within the membrane. Such a "sliding" along the enzyme would be supported by dynamics of the substrate TMD (Fluhrer et al., 2008). Local unfolding and stretching of the substrate's α-helix enable access of the cleavage sites by the catalytic residues. It is tempting to speculate that physiological reasons for this consecutive cleavage exist, especially as it can be modified by palmitoylation of the TNFα

ICD. This lipid modification of the cytosolic cysteine enables modulation of the consecutive cleavage by anchoring the ICD to the membrane. Since palmitoylation is a reversible modification, the cell might be able to increase TNFα palmitoylation guiding the membrane-associated proteins to lipid rafts (Poggi et al., 2013) but also enabling a consecutive cleavage upon interaction with SPPL2. In contrast, removal of the palmitoylation would decrease lipid raft association and either accelerate consecutive cleavage or reduce it to fewer cleavages. Thus, consecutive cleavage could serve merely a degradational purpose, as a slower turnover would result in less ICD release, which reduces the intracellular signalling. Conversely, the removal of the palmitoylation may result in a fast release of the ICD to induce intracellular signalling. On the contrary, a slow consecutive cleavage might keep the TICD in close proximity to the membrane enabling recruitment of other proteins to the site of action and a fast release from the membrane might reduce recruitment by fast intracellular degradation of the TICD.

6. OUTLOOK AND FUTURE IMPLICATIONS

The results of this study have provided insights into the cleavage mechanism of SPPL2a and SPPL2b. Besides the identification of a non-canonical shedding function of SPPL2a, substrate determinants of TNFα such as the flexibility of the TMD but also charges in the luminal JMD have been identified. However, in a cellular context modifications of the substrates seemed to enable cleavage by proteases other than SPPL2 or ADAM10/17. Thus, the development of an *in vitro* assay in which purified substrate and protease encounter each other under specific, controlled conditions would be crucial. This would help to conclude more certainly if and to what extent modifications affect SPPL2 cleavage and thus substrate properties can be deducted more easily. Therefore, future work will be needed to pinpoint additional characteristics that distinguish random proteins form SPPL2 substrates.

Even though results showed that negative charges affect shedding by ADAM10/17 and SPPL2 as well as initial cleavage, the role of positive charges and charges in the TICD was so far not investigated. Indications that positive charges in both cytosolic and luminal JMD are important for TNFα processing by SPPL2 proteases would need to be addressed in experiments substituting these residues. As charges in the luminal TNFα JMD that were distant from the actual cleavage site affected the cleavage efficiency of SPPL2 it would be interesting to see whether a similar effect for the cytosolic JMD residues can be observed. Substitutions of these residues would yield insights into whether also the positive charges affect processing. To verify the results, which indicated that an increased amount of positive charges in the luminal JMD inhibited initial cleavage, targeted insertions of positively charged residues, for instance by substituting the negative residues at E61, E62 and D66 with positively charged residues would be required.

In the context of ICD modifications, it was established that the removal of palmitoylation increases on non-canonical shedding and consecutive cleavage. It has been shown that for peripheral membrane proteins mutations distal to the sites of palmitoylation can strongly impact the likelihood of lipidation (Ko and Dixon, 2018). Therefore, it would be interesting to test whether proline substitutions in the membrane effected the palmitoylation status of TNFα. If proline substitutions in the TNFα TMD

actually reduce ICD palmitoylation, increased processivity of these mutants by SPPL2 might also be induced by the lack of lipidation.

The SPPL2 substrate TNFα is a cytokine, crucial for initiating and regulating many essential signalling pathways and thus to be fundamental for inflammatory processes and host defence. Therefore, investigating its lifecycle and the physiological role of its cleavage products might be essential in improving the treatment of TNFα-related diseases.

Even though in this study endogenous levels of SPPL2a displayed non-canonical release of sTNFα(L2) from transfected TNFα, in this experimental setup levels of soluble TNFα peptides are much higher as under physiological conditions. Thus, in the future, it would be of interest to investigate the amount of non-canonical shedding in the context of physiological TNFα levels. These experiments would require a cell line with detectable endogenous amounts of SPPL2a and TNFα. A cell line probably most suitable for experimental use would be HMC-1 that displays relative high levels of both proteins (Figure 6.1). HMC-1 is a mast-cell cell line derived from a patient with leukaemia. Although secretion of TNFα could be further enhanced by LPS stimulation, an HMC-1 SPPL2a/b-deficient clone would need to be established to conclude about the specificity of the possibly generated fragments. Furthermore, the investigation of whether adaptor proteins in different cells might help facilitating non-canonical shedding would be interesting.

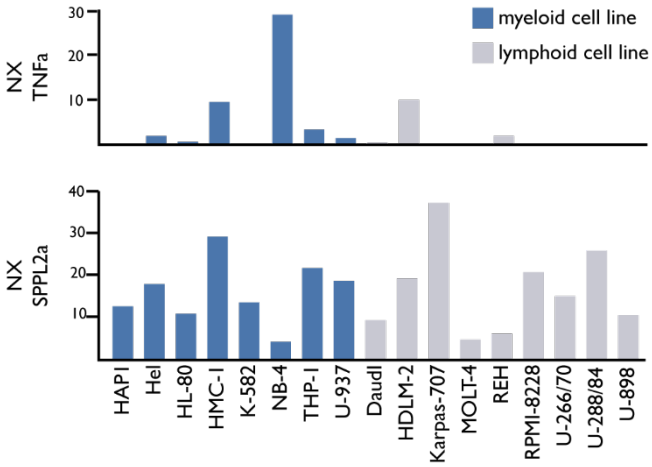

Figure 6.1 Immortalised cell lines that express TNFα and SPPL2a endogenously. Generally, myeloid cell lines express the highest levels of TNFα. Especially NB-4 cells that are derived from bone marrow of a patient with progressive leukaemia. Also, solid tumours upregulate TNFα, therefore, medium levels can be found in the lymphoid cell line HDLM-2. SPPL2a is ubiquitously expressed and can be found in myeloid and lymphoid cell lines. Highest levels are found in HMC-1 mast cells and Karpas-707 cells originated from myeloma cells (www.proteinatlas.org).

Besides the amount of physiologically released sTNFα(L2), its fate and function within the cell might be of interest. Design of sTNFα(L2) peptides that can be used in cellular assays could give insights about their signalling capacity. Cells with detectable amounts of TNFR such as HeLa cells could be analysed for changes in the intracellular

signalling pathways. Analysis of mRNA levels using qPCR or on protein level using WB might yield interesting results of whether sTNFα(L2) alters signalling of sTNFα. To explore whether sTNFα(L2) is able to aggregate such as Aβ peptides, aggregation capacity could be investigated by MD simulations or by SEC-MALS (size exclusion chromatography with multiple-angle light scattering analysis). In addition, mouse models overexpressing SPPL2a could give a hint towards a phenotype generated by the longer TNFα fragment.

Anti-TNFα antibodies that antagonise the receptor or neutralize soluble TNFα are the gold standard in the treatment of TNFα-related diseases and among the most sold drugs worldwide. Other approaches such as to inhibit ADAM17 to reduce sTNFα failed to reach clinical trials as the broad substrate spectrum elicits severe side effects (López-Otín et al., 2009, Vandenbroucke and Libert, 2014). However, as specifically long-term treatments increase the risk of developing autoantibodies or decrease the physiological response (Tack et al., 2009, Tseng et al., 2018) other strategies that make use TNFα variants are being pursued. Soluble TNFα variants are developed that compared to the antibodies are less likely to be recognised as foreign. Non-naturally occurring sTNFα monomers would interact with endogenous sTNFα wt monomers resulting in mixed trimers incapable of activating the TNFR. This regulates the activation of the TNFRs and therefore adjusts the host immune response. These sTNFα variants could be used for (short-term) treatment of patients as an alternative for classical treatment (Dahiyat and Filikov, 2006). Depending on the outcome of how sTNFα(L2) behaves in physiological conditions it might be of interest to increase non-canonical shedding by SPPL2a. Additionally, it might be of interest to investigate whether gene or protein variations of SPPL2a affect physiological cleavage of TNFα and thus sTNFα(L2) release, especially in the context of patients with TNFα-related diseases that do not respond to classical treatment approaches.

In summary, the processing of TNFα is more diverse than previously thought, and SPPL2a and SPPL2b differ in their processing capacity of this substrate. Instead of the conventional process of RIP with a preceding removal of the ECD by an accompanying full-time sheddase such as ADAM10/17 and subsequent processing by SPPL2, TNFα can directly be shedded in a non-canonical fashion by SPPL2a but not SPPL2b. The subsequent consecutive cleavage however, is more efficiently facilitated by SPPL2b whereas SPPL2a displays most likely slower cleavage kinetics. The cleavage of TNFα by SPPL2a and SPPL2b is not enabled by a consensus sequence but rather by structural properties throughout domains close to the membrane. Nevertheless, the substrate determinants in TNFα did not apply for other SPPL2 substrates. Thus, it would be of interest to analyse other physiologically relevant substrates of SPPL2a and SPPL2bin more detail to finally conclude about the recognition and cleavage process. Nevertheless, the implication of SPPL2a in the processing of important proteins such as TNFα and CD74 emphasises an essential role of the protease in a functioning host defence mechanism. Even if not as a single trigger for disease, increased as well as decreased SPPL2a expression might affect the disease severity or outcome of a certain treatment.

REFERENCES

ARICAN, O., ARAL, M., SASMAZ, S. & CIRAGIL, P. 2005. Serum levels of TNF-α, IFN-γ, IL-6, IL-8, IL-12, IL-17, and IL-18 in patients with active psoriasis and correlation with disease severity. *Mediators of inflammation,* 2005.

ARMSTRONG, K. M. & BALDWIN, R. L. 1993. Charged histidine affects alpha-helix stability at all positions in the helix by interacting with the backbone charges. *Proceedings of the National Academy of Sciences,* 90**,** 11337-11340.

BAI, X.-C., YAN, C., YANG, G., LU, P., MA, D., SUN, L., ZHOU, R., SCHERES, S. H. W. & SHI, Y. 2015. An atomic structure of human γ-secretase. *Nature,* 525**,** 212-217.

BALIGA, R. R., PIMENTAL, D. R., ZHAO, Y.-Y., SIMMONS, W. W., MARCHIONNI, M. A., SAWYER, D. B. & KELLY, R. A. 1999. NRG-1-induced cardiomyocyte hypertrophy. Role of PI-3-kinase, p70S6K, and MEK-MAPK-RSK. *American Journal of Physiology-Heart and Circulatory Physiology,* 277**,** H2026-H2037.

BAO, J., WOLPOWITZ, D., ROLE, L. W. & TALMAGE, D. A. 2003. Back signaling by the Nrg-1 intracellular domain. *The Journal of cell biology,* 161**,** 1133-1141.

BEARD, H. A., BARNIOL-XICOTA, M., YANG, J. & VERHELST, S. H. L. 2019. Discovery of Cellular Roles of Intramembrane Proteases. *ACS Chem Biol,* 14**,** 2372-2388.

BECKER-HERMAN, S., ARIE, G., MEDVEDOVSKY, H., KEREM, A. & SHACHAR, I. 2005. CD74 Is a Member of the Regulated Intramembrane Proteolysis-processed Protein Family. *Molecular Biology of the Cell,* 16**,** 5061-5069.

BEHNKE, J., SCHNEPPENHEIM, J., KOCH-NOLTE, F., HAAG, F., SAFTIG, P. & SCHRODER, B. 2011. Signal-peptide-peptidase-like 2a (SPPL2a) is targeted to lysosomes/late endosomes by a tyrosine motif in its C-terminal tail. *FEBS Lett,* 585**,** 2951-7.

BELL, J. H., HERRERA, A. H., LI, Y. & WALCHECK, B. 2007. Role of ADAM17 in the ectodomain shedding of TNF-alpha and its receptors by neutrophils and macrophages. *J Leukoc Biol,* 82**,** 173-6.

BERGBOLD, N. & LEMBERG, M. K. 2013. Emerging role of rhomboid family proteins in mammalian biology and disease. *Biochim Biophys Acta,* 1828**,** 2840-8.

BIS, J. C., JIAN, X., KUNKLE, B. W., CHEN, Y., HAMILTON-NELSON, K. L., BUSH, W. S., SALERNO, W. J., LANCOUR, D., MA, Y. & RENTON, A. E. 2018. Whole exome sequencing study identifies novel rare and common Alzheimer's-Associated variants involved in immune response and transcriptional regulation. *Molecular psychiatry***,** 1-17.

BLAND, F. A., LEMBERG, M. K., MCMICHAEL, A. J., MARTOGLIO, B. & BRAUD, V. M. 2003. Requirement of the proteasome for the trimming of signal peptide-derived epitopes presented by the nonclassical major histocompatibility complex class I molecule HLA-E. *Journal of Biological Chemistry,* 278**,** 33747-33752.

BOEUF, S., BORGER, M., HENNIG, T., WINTER, A., KASTEN, P. & RICHTER, W. 2009. Enhanced ITM2A expression inhibits chondrogenic differentiation of mesenchymal stem cells. *Differentiation,* 78**,** 108-15.

BOND, J. S. 2019. Proteases: History, discovery, and roles in health and disease. *Journal of Biological Chemistry,* 294**,** 1643-1651.

BRADY, O. A., ZHOU, X. & HU, F. 2014. Regulated intramembrane proteolysis of the frontotemporal lobar degeneration risk factor, TMEM106B, by signal peptide peptidase-like 2a (SPPL2a). *Journal of Biological Chemistry,* 289**,** 19670-19680.

BUDENHOLZER, L., CHENG, C. L., LI, Y. & HOCHSTRASSER, M. 2017. Proteasome Structure and Assembly. *J Mol Biol,* 429**,** 3500-3524.

BUSEYNE, F., BETSEM, E., MONTANGE, T., NJOUOM, R., BILOUNGA NDONGO, C., HERMINE, O. & GESSAIN, A. 2018. Clinical Signs and Blood Test Results Among Humans Infected With Zoonotic Simian Foamy Virus: A Case-Control Study. *The Journal of Infectious Diseases,* 218**,** 144-151.

CAI, T. & TOMITA, T. 2020. Structure-activity relationship of presenilin in gamma-secretase-mediated intramembrane cleavage. *Semin Cell Dev Biol,* 105**,** 102-109.

CARSWELL, E. A., OLD, L. J., KASSEL, R. L., GREEN, S., FIORE, N. & WILLIAMSON, B. 1975. An endotoxin-induced serum factor that causes necrosis of tumors. *Proc Natl Acad Sci U S A,* 72**,** 3666-70.

CHÁVEZ-GUTIÉRREZ, L. & DE STROOPER, B. 2016. Probing γ-secretase–substrate interactions at the single amino acid residue level. *The EMBO journal,* 35**,** 1597-1599.

CHEN, A. C., KIM, S., SHEPARDSON, N., PATEL, S., HONG, S. & SELKOE, D. J. 2015. Physical and functional interaction between the α-and γ-secretases: a new model of regulated intramembrane proteolysis. *Journal of Cell Biology,* 211**,** 1157-1176.

CHEN, C. Y., MALCHUS, N. S., HEHN, B., STELZER, W., AVCI, D., LANGOSCH, D. & LEMBERG, M. K. 2014a. Signal peptide peptidase functions in ERAD to cleave the unfolded protein response regulator XBP1u. *EMBO J,* 33**,** 2492-506.

CHEN, C. Y., MALCHUS, N. S., HEHN, B., STELZER, W., AVCI, D., LANGOSCH, D. & LEMBERG, M. K. 2014b. Signal peptide peptidase functions in ERAD to cleave the unfolded protein response regulator XBP 1u. *The EMBO journal,* 33**,** 2492-2506.

CHEN, G. & ZHANG, X. 2010. New insights into S2P signaling cascades: regulation, variation, and conservation. *Protein Sci,* 19**,** 2015-30.

CHI, A., VALENCIA, J. C., HU, Z.-Z., WATABE, H., YAMAGUCHI, H., MANGINI, N. J., HUANG, H., CANFIELD, V. A., CHENG, K. C. & YANG, F. 2006. Proteomic and bioinformatic characterization of the biogenesis and function of melanosomes. *Journal of proteome research,* 5**,** 3135-3144.

CHO, C. 2012. Testicular and epididymal ADAMs: expression and function during fertilization. *Nature Reviews Urology,* 9**,** 550.

CHOI, S. I., VIDAL, R., FRANGIONE, B. & LEVY, E. 2004. Axonal transport of British and Danish amyloid peptides via secretory vesicles. *FASEB J,* 18**,** 373-5.

COESHOTT, C., OHNEMUS, C., PILYAVSKAYA, A., ROSS, S., WIECZOREK, M., KROONA, H., LEIMER, A. H. & CHERONIS, J. 1999. Converting enzyme-independent release of tumor necrosis factor α and IL-1β from a stimulated human monocytic cell line in the presence of activated neutrophils or purified proteinase 3. *Proceedings of the National Academy of Sciences,* 96**,** 6261-6266.

CORDES, F. S., BRIGHT, J. N. & SANSOM, M. S. 2002. Proline-induced distortions of transmembrane helices. *J Mol Biol,* 323**,** 951-60.

CRAIG, V. J., ZHANG, L., HAGOOD, J. S. & OWEN, C. A. 2015. Matrix metalloproteinases as therapeutic targets for idiopathic pulmonary fibrosis. *Am J Respir Cell Mol Biol,* 53**,** 585-600.

CUKALEVSKI, R., YANG, X., MEISL, G., WEININGER, U., BERNFUR, K., FROHM, B., KNOWLES, T. P. & LINSE, S. 2015. The Aβ40 and Aβ42 peptides self-assemble into separate homomolecular fibrils in binary mixtures but cross-react during primary nucleation. *Chemical science,* 6**,** 4215-4233.

DAHIYAT, B. I. & FILIKOV, A. 2006. TNF-α variants. Google Patents.

DAVDA, D., EL AZZOUNY, M. A., TOM, C. T., HERNANDEZ, J. L., MAJMUDAR, J. D., KENNEDY, R. T. & MARTIN, B. R. 2013. Profiling targets of the irreversible palmitoylation inhibitor 2-bromopalmitate. *ACS chemical biology,* 8**,** 1912-1917.

DE STROOPER, B. 2005. Nicastrin: gatekeeper of the γ-secretase complex. *Cell,* 122**,** 318-320.

DEL CAMPO, M. & TEUNISSEN, C. E. 2014. Role of BRI2 in dementia. *J Alzheimers Dis,* 40**,** 481-94.

DI CERA, E. 2009. Serine proteases. *IUBMB life,* 61**,** 510-515.

DIJKSTRA, J. M. & YAMAGUCHI, T. 2019. Ancient features of the MHC class II presentation pathway, and a model for the possible origin of MHC molecules. *Immunogenetics,* 71**,** 233-249.

DRAG, M. & SALVESEN, G. S. 2010. Emerging principles in protease-based drug discovery. *Nat Rev Drug Discov,* 9**,** 690-701.

DRAPER, J. M. & SMITH, C. D. 2009. Palmitoyl acyltransferase assays and inhibitors (Review). *Mol Membr Biol,* 26**,** 5-13.

DRECOURT, A., BABDOR, J., DUSSIOT, M., PETIT, F., GOUDIN, N., GARFA-TRAORÉ, M., HABAROU, F., BOLE-FEYSOT, C., NITSCHKÉ, P. & OTTOLENGHI, C. 2018. Impaired transferrin receptor palmitoylation and recycling in neurodegeneration with brain iron accumulation. *The American Journal of Human Genetics,* 102**,** 266-277.

DUDA, A., STANGE, A., LÜFTENEGGER, D., STANKE, N., WESTPHAL, D., PIETSCHMANN, T., EASTMAN, S. W., LINIAL, M. L., RETHWILM, A. & LINDEMANN, D. 2004. Prototype foamy virus envelope glycoprotein leader peptide processing is mediated by a furin-like cellular protease, but cleavage is not essential for viral infectivity. *Journal of virology,* 78**,** 13865-13870.

DUFFY, M. J., MCKIERNAN, E., O'DONOVAN, N. & MCGOWAN, P. M. 2009. The role of ADAMs in disease pathophysiology. *Clinica Chimica Acta,* 403**,** 31-36.

DUNCAN, E. A., DAVE, U. P., SAKAI, J., GOLDSTEIN, J. L. & BROWN, M. S. 1998. Second-site cleavage in sterol regulatory element-binding protein occurs at transmembrane junction as determined by cysteine panning. *J Biol Chem,* 273**,** 17801-9.

DUSTERHOFT, S., BABENDREYER, A., GIESE, A. A., FLASSHOVE, C. & LUDWIG, A. 2019. Status update on iRhom and ADAM17: It's still complicated. *Biochim Biophys Acta Mol Cell Res,* 1866**,** 1567-1583.

ECK, M. J. & SPRANG, S. R. 1989. The structure of tumor necrosis factor-alpha at 2.6 A resolution. Implications for receptor binding. *J Biol Chem,* 264**,** 17595-605.

EDWARDS, D. R., HANDSLEY, M. M. & PENNINGTON, C. J. 2008. The ADAM metalloproteinases. *Mol Aspects Med,* 29**,** 258-89.

EL-TAHAN, R. R., GHONEIM, A. M. & EL-MASHAD, N. 2016. TNF-α gene polymorphisms and expression. *Springerplus,* 5**,** 1508.

FARR, L., GHOSH, S. & MOONAH, S. 2020. Role of MIF Cytokine/CD74 Receptor Pathway in Protecting Against Injury and Promoting Repair. *Front Immunol,* 11**,** 1273.

FENG, L., YAN, H., WU, Z., YAN, N., WANG, Z., JEFFREY, P. D. & SHI, Y. 2007. Structure of a site-2 protease family intramembrane metalloprotease. *Science,* 318**,** 1608-12.

FENG, T., SHENG, R. R., SOLÉ-DOMÈNECH, S., ULLAH, M., ZHOU, X., MENDOZA, C. S., ENRIQUEZ, L. C. M., KATZ, II, PAUSHTER, D. H., SULLIVAN, P. M., WU, X., MAXFIELD, F. R. & HU, F. 2020. A role of the frontotemporal lobar degeneration risk factor TMEM106B in myelination. *Brain,* 143**,** 2255-2271.

FLECK, D., VAN BEBBER, F., COLOMBO, A., GALANTE, C., SCHWENK, B. M., RABE, L., HAMPEL, H., NOVAK, B., KREMMER, E., TAHIROVIC, S., EDBAUER, D., LICHTENTHALER, S. F., SCHMID, B., WILLEM, M. & HAASS, C. 2013. Dual cleavage of neuregulin 1 type III by BACE1 and ADAM17 liberates its EGF-like domain and allows paracrine signaling. *J Neurosci,* 33**,** 7856-69.

FLECK, D., VOSS, M., BRANKATSCHK, B., GIUDICI, C., HAMPEL, H., SCHWENK, B., EDBAUER, D., FUKUMORI, A., STEINER, H., KREMMER, E., HAUG-KROPER, M., ROSSNER, M. J., FLUHRER, R., WILLEM, M. & HAASS, C. 2016. Proteolytic Processing of Neuregulin 1 Type III by Three Intramembrane-cleaving Proteases. *J Biol Chem,* 291**,** 318-33.

FLUHRER, R., FUKUMORI, A., MARTIN, L., GRAMMER, G., HAUG-KROPER, M., KLIER, B., WINKLER, E., KREMMER, E., CONDRON, M. M., TEPLOW, D. B., STEINER, H. & HAASS, C. 2008. Intramembrane proteolysis of GXGD-type aspartyl proteases is slowed by a familial Alzheimer disease-like mutation. *J Biol Chem,* 283**,** 30121-8.

FLUHRER, R., GRAMMER, G., ISRAEL, L., CONDRON, M. M., HAFFNER, C., FRIEDMANN, E., BOHLAND, C., IMHOF, A., MARTOGLIO, B., TEPLOW, D. B. & HAASS, C. 2006. A gamma-secretase-like intramembrane cleavage of TNFalpha by the GxGD aspartyl protease SPPL2b. *Nat Cell Biol,* 8**,** 894-6.

FLUHRER, R., MARTIN, L., KLIER, B., HAUG-KROPER, M., GRAMMER, G., NUSCHER, B. & HAASS, C. 2012. The alpha-helical content of the transmembrane domain of the British dementia protein-2 (Bri2) determines its processing by signal peptide peptidase-like 2b (SPPL2b). *J Biol Chem,* 287**,** 5156-63.

FLUHRER, R., STEINER, H. & HAASS, C. 2009. Intramembrane proteolysis by signal peptide peptidases: a comparative discussion of GXGD-type aspartyl proteases. *J Biol Chem,* 284**,** 13975-9.

FLYNN, J. L., GOLDSTEIN, M. M., CHAN, J., TRIEBOLD, K. J., PFEFFER, K., LOWENSTEIN, C. J., SCHREIBER, R., MAK, T. W. & BLOOM, B. R. 1995. Tumor necrosis factor-alpha is required in the protective immune response against Mycobacterium tuberculosis in mice. *Immunity,* 2**,** 561-72.

FOUQUE, A., DEBURE, L. & LEGEMBRE, P. 2014. The CD95/CD95L signaling pathway: a role in carcinogenesis. *Biochim Biophys Acta,* 1846**,** 130-41.

FRIEDMANN, E., HAUBEN, E., MAYLANDT, K., SCHLEEGER, S., VREUGDE, S., LICHTENTHALER, S. F., KUHN, P. H., STAUFFER, D., ROVELLI, G. & MARTOGLIO, B. 2006. SPPL2a and SPPL2b promote intramembrane proteolysis of TNFalpha in activated dendritic cells to trigger IL-12 production. *Nat Cell Biol,* 8**,** 843-8.

FRIEDMANN, E., LEMBERG, M. K., WEIHOFEN, A., DEV, K. K., DENGLER, U., ROVELLI, G. & MARTOGLIO, B. 2004. Consensus analysis of signal peptide peptidase and homologous human aspartic proteases reveals opposite topology of catalytic domains compared with presenilins. *J Biol Chem,* 279**,** 50790-8.

FUKUMORI, A., FLUHRER, R., STEINER, H. & HAASS, C. 2010. Three-amino acid spacing of presenilin endoproteolysis suggests a general stepwise cleavage of γ-secretase-mediated intramembrane proteolysis. *Journal of Neuroscience,* 30**,** 7853-7862.

GLOBA, A. K. & BAMJI, S. X. 2017. Protein palmitoylation in the development and plasticity of neuronal connections. *Curr Opin Neurobiol,* 45**,** 210-220.

GOLDE, T. E., WOLFE, M. S. & GREENBAUM, D. C. Signal peptide peptidases: a family of intramembrane-cleaving proteases that cleave type 2 transmembrane proteins. Seminars in cell & developmental biology, 2009. Elsevier, 225-230.

GONG, Y., WU, J., QIANG, H., LIU, B., CHI, Z., CHEN, T., YIN, B., PENG, X. & YUAN, J. 2008. BRI3 associates with SCG10 and attenuates NGF-induced neurite outgrowth in PC12 cells. *BMB Rep,* 41**,** 287-93.

GÖTZ, A., MYLONAS, N., HÖGEL, P., SILBER, M., HEINEL, H., MENIG, S., VOGEL, A., FEYRER, H., HUSTER, D. & LUY, B. 2018. Stabilization/destabilization of the APP transmembrane domain by mutations in the di-glycine hinge alter helical structure and dynamics, and impair cleavage by γ-secretase. *bioRxiv***,** 375006.

GÖTZ, A., MYLONAS, N., HÖGEL, P., SILBER, M., HEINEL, H., MENIG, S., VOGEL, A., FEYRER, H., HUSTER, D. & LUY, B. 2019. Modulating hinge flexibility in the APP transmembrane domain alters γ-secretase cleavage. *Biophysical journal,* 116**,** 2103-2120.

GRAY, T. & MATTHEWS, B. 1984. Intrahelical hydrogen bonding of serine, threonine and cysteine residues within α-helices and its relevance to membrane-bound proteins. *Journal of molecular biology,* 175**,** 75-81.

GRELL, M., DOUNI, E., WAJANT, H., LOHDEN, M., CLAUSS, M., MAXEINER, B., GEORGOPOULOS, S., LESSLAUER, W., KOLLIAS, G., PFIZENMAIER, K. & SCHEURICH, P. 1995. The transmembrane form of tumor necrosis factor is the prime activating ligand of the 80 kDa tumor necrosis factor receptor. *Cell,* 83**,** 793-802.

GROSS, O., GEWIES, A., FINGER, K., SCHÄFER, M., SPARWASSER, T., PESCHEL, C., FÖRSTER, I. & RULAND, J. 2006. Card9 controls a non-TLR signalling pathway for innate anti-fungal immunity. *Nature,* 442**,** 651-6.

GUARDIOLA-SERRANO, F., ROSSIN, A., CAHUZAC, N., LÜCKERATH, K., MELZER, I., MAILFERT, S., MARGUET, D., ZÖRNIG, M. & HUEBER, A. 2010. Palmitoylation of human FasL modulates its cell death-inducing function. *Cell death & disease,* 1**,** e88-e88.

GUILLEMOT, J., CANUEL, M., ESSALMANI, R., PRAT, A. & SEIDAH, N. G. 2013. Implication of the proprotein convertases in iron homeostasis: proprotein convertase 7 sheds human transferrin receptor 1 and furin activates hepcidin. *Hepatology,* 57**,** 2514-24.

GUNČAR, G., PUNGERČIČ, G., KLEMENČIČ, I., TURK, V. & TURK, D. 1999. Crystal structure of MHC class II-associated p41 Ii fragment bound to cathepsin L reveals the structural basis for differentiation between cathepsins L and S. *The EMBO journal,* 18**,** 793-803.

GURUMALLESH, P., ALAGU, K., RAMAKRISHNAN, B. & MUTHUSAMY, S. 2019. A systematic reconsideration on proteases. *Int J Biol Macromol,* 128**,** 254-267.

HALIM, A., RÜETSCHI, U., LARSON, G. R. & NILSSON, J. 2013. LC–MS/MS characterization of O-glycosylation sites and glycan structures of human cerebrospinal fluid glycoproteins. *Journal of proteome research,* 12**,** 573-584.

HAMBLET, C. E., MAKOWSKI, S. L., TRITAPOE, J. M. & POMERANTZ, J. L. 2016. NK Cell Maturation and Cytotoxicity Are Controlled by the Intramembrane Aspartyl Protease SPPL3. *The Journal of Immunology,* 196**,** 2614-2626.

HAMPTON, S. E., DORE, T. M. & SCHMIDT, W. K. 2018. Rce1: mechanism and inhibition. *Crit Rev Biochem Mol Biol,* 53**,** 157-174.

HARDY, J. 2003. The relationship between amyloid and tau. *Journal of Molecular Neuroscience,* 20**,** 203-206.

HARO, H., CRAWFORD, H. C., FINGLETON, B., SHINOMIYA, K., SPENGLER, D. M. & MATRISIAN, L. M. 2000. Matrix metalloproteinase-7–dependent release of tumor necrosis factor-α in a model of herniated disc resorption. *The Journal of Clinical Investigation,* 105**,** 143-150.

HATUNIC, M., STAPLETON, M., HAND, E., DELONG, C., CROWLEY, V. & NOLAN, J. 2009. The Leu262Val polymorphism of presenilin associated rhomboid like protein (PARL) is associated with earlier onset of type 2 diabetes and increased urinary microalbumin creatinine ratio in an Irish case–control population. *Diabetes research and clinical practice,* 83**,** 316-319.

HAYES, G. R., ENNS, C. A. & LUCAS, J. J. 1992. Identification of the O-linked glycosylation site of the human transferrin receptor. *Glycobiology,* 2**,** 355-359.

HENNE, C., SCHWENK, F., KOCH, N. & MÖLLER, P. 1995. Surface expression of the invariant chain (CD74) is independent of concomitant expression of major histocompatibility complex class II antigens. *Immunology,* 84**,** 177.

HITZENBERGER, M., GOTZ, A., MENIG, S., BRUNSCHWEIGER, B., ZACHARIAS, M. & SCHARNAGL, C. 2020. The dynamics of gamma-secretase and its substrates. *Semin Cell Dev Biol*.

HITZENBERGER, M. & ZACHARIAS, M. 2019. γ-secretase studied by atomistic molecular dynamics simulations: Global dynamics, enzyme activation, water distribution and lipid binding. *Frontiers in chemistry,* 6**,** 640.

HÖGEL, P., GÖTZ, A., KUHNE, F., EBERT, M., STELZER, W., RAND, K. D., SCHARNAGL, C. & LANGOSCH, D. 2018. Glycine perturbs local and global conformational flexibility of a transmembrane helix. *Biochemistry,* 57**,** 1326-1337.

HOHJOH, H. & TOKUNAGA, K. 2001. Allele-specific binding of the ubiquitous transcription factor OCT-1 to the functional single nucleotide polymorphism (SNP) sites in the tumor necrosis factor-alpha gene (TNFA) promoter. *Genes & Immunity,* 2**,** 105-109.

HOLCOMB, L., GORDON, M. N., MCGOWAN, E., YU, X., BENKOVIC, S., JANTZEN, P., WRIGHT, K., SAAD, I., MUELLER, R. & MORGAN, D. 1998. Accelerated Alzheimer-type phenotype in transgenic mice carrying both mutant amyloid precursor protein and presenilin 1 transgenes. *Nature medicine,* 4**,** 97-100.

HSU, F.-F., CHOU, Y.-T., CHIANG, M.-T., LI, F.-A., YEH, C.-T., LEE, W.-H. & CHAU, L.-Y. 2019. Signal peptide peptidase promotes tumor progression via facilitating FKBP8 degradation. *Oncogene,* 38**,** 1688-1701.

HU, X., FAN, Q., HOU, H. & YAN, R. 2016. Neurological dysfunctions associated with altered BACE1-dependent Neuregulin-1 signaling. *J Neurochem,* 136**,** 234-49.

HÜTTL, S., HELFRICH, F., MENTRUP, T., HELD, S., FUKUMORI, A., STEINER, H., SAFTIG, P., FLUHRER, R. & SCHRÖDER, B. 2016. Substrate determinants of signal peptide peptidase-like 2a (SPPL2a)-mediated intramembrane proteolysis of the invariant chain CD74. *Biochemical Journal,* 473**,** 1405-1422.

HUTTL, S., KLASENER, K., SCHWEIZER, M., SCHNEPPENHEIM, J., OBERG, H. H., KABELITZ, D., RETH, M., SAFTIG, P. & SCHRODER, B. 2015. Processing of CD74 by the Intramembrane Protease SPPL2a Is Critical for B Cell Receptor Signaling in Transitional B Cells. *J Immunol,* 195**,** 1548-63.

IDRISS, H. T. N., J. 2000. TNF alpha and the TNF Receptor Superfamily: Structure-Function Relationship(s). *Microscopy research and technique,* 50**,** 184-195.

JING, S. & TROWBRIDGE, I. 1987. Identification of the intermolecular disulfide bonds of the human transferrin receptor and its lipid-attachment site. *The EMBO journal,* 6**,** 327-331.

KAETHER, C., HAASS, C. & STEINER, H. 2006. Assembly, Trafficking and Function of γ-Secretase. *Neurodegenerative Diseases,* 3**,** 275-283.

KALIA, N., KAUR, M., SHARMA, S. & SINGH, J. 2018. A comprehensive in silico analysis of regulatory SNPs of human CLEC7A gene and its validation as genotypic and phenotypic disease marker in recurrent vulvovaginal infections. *Frontiers in cellular and infection microbiology,* 8**,** 65.

KALLIOLIAS, G. D. & IVASHKIV, L. B. 2016. TNF biology, pathogenic mechanisms and emerging therapeutic strategies. *Nat Rev Rheumatol,* 12**,** 49-62.

KANDEL, R. R. & NEAL, S. E. 2020. The role of rhomboid superfamily members in protein homeostasis: Mechanistic insight and physiological implications. *Biochim Biophys Acta Mol Cell Res,* 1867**,** 118793.

KIM, S.-H., WANG, R., GORDON, D. J., BASS, J., STEINER, D. F., LYNN, D. G., THINAKARAN, G., MEREDITH, S. C. & SISODIA, S. S. 1999. Furin mediates enhanced production of fibrillogenic ABri peptides in familial British dementia. *Nature neuroscience,* 2**,** 984-988.

KIRKIN, V., CAHUZAC, N., GUARDIOLA-SERRANO, F., HUAULT, S., LUCKERATH, K., FRIEDMANN, E., NOVAC, N., WELS, W. S., MARTOGLIO, B., HUEBER, A. O. & ZORNIG, M. 2007. The Fas ligand intracellular domain is released by ADAM10 and SPPL2a cleavage in T-cells. *Cell Death Differ,* 14**,** 1678-87.

KO, P. J. & DIXON, S. J. 2018. Protein palmitoylation and cancer. *EMBO Rep,* 19.

KOJRO, E. & FAHRENHOLZ, F. 2005. The non-amyloidogenic pathway: structure and function of alpha-secretases. *Subcell Biochem,* 38**,** 105-27.

KONG, X.-F., MARTINEZ-BARRICARTE, R., KENNEDY, J., MELE, F., LAZAROV, T., DEENICK, E. K., MA, C. S., BRETON, G., LUCERO, K. B., LANGLAIS, D., BOUSFIHA, A., AYTEKIN, C., MARKLE, J., TROUILLET, C., JABOT-HANIN, F., ARLEHAMN, C. S. L., RAO, G., PICARD, C., LASSEAU, T., LATORRE, D., HAMBLETON, S., DESWARTE, C., ITAN, Y., ABARCA, K., MORAES-VASCONCELOS, D., AILAL, F., IKINCIOGULLARI, A., DOGU, F., BENHSAIEN, I., SETTE, A., ABEL, L., BOISSON-DUPUIS, S., SCHRÖDER, B., NUSSENZWEIG, M. C., LIU, K., GEISSMANN, F., TANGYE, S. G., GROS, P., SALLUSTO, F., BUSTAMANTE, J. & CASANOVA, J.-L. 2018. Disruption of an antimycobacterial circuit between dendritic and helper T cells in human SPPL2a deficiency. *Nature Immunology,* 19**,** 973-985.

KOSTER, K. P. & YOSHII, A. 2019. Depalmitoylation by palmitoyl-protein thioesterase 1 in neuronal health and degeneration. *Frontiers in synaptic neuroscience,* 11**,** 25.

KRAUT, J. 1977. Serine proteases: structure and mechanism of catalysis. *Annual review of biochemistry,* 46**,** 331-358.

KRAWITZ, P., HAFFNER, C., FLUHRER, R., STEINER, H., SCHMID, B. & HAASS, C. 2005. Differential localization and identification of a critical aspartate suggest non-redundant proteolytic functions of the presenilin homologues SPPL2b and SPPL3. *J Biol Chem,* 280**,** 39515-23.

KUHN, P.-H., VOSS, M., HAUG-KRÖPER, M., SCHRÖDER, B., SCHEPERS, U., BRÄSE, S., HAASS, C., LICHTENTHALER, S. F. & FLUHRER, R. 2015. Secretome analysis identifies novel signal Peptide peptidase-like 3 (Sppl3) substrates and reveals a role of Sppl3 in multiple Golgi glycosylation pathways. *Molecular & Cellular Proteomics,* 14**,** 1584-1598.

KUHNLE, N., DEDERER, V. & LEMBERG, M. K. 2019. Intramembrane proteolysis at a glance: from signalling to protein degradation. *J Cell Sci,* 132.

KUMANO-KURAMOCHI, M., XIE, Q., KAJIWARA, S., KOMBA, S., MINOWA, T. & MACHIDA, S. 2013. Lectin-like oxidized LDL receptor-1 is palmitoylated and internalizes ligands via caveolae/raft-dependent endocytosis. *Biochemical and biophysical research communications,* 434**,** 594-599.

KUNZEL, U., GRIEVE, A. G., MENG, Y., SIEBER, B., COWLEY, S. A. & FREEMAN, M. 2018. FRMD8 promotes inflammatory and growth factor signalling by stabilising the iRhom/ADAM17 sheddase complex. *Elife,* 7.

LANG, C. M., FELLERER, K., SCHWENK, B. M., KUHN, P.-H., KREMMER, E., EDBAUER, D., CAPELL, A. & HAASS, C. 2012. Membrane orientation and subcellular localization of transmembrane protein 106B (TMEM106B), a major risk factor for frontotemporal lobar degeneration. *Journal of Biological Chemistry,* 287**,** 19355-19365.

LANGOSCH, D., SCHARNAGL, C., STEINER, H. & LEMBERG, M. K. 2015. Understanding intramembrane proteolysis: from protein dynamics to reaction kinetics. *Trends Biochem Sci,* 40**,** 318-27.

LANGOSCH, D. & STEINER, H. 2017. Substrate processing in intramembrane proteolysis by gamma-secretase - the role of protein dynamics. *Biol Chem,* 398**,** 441-453.

LANIER, L. L. 2015. NKG2D Receptor and Its Ligands in Host Defense. *Cancer Immunol Res,* 3**,** 575-82.

LAVOIE, M. J. & SELKOE, D. J. 2003. The Notch ligands, Jagged and Delta, are sequentially processed by α-secretase and presenilin/γ-secretase and release signaling fragments. *Journal of Biological Chemistry,* 278**,** 34427-34437.

LAWRENCE, C. M., RAY, S., BABYONYSHEV, M., GALLUSER, R., BORHANI, D. W. & HARRISON, S. C. 1999. Crystal structure of the ectodomain of human transferrin receptor. *Science,* 286**,** 779-782.

LEMBERG, M. K. & ADRAIN, C. 2016. Inactive rhomboid proteins: New mechanisms with implications in health and disease. *Semin Cell Dev Biol,* 60**,** 29-37.

LEMBERG, M. K. & MARTOGLIO, B. 2002. Requirements for signal peptide peptidase-catalyzed intramembrane proteolysis. *Mol Cell,* 10**,** 735-44.

LEMBERG, M. K. & MARTOGLIO, B. 2004. On the mechanism of SPP-catalysed intramembrane proteolysis; conformational control of peptide bond hydrolysis in the plane of the membrane. *FEBS Lett,* 564**,** 213-8.

LETTAU, M., PAULSEN, M., KABELITZ, D. & JANSSEN, O. 2009. FasL expression and reverse signalling. *Death Receptors and Cognate Ligands in Cancer***,** 49-61.

LEVOIN, N., JEAN, M. & LEGEMBRE, P. 2020. CD95 Structure, Aggregation and Cell Signaling. *Front Cell Dev Biol,* 8**,** 314.

LI, S. C. & DEBER, C. M. 1994. A measure of helical propensity for amino acids in membrane environments. *Nat Struct Biol,* 1**,** 558.

LICHTENTHALER, S. F., LEMBERG, M. K. & FLUHRER, R. 2018. Proteolytic ectodomain shedding of membrane proteins in mammals-hardware, concepts, and recent developments. *EMBO J,* 37.

LIN, D. T. S. & CONIBEAR, E. 2015. ABHD17 proteins are novel protein depalmitoylases that regulate N-Ras palmitate turnover and subcellular localization. *Elife,* 4**,** e11306.

LINKERMANN, A., QIAN, J. & JANSSEN, O. 2003. Slowly getting a clue on CD95 ligand biology. *Biochem Pharmacol,* 66**,** 1417-26.

LIU, P., CLEVELAND, T. E. T., BOUYAIN, S., BYRNE, P. O., LONGO, P. A. & LEAHY, D. J. 2012. A single ligand is sufficient to activate EGFR dimers. *Proc Natl Acad Sci U S A,* 109**,** 10861-6.

LIU, W., RAMAGOPAL, U., CHENG, H., BONANNO, JEFFREY B., TORO, R., BHOSLE, R., ZHAN, C. & ALMO, STEVEN C. 2016. Crystal Structure of the Complex of Human FasL and Its Decoy Receptor DcR3. *Structure,* 24**,** 2016-2023.

LIU, Y., HELMS, C., LIAO, W., ZABA, L. C., DUAN, S., GARDNER, J., WISE, C., MINER, A., MALLOY, M. & PULLINGER, C. R. 2008. A genome-wide association study of psoriasis and psoriatic arthritis identifies new disease loci. *PLoS Genet,* 4**,** e1000041.

LÓPEZ-OTÍN, C., PALAVALLI, L. H. & SAMUELS, Y. 2009. Protective roles of matrix metalloproteinases: from mouse models to human cancer. *Cell Cycle,* 8**,** 3657-3662.

LYSYK, L., BRASSARD, R., TOURET, N. & LEMIEUX, M. J. 2020. PARL Protease: A Glimpse at Intramembrane Proteolysis in the Inner Mitochondrial Membrane. *J Mol Biol,* 432**,** 5052-5062.

MANDAL, A., KLOTZ, K. L., SHETTY, J., JAYES, F. L., WOLKOWICZ, M. J., BOLLING, L. C., COONROD, S. A., BLACK, M. B., DIEKMAN, A. B., HAYSTEAD, T. A., FLICKINGER, C. J. & HERR, J. C. 2003. SLLP1, a unique, intra-acrosomal, non-bacteriolytic, c lysozyme-like protein of human spermatozoa. *Biol Reprod,* 68**,** 1525-37.

MANOLARIDIS, I., KULKARNI, K., DODD, R. B., OGASAWARA, S., ZHANG, Z., BINEVA, G., O'REILLY, N., HANRAHAN, S. J., THOMPSON, A. J., CRONIN, N., IWATA, S. & BARFORD, D. 2013. Mechanism of farnesylated CAAX protein processing by the intramembrane protease Rce1. *Nature,* 504**,** 301-305.

MARETZKY, T., MCILWAIN, D. R., ISSUREE, P. D., LI, X., MALAPEIRA, J., AMIN, S., LANG, P. A., MAK, T. W. & BLOBEL, C. P. 2013. iRhom2 controls the substrate selectivity of stimulated ADAM17-dependent ectodomain shedding. *Proc Natl Acad Sci U S A,* 110**,** 11433-8.

MARINO, M. W., DUNN, A., GRAIL, D., INGLESE, M., NOGUCHI, Y., RICHARDS, E., JUNGBLUTH, A., WADA, H., MOORE, M., WILLIAMSON, B., BASU, S. & OLD, L. J. 1997. Characterization of tumor necrosis factor-deficient mice. *Proceedings of the National Academy of Sciences,* 94**,** 8093-8098.

MARTIN, L., FLUHRER, R. & HAASS, C. 2009. Substrate requirements for SPPL2b-dependent regulated intramembrane proteolysis. *J Biol Chem,* 284**,** 5662-70.

MARTIN, L., FLUHRER, R., REISS, K., KREMMER, E., SAFTIG, P. & HAASS, C. 2008. Regulated intramembrane proteolysis of Bri2 (Itm2b) by ADAM10 and SPPL2a/SPPL2b. *J Biol Chem,* 283**,** 1644-52.

MATSUDA, S., MATSUDA, Y. & D'ADAMIO, L. 2009. BRI3 inhibits amyloid precursor protein processing in a mechanistically distinct manner from its homologue dementia gene BRI2. *J Biol Chem,* 284**,** 15815-25.

MATSUDA, S., MATSUDA, Y., SNAPP, E. L. & D'ADAMIO, L. 2011. Maturation of BRI2 generates a specific inhibitor that reduces APP processing at the plasma membrane and in endocytic vesicles. *Neurobiology of aging,* 32**,** 1400-1408.

MATSUDA, S. & SENDA, T. 2019. BRI2 as an anti-Alzheimer gene. *Med Mol Morphol,* 52**,** 1-7.

MATSUMURA, N., TAKAMI, M., OKOCHI, M., WADA-KAKUDA, S., FUJIWARA, H., TAGAMI, S., FUNAMOTO, S., IHARA, Y. & MORISHIMA-KAWASHIMA, M. 2014. gamma-Secretase associated with lipid rafts: multiple interactive pathways in the stepwise processing of beta-carboxyl-terminal fragment. *J Biol Chem,* 289**,** 5109-21.

MCGEEHAN, G. M., BECHERER, J. D., BAST, R. C., JR., BOYER, C. M., CHAMPION, B., CONNOLLY, K. M., CONWAY, J. G., FURDON, P., KARP, S., KIDAO, S. & ET AL. 1994. Regulation of tumour necrosis factor-alpha processing by a metalloproteinase inhibitor. *Nature,* 370**,** 558-61.

MEAD, S., JAMES-GALTON, M., REVESZ, T., DOSHI, R. B., HARWOOD, G., PAN, E. L., GHISO, J., FRANGIONE, B. & PLANT, G. 2000. Familial British dementia with amyloid angiopathy: Early clinical, neuropsychological and imaging findings. *Brain,* 123**,** 975-991.

MENTRUP, T., CABRERA-CABRERA, F., FLUHRER, R. & SCHRODER, B. 2020. Physiological functions of SPP/SPPL intramembrane proteases. *Cell Mol Life Sci,* 77**,** 2959-2979.

MENTRUP, T., FLUHRER, R. & SCHRODER, B. 2017. Latest emerging functions of SPP/SPPL intramembrane proteases. *Eur J Cell Biol,* 96**,** 372-382.

MENTRUP, T., THEODOROU, K., CABRERA-CABRERA, F., HELBIG, A. O., HAPP, K., GIJBELS, M., GRADTKE, A. C., RABE, B., FUKUMORI, A., STEINER, H., THOLEY, A., FLUHRER, R., DONNERS, M. & SCHRODER, B. 2019. Atherogenic LOX-1 signaling is controlled by SPPL2-mediated intramembrane proteolysis. *J Exp Med,* 216**,** 807-830.

MOHAN, M. J., SEATON, T., MITCHELL, J., HOWE, A., BLACKBURN, K., BURKHART, W., MOYER, M., PATEL, I., WAITT, G. M., BECHERER, J. D., MOSS, M. L. & MILLA, M. E. 2002. The tumor necrosis factor-alpha converting enzyme (TACE): a unique metalloproteinase with highly defined substrate selectivity. *Biochemistry,* 41**,** 9462-9.

MOORE, B. D., MARTIN, J., DE MENA, L., SANCHEZ, J., CRUZ, P. E., CEBALLOS-DIAZ, C., LADD, T. B., RAN, Y., LEVITES, Y., KUKAR, T. L., KURIAN, J. J., MCKENNA, R., KOO, E. H., BORCHELT, D. R., JANUS, C., RINCON-LIMAS, D., FERNANDEZ-FUNEZ, P. & GOLDE, T. E. 2017. Short Aβ peptides attenuate Aβ42 toxicity in vivo. *Journal of Experimental Medicine,* 215**,** 283-301.

MORENO-DE-LUCA, A., HELMERS, S. L., MAO, H., BURNS, T. G., MELTON, A. M., SCHMIDT, K. R., FERNHOFF, P. M., LEDBETTER, D. H. & MARTIN, C. L. 2011. Adaptor protein complex-4 (AP-4) deficiency causes a novel autosomal recessive cerebral palsy syndrome with microcephaly and intellectual disability. *Journal of medical genetics,* 48**,** 141-144.

MOSS, M. L., JIN, S.-L. C., MILLA, M. E., BURKHART, W., CARTER, H. L., CHEN, W.-J., CLAY, W. C., DIDSBURY, J. R., HASSLER, D. & HOFFMAN, C. R. 1997. Cloning of a disintegrin metalloproteinase that processes precursor tumour-necrosis factor-α. *Nature,* 385**,** 733-736.

MUKAI, Y., NAKAMURA, T., YOSHIKAWA, M., YOSHIOKA, Y., TSUNODA, S., NAKAGAWA, S., YAMAGATA, Y. & TSUTSUMI, Y. 2010. Solution of the structure of the TNF-TNFR2 complex. *Sci Signal,* 3**,** ra83.

MUKAI, Y., SHIBATA, H., NAKAMURA, T., YOSHIOKA, Y., ABE, Y., NOMURA, T., TANIAI, M., OHTA, T., IKEMIZU, S., NAKAGAWA, S., TSUNODA, S.-I., KAMADA, H., YAMAGATA, Y. & TSUTSUMI, Y. 2009. Structure–Function Relationship of Tumor Necrosis Factor (TNF) and Its Receptor Interaction Based on 3D Structural Analysis of a Fully Active TNFR1-Selective TNF Mutant. *Journal of Molecular Biology,* 385**,** 1221-1229.

NAGASE, H., VISSE, R. & MURPHY, G. 2006. Structure and function of matrix metalloproteinases and TIMPs. *Cardiovascular research,* 69**,** 562-573.

NAITO, Y., MASUYAMA, T. & ISHIHARA, M. 2020. Iron and cardiovascular diseases. *J Cardiol*.

NICHOLSON, A. M. & RADEMAKERS, R. 2016. What we know about TMEM106B in neurodegeneration. *Acta Neuropathol,* 132**,** 639-651.

NIEMEYER, J., MENTRUP, T., HEIDASCH, R., MÜLLER, S. A., BISWAS, U., MEYER, R., PAPADOPOULOU, A. A., DEDERER, V., HAUG-KRÖPER, M. & ADAMSKI, V. 2019. The intramembrane protease SPPL 2c promotes male germ cell development by cleaving phospholamban. *EMBO reports,* 20**,** e46449.

NOVIKOVA, G., KAPOOR, M., JULIA, T., ABUD, E. M., EFTHYMIOU, A. G., CHENG, H., FULLARD, J. F., BENDL, J., ROUSSOS, P. & POON, W. W. 2019. Integration of Alzheimer's disease genetics and myeloid genomics reveals novel disease risk mechanisms. *Biorxiv***,** 694281.

O'MALLEY, W. E., ACHINSTEIN, B. & SHEAR, M. J. 1962. Action of bacterial polysaccharide on tumors. II. Damage of sarcoma 37 by serum of mice treated with Serratia marcescens polysaccharide, and induced tolerance. *Journal of the National Cancer Institute,* 29**,** 1169-1175.

OHKI, I., ISHIGAKI, T., OYAMA, T., MATSUNAGA, S., XIE, Q., OHNISHI-KAMEYAMA, M., MURATA, T., TSUCHIYA, D., MACHIDA, S. & MORIKAWA, K. 2005. Crystal structure of human lectin-like, oxidized low-density lipoprotein receptor 1 ligand binding domain and its ligand recognition mode to OxLDL. *Structure,* 13**,** 905-917.

OKOCHI, M., FUKUMORI, A., JIANG, J., ITOH, N., KIMURA, R., STEINER, H., HAASS, C., TAGAMI, S. & TAKEDA, M. 2006. Secretion of the Notch-1 Abeta-like peptide during Notch signaling. *J Biol Chem,* 281**,** 7890-8.

OLSSON, F., SCHMIDT, S., ALTHOFF, V., MUNTER, L. M., JIN, S., ROSQVIST, S., LENDAHL, U., MULTHAUP, G. & LUNDKVIST, J. 2014. Characterization of intermediate steps in amyloid beta (Abeta) production under near-native conditions. *J Biol Chem,* 289**,** 1540-50.

ORDÁS, I., MOULD, D. R., FEAGAN, B. G. & SANDBORN, W. J. 2012. Anti-TNF monoclonal antibodies in inflammatory bowel disease: pharmacokinetics-based dosing paradigms. *Clinical Pharmacology & Therapeutics,* 91**,** 635-646.

ORLANDO, G., SILVA, A., MACEDO-RIBEIRO, S., RAIMONDI, D. & VRANKEN, W. 2020. Accurate prediction of protein beta-aggregation with generalized statistical potentials. *Bioinformatics,* 36**,** 2076-2081.

OSENKOWSKI, P., LI, H., YE, W., LI, D., AESCHBACH, L., FRAERING, P. C., WOLFE, M. S., SELKOE, D. J. & LI, H. 2009. Cryoelectron Microscopy Structure of Purified γ-Secretase at 12 Å Resolution. *Journal of Molecular Biology,* 385**,** 642-652.

PAPADOPOULOU, A. A., MULLER, S. A., MENTRUP, T., SHMUELI, M. D., NIEMEYER, J., HAUG-KROPER, M., VON BLUME, J., MAYERHOFER, A., FEEDERLE, R., SCHRODER, B., LICHTENTHALER, S. F. & FLUHRER, R. 2019. Signal Peptide Peptidase-Like 2c (SPPL2c) impairs vesicular transport and cleavage of SNARE proteins. *EMBO Rep,* 20.

PARAMESWARAN, N. P. S. 2010. Tumor necrosis factor alpha signaling in macrophages. *Crit Rev Eukaryot Gene Expr,* 20**,** 87-103.

PARDOSSI-PIQUARD, R., YANG, S.-P., KANEMOTO, S., GU, Y., CHEN, F., BÖHM, C., SEVALLE, J., LI, T., WONG, P. C. & CHECLER, F. 2009. APH1 polar transmembrane residues regulate the assembly and activity of presenilin complexes. *Journal of Biological Chemistry,* 284**,** 16298-16307.

PESCHON, J. J., SLACK, J. L., REDDY, P., STOCKING, K. L., SUNNARBORG, S. W., LEE, D. C., RUSSELL, W. E., CASTNER, B. J., JOHNSON, R. S., FITZNER, J. N., BOYCE, R. W., NELSON, N., KOZLOSKY, C. J., WOLFSON, M. F., RAUCH, C. T., CERRETTI, D. P., PAXTON, R. J., MARCH, C. J. & BLACK, R. A. 1998. An Essential Role for Ectodomain Shedding in Mammalian Development. *Science,* 282**,** 1281-1284.

PFEFFER, K., MATSUYAMA, T., KÜNDIG, T. M., WAKEHAM, A., KISHIHARA, K., SHAHINIAN, A., WIEGMANN, K., OHASHI, P. S., KRÖNKE, M. & MAK, T. W. 1993. Mice deficient for the 55 kd tumor necrosis factor receptor are resistant to endotoxic shock, yet succumb to L. monocytogenes infection. *Cell,* 73**,** 457-67.

PICKFORD, F., COOMARASWAMY, J., JUCKER, M. & MCGOWAN, E. 2006. Modeling familial British dementia in transgenic mice. *Brain pathology,* 16**,** 80-85.

PLANEY, S. L. & ZACHARIAS, D. A. 2010. Identification of targets and inhibitors of protein palmitoylation. *Expert Opinion on Drug Discovery,* 5**,** 155-164.

POGGI, M., KARA, I., BRUNEL, J. M., LANDRIER, J. F., GOVERS, R., BONARDO, B., FLUHRER, R., HAASS, C., ALESSI, M. C. & PEIRETTI, F. 2013. Palmitoylation of TNF alpha is involved in the regulation of TNF receptor 1 signalling. *Biochim Biophys Acta,* 1833**,** 602-12.

PRUESSMEYER, J. & LUDWIG, A. The good, the bad and the ugly substrates for ADAM10 and ADAM17 in brain pathology, inflammation and cancer. Seminars in cell & developmental biology, 2009. Elsevier, 164-174.

QIAN, Y., ZHANG, X., ZHOU, L., YUN, X., XIE, J., XU, J., RUAN, Y. & REN, S. 2012. Site-specific N-glycosylation identification of recombinant human lectin-like oxidized low density lipoprotein receptor-1 (LOX-1). *Glycoconjugate journal,* 29**,** 399-409.

QUINT, S., WIDMAIER, S., MINDE, D., HORNBURG, D., LANGOSCH, D. & SCHARNAGL, C. 2010. Residue-specific side-chain packing determines the backbone dynamics of transmembrane model helices. *Biophys J,* 99**,** 2541-9.

RAN, F. A., HSU, P. D., WRIGHT, J., AGARWALA, V., SCOTT, D. A. & ZHANG, F. 2013. Genome engineering using the CRISPR-Cas9 system. *Nat Protoc,* 8**,** 2281-2308.

RAWSON, R. B. 2013. The site-2 protease. *Biochim Biophys Acta,* 1828**,** 2801-7.

RIESE, R. J., WOLF, P. R., BRÖMME, D., NATKIN, L. R., VILLADANGOS, J. A., PLOEGH, H. L. & CHAPMAN, H. A. 1996. Essential role for cathepsin S in MHC class II–associated invariant chain processing and peptide loading. *Immunity,* 4**,** 357-366.

ROSSIN, A., MILORO, G. & HUEBER, A. O. 2019. TRAIL and FasL Functions in Cancer and Autoimmune Diseases: Towards an Increasing Complexity. *Cancers (Basel),* 11.

SASTRE, M., STEINER, H., FUCHS, K., CAPELL, A., MULTHAUP, G., CONDRON, M. M., TEPLOW, D. B. & HAASS, C. 2001. Presenilin-dependent γ-secretase processing of β-amyloid precursor protein at a site corresponding to the S3 cleavage of Notch. *EMBO reports,* 2**,** 835-841.

SCHARNAGL, C., PESTER, O., HORNBURG, P., HORNBURG, D., GÖTZ, A. & LANGOSCH, D. 2014. Side-chain to main-chain hydrogen bonding controls the intrinsic backbone dynamics of the amyloid precursor protein transmembrane helix. *Biophysical journal,* 106**,** 1318-1326.

SCHAUENBURG, L., LIEBSCH, F., ERAVCI, M., MAYER, M. C., WEISE, C. & MULTHAUP, G. 2018. APLP1 is endoproteolytically cleaved by gamma-secretase without previous ectodomain shedding. *Sci Rep,* 8**,** 1916.

SCHNEPPENHEIM, J., HUTTL, S., KRUCHEN, A., FLUHRER, R., MULLER, I., SAFTIG, P., SCHNEPPENHEIM, R., MARTIN, C. L. & SCHRODER, B. 2014. Signal-peptide-peptidase-like 2a is required for CD74 intramembrane proteolysis in human B cells. *Biochem Biophys Res Commun,* 451**,** 48-53.

SCHRODER, B. 2016. The multifaceted roles of the invariant chain CD74--More than just a chaperone. *Biochim Biophys Acta,* 1863**,** 1269-81.

SCHULTE, M., REISS, K., LETTAU, M., MARETZKY, T., LUDWIG, A., HARTMANN, D., DE STROOPER, B., JANSSEN, O. & SAFTIG, P. 2007. ADAM10 regulates FasL cell surface expression and modulates FasL-induced cytotoxicity and activation-induced cell death. *Cell Death & Differentiation,* 14**,** 1040-1049.

SHI, G., LEE, J. R., GRIMES, D. A., RACACHO, L., YE, D., YANG, H., ROSS, O. A., FARRER, M., MCQUIBBAN, G. A. & BULMAN, D. E. 2011. Functional alteration of PARL contributes to mitochondrial dysregulation in Parkinson's disease. *Human molecular genetics,* 20**,** 1966-1974.

SPITZ, C., SCHLOSSER, C., GUSCHTSCHIN-SCHMIDT, N., STELZER, W., MENIG, S., GÖTZ, A., HAUG-KRÖPER, M., SCHARNAGL, C., LANGOSCH, D. & MUHLE-GOLL, C. 2020. Non-Canonical shedding of TNFα by SPPL2a is determined by the conformational flexibility of its transmembrane helix. *iScience***,** 101775.

STEVENSON, F., BURSTEN, S., LOCKSLEY, R. & LOVETT, D. 1992. Myristyl acylation of the tumor necrosis factor alpha precursor on specific lysine residues. *The Journal of experimental medicine,* 176**,** 1053-1062.

STRAND, V., SHARP, V., KOENIG, A. S., PARK, G., SHI, Y., WANG, B., ZACK, D. J. & FIORENTINO, D. 2012. Comparison of health-related quality of life in rheumatoid arthritis, psoriatic arthritis and psoriasis and effects of etanercept treatment. *Annals of the rheumatic diseases,* 71**,** 1143-1150.

SUN, L., LI, X. & SHI, Y. 2016. Structural biology of intramembrane proteases: mechanistic insights from rhomboid and S2P to γ-secretase. *Curr Opin Struct Biol,* 37**,** 97-107.

SUN, L. & ZHAO, Y. 2007. The biological role of dectin-1 in immune response. *Int Rev Immunol,* 26**,** 349-64.

TACK, C. J., KLEIJWEGT, F. S., VAN RIEL, P. L. & ROEP, B. O. 2009. Development of type 1 diabetes in a patient treated with anti-TNF-alpha therapy for active rheumatoid arthritis. *Diabetologia,* 52**,** 1442-4.

TAKAKURA-YAMAMOTO, R., YAMAMOTO, S., FUKUDA, S. & KURIMOTO, M. 1996. O-Glycosylated Species of Natural Human Tumor-Necrosis Factor-α. *European journal of biochemistry,* 235**,** 431-437.

TANAKA, M., ITAI, T., ADACHI, M. & NAGATA, S. 1998. Downregulation of Fas ligand by shedding. *Nature medicine,* 4**,** 31-36.

TARTAGLIA, L. A., PENNICA, D. & GOEDDEL, D. V. 1993a. Ligand passing: the 75-kDa tumor necrosis factor (TNF) receptor recruits TNF for signaling by the 55-kDa TNF receptor. *J Biol Chem,* 268**,** 18542-8.

TARTAGLIA, L. A., ROTHE, M., HU, Y. F. & GOEDDEL, D. V. 1993b. Tumor necrosis factor's cytotoxic activity is signaled by the p55 TNF receptor. *Cell,* 73**,** 213-6.

TARTAGLIA, L. A., WEBER, R. F., FIGARI, I. S., REYNOLDS, C., PALLADINO, M. A. & GOEDDEL, D. V. 1991. The two different receptors for tumor necrosis factor mediate distinct cellular responses. *Proceedings of the National Academy of Sciences,* 88**,** 9292-9296.

TESTI, C., BOFFI, A. & MONTEMIGLIO, L. C. 2019. Structural analysis of the transferrin receptor multifaceted ligand(s) interface. *Biophys Chem,* 254**,** 106242.

THINON, E., SERWA, R. A., BRONCEL, M., BRANNIGAN, J. A., BRASSAT, U., WRIGHT, M. H., HEAL, W. P., WILKINSON, A. J., MANN, D. J. & TATE, E. W. 2014. Global profiling of co-and post-translationally N-myristoylated proteomes in human cells. *Nature communications,* 5**,** 1-13.

TONE, K., STAPPERS, M. H. T., WILLMENT, J. A. & BROWN, G. D. 2019. C-type lectin receptors of the Dectin-1 cluster: Physiological roles and involvement in disease. *Eur J Immunol,* 49**,** 2127-2133.

TORRES-ARANCIVIA, C., ROSS, C. M., CHAVEZ, J., ASSUR, Z., DOLIOS, G., MANCIA, F. & UBARRETXENA-BELANDIA, I. 2010. Identification of an archaeal presenilin-like intramembrane protease. *PLoS One,* 5.

TSACHAKI, M., GHISO, J. & EFTHIMIOPOULOS, S. 2008. BRI2 as a central protein involved in neurodegeneration. *Biotechnol J,* 3**,** 1548-54.

TSACHAKI, M., SERLIDAKI, D., FETANI, A., ZARKOU, V., ROZANI, I., GHISO, J. & EFTHIMIOPOULOS, S. 2011. Glycosylation of BRI2 on asparagine 170 is involved in its trafficking to the cell surface but not in its processing by furin or ADAM10. *Glycobiology,* 21**,** 1382-1388.

TSENG, W.-Y., HUANG, Y.-S., LIN, H.-H., LUO, S.-F., MCCANN, F., MCNAMEE, K., CLANCHY, F. & WILLIAMS, R. 2018. TNFR signalling and its clinical implications. *Cytokine,* 101**,** 19-25.

URBAN, S. 2013. Mechanisms and cellular functions of intramembrane proteases. *Biochim Biophys Acta,* 1828**,** 2797-800.

UTSUMI, T., TAKESHIGE, T., TANAKA, K., TAKAMI, K., KIRA, Y., KLOSTERGAARD, J. & ISHISAKA, R. 2001. Transmembrane TNF (pro-TNF) is palmitoylated. *FEBS letters,* 500**,** 1-6.

VALATAS, V., KOLIOS, G. & BAMIAS, G. 2019. TL1A (TNFSF15) and DR3 (TNFRSF25): A Co-stimulatory System of Cytokines With Diverse Functions in Gut Mucosal Immunity. *Front Immunol,* 10**,** 583.

VAN OSTADE, X., TAVERNIER, J., PRANGE, T. & FIERS, W. 1991. Localization of the active site of human tumour necrosis factor (hTNF) by mutational analysis. *EMBO J,* 10**,** 827-36.

VANDENBROUCKE, R. E. & LIBERT, C. 2014. Is there new hope for therapeutic matrix metalloproteinase inhibition? *Nature reviews Drug discovery,* 13**,** 904-927.

VARGO-GOGOLA, T., CRAWFORD, H. C., FINGLETON, B. & MATRISIAN, L. M. 2002. Identification of novel matrix metalloproteinase-7 (matrilysin) cleavage sites in murine and human Fas ligand. *Archives of Biochemistry and Biophysics,* 408**,** 155-161.

VOSS, M., FUKUMORI, A., KUHN, P.-H., KÜNZEL, U., KLIER, B., GRAMMER, G., HAUG-KRÖPER, M., KREMMER, E., LICHTENTHALER, S. F. & STEINER, H. 2012. Foamy virus envelope protein is a substrate for signal peptide peptidase-like 3 (SPPL3). *Journal of Biological Chemistry,* 287**,** 43401-43409.

VOSS, M., KUNZEL, U., HIGEL, F., KUHN, P. H., COLOMBO, A., FUKUMORI, A., HAUG-KROPER, M., KLIER, B., GRAMMER, G., SEIDL, A., SCHRODER, B., OBST, R., STEINER, H., LICHTENTHALER, S. F., HAASS, C. & FLUHRER, R. 2014. Shedding of glycan-modifying enzymes by signal peptide peptidase-like 3 (SPPL3) regulates cellular N-glycosylation. *EMBO J,* 33**,** 2890-905.

VOSS, M., SCHRODER, B. & FLUHRER, R. 2013. Mechanism, specificity, and physiology of signal peptide peptidase (SPP) and SPP-like proteases. *Biochim Biophys Acta,* 1828**,** 2828-39.

WANG, J., BEHER, D., NYBORG, A. C., SHEARMAN, M. S., GOLDE, T. E. & GOATE, A. 2006. C-terminal PAL motif of presenilin and presenilin homologues required for normal active site conformation. *Journal of Neurochemistry,* 96**,** 218-227.

WEIHOFEN, A., BINNS, K., LEMBERG, M. K., ASHMAN, K. & MARTOGLIO, B. 2002. Identification of signal peptide peptidase, a presenilin-type aspartic protease. *Science,* 296**,** 2215-8.

WILLEM, M. 2016. Proteolytic processing of Neuregulin-1. *Brain Res Bull,* 126**,** 178-182.

WITTMANN, L. 2017. *In-silico Investigation of the Dynamic Fingerprints of the Transmembrane Domains of Signal Peptide Peptidase Substrates and Non-Substrates.* B.Sc., Technical University Munich.

WOLFE, M. S. & HAASS, C. 2001. The Role of presenilins in gamma-secretase activity. *J Biol Chem,* 276**,** 5413-6.

WON, S. J., CHEUNG SEE KIT, M. & MARTIN, B. R. 2018. Protein depalmitoylases. *Critical reviews in biochemistry and molecular biology,* 53**,** 83-98.

WORKMAN, L. M. & HABELHAH, H. 2013. TNFR1 signaling kinetics: spatiotemporal control of three phases of IKK activation by posttranslational modification. *Cellular signalling,* 25**,** 1654-1664.

WU, H., LIU, G., LI, C. & ZHAO, S. 2003. bri3, a novel gene, participates in tumor necrosis factor-alpha-induced cell death. *Biochem Biophys Res Commun,* 311**,** 518-24.

XU, W., BARRIENTOS, T., MAO, L., ROCKMAN, H. A., SAUVE, A. A. & ANDREWS, N. C. 2015. Lethal cardiomyopathy in mice lacking transferrin receptor in the heart. *Cell reports,* 13**,** 533-545.

YI, F., SHI, X., PEI, X. & WU, X. 2018. Tumor necrosis factor-alpha-308 gene promoter polymorphism associates with survival of cancer patients: A meta-analysis. *Medicine (Baltimore),* 97**,** e13160.

YIN, L., CALVO-CALLE, J. M., DOMINGUEZ-AMOROCHO, O. & STERN, L. J. 2012. HLA-DM Constrains Epitope Selection in the Human CD4 T Cell Response to Vaccinia Virus by Favoring the Presentation of Peptides with Longer HLA-DM–Mediated Half-Lives. *The Journal of Immunology,* 189**,** 3983-3994.

YUCEL, S. S., STELZER, W., LORENZONI, A., WOZNY, M., LANGOSCH, D. & LEMBERG, M. K. 2019. The Metastable XBP1u Transmembrane Domain Defines Determinants for Intramembrane Proteolysis by Signal Peptide Peptidase. *Cell Rep,* 26**,** 3087-3099 e11.

ZAHN, C., KAUP, M., FLUHRER, R. & FUCHS, H. 2013. The transferrin receptor-1 membrane stub undergoes intramembrane proteolysis by signal peptide peptidase-like 2b. *Febs j,* 280**,** 1653-63.

ZETTL, M., ADRAIN, C., STRISOVSKY, K., LASTUN, V. & FREEMAN, M. 2011. Rhomboid family pseudoproteases use the ER quality control machinery to regulate intercellular signaling. *Cell,* 145**,** 79-91.

ZHENG, B., DERAN, M., LI, X., LIAO, X., FUKATA, M. & WU, X. 2013. 2-Bromopalmitate analogues as activity-based probes to explore palmitoyl acyltransferases. *Journal of the American Chemical Society,* 135**,** 7082-7085.

ZHENG, Y., SAFTIG, P., HARTMANN, D. & BLOBEL, C. 2004. Evaluation of the contribution of different ADAMs to tumor necrosis factor alpha (TNFalpha) shedding and of the function of the TNFalpha ectodomain in ensuring selective stimulated shedding by the TNFalpha convertase (TACE/ADAM17). *J Biol Chem,* 279**,** 42898-906.

ZHU, X. & PAPAYANNOPOULOS, I. A. 2003. Improvement in the detection of low concentration protein digests on a MALDI TOF/TOF workstation by reducing α-cyano-4-hydroxycinnamic acid adduct ions. *Journal of biomolecular techniques: JBT,* 14**,** 298.

ZMUDA, F. & CHAMBERLAIN, L. H. 2020. Regulatory Effects of Post-Translational Modifications on zDHHC S-acyltransferases. *J Biol Chem*.

ZUCCATO, E., BLOTT, E. J., HOLT, O., SIGISMUND, S., SHAW, M., BOSSI, G. & GRIFFITHS, G. M. 2007. Sorting of Fas ligand to secretory lysosomes is regulated by mono-ubiquitylation and phosphorylation. *Journal of cell science,* 120**,** 191-199.

ZUNKE, F. & ROSE-JOHN, S. 2017. The shedding protease ADAM17: Physiology and pathophysiology. *Biochim Biophys Acta Mol Cell Res,* 1864**,** 2059-2070.

REFERENCES TABLE 1.1

* prediction according to sequence

[1] FRIEDMANN, E., HAUBEN, E., MAYLANDT, K., SCHLEEGER, S., VREUGDE, S., LICHTENTHALER, S. F., KUHN, P. H., STAUFFER, D., ROVELLI, G. & MARTOGLIO, B. 2006. SPPL2a and SPPL2b promote intramembrane proteolysis of TNFalpha in activated dendritic cells to trigger IL-12 production. *Nat Cell Biol,* 8 843-8.

[2] ECK, M. J. & SPRANG, S. R. 1989. The structure of tumor necrosis factor-alpha at 2.6 A resolution. Implications for receptor binding. *J Biol Chem,* 264 17595-605.

[3] MOSS, M. L., JIN, S.-L. C., MILLA, M. E., BURKHART, W., CARTER, H. L., CHEN, W.-J., CLAY, W. C., DIDSBURY, J. R., HASSLER, D. & HOFFMAN, C. R. 1997. Cloning of a disintegrin metalloproteinase that processes precursor tumour-necrosis factor-α. *Nature,* 385 733-736.

[4] ZHENG, Y., SAFTIG, P., HARTMANN, D. & BLOBEL, C. 2004. Evaluation of the contribution of different ADAMs to tumor necrosis factor alpha (TNFalpha) shedding and of the function of the TNFalpha ectodomain in ensuring selective stimulated shedding by the TNFalpha convertase (TACE/ADAM17). *J Biol Chem,* 279 42898-906.

[5] FLUHRER, R., GRAMMER, G., ISRAEL, L., CONDRON, M. M., HAFFNER, C., FRIEDMANN, E., BOHLAND, C., IMHOF, A., MARTOGLIO, B., TEPLOW, D. B. & HAASS, C. 2006. A gamma-secretase-like intramembrane cleavage of TNFalpha by the GxGD aspartyl protease SPPL2b. *Nat Cell Biol,* 8 894-6.

[6] FLUHRER, R., FUKUMORI, A., MARTIN, L., GRAMMER, G., HAUG-KROPER, M., KLIER, B., WINKLER, E., KREMMER, E., CONDRON, M. M., TEPLOW, D. B., STEINER, H. & HAASS, C. 2008. Intramembrane proteolysis of GXGD-type aspartyl proteases is slowed by a familial Alzheimer disease-like mutation. *J Biol Chem,* 283 30121-8.

[7] FRIEDMANN, E., HAUBEN, E., MAYLANDT, K., SCHLEEGER, S., VREUGDE, S., LICHTENTHALER, S. F., KUHN, P. H., STAUFFER, D., ROVELLI, G. & MARTOGLIO, B. 2006. SPPL2a and SPPL2b promote intramembrane proteolysis of TNFalpha in activated dendritic cells to trigger IL-12 production. *Nat Cell Biol,* 8 843-8.

[8] TAKAKURA-YAMAMOTO, R., YAMAMOTO, S., FUKUDA, S. & KURIMOTO, M. 1996. O-Glycosylated Species of Natural Human Tumor-Necrosis Factor-α. *European journal of biochemistry,* 235 431-437.

[9] STEVENSON, F., BURSTEN, S., LOCKSLEY, R. & LOVETT, D. 1992. Myristyl acylation of the tumor necrosis factor alpha precursor on specific lysine residues. *The Journal of experimental medicine,* 176 1053-1062.

[10] UTSUMI, T., TAKESHIGE, T., TANAKA, K., TAKAMI, K., KIRA, Y., KLOSTERGAARD, J. & ISHISAKA, R. 2001. Transmembrane TNF (pro-TNF) is palmitoylated. *FEBS letters,* 500 1-6.

[11] TANAKA, M., ITAI, T., ADACHI, M. & NAGATA, S. 1998. Downregulation of Fas ligand by shedding. *Nature medicine,* 4 31-36.

[12] ZUCCATO, E., BLOTT, E. J., HOLT, O., SIGISMUND, S., SHAW, M., BOSSI, G. & GRIFFITHS, G. M. 2007. Sorting of Fas ligand to secretory lysosomes is regulated by mono-ubiquitylation and phosphorylation. *Journal of cell science,* 120 191-199.

[13] LIU, W., RAMAGOPAL, U., CHENG, H., BONANNO, JEFFREY B., TORO, R., BHOSLE, R., ZHAN, C. & ALMO, STEVEN C. 2016. Crystal Structure of the Complex of Human FasL and Its Decoy Receptor DcR3. *Structure,* 24 2016-2023.

[14] VARGO-GOGOLA, T., CRAWFORD, H. C., FINGLETON, B. & MATRISIAN, L. M. 2002. Identification of novel matrix metalloproteinase-7 (matrilysin) cleavage sites in murine and human Fas ligand. *Archives of Biochemistry and Biophysics,* 408**,** 155-161.
[15] LETTAU, M., PAULSEN, M., KABELITZ, D. & JANSSEN, O. 2009. FasL expression and reverse signalling. *Death Receptors and Cognate Ligands in Cancer***,** 49-61.
[16] GUARDIOLA-SERRANO, F., ROSSIN, A., CAHUZAC, N., LÜCKERATH, K., MELZER, I., MAILFERT, S., MARGUET, D., ZÖRNIG, M. & HUEBER, A. 2010. Palmitoylation of human FasL modulates its cell death-inducing function. *Cell death & disease,* 1**,** e88-e88.
[17] TSACHAKI, M., SERLIDAKI, D., FETANI, A., ZARKOU, V., ROZANI, I., GHISO, J. & EFTHIMIOPOULOS, S. 2011. Glycosylation of BRI2 on asparagine 170 is involved in its trafficking to the cell surface but not in its processing by furin or ADAM10. *Glycobiology,* 21**,** 1382-1388.
[18] MATSUDA, S., MATSUDA, Y., SNAPP, E. L. & D'ADAMIO, L. 2011. Maturation of BRI2 generates a specific inhibitor that reduces APP processing at the plasma membrane and in endocytic vesicles. *Neurobiology of aging,* 32**,** 1400-1408.
[19] CHOI, S. I., VIDAL, R., FRANGIONE, B. & LEVY, E. 2004. Axonal transport of British and Danish amyloid peptides via secretory vesicles. *FASEB J,* 18**,** 373-5.
[20] MARTIN, L., FLUHRER, R., REISS, K., KREMMER, E., SAFTIG, P. & HAASS, C. 2008. Regulated intramembrane proteolysis of Bri2 (Itm2b) by ADAM10 and SPPL2a/SPPL2b. *J Biol Chem,* 283**,** 1644-52.
[21] SCHRODER, B. 2016. The multifaceted roles of the invariant chain CD74--More than just a chaperone. *Biochim Biophys Acta,* 1863**,** 1269-81.
[22] HENNE, C., SCHWENK, F., KOCH, N. & MÖLLER, P. 1995. Surface expression of the invariant chain (CD74) is independent of concomitant expression of major histocompatibility complex class II antigens. *Immunology,* 84**,** 177.
[23] GUNČAR, G., PUNGERČIČ, G., KLEMENČIČ, I., TURK, V. & TURK, D. 1999. Crystal structure of MHC class II-associated p41 Ii fragment bound to cathepsin L reveals the structural basis for differentiation between cathepsins L and S. *The EMBO journal,* 18**,** 793-803.
[24] RIESE, R. J., WOLF, P. R., BRÖMME, D., NATKIN, L. R., VILLADANGOS, J. A., PLOEGH, H. L. & CHAPMAN, H. A. 1996. Essential role for cathepsin S in MHC class II–associated invariant chain processing and peptide loading. *Immunity,* 4**,** 357-366.
[25] BECKER-HERMAN, S., ARIE, G., MEDVEDOVSKY, H., KEREM, A. & SHACHAR, I. 2005. CD74 Is a Member of the Regulated Intramembrane Proteolysis-processed Protein Family. *Molecular Biology of the Cell,* 16**,** 5061-5069.
[26] HALIM, A., RUETSCHI, U., LARSON, G. R. & NILSSON, J. 2013. LC–MS/MS characterization of O-glycosylation sites and glycan structures of human cerebrospinal fluid glycoproteins. *Journal of proteome research,* 12**,** 573-584.
[27] HÜTTL, S., HELFRICH, F., MENTRUP, T., HELD, S., FUKUMORI, A., STEINER, H., SAFTIG, P., FLUHRER, R. & SCHRÖDER, B. 2016. Substrate determinants of signal peptide peptidase-like 2a (SPPL2a)-mediated intramembrane proteolysis of the invariant chain CD74. *Biochemical Journal,* 473**,** 1405-1422.
[28] LANG, C. M., FELLERER, K., SCHWENK, B. M., KUHN, P.-H., KREMMER, E., EDBAUER, D., CAPELL, A. & HAASS, C. 2012. Membrane orientation and subcellular localization of transmembrane protein 106B (TMEM106B), a major risk factor for frontotemporal lobar degeneration. *Journal of Biological Chemistry,* 287**,** 19355-19365.
[29] THINON, E., SERWA, R. A., BRONCEL, M., BRANNIGAN, J. A., BRASSAT, U., WRIGHT, M. H., HEAL, W. P., WILKINSON, A. J., MANN, D. J. & TATE, E. W. 2014. Global profiling of co-and post-translationally N-myristoylated proteomes in human cells. *Nature communications,* 5**,** 1-13.

[30] MENTRUP, T., THEODOROU, K., CABRERA-CABRERA, F., HELBIG, A. O., HAPP, K., GIJBELS, M., GRADTKE, A. C., RABE, B., FUKUMORI, A., STEINER, H., THOLEY, A., FLUHRER, R., DONNERS, M. & SCHRODER, B. 2019. Atherogenic LOX-1 signaling is controlled by SPPL2-mediated intramembrane proteolysis. *J Exp Med,* 216**,** 807-830.
[31] OHKI, I., ISHIGAKI, T., OYAMA, T., MATSUNAGA, S., XIE, Q., OHNISHI-KAMEYAMA, M., MURATA, T., TSUCHIYA, D., MACHIDA, S. & MORIKAWA, K. 2005. Crystal structure of human lectin-like, oxidized low-density lipoprotein receptor 1 ligand binding domain and its ligand recognition mode to OxLDL. *Structure,* 13**,** 905-917.
[32] QIAN, Y., ZHANG, X., ZHOU, L., YUN, X., XIE, J., XU, J., RUAN, Y. & REN, S. 2012. Site-specific N-glycosylation identification of recombinant human lectin-like oxidized low density lipoprotein receptor-1 (LOX-1). *Glycoconjugate journal,* 29**,** 399-409.
[33] KUMANO-KURAMOCHI, M., XIE, Q., KAJIWARA, S., KOMBA, S., MINOWA, T. & MACHIDA, S. 2013. Lectin-like oxidized LDL receptor-1 is palmitoylated and internalizes ligands via caveolae/raft-dependent endocytosis. *Biochemical and biophysical research communications,* 434**,** 594-599.
[34] CHI, A., VALENCIA, J. C., HU, Z.-Z., WATABE, H., YAMAGUCHI, H., MANGINI, N. J., HUANG, H., CANFIELD, V. A., CHENG, K. C. & YANG, F. 2006. Proteomic and bioinformatic characterization of the biogenesis and function of melanosomes. *Journal of proteome research,* 5**,** 3135-3144.
[35] LAWRENCE, C. M., RAY, S., BABYONYSHEV, M., GALLUSER, R., BORHANI, D. W. & HARRISON, S. C. 1999. Crystal structure of the ectodomain of human transferrin receptor. *Science,* 286**,** 779-782.
[36] GUILLEMOT, J., CANUEL, M., ESSALMANI, R., PRAT, A. & SEIDAH, N. G. 2013. Implication of the proprotein convertases in iron homeostasis: proprotein convertase 7 sheds human transferrin receptor 1 and furin activates hepcidin. *Hepatology,* 57**,** 2514-24.
[37] ZAHN, C., KAUP, M., FLUHRER, R. & FUCHS, H. 2013. The transferrin receptor-1 membrane stub undergoes intramembrane proteolysis by signal peptide peptidase-like 2b. *Febs j,* 280**,** 1653-63.
[38] HAYES, G. R., ENNS, C. A. & LUCAS, J. J. 1992. Identification of the O-linked glycosylation site of the human transferrin receptor. *Glycobiology,* 2**,** 355-359.
[39] JING, S. & TROWBRIDGE, I. 1987. Identification of the intermolecular disulfide bonds of the human transferrin receptor and its lipid-attachment site. *The EMBO journal,* 6**,** 327-331.
[40] FLECK, D., VAN BEBBER, F., COLOMBO, A., GALANTE, C., SCHWENK, B. M., RABE, L., HAMPEL, H., NOVAK, B., KREMMER, E., TAHIROVIC, S., EDBAUER, D., LICHTENTHALER, S. F., SCHMID, B., WILLEM, M. & HAASS, C. 2013. Dual cleavage of neuregulin 1 type III by BACE1 and ADAM17 liberates its EGF-like domain and allows paracrine signaling. *J Neurosci,* 33**,** 7856-69.
[41] LIU, P., CLEVELAND, T. E. T., BOUYAIN, S., BYRNE, P. O., LONGO, P. A. & LEAHY, D. J. 2012. A single ligand is sufficient to activate EGFR dimers. *Proc Natl Acad Sci U S A,* 109**,** 10861-6.
[42] FLECK, D., VOSS, M., BRANKATSCHK, B., GIUDICI, C., HAMPEL, H., SCHWENK, B., EDBAUER, D., FUKUMORI, A., STEINER, H., KREMMER, E., HAUG-KROPER, M., ROSSNER, M. J., FLUHRER, R., WILLEM, M. & HAASS, C. 2016. Proteolytic Processing of Neuregulin 1 Type III by Three Intramembrane-cleaving Proteases. *J Biol Chem,* 291**,** 318-33.
[43] BAO, J., WOLPOWITZ, D., ROLE, L. W. & TALMAGE, D. A. 2003. Back signaling by the Nrg-1 intracellular domain. *The Journal of cell biology,* 161**,** 1133-1141.
[44] DUDA, A., STANGE, A., LÜFTENEGGER, D., STANKE, N., WESTPHAL, D., PIETSCHMANN, T., EASTMAN, S. W., LINIAL, M. L., RETHWILM, A. & LINDEMANN, D. 2004. Prototype foamy virus envelope glycoprotein leader peptide processing is mediated by a furin-like cellular protease, but cleavage is not essential for viral infectivity. *Journal of virology,* 78**,** 13865-13870.
[45] VOSS, M., FUKUMORI, A., KUHN, P.-H., KÜNZEL, U., KLIER, B., GRAMMER, G., HAUG-KRÖPER, M., KREMMER, E., LICHTENTHALER, S. F. & STEINER, H. 2012. Foamy virus envelope protein is a substrate for signal peptide peptidase-like 3 (SPPL3). *Journal of Biological Chemistry,* 287**,** 43401-43409.

DANKSAGUNG

An dieser Stelle möchte ich mich bei all denjenigen bedanken, die mich nicht nur beim Schreiben dieser Dissertation, sondern auch in den letzten fünf Jahren beim (Über-) Leben inner- und außerhalb des Labors unterstützt haben.

Zuerst gebührt mein besonderer Dank Prof. Dr. Regina Fluhrer, die mir die Möglichkeit gegeben hat an ihrem Institut unter hervorragender Betreuung zu promovieren. Ich habe dabei nicht nur im Bereich der unendlich komplizierten Biochemie viel gelernt, sondern mich auch kreativ jederzeit ausleben dürfen. Ich möchte mich für ihre nahezu unendliche Geduld beim Lesen und Korrigieren dieser Arbeit bedanken und hoffe, dass ich mich mit der graphischen „Rettung" eines kleinen Biochemie Buchs revanchieren konnte.

Ich bedanke mich außerdem bei der Forschergruppe 2290 für die finanzielle Unterstützung meines Projekts und bei allen FOR-Mitgliedern für ihren Beitrag bei der Publikation. Der wissenschaftliche Austausch quer durchs Land war immer hilfreich oder zumindest lustig, auch wenn uns die Gnocchi manchmal schwer im Magen lagen.

Danke an meine Laborkolleginnen Alkmini Papadopoulou, Martina Haug-Kröper, Christine Schlosser und Sabine Höppner. Ohne die Hilfe von Christine und Martina würde ich wahrscheinlich heute noch an Fig.1 sitzen. Außerdem gibt es niemanden, der so schöne Timecourses zaubert wie Martina. Vielen Dank an Sabine, deren Input für zukünftige Experimente schon jetzt von großem Wert ist. Ganz besonders möchte ich mich bei Alkmini für die überlebenswichtige Unterstützung mit Sushi und Spaß bedanken. Ich hätte mir keine bessere Bench-/Konferenzpartnerin und Freundin wünschen können, auch wenn der Bus nach Toronto das sicherlich anders gesehen hat.

Vielen Dank auch an die Beteiligten des γ-Sekretasemeetings, ohne die diese Arbeit vermutlich um einige Mutanten ärmer wäre. Danke den Mitgliedern der Fremdgruppe, die uns heimlich „Praktikumsplätze" zur Verfügung gestellt haben und unheimlich oft mit Rat und Tat zu Seite standen. Deshalb geht mein Dank auch an Johannes Trambauer, ohne den es die γ-Sekretase wahrscheinlich gar nicht geben würde - oder zumindest nicht den Abschnitt über sie in dieser Arbeit. Ich hoffe, es gingen nicht zu viele Informationen auf langen Fluren des DZNE oder zwischen Plexiglasscheiben verloren.

Ich möchte mich außerdem bei meiner Freundin Jacky für ihre unerbittlichen Motivationskünste bedanken. Ich glaube wir haben zusammen einen kleinen Regenwald gepflanzt, der nach dem Druck unserer Manuskripte wahrscheinlich wieder abgeholzt ist.

Abschließend möchte ich mich bei meinem Freund und Lebensgefährten Ingo bedanken, ohne den der ein oder andere Laptop und andere Bürogegenstände sicherlich Schaden genommen hätten. Vielen Dank auch an meine Eltern, die mich auf meinen manchmal etwas konfusen Weg immer unterstützt haben. Ich hoffe, dass ihr nun wisst was diese Intramembrandingsbumse sind und ich endlich wie deutsche Interpunktion funktioniert,..;.?

AFFIDAVIT

LMU LUDWIG-MAXIMILIANS-UNIVERSITÄT MÜNCHEN

Promotionsbüro
Medizinische Fakultät

MMRS

Eidesstattliche Versicherung

Spitz, Charlotte

Name, Vorname

Ich erkläre hiermit an Eides statt, dass ich die vorliegende Dissertation mit dem Titel:

Characterisation of the cleavage mechanism of SPPL2 proteases

selbständig verfasst, mich außer der angegebenen keiner weiteren Hilfsmittel bedient und alle Erkenntnisse, die aus dem Schrifttum ganz oder annähernd übernommen sind, als solche kenntlich gemacht und nach ihrer Herkunft unter Bezeichnung der Fundstelle einzeln nachgewiesen habe.

Ich erkläre des Weiteren, dass die hier vorgelegte Dissertation nicht in gleicher oder in ähnlicher Form bei einer anderen Stelle zur Erlangung eines akademischen Grades eingereicht wurde.

28.10.2021, München — *Charlotte Spitz*

Ort, Datum — Unterschrift Doktorandin bzw. Doktorand